Université de Toulouse

THÈSE

En vue de l'obtention du

DOCTORAT DE L'UNIVERSITÉ DE TOULOUSE

Délivré par :
Université Toulouse III Paul Sabatier (UT3 Paul Sabatier)

Discipline ou spécialité :

Pharmacologie

Présentée et soutenue par :
Isabelle Vila

le : 8 Juillet 2013

Titre :

Rôle du Toll-like receptor 4 (TLR4) immun dans le développement de la fibrose du tissu adipeux

---

Ecole doctorale :
Biologie, Santé, Biotechnologies (BSB)

Unité de recherche :
INSERM, U1048, Institut des maladies métaboliques et cardiovasculaires

Directeur(s) de Thèse :

Pr Dominique Langin

Rapporteurs :

Pr Anne Dutour
Dr Philippe Gual

Membre(s) du jury :
Pr Isabelle Castan-Laurell (président)
Pr Anne Dutour
Dr Philippe Gual
Pr Karine Clément
Dr Jean-Sébastien Saulnier-Blache
Pr Dominique Langin

REMERCIEMENTS

Voici venu le temps d'écrire, ce que l'on lit en premier mais qui pourtant s'écrit en dernier, les pages les plus personnelles de la thèse. Tout d'abord, cela signifie que la fin est proche, ce qui en soi est une très bonne nouvelle, mais qui veut aussi dire que le compte à rebours avant le départ a déjà commencé. Ces quelques lignes vont me permettre de remercier toutes les personnes qui ont supporté de travailler avec moi de près ou de loin, malgré mes goûts douteux en musique et mes tendances à pousser la chansonnette à longueur de journée.

Je souhaite remercier en premier lieu mon directeur de thèse, Dominique Langin, pour m'avoir accueilli au sein de son équipe. Malgré un départ un peu difficile, mon hypothèse de thèse ayant été invalidée dès les premiers mois, on s'en est finalement plutôt pas mal sorti. Je te remercie de m'avoir accordé ta confiance et une grande liberté de recherche durant ces quatre années. Merci pour m'avoir donné la chance d'intégrer et de grandir dans cette équipe.

Je voudrais remercier les rapporteurs de cette thèse, le Pr Anne Dutour et le Dr Philippe Gual, ainsi que les membres du jury le Pr Karine Clément et le Dr Jean-Sébastien Saulnier-Blache, pour l'intérêt qu'ils ont porté à mon travail. Un grand merci au Pr Isabelle Castan-Laurell d'avoir accepté d'être présidente de mon jury de thèse.

Je voudrais surtout profiter de ces pages de remerciements pour souligner que cette thèse est surtout le résultat d'un travail d'équipe important. Ce travail n'aurait sans doute jamais vu le jour sans le soutien indéfectible de nombreuses personnes.

Je voudrais tout d'abord remercier infiniment Marie-Adeline Marques. Elle a été au cours de mes quatre années « d'apprentie-chercheuse » ma deuxième moitié de cerveau et ma

deuxième paire de bras ! Toujours partante pour mettre au point une nouvelle manip (et Dieu sait s'il y en a eu !), j'ai eu beaucoup de plaisir à travailler avec toi.

Un grand merci à Laurent Monbrun qui m'a pratiquement tout appris à la paillasse. Merci d'avoir partagé ton expérience avec moi, merci pour ton aide et merci d'avoir rendu moins pénibles les DNAsage/RT avec nos conversations de geeks !

Je tiens à remercier Geneviève Tavernier tout d'abord pour avoir initié ce travail, pour son aide précieuse et pour m'avoir formé en expérimentation animale. On ne devient pas la reine de l'ITT/GTT sans un bon maître ! Merci aussi de soutenir l'USAP (même si entre le Stade et l'USAP ton cœur balance), on se sent moins seule en pays toulousain.

Je voudrais tout particulièrement remercier les musclés qui m'ont accepté parmi eux, même si la fibrose du tissu adipeux c'est quand même moins couillu que les lipases dans le muscle ! Vous avez su créer un véritable esprit de famille et cela a été vachement chouette d'en faire partie pendant ces quelques années.

Merci à Cédric Moro d'avoir été là pour moi quand j'avais des questions et de m'avoir suivi scientifiquement pendant toute ma thèse. Quand je lis un papier et que je me dis « Tiens Moro aussi il penserait que c'est bullshit » et bien je me dis que peut-être tout n'est pas perdu pour moi scientifiquement.

Ensuite, je souhaite remercier Katie Louche. Merci pour ta bonne humeur, merci pour ta disponibilité, ta gentillesse et merci pour ton rire. Travailler toute la semaine à tes côtés en tant que collègue a été super agréable et boire l'apéro le week-end en tant qu'amie l'a été encore plus.

Merci à Virginie Bourlier, pour sa disponibilité et pour nos nombreuses discussions qui ont été très enrichissantes pour moi. Merci aussi de m'avoir mis des rats morts de côté quand j'en avais besoin, même si à l'époque tu devais me prendre pour une sataniste ratophile !

Merci à Claire, Diane et Marine, la relève est là ! Et courage pour la suite, vous verrez la dernière année de thèse est encore pire que les autres !! Allez Emilie c'est la dernière ligne droite !

Un grand Merci à mes anciens et nouveaux acolytes de bureau. Ma première pensée va tout naturellement vers nos M2 de choc : Aurèle, Philippe et Camille. J'ai passé à vos côtés une année inoubliable (OMGPOP !!). Merci à Marion avec qui j'ai pu parler fromage et pinard même à 9h du matin. Merci à Marianne, Etienne et Valentin pour nos soirées « poker », soirées qui m'ont permis de comprendre qu'en fait aux cartes il n'y a vraiment que la chance qui compte (hein Marianne !?). Merci à Corinne pour être à l'origine des meilleures crêpes de Toulouse. Merci Lucille pour ta fraicheur et pour ton aide à venir.

Merci Aline pour ton aide, ta disponibilité, ta bonne humeur et ton humour. « Allez tchao !! »

Merci François pour la relecture de ce travail et pour nous éviter de manger trop vite le midi ! Merci Balbine et Nathalie pour votre expertise en stats, pour moi vous parlez toujours chinois ! Merci Sylvie pour ta bonne humeur et ta gentillesse. Merci Dominique L pour nos petites discussions « chasse et nature » mais surtout pour m'avoir permis de réaliser un rêve inaccessible pour beaucoup d'individus de la gent féminine : un tour dans le camion « du surfeur ».

Je souhaiterais aussi remercier d'autres personnes de l'Université, l'I2MC et de Stromalab : Claude K (pour les apéros de dernière minute), Anne D et Chantal B (d'avoir rendu les cours d'expérimentation animale plus sympa !), Coralie S (merci d'avoir relu ce manuscrit, merci pour ta disponibilité et tes bons conseils), Mano (pour ta gentillesse, bonne chance pour la suite), Marie-Josée (merci d'avoir été là pour moi en M2, on a passé de merveilleux moments !) mais également toutes les plateformes techniques. Merci au sergent chef Mortier pour sa bonne humeur et son efficacité redoutable.

Je voudrais également remercier Aurélien pour nos soirées épiques et pour m'avoir rapproché de celui qui par la suite est devenu beaucoup de choses : mon voisin de bureau, le copremier auteur de mon premier papier, mon copilote au labo comme dans la vie. Avec

cette thèse PM, nous tournons une page ensemble, une autre s'ouvre… Fais en sorte que ce soit à un endroit où on capte un peu ce qu'ils disent. Tout le monde a eu droit à un merci alors merci surtout de me supporter 24h/24h. Je t'aime. Merci aussi d'avoir une famille aussi géniale même si je ne comprends pas toujours leur dialecte !

Je tiens à remercier toutes les personnes que j'ai rencontrées au cours de mes pérégrinations et qui ont fait de moi ce que je suis. Merci du fond du cœur à mes amis qui m'ont toujours accompagnée, pour leur présence et leur soutien. Je pense en particulier à mes amis de toujours Greg, Freud et Pierrot mais aussi à Jessica qui a été « mon repère » tout au long de ces années toulousaines, à ma petite Céline et à ma Madège. On a vraiment vécu des moments inoubliables depuis toutes ces années, merci d'être encore là !

J'aimerais remercier ma famille et tout particulièrement mes parents. Ils ont toujours cru en moi et m'ont toujours dit de viser plus haut. Ils m'ont toujours soutenu, même si mes études ont battu des records de longueur. Pour mon père, les études c'est comme un fusil, il n'y a que deux cartouches. Après ma première année de médecine (ratée évidemment !), il m'a dit « il ne te reste plus qu'une seule cartouche ! » T'as vu Papa, j'ai écouté, la deuxième est encore au chaud ! Merci Maman d'avoir ouvert mon appétit scientifique en me demandant ce que je pensais de la théorie des cordes ou encore comment je concevais un trou noir, le tout au réveil à 8h du matin et avant mon café !

Je tiens enfin à remercier mes grands-parents. Merci pour les doux souvenirs d'enfance que vous m'avez laissés. Où que vous soyez, je sais que vous êtes fiers de moi.

Molts petons a tots

« Dans les champs de l'observation,

le hasard ne favorise que les esprits préparés ».

Louis Pasteur

TABLE DES MATIERES

LISTE DES ILLUSTRATIONS

FIGURES

LISTE DES ABREVIATIONS

AC	Adénylate cyclase
ACC	Acétyl-CoA carboxylase
Acyl-CoA	Acyl-coenzyme A
AG	Acide gras
AGL	Acide gras libre
AMPc	Adénosine monophosphate cyclique
AMPK	AMP-activated protein kinase
ARN	Acide ribonucléique
AS160	Akt substrate of 160 kDa
ATGL	Adipose triglyceride lipase
ATP	Adénosine-5'-triphosphate
C/EBP	CCAAT/Enhancer binding proteins
CD	Cluster of Differentiation
CGI-58	Comparative Gene Identification-58
CLS	Crown like structure
CRP	C-Réactive Protéine
CSM	Cellule stromale mésenchymateuse
CTGF	Connective tissue growth factor
DAG	Diacylglycérol
DGAT-1	Diacylglycerol acyltransferase
ERK	Extracellular signal-regulated kinase
FABP	Fatty acid binding protein

FABPpm	Fatty acid binding protein plasma membrane
FAS	Fatty acid synthase
FAT	Fatty Acid Translocase
FATP	Fatty Acid Transport Protein
G0S2	G0/G1 switch gene 2
GC	Guanylate cyclase
GLUT	Glucose transporter
GM-CSF	Granulocyte Macrophage Colony Stimulating Factor
GMPc	Guanosine monophosphate cyclique
HGF	Hepatocyte growth factor
HGFR	Hepatocyte Growth Factor Receptor
HIF-1α	Hypoxia inducible factor 1 alpha
HSC	Hepatic stellate cell
IFNγ	Interferon gamma
IKK-β	Inhibitor of nuclear factor kappa-B kinase subunit beta
IL	Interleukine
IMC	Indice de masse corporelle
IRAK	IL-1 Receptor Associated-Kinases
IRS	Insulin Receptor Substrates
ITT	Test de tolérance à l'insuline
JNK	C-Jun N-terminal kinases
LAP	Latency associated peptide
LBP	LPS binding protein
LHS	Lipase hormone-sensible

LPL	Lipoprotéine lipase
LPS	Lipopolysaccharide
MAG	Monoacylglycérol
MAPK	Mitogen-activated protein kinases
MCK	Muscle creatine kinase
MCP-1	Monocyte chemoattractant protein 1
M-CSF	Macrophate colony-stimulating factor
MEC	Matrice extracellulaire
MGL	Monoglyceride lipase
MMP	Matrix metalloproteinase
Myd88	Myeloid differentiation (88)
NF-kB	Nuclear factor-kappa B
NPR-A	Atrial natriuretic peptide receptor
PDGF	Platelet derived growth factor
PDH	Pyruvate deshydrogenase
PDK-1	3-phosphoinositide-dependent protein kinase 1
PH	Pleckstrin homology
PI3K	Phosphatidylinositol'3 kinase
PIP-3	Phosphatidylinositol 3,4,5 trisphosphate
PKA	Protéine kinase A
PKG	Protéine kinase G
PKC	Protéine kinase C
PLIN	Périlipine
PP2A	Protéine phosphatase 2A

PPAR	Peroxisome proliferator activated receptor
PREF-1	Preadipocyte factor 1
SCF	Stem cell factor
SH2	Src Homology 2 Domain
SOCS	Suppressor of cytokine signaling
SVF	Stroma-vascular fraction
TA	Tissu adipeux
TAG	Triacylglycérol
TGFβ	Transforming growth factor beta
TIMP	Tissue inhibitor of metalloproteinase
TIR	Toll/interleukin-1 receptor
TLR4	Toll like receptor 4
TNC	Ténascine C
TNF-α	Tumor necrosis factor alpha
TRAF	TNF receptor associated factor
TRIF	TIR domain containing adaptator interferon beta
TβRI	TGF beta receptor 1
VLDL	Very low density lipoprotein
WT	Wild type ou contrôle
αSMA	Alpha smooth muscle actine
βAR	Récepteur β-adrénergique

La première partie de ce manuscrit va traiter de la partie principale de ma thèse qui porte sur la fibrose du tissu adipeux et le rôle du TLR4 immun dans sa mise en place. Vous trouverez tout d'abord une présentation du tissu adipeux puis je vous parlerai de l'inflammation de «bas bruit» retrouvé au cours de l'obésité. Je vous présenterai par la suite la matrice extracellulaire et son remodelage. Enfin nous parlerons du processus pathologique de fibrose du tissu adipeux et de ces conséquences. Cette introduction bibliographique sera suivie de l'article, qui sera prochainement soumis pour publication, puis d'une discussion et conclusion sur les résultats de cet article ainsi que sur ceux qui ne seront pas publiés.

Dans une deuxième partie, je vous parlerai d'un sujet annexe à ma thèse, suivi en collaboration avec des collègues de l'équipe, portant sur la dérégulation de la lipolyse musculaire et ses conséquences sur l'insulinorésistance musculaire. Je vous présenterai de manière succincte les mécanismes d'insulinorésistance musculaire et les voies d'accumulation des lipides intermédiaires. Cette petite introduction sera suivie de l'article publié (Badin, Vila et al. 2013) et d'une discussion.

FIBROSE DU TISSU ADIPEUX

PARTIE I: FIBROSE DU TISSU ADIPEUX

I Le tissu adipeux blanc

1.1) Fonction du tissu adipeux blanc: un organe de stockage

Au-delà de son rôle d'isolant thermique et mécanique, le tissu adipeux blanc est la principale réserve énergétique de l'organisme. Il permet de réguler la balance énergétique en stockant le surplus de substrats sous forme de triacylglycérols (TAG). Ce stock de lipides reste mobilisable en fonction des besoins métaboliques des autres tissus et de l'organisme dans sa totalité. Globalement la gestion de l'énergie se fait grâce à deux voies métaboliques principales: la lipogenèse et la lipolyse.

1.1.1) Le stockage des lipides: lipogenèse et synthèse des triacylglycérols

Dans l'adipocyte, le stockage des lipides peut se faire grâce 2 voies. (figure 1)

La première voie correspond à la lipogenèse à partir de la capture directe des acides gras (AG) au niveau circulant. Ces derniers proviennent soit de l'alimentation en période post-prandiale soit de la lipogenèse hépatique. Ils arrivent au tissu adipeux (TA) *via* la circulation, soit directement sous forme de TAG associés aux chylomicrons et aux lipoprotéines de très faible densité (ou VLDL pour « *very low density lipoprotein* »). Les TAG sont alors hydrolysés par la lipoprotéine lipase (LPL) ancrée à la surface des cellules endothéliales (Goldberg 1996; Tacken, Teusink et al. 2000). Les AG non estérifiés entrent ensuite dans l'adipocyte, soit par diffusion simple, soit *via* des transporteurs d'AGL (acide gras libre) au niveau de la membrane plasmique. Les adipocytes blancs humains expriment différents transporteurs d'acides gras qui facilitent et régulent le transport des acides gras à travers la membrane plasmique : la protéine CD36 (homologue à la protéine murine «*Fatty Acid Translocase*» FAT), la «*Fatty Acid Transport Protein*» (FATP) et la «*Fatty Acid Binding Protein plasma membrane* » (FABPpm) (Abumrad, el-Maghrabi et al. 1993; Schaffer and Lodish 1994; Abumrad, Coburn et al. 1999). A l'intérieur de l'adipocyte, ces AGL seront transformés en Acyl-Co

enzyme A (Acyl-CoA) par l'Acyl-CoA synthétase. Ils seront ensuite ré-estérifiés en TAG en présence de glycérol-3P par l'action de différentes acyl transférases.

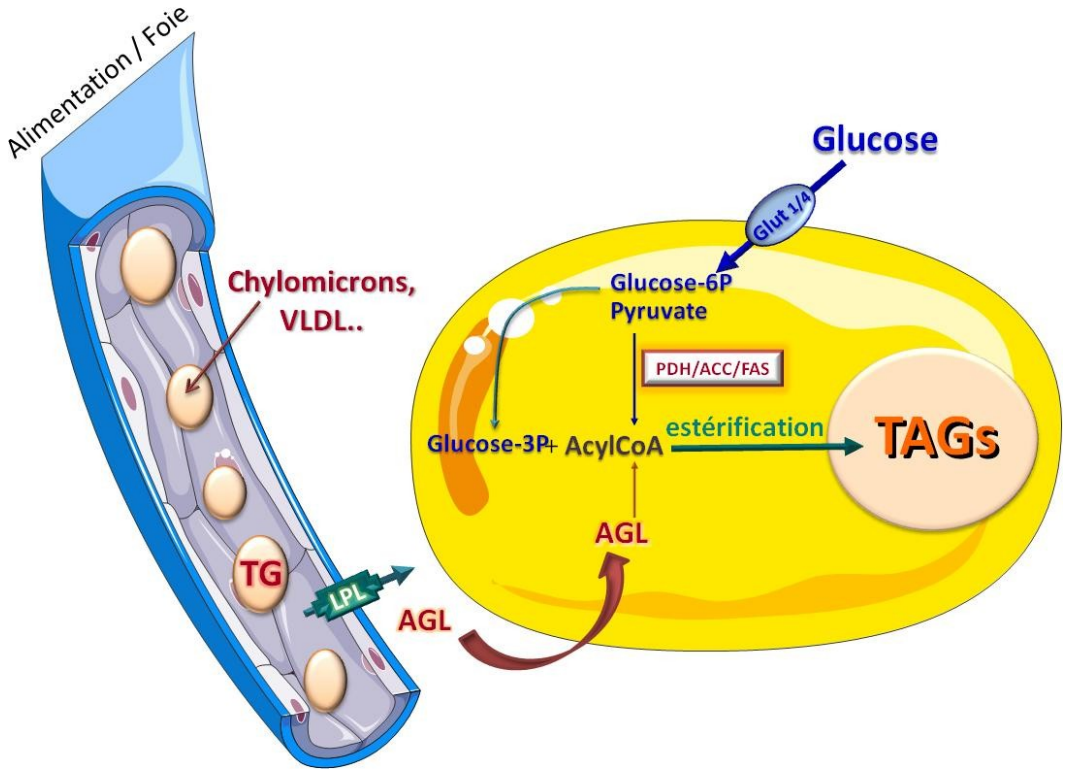

Figure 1: Stockage des lipides dans l'adipocyte

ACC: acétyl-CoA carboxylase, AGL: acide gras libre; FAS: fatty acid synthase; GLUT: tramporteur du glucose; LPL: lipoprotèine lipase; PDH: pyruvate déshydrogénase; TAGs: triacylglycérols; VLDL: very low density lipoprotein.

La deuxième voie de stockage des lipides dans l'adipocyte correspond à la lipogenèse *de novo*; ce terme désigne la néosynthèse d'AG à partir du glucose. La première étape de cette voie est l'entrée du glucose dans l'adipocyte, grâce à des transporteurs spécifiques (GLUT-1 et 4). Dans l'adipocyte, le glucose est alors transformé en pyruvate par la glycolyse. A la fin de ce processus, la pyruvate déshydrogénase (PDH), l'acétyl-CoA carboxylase (ACC) et la synthase des acides gras (FAS, « *Fatty Acid Synthase* ») interviennent successivement pour catalyser la formation des AG à longue chaîne saturée. L'action de différentes désaturases permet de synthétiser des AG plus ou moins saturés. Comme précédemment, ces AG sont ensuite ré-estérifiés pour donner des TAG. Il est nécessaire de préciser que chez les rongeurs, la lipogenèse est réalisée dans le foie et le TA alors que chez l'Homme celle-ci est majoritairement hépatique dans des conditions nutritionnelles habituelles (Collins, Neville et al. 2011; Lodhi, Wei et al. 2011).

1.1.2) La mobilisation des lipides: la lipolyse

La lipolyse assure la dégradation des TAG contenus au sein de la gouttelette lipidique de l'adipocyte (figure 2). Quand elle est compète, elle aboutit à l'hydrolyse des TAG en trois molécules d'acides gras et une molécule de glycérol. La libération des AG dans le sang permet de fournir l'énergie nécessaire aux tissus périphériques. Plusieurs lipases interviennent de façon séquentielle dans cette hydrolyse (Bezaire and Langin 2009; Lafontan and Langin 2009).

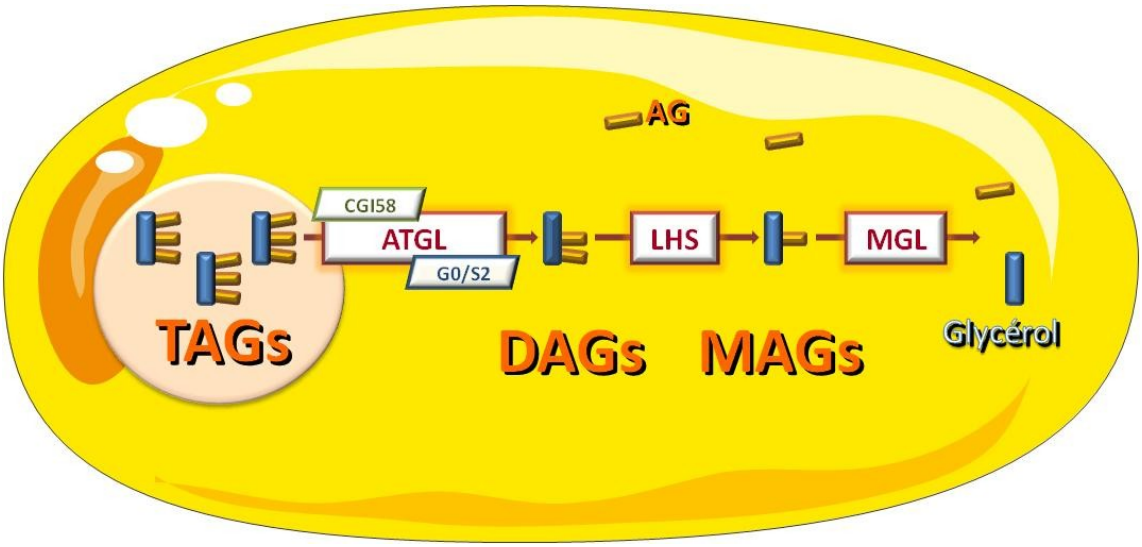

Figure 2: Cascade lipolytique dans l'adipocyte

AG: acide gras, ATGL: adipose triglyceride lipase; CGI58: comparative gene identification 58; DAGs: diacylglycérols; G0/S2: G0/G1 Switch gene 2; LHS: lipase hormonosensible; MAGs: monoacylglycérols; MGL: monoglycerol lipase; TAGs: triacylglycérols.

La première lipase intervenant est l'ATGL (*Adipose TriGlyceride Lipase*) (Jenkins, Mancuso et al. 2004; Zimmermann, Strauss et al. 2004; Haemmerle, Lass et al. 2006). Celle-ci a une grande affinité pour les TAG. Elle hydrolyse donc les TAG de la gouttelette lipidique en diacylglycérols (DAG). Cette lipase fonctionne en duo avec CGI-58 (*Comparative Gene Identification 58*) son cofacteur qui potentialise son activité TAG hydrolase (Lass, Zimmermann et al. 2006). Lorsque les adipocytes ne sont pas stimulés, CGI-58 est lié à la protéine périlipine 1, protéine structurale de la gouttelette lipidique adipocytaire. Dans cette configuration CGI-58 se trouve dans l'incapacité d'activer l'ATGL. A contrario la stimulation des adipocytes permet la phosphorylation des périlipines. Ceci entraîne la «libération» de CGI-58 qui pourra alors interagir avec l'ATGL et potentialiser l'hydrolyse des TAG (Granneman, Moore et al. 2007). A l'inverse

l'activité de l'ATGL est également régulée négativement par une autre protéine «*G0/G1 Switch gene 2*» (G0S2) dont l'effet sur l'ATGL vient d'être rapporté récemment *in vitro* ainsi que dans des adipocytes murins et humains (Cornaciu, Boeszoermenyi et al. 2011; Schweiger, Paar et al. 2012).

La deuxième lipase intervenant dans la cascade lipolytique est la lipase hormono-sensible (LHS) (Kolditz and Langin 2010). Elle clive les DAG en monoacylglycérols (MAG). L'activité de cette lipase dépend essentiellement de sa phosphorylation par une kinase dépendante de l'AMPc (par la protéine kinase A ou PKA) (Holm, Osterlund et al. 2000) ou du GMPc (par la protéine kinase G ou PKG) (Sengenes, Bouloumie et al. 2003). Cette phosphorylation active la LHS démasquant ainsi son site catalytique. Par ailleurs, cette phosphorylation permet une redistribution de la lipase du cytoplasme vers la gouttelette lipidique. La phosphorylation des périlipines par la PKA et la PKG, quant à elle, réduit leurs ancrages à la gouttelette lipidique et favorise ainsi l'accès de la LHS à ses substrats lipidiques (Miyoshi, Souza et al. 2006). La lipase des monoglycérides (MGL) hydrolyse ensuite les MAG en glycérol et AG non estérifiés (Zechner, Kienesberger et al. 2009). Cette enzyme est fortement exprimée dans l'adipocyte, on la trouve dans le cytoplasme, la membrane plasmique et la gouttelette lipidique (Karlsson, Contreras et al. 1997). Sa forte présence dans le tissu adipeux et sa grande spécificité pour les MAG suggèrent que la dernière étape de la lipolyse n'est pas extrêmement régulée. Une fois dans la circulation, les AG vont être véhiculés par l'albumine et vont servir de carburant pour les tissus métaboliquement actifs *via* leur oxydation qui génère de l'ATP. C'est le procédé majoritairement utilisé par les cellules pour obtenir de l'énergie à partir des AG.

1.1.3) Contrôle neuro-humoral de la synthèse et de l'hydrolyse des TAG

L'adipocyte présente donc deux fonctions principales, le stockage des lipides et leur mobilisation en cas de besoin. Ces activités métaboliques sont étroitement régulées par des signaux neuro-humoraux (Fain and Garcija-Sainz 1983; Lafontan, Moro et al. 2008). En effet l'activité lipolytique de l'adipocyte humain est sous le contrôle permanent des voies lipolytiques et anti-lipolytiques (figure 3) (Lafontan, Moro et al. 2005; Lafontan and Langin 2009).

Les catécholamines sont des agents lipolytiques majeurs *via* des récepteurs β-adrénergiques (β-AR) couplés à une protéine Gs. Elles induisent ainsi une stimulation

de l'adénylate cyclase (AC), entrainant une production d'AMPc, provoquant l'activation de la lipolyse par la PKA (Lafontan and Berlan 1993). Les peptides natriurétiques *via* leurs récepteurs actifs NPR-A permettent la production de GMPc par une guanylate cyclase (GC) induisant une stimulation de la lipolyse par la PKG (Sengenes, Moro et al. 2005).

Dans l'adipocyte, l'insuline est l'hormone anti-lipolytique principale. Elle agit en inhibant la production d'AMPc, diminuant ainsi l'activité de la PKA. Outre cette hormone il existe plusieurs familles de récepteurs à 7 domaines transmembranaires couplés négativement, *via* une protéine Gi, à l'adénylate cyclase. Ces récepteurs anti-lipolitiques permettent d'engendrer une inhibition de la lipolyse suite à la liaison de leurs agonistes spécifiques (exemple: les récepteurs α2-adrénergiques (α2-AR), les récepteurs adénosine de type A1 (A1-R), les récepteurs des prostaglandines E de type EP3 (EP3-PG-R), les récepteurs du neuropeptideY/peptide YY (NPY-Y)).

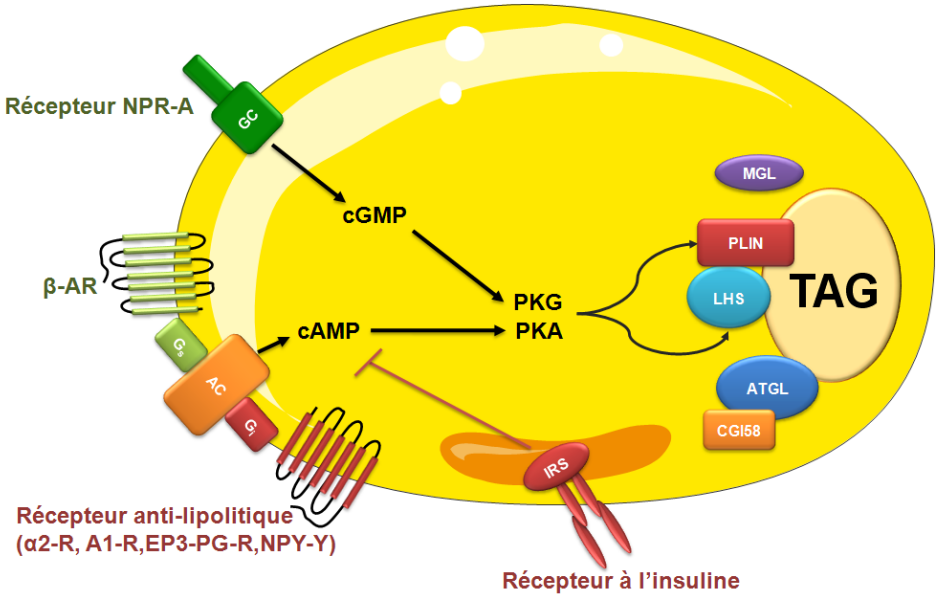

Figure 3: Contrôle neuro-humoral de la lipolyse adipocytaire

α2-AR: récepteur α2-adrénergique; β-AR: récepteur β-adrénergique; A1-R: récepteur adénosine de type A1; AC: adénylate cyclase, ATGL: adipose triglyceride lipase; cAMP: adénosine monophosphate cyclique, cGMP: guanosine 3',5'monophosphate cyclique; CGI58: Comparative Gene Identification 58; EP3-PG-R: récepteur des prostaglandines E de type EP3; GC:guanylate cyclase; IRS: substrat du récepteur à l'insuline; LHS: lipase hormonosensible; MGL: monoglycerol lipase; NPY-Y: récepteur du neuropeptide Y/peptide YY; PKG: protéine kinase G; PKA: protéine kinase A; TAGs: triacylglycérols.

L'augmentation de masse grasse, observée au cours de l'obésité, est accompagnée de modifications métaboliques du tissu adipeux. L'excès de TA s'accompagne d'une diminution de sa fonction lipolytique chez des sujets au repos mais également soumis à

un exercice physique (Horowitz 2001). Au repos ces altérations lipolytiques, chez l'obèse, pourraient s'expliquer par une baisse de l'expression/activité des lipases adipocytaires En effet chez l'obèse, les expressions protéiques des deux protéines majeures de la lipolyse, l'ATGL (Jocken, Langin et al. 2007) et la LHS, sont diminuées (Large, Reynisdottir et al. 1999; Langin, Dicker et al. 2005). A l'exercice, des mesures réalisées par micro-dialyse *in situ,* du dépôt sous cutané abdominal ont montré chez l'obèse une diminution de la réponse lipolytique au cours de l'exercice physique. Cette diminution de réponse s'explique essentiellement par une augmentation de la réceptivité α_2-adrénergique ainsi qu'une diminution de la réponse β-adrénergique (Stich, De Glisezinski et al. 2000; Horowitz 2001).

1.2) La composition du tissu adipeux blanc: un organe complexe

Au côté des adipocytes qui contiennent de grandes quantités de TAG, le tissu adipeux blanc comporte, en réalité, une grande diversité cellulaire. Après digestion par l'action de collagénases puis d'une centrifugation (Rodbell 1964), les cellules du TA blanc peuvent être séparées en deux grandes populations: les adipocytes matures et la fraction stroma-vasculaire (SVF). Cette fraction cellulaire non adipocytaire est composée de cellules stromales comprenant des cellules souches, dont certaines sont déjà des progéniteurs adipocytaires, ainsi que des cellules endothéliales. Cette fraction comprend également des cellules immunes principalement des macrophages et des lymphocytes (figure 4).

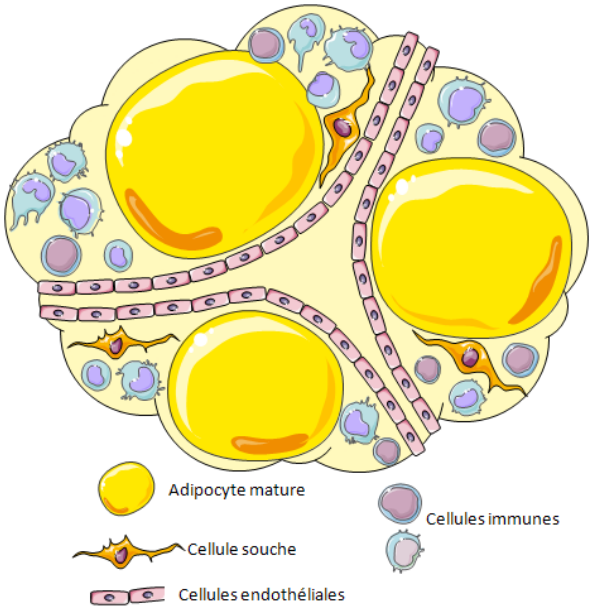

Figure 4: Le tissu adipeux, une diversité cellulaire

1.2.1) Les adipocytes

L'adipocyte blanc mature représente le type cellulaire majoritaire du tissu adipeux. Cette cellule a une énorme capacité de stockage d'énergie sous forme de TAG, ceux-ci sont stockés dans une gouttelette lipidique unique pouvant représenter 95% de son volume.

1.2.1.1) Hypertrophie et hyperplasie adipocytaire

L'obésité et le surpoids se caractérisent par le développement excessif du TA. Chez l'Homme, une personne est considérée obèse si son indice de masse corporelle (IMC = masse (Kg) / taille au carré (m²)) est supérieur ou égal à 30kg/m², et en surpoids si l'IMC se situe entre 25 et 29.9 kg/m². Un surplus de calories alimentaires entraîne une accumulation de TAG au niveau adipocytaire. A l'opposé, une diminution des apports énergétiques ou une augmentation de leur utilisation permet une diminution de la masse du TA. De manière intéressante, le «turnover» des TAG est un déterminant de la mise en place d'une obésité. En effet un stockage important et une faible hydrolyse des TAG du TA favorisent l'obésité, tandis qu'un faible stockage et une faible hydrolyse favorisent le développement d'une dyslipidémie chez l'Homme (Arner, Bernard et al. 2011).

L'augmentation de masse du tissu adipeux est associée à une augmentation de la taille puis du nombre d'adipocytes en cas d'obésité sévère (Prins and O'Rahilly 1997). L'équipe de Peter Arner a récemment démontré que le nombre d'adipocytes est un déterminant majeur de la masse grasse totale chez les adultes (Spalding, Arner et al. 2008). Le taux de renouvellement du TA atteint 10% chez l'Homme et reste constant à l'âge adulte sur une large gamme de masse corporelle, suggérant un rôle important de l'augmentation de la taille des adipocytes (hypertrophie). Selon l'hypothèse de la «taille critique», il existerait une taille cellulaire maximale. Ainsi, la cellule adipeuse différenciée se charge de triglycérides jusqu'à atteindre une taille critique au-delà de laquelle elle «recrute» un nouvel adipocyte (MacDougald and Mandrup 2002). L'adipocyte mature étant incapable de proliférer, la «création» de nouveaux adipocytes (hyperplasie) provient donc de la prolifération et la différenciation des progéniteurs adipocytaires présents en grande quantité dans la SVF (Bjorntorp, Gustafson et al. 1971; Geloen, Collet et al. 1989). Selon les travaux d'Arner, cette phase aurait lieu essentiellement durant l'enfance et l'adolescence.

1.2.1.2) La différenciation adipocytaire

Le feuillet embryonnaire à l'origine du TA est commun à celui des os et des muscles : il s'agit du mésoderme (Gesta, Tseng et al. 2007). Le processus de différenciation adipocytaire, appelé adipogenèse, est le passage d'une cellule stromale mésenchymateuse (CSM) en pré-adipocyte puis en adipocyte mature (figure 5). Le marqueur Pref-1 (*Preadipocyte factor 1*) est utilisé pour différentier les pré-adipocytes des adipocytes matures puisque celui-ci apparaît très tôt dans le lignage adipocytaire et disparaît au cours de la différenciation (Smas and Sul 1993). A l'inverse l'expression des enzymes et protéines de la synthèse et de la mobilisation des TAG augmente au cours de la différenciation adipocytaire et sont utilisées comme marqueurs des adipocytes matures. La différenciation adipocytaire est contrôlée par une expression génique finement régulée dans le temps (Koutnikova and Auwerx 2001). Les facteurs de transcription de la famille des C/EBPs *(CCAAT/Enhancer Binding Proteins)* et des PPARs *(Peroxisome Proliferator Activated Receptor)* interviennent largement dans ce processus de différenciation.

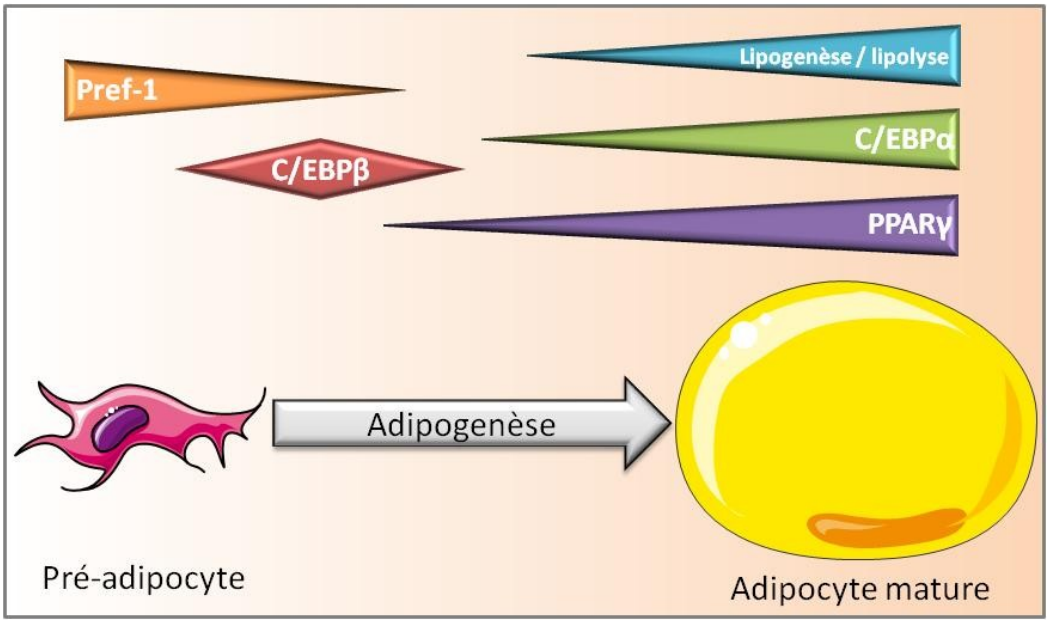

Figure 5: L'adipogenèse du pré-adipocyte à l'adipocyte mature

C/EBP: CCAAT/Enhancer Binding Proteins, Pref-1: preadipocyte factor 1, PPARγ: peroxisome proliferator activated receptor.

1.2.2) La fraction stroma-vasculaire

1.2.2.1) Les progéniteurs adipocytaires et les cellules endothéliales

La fraction stroma-vasculaire comprend des cellules dîtes non leucocytaires, n'exprimant pas le marqueur de surface CD45 (figure 6). Ces cellules sont différenciées sur la base de deux marqueurs membranaires CD34 et CD31. Chez la souris le marqueur Sca1 est utilisé en plus du CD34.

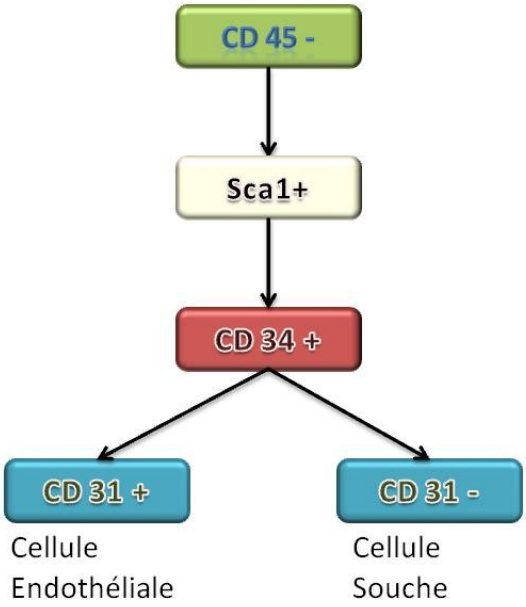

Figure 6: Marqueurs membranaires des cellules souches et endothéliales du TA murin

Les cellules CD34+/CD31- sont des cellules souches capables, en milieu adipogénique, de se différencier en adipocytes fonctionnels (Sengenes, Lolmede et al. 2005). Certaines de ces cellules appelées «*adipose stem cells*» sont assimilées à des CSM malgré quelques différences notamment sur la présence du marqueur CD34+ ou leur capacité de différenciation. Ces cellules peuvent se différencier *in vitro* en trois types cellulaires: ostéoblates, chondroblastes et adipocytes (Pittenger, Mackay et al. 1999). D'autres cellules communément appelées pré-adipocytes sont des cellules unipotentes et déjà engagées dans la voie de différenciation adipocytaire.

Les cellules CD34+/CD31+ sont des cellules endothéliales capillaires qui participent à la néovascularisation du TA et permettent ainsi son développement (Hausman and Richardson 2004). En effet, le pourcentage de cellules endothéliales capillaires,

caractérisées par la double expression CD34 et CD31, reste constant avec l'augmentation de l'IMC (Miranville, Heeschen et al. 2004). Grâce à de récents travaux, la dépendance du TA vis-à-vis de son réseau vasculaire, au cours de l'obésité, a été mise en évidence. Ces travaux ont montré que l'utilisation de facteurs anti-angiogéniques permet de limiter le développement de la masse grasse dans différents modèles de souris obèses (Rupnick, Panigrahy et al. 2002; Brakenhielm, Cao et al. 2004). Des études ont montré que le réseau vasculaire du TA est aussi important que celui du muscle squelettique et que chaque adipocyte présente des contacts étroits avec au moins un capillaire sanguin (Gersh and Still 1945; Hausberger and Widelitz 1963). L'endothélium joue également un rôle clé dans le contrôle de la lipogenèse adipocytaire *via* la LPL mais aussi un rôle direct dans les phénomènes de trafic cellulaire.

1.2.2.2) Les cellules immunes

La fraction stroma-vasculaire comprend une population d'origine hématopoïétique dite leucocytaire. Ces cellules présentent toutes le marqueur membranaire pan-leucocytaire CD45 (figure 7). Le marqueur CD3 permet ensuite de discriminer les lymphocytes des macrophages et cellules dendritiques.

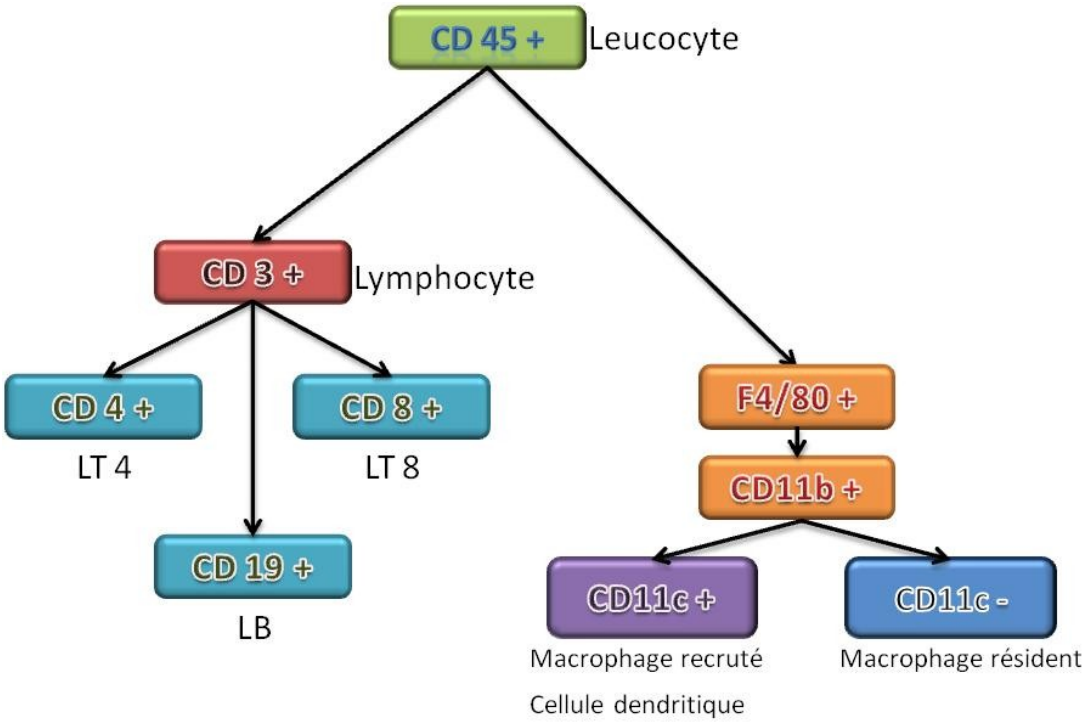

Figure 7: Marqueurs membranaires des cellules immunes du TA murin

Les lymphocytes

En termes de structure et de fonction, on distingue deux grandes lignées lymphocytaires différentes : les lymphocytes T qui sont soit CD4+ soit CD8+ et les lymphocytes B qui sont CD19+. Les lymphocytes T auxiliaires (CD4) sont des intermédiaires de la réponse immunitaire, qui prolifèrent après contact avec une cellule présentatrice d'antigènes. Les cellules CD4 «aident» à la réalisation d'autres fonctions lymphocytaires. Ces cellules CD4 stimulent la prolifération clonale et la différenciation des lymphocytes CD8 en lymphocytes cytotoxiques et des lymphocytes B en plasmocytes. Les lymphocytes T cytotoxiques (CD8) détruisent les cellules infectées exprimant l'antigène spécifique qu'ils reconnaissent. Les lymphocytes B sont des lymphocytes qui jouent un grand rôle dans l'immunité humorale, par opposition à l'immunité cellulaire induite par les lymphocytes T. Une fois activés *via* la présentation d'un antigène par une autre cellule immunitaire, les lymphocytes B se transforment en plasmocytes, cellules capables de produire en masse des anticorps dirigés contre l'antigène présenté (Fagarasan and Honjo 2000).

Il existe également des lymphocytes NK pour «natural killer» qui ne sont ni T (CD3-), ni B (CD19-). Ces cellules de l'immunité innée sont capables de lyser des cellules étrangènes à l'organisme de manière antigène indépendantte. Il existe sur la membrane cellulaire des NK des récepteurs activateurs (portant des séquences «ITAM»: immunoreceptor tyrosine-based activation motif) ou inhibiteurs (portant des séquences « ITIM » : immunoreceptor tyrosine-based inhibition motif). Lorsqu'un NK rencontre une autre cellule, la lyse de cette cellule ne se produira que si les signaux d'activation surpassent les signaux d'inhibition. Enfin il existe des lymphocytes NKT, pour «natural killer T», qui sont un groupe hétérogène de lymphocyte T. Ils possèdent des marqueurs de lymphocytes T et de lymphocytes NK. La plupart de ces cellules reconnaissent la molécule non-polymorphique CD1d, une molécule analogue aux protéines du complexe majeur d'histocompatibilité de classe un, qui est une molécule présentatrice des antigènes lipidiques et glycolipidiques. Lors de leur activation, les NKT sont capables de produire de grandes quantités d'interféron gamma, d'interleukine 4 (IL-4), et de «*Granulocyte macrophage colony-stimulating factor»* (GM-CSF), ainsi que de nombreuses cytokines et chimiokines.

Kintscher et al. ont mis en évidence la présence de lymphocytes au sein du TA de sujets diabétiques, la quantité de lymphocytes étant corrélée avec le tour de taille des

patients. De plus, des souris soumises à un régime enrichi en graisse présentent une forte infiltration de lymphocytes T dans le TA viscéral (Kintscher, Hartge et al. 2008). Cependant, l'étude des souris ($rag^{-/-}$) obèses et déficientes en lymphocytes (Duffaut, Zakaroff-Girard et al. 2009) a montré que cette absence ne suffisait pas à normaliser les paramètres métaboliques comme cela avait été montré avec les macrophages. En effet la déplétion en cellules immunes CD11c+ à l'aide d'une manipulation d'irradiation/reconstitution de moelle osseuse , dans des souris obèses, a permis de diminuer les macrophages du tissu adipeux et de normaliser les paramètres métaboliques (Patsouris, Li et al. 2008). Cependant des études récentes ont montré un rôle potentiel des cellules LT CD8+, dont l'infiltration précoce au cours de l'obésité pourrait être à l'origine du recrutement des macrophages (Lumeng, Maillard et al. 2009; Nishimura, Manabe et al. 2009).

Les macrophages

Les macrophages sont des cellules issues de la lignée myéloïde. Ils expriment le F4/80 chez la souris ou le CD14 chez l'Homme comme marqueurs membranaires. La stimulation des précurseurs macrophagiques par des facteurs tels M-CSF ou GM-CSF (*Macrophage colony-stimulating factor / Granulocyte macrophage colony-stimulating factor*) va permettre leur différenciation en monocytes. Les monocytes quittent la moelle osseuse sous l'action de facteurs chimioattractants et deviennent circulants. Ils vont pouvoir ensuite infiltrer les tissus en réponse à des stimuli inflammatoires en adhérant à l'endothélium vasculaire. Les monocytes migrent dans les tissus par diapédèse puis se différencient en macrophages (Curat, Miranville et al. 2004). Il existe deux types de macrophages dans les tissus, les macrophages résidents du tissu et les macrophages recrutés sur un site d'inflammation sous l'effet de cytokines. Les monocytes et les macrophages sont des cellules capables de phagocytose. Leur rôle est de phagocyter les débris cellulaires et les pathogènes. Ils participent en cela à l'immunité innée en tant que défense non-spécifique. Le rôle des macrophages dans le TA sera évoqué plus tard dans la partie «Inflammation du tissu adipeux».

Les cellules dendritiques

Les cellules dendritiques, dont le précurseur est commun avec le macrophage, sont des cellules présentatrices d'antigène, ces cellules sont capables de présenter des antigènes aux autres cellules immunes notamment les lymphocytes T naïfs (Wu and Liu 2007). Le marqueur CD11c est un marqueur spécifique des cellules dendritiques chez

la souris (Nguyen, Favelyukis et al. 2007), cependant ce marqueur est également utilisé pour identifier les macrophages recrutés dans le tissu (Lumeng, Bodzin et al. 2007). Les cellules F4/80+/CD11c+ infiltrant le tissu adipeux au cours de l'obésité sont donc majoritairement des macrophages mais une petite fraction sont des cellules dendritiques (Stefanovic-Racic, Yang et al. 2012). Les cellules dendritiques ont un rôle d'activation des lymphocytes T mais ils peuvent également induire le recrutement et l'activation des macrophages dans les tissus (Banchereau and Steinman 1998; Heymann, Meyer-Schwesinger et al. 2009; Stefanovic-Racic, Yang et al. 2012). Une étude récente a montré la présence dans le tissu adipeux de la souris obèse, mais également chez l'Homme obèse, de cellules dendritiques dites proinflammatoires ayant un rôle prépondérant dans l'orientation des cellules LT4 (Bertola, Ciucci et al. 2012).

Les mastocytes

Le mastocyte est une cellule granuleuse présente essentiellement dans les tissus conjonctifs, qui se caractérise par la présence dans son cytoplasme de très nombreuses granulations contenant des médiateurs chimiques comme la sérotonine, l'histamine, la tryptase ou l'héparine. Chez les rongeurs, comme chez l'Homme, les mastocytes dérivent des cellules souches hématopoïétiques présentes dans la moelle osseuse. Chez l'Homme, ces cellules souches donnent naissance à des progéniteurs mastocytaires de phénotype CD34+, KIT+ (le récepteur au «*Stem Cell Factor*» ou SCF), et CD13+. Ces progéniteurs passent dans le sang et colonisent les tissus où ils terminent leur différenciation en mastocytes, toujours sous l'effet de cytokines libérées localement, essentiellement encore le SCF, mais aussi l'Interleukine-4 ou l'Interféron-gamma (Metcalfe, Baram et al. 1997). Chez l'obèse, le nombre de mastocytes augmente dans le tissu adipeux viscéral, ces mastocytes sont, dans ce cas là, des sécréteurs de TNF-α (*Tumor Necrosis Factor alpha*) (Altintas, Azad et al. 2011). Cette augmentation des mastocytes dans le tissu adipeux viscéral de la souris obèse suggère un rôle de ces cellules immunes dans la pathogénicité de l'obésité et la mise en place de l'insulinorésistance. En effet la déplétion ou l'inactivation des mastocytes améliore le profil métabolique de souris placées en régime gras (Liu, Divoux et al. 2009; Divoux, Moutel et al. 2012; Shi and Shi 2012).

1.3) Le tissu adipeux blanc: un organe sécrétoire

Pendant longtemps, le tissu adipeux n'a été considéré que comme un tissu de «stockage» emmagasinant les lipides en période d'abondance et les relargant lors de périodes de jeûne. Or le tissu adipeux sécrète diverses protéines dotées de propriétés régulatrices appelées adipokines. Certaines de ces protéines (leptine, adiponectine…) agissent à distance, par voie endocrine, sur leurs tissus-cibles, et d'autres agissent localement par voie autocrine ou paracrine (TNF-α, facteurs angiogéniques et mitogéniques…) (figure 8). Toute hausse ou baisse, de la masse grasse s'accompagne inévitablement d'une modification de production de ces protéines. Le profil sécrétoire du TA varie donc au cours de l'obésité et du statut d'insulinosensibilité.

Ce terme d'adipokine est utilisé pour décrire des protéines ou des lipides qui sont synthétisés et sécrétés par le tissu adipeux dans son ensemble. Parmi le nombre considérable de sécrétions du TA, la part revenant aux sécrétions de l'adipocyte semble faible. En effet, une étude a pu identifier 80 protéines sécrétées par l'adipocyte isolé de rat (Chen, Cushman et al. 2005). Différentes études montrent en effet que la SVF, plus particulièrement les macrophages qui sont en nombre important dans le TA des sujets obèses, est responsable de la majorité des sécrétions du TA (Fain, Madan et al. 2004; Fain 2006).

Nous avons choisi de présenter quelques unes des adipokines qui interviennent dans les pathologies de l'insulinorésistance et dans les complications cardiovasculaires associées à l'obésité : l'adiponectine, la leptine, le facteur de nécrose tumorale α (TNF-α), le chimioattractant des macrophages (MCP-1) (*Monocyte Chimioattractant Protein 1*) et l'Interleukine-6 (IL-6).

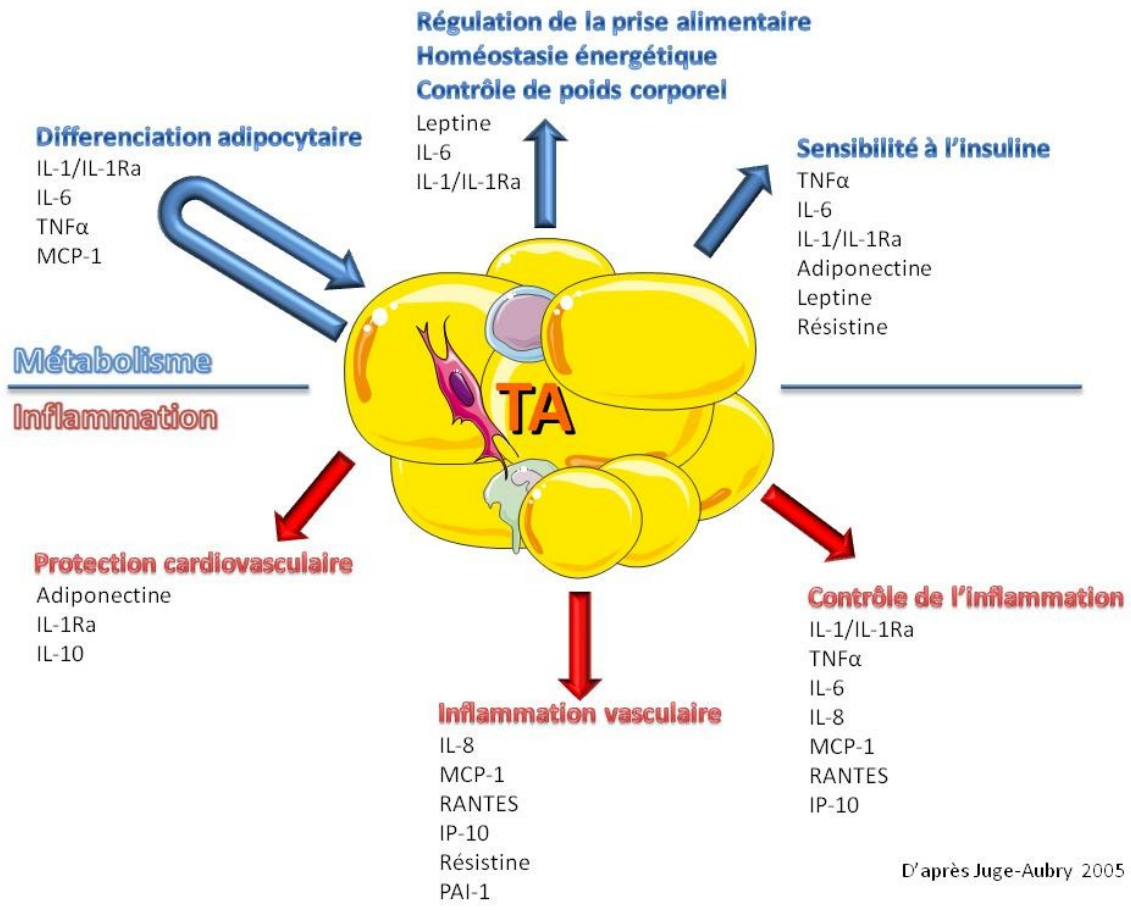

Figure 8: Le tissu adipeux, un organe sécrétoire

IL: interleukine; IP10: interferon gamma-induced protein 10; MCP1: monocyte chemioattractant protein 1; RANTES: regulated on activation, normal T cell expressed and secreted; PAI-1: plasminogen activator inhibitor-1; TNFα: tumor necrosis factor alpha.

1.3.1) Les adipokines à fonction métabolique

Chez l'Homme deux protéines sont bien connues pour être principalement sécrétées par l'adipocyte: l'adiponectine et la leptine (Fain, Madan et al. 2004).

La leptine est une hormone codée par le gène ob (*obese*) et sécrétée par l'adipocyte. Elle agit principalement au niveau de l'hypothalamus après s'être liée à son récepteur (ob-Rb). La leptine module ensuite l'expression de neuropeptides hypothalamiques: en augmentant la production de peptides cataboliques et en diminuant celle de peptides anaboliques et orexigènes (Schwartz, Seeley et al. 1996). Elle exerce ainsi ses principaux effets centraux d'induction de satiété et d'adaptation neuroendocrinienne au jeûne. La concentration plasmatique de leptine est directement proportionnelle à la masse grasse ce qui fait d'elle un indicateur d'adiposité (Frederich, Hamann et al.

1995). En réponse à l'augmentation des réserves adipeuses, elle va provoquer la diminution de la prise alimentaire et exercer ainsi un rétrocontrôle négatif sur la prise de masse grasse. Il existe chez certain obèse une mise en place d'une résistance à la leptine, en effet les taux plasmatiques de leptine augmentent mais il n'y a pas en réponse de baisse de la prise alimentaire (Munzberg, Bjornholm et al. 2005).

Comme la leptine, l'adiponectine est une protéine essentiellement sécrétée par les adipocytes (Scherer, Williams et al. 1995). Contrairement aux autres adipokines elle voit sa concentration plasmatique diminuer chez le sujet obèse et/ou diabétique. L'adiponectine agit sur ses principaux tissus cibles (muscles, foie…) après s'être liée à des récepteurs spécifiques AdipoR1 et AdipoR2 appartenant à la famille des récepteurs à sept domaines transmembranaires: AdipoR1 dans le muscle et AdipoR2 dans le foie (Yamauchi, Kamon et al. 2003). Les voies de signalisation mises en jeu après fixation de l'adiponectine sur ses récepteurs impliquent l'AMPK (kinase activée par l'AMP), enzyme connue pour favoriser le métabolisme glucidique. L'adiponectine présente donc des propriétés antidiabétiques. De plus, très étudiée chez le rongeur, elle stimule la thermogenèse, l'oxydation des acides gras (Tomas, Tsao et al. 2002) et exerce des effets hypolipémiants.

1.3.2) Les adipokines à fonction inflammatoire

Classiquement sécrétées par les cellules immunes, les adipocytes matures sont également capables de produire des cytokines et chimiokines comme le TNF-α, MCP-1 ou l'IL-6.

1.3.2.1) Le TNF-α

Découvert en 1975, le TNF-α a été décrit comme une substance d'origine macrophagique capable de provoquer la nécrose hémorragique de tumeurs solides. Le TNF-α est une cytokine aux actions multiples (Chu 2013). Facteur de nécrose tumorale, à l'origine de lésions tissulaires ou des effets hémodynamiques du choc septique, inducteur d'apoptose, il agit principalement sur les mécanismes de l'immunité et de l'inflammation. Les monocytes et macrophages sont les principales cellules productrices de TNF-α. Les facteurs induisant la synthèse de TNF-α sont principalement d'origine infectieuse, le lipopolysaccharide (LPS) en étant le facteur principal. Le premier lien entre TNF-α et obésité a été démontré chez des souris obèses et diabétiques génétiquement modifiées par invalidation du gène codant pour le récepteur à la leptine

ou souris db/db. En effet leur tissu adipeux épididymaire sécrète du TNF-α à un niveau significativement très élevé (Hotamisligil, Shargill et al. 1993). Le TNF-α pourrait également avoir un rôle dans le développement de l'insulinorésistance. En effet celui-ci augmenterait la phosphorylation inhibitrice d'IRS1 (*Insulin Receptor Subtrate 1*), le principal substrat du récepteur à l'insuline (Hotamisligil, Peraldi et al. 1996) et diminuerait la sensibilité à l'insuline. De plus, il modulerait l'expression de GLUT4, transporteur insulinodépendant du glucose, dans le tissu adipeux et dans le muscle (Stephens and Pekala 1991; Moller 2000). Le TNF-α possède également un effet lipolytique en induisant une augmentation des taux intracellulaires d'AMPc et une phosphorylation activatrice de la LHS (Grunfeld and Feingold 1991; Spiegelman and Hotamisligil 1993; Zhang, Halbleib et al. 2002).

1.3.2.2) MCP-1

MCP-1 est une protéine chimioattractante (chimiokine) qui permet le recrutement des précurseurs macrophagiques, les monocytes. En effet chez la souris une perfusion de MCP-1 augmente le nombre de monocytes sanguins (Takahashi, Mizuarai et al. 2003). L'expression basale de la cytokine MCP-1 est en général très faible. Cependant son expression peut être induite par différents stimuli tels que l'IL-1 (Interleukine 1), le TNF-α ou le LPS. En effet MCP-1 a été détecté dans des processus inflammatoires associés à une infiltration de cellules mononuclées telle que lors de l'athérosclérose (Ross 1999). Dans les situations d'obésité, le tissu adipeux, et essentiellement ses macrophages, est un producteur de MCP-1. Par exemple, il a été montré une production de MCP-1 par le tissu adipeux épicardiaque parallèlement à une augmentation de l'infiltration de cellules inflammatoires (Mazurek, Zhang et al. 2003). Le taux circulant de MCP-1, très élevé, chez l'obèse diminue avec la perte de poids (Christiansen, Richelsen et al. 2005). Ceci renforce l'hypothèse que les macrophages présents dans le tissu adipeux contribuent de manière importante à la production locale de cytokines, tout ceci montrant un rôle clé de MCP-1 dans l'initiation de l'inflammation du TA au cours de l'obésité (Weisberg, Hunter et al. 2006).

1.3.2.3) L'interleukine 6 (IL-6)

L'IL-6 est produit par un grand nombre de cellules notamment les cellules endothéliales ou encore les macrophages (Akira, Taga et al. 1993). L'IL-6 est également produite par le TA, mais il semble cependant que sa production soit majoritairement dépendante des cellules de la SVF (Fried, Bunkin et al. 1998). Les taux plasmatiques d'IL-6 sont

étroitement corrélés avec l'IMC et inversement reliés à la sensibilité à l'insuline (Bastard, Jardel et al. 2000). Des études *in vitro* sur hépatocytes ont montré que l'IL-6 inhibe l'autophosphorylation du récepteur à l'insuline et diminuerait donc la sensibilité à l'insuline (Senn, Klover et al. 2002). Cependant l'invalidation génique de l'IL-6 chez la souris donne un phénotype obèse associé à une intolérance au glucose (Wallenius, Wallenius et al. 2002). L'IL-6 pourrait donc avoir différents effets au niveau central ou périphérique pour moduler la prise de poids et/ou la sensibilité à l'insuline.

II Inflammation du tissu adipeux associée à l'obésité

2.1) Inflammation de «bas bruit» du tissu adipeux et obésité

2.1.1) Rôle des adipokines

Peu à peu s'est dégagée l'évidence que la cellule adipeuse peut partager avec les cellules du système immunitaire un certain nombre de propriétés, telles que la production de cytokines pro-inflammatoires. Avec l'obésité, le tissu adipeux va être à l'origine d'une production anormale d'adipokines et de cytokines inflammatoires (Hotamisligil, Shargill et al. 1993; Samad, Yamamoto et al. 1997; Fried, Bunkin et al. 1998). Ceci conduit chez l'obèse à une élévation des concentrations plasmatiques de marqueurs de l'inflammation (la protéine C réactive, le TNF-α et l'IL-6) (Ford 2003; Das 2004). L'obésité est donc associée à une situation inflammatoire chronique dite de «bas bruit» (Wellen and Hotamisligil 2003; Clement, Viguerie et al. 2004). Il paraît évident que l'adipocyte puisse jouer un rôle central dans les altérations métaboliques mais il semble assez peu probable qu'il soit entièrement responsable du phénomène inflammatoire.

2.1.2) Infiltration macrophagique du tissu adipeux

La présence de macrophages dans le TA a été mise en évidence dans les années 60 par des histologistes. Depuis peu, la communauté scientifique s'intéresse de près à leur rôle potentiel dans la mise en place de l'état d'inflammation du TA durant l'obésité. En effet l'obésité chez le rongeur s'accompagne d'une augmentation du nombre de macrophages (Weisberg, McCann et al. 2003; Xu, Barnes et al. 2003). Cette augmentation a été confirmée chez l'Homme par cytométrie en flux et immunohistochimie (Curat, Wegner et al. 2006). Chez l'obèse, plusieurs équipes ont observé que les macrophages du TA pouvaient être jusqu'à six fois plus nombreux que chez un «patient normo-pondéré» (Cancello, Henegar et al. 2005; Cousin, Caspar-Bauguil et al. 2006). Le contenu tissulaire en cette population est d'ailleurs corrélé positivement avec la masse grasse et diminue lors d'une perte de poids (Clement, Viguerie et al. 2004; Cancello, Henegar et al. 2005). Au cours de l'obésité de nombreux

chimio-attractants sécrétés par le TA comme MCP-1 sont augmentés (Kanda, Tateya et al. 2006). Ceci induit l'entrée des monocytes circulants dans le TA et pourrait expliquer ainsi l'augmentation du nombre de macrophages. (Weisberg, McCann et al. 2003).

2.1.3) Activation des macrophages

L'inflammation consécutive à des lésions tissulaires se traduit par l'activation et la polarisation des macrophages résidents. Ceci conduit à l'augmentation de la production de cytokines et d'autres médiateurs de l'inflammation, et au recrutement de monocytes sanguins. Dans le contexte de la réponse immunitaire adaptative, l'environnement cytokinique produit par les lymphocytes T a pour conséquence l'activation des macrophages. L'activation des macrophages a d'abord été définie par les états de polarisation M1 et M2 reflétant la nomenclature Th1/Th2 des lymphocytes (Olefsky and Glass 2010). La polarisation M1 dite «classique» induite par des cytokines Th1 (Interferon gamma ou IFNγ, TNF-α) conférait aux macrophages un profil pro-inflammatoire dû au type de cytokines sécrétées (TNF-α, IL6…). En revanche, la polarisation M2 induite par des cytokines Th2 (IL-4, IL-13) conférait aux macrophages un profil d'activation dite «alternative» ou anti-inflammatoire (exemple de cytokine sécrétée en retour: l'IL-10) (figure 9).

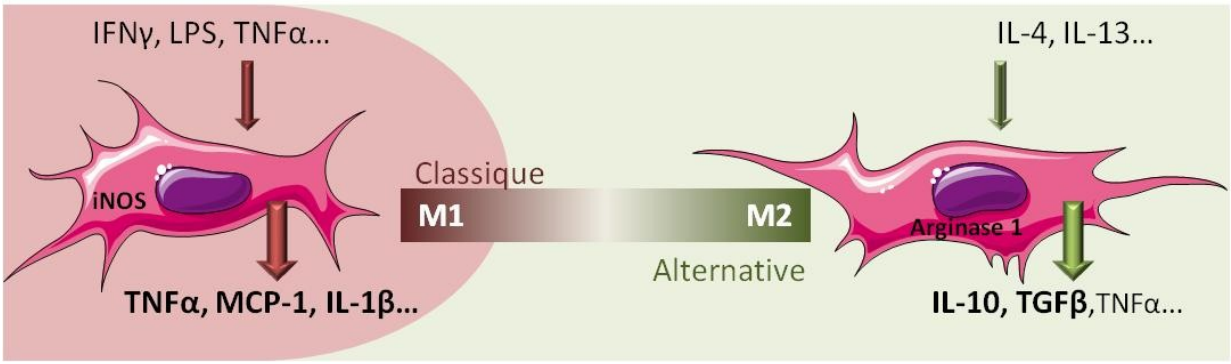

Figure 9: Classification M1/M2 des macrophages

IL: interleukine; IFNγ: interferon gamma; LPS: lipopolysaccharide; MCP1: monocyte chemioattractant protein 1; TGFB: transforming growth factor beta; TNFα: tumor necrosis factor alpha.

D'autres états d'activation basés sur la présence de récepteurs membranaires ont permis de nuancer cette catégorisation chez la souris. Ces études sont fondées sur l'existence de deux marqueurs membranaires: CD11c et CD206 (Shaul, Bennett et al. 2010). Les macrophages pouvaient alors être doublement positifs (CD11c+/CD206+ (M1/M2 ou type 1b)) et présentaient donc un phénotype mixte (Shaul, Bennett et al.

2010). D'autres étaient simple positifs (CD11c+/CD206- ou CD11-/CD206+ soit type 1a et type 2) soient les M1 et M2 classiquement connus. Enfin certains semblaient être double négatifs (CD11c-/CD206- ou type 3). Cette population de macrophages doublement négatives a été trouvée dans le tissu adipeux murin, ces macrophages semblent présentés un phénotype de «réparateurs tissulaires».(Zeyda, Gollinger et al. 2010).

Différents types de nomenclature ont depuis quelques années été proposés en tenant compte par exemple des signaux inducteurs (Mantovani, Sica et al. 2004) ou de la fonction du macrophage (Mosser and Edwards 2008). A ce jour, il n'y a pas encore de consensus sur la classification des macrophages. Cependant il est important de garder à l'esprit qu'il existe un large spectre d'activation des macrophages entre les M1 et M2 (figure 10) (Mosser and Edwards 2008). Ces macrophages ont alors un éventail de récepteurs et de fonctions conditionnés par leur microenvironnement.

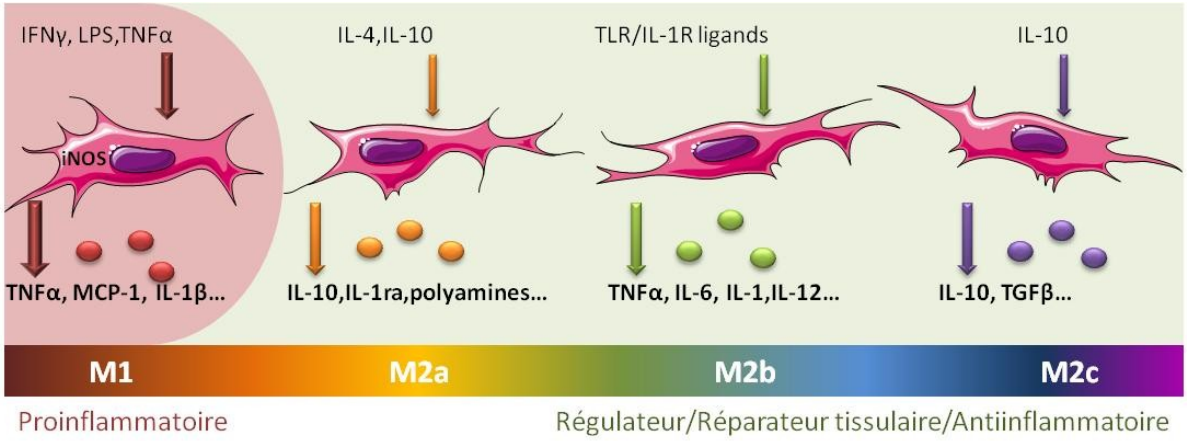

Figure 10: Classification des macrophages selon leur fonction

IL: interleukine; IFNγ: interferon gamma; LPS: lipopolysaccharide; MCP1: monocyte chemioattractant protein 1; TGFB: transforming growth factor beta; TLR: Toll-like receptor; TNFα: tumor necrosis factor alpha.

Il existe des différences entre les marqueurs macrophagiques utilisés selon si l'on se trouve chez l'Homme ou chez la souris. Classiquement le marqueur CD14 est utilisé chez l'Homme pour identifier les macrophages alors que chez la souris on utilise le marqueur F4/80. Chez la souris, l'activation alternative en macrophage M2 induit l'expression de l'arginase-1 (Lumeng, Bodzin et al. 2007) alors que celle-ci est très peu exprimée dans les macrophages chez l'Homme (Raes, Van den Bergh et al. 2005; Bourlier, Zakaroff-Girard et al. 2008). Le CD11c est également utilisé chez la souris

pour visualiser les macrophages recrutés alors que ce marqueur est peu ou pas exprimé chez l'Homme (Zeyda, Farmer et al. 2007).

Chez la souris, un régime riche en gras provoque le recrutement de macrophages M1 (Lumeng, Bodzin et al. 2007). Une étude cinétique sous régime gras suggère tout d'abord une accumulation de macrophages de type M1 jusqu'à 16 semaines de régime puis leur diminution au profit de macrophages de type M2. Cependant un point reste à éclaircir s'agit il d'un recrutement ou d'une repolarisation des macrophages M1 dans le tissu (Strissel, Stancheva et al. 2007). La présence de macrophages au phénotype intermédiaire M1/M2, dans le tissu adipeux de souris en régime gras, appuie la thèse de la repolarisation (Shaul, Bennett et al. 2010). Dans le tissu adipeux humain, les macrophages sont essentiellement de phénotype mixte intermédiaire entre les états de polarisation M1 et M2 (Zeyda, Farmer et al. 2007; Bourlier, Zakaroff-Girard et al. 2008). Cependant dans une population de sujets massivement obèses il a été montré une forte augmentation du ratio M1 sur M2 dû à l'infiltration de macrophages M1, ratio qui diminue en cas de perte de poids (Aron-Wisnewsky, Tordjman et al. 2009).

2.1.4) Communication Adipocyte/Macrophage

Les macrophages du TA montrent une grande hétérogénéité en terme d'état d'activation (Gordon and Taylor 2005), reflétant la complexité des événements se déroulant au cours de l'obésité. Chez la personne mince, les macrophages ont un phénotype M2 «anti-inflammatoire» (Lumeng, Bodzin et al. 2007). Les différents facteurs sécrétés par ces macrophages M2 aident à maintenir un environnement normal préservant la fonction adipocytaire. A l'inverse le nombre et l'activité des macrophages M1 augmente chez l'obèse (Olefsky and Glass 2010), l'obésité est donc caractérisée par une forte infiltration de macrophages proinflammatoires. Ces macrophages M1 expriment des facteurs tels que le TNF-α (Lumeng, Deyoung et al. 2007). Il existe donc une balance fine dans la polarisation des macrophages du tissu adipeux en fonction de l'environnement des adipocytes.

Des études de coculture adipocytes/macrophages ont montré l'existence d'une boucle paracrine impliquant les AG ainsi que le TNF-α. Ces AG provenant des adipocytes et le TNF-α des macrophages formeraient ainsi un cercle vicieux augmentant l'expression de cytokines pro-inflammtoires et la diminution de l'adiponectine (Suganami, Nishida et al. 2005). En effet le TNF-α macrophagique agit sur l'adipocyte en induisant l'expression

de cytokines pro-inflammtoires et en stimulant la lipolyse, de son côté l'adipocyte fournit des AG, ligands du TLR4 (*Toll-Like Receptor 4*) et activateurs de la voie NF-kB *(Nuclear Factor Kappa B*) du macrophage (Shi, Kokoeva et al. 2006). Il existerait donc une communication étroite entre l'adipocyte et le macrophage, ce lien pourrait être à l'origine de l'inflammation chronique observée durant l'obésité (Suganami and Ogawa 2010).

Cependant une étude récente du laboratoire montre, dans un modèle *in vitro* de milieux conditionnés, l'incapacité des acides gras issus de la lipolyse à activer des macrophages *via* leur récepteur TLR4. Ces résultats ont été confirmés *in vivo* dans un modèle murin. En effet l'inhibition chronique de la lipolyse, à l'aide d'un inhibiteur de la LHS, diminuant ainsi les acides gras circulants, n'a pas eu d'effet sur les marqueurs de l'inflammation. Le sujet reste donc encore largement débattu.

2.2) Le rôle du TLR4 dans l'inflammation du TA

2.2.1) Implication du TLR4

En plus des cellules immunes, les pré-adipocytes ainsi que les adipocytes matures *in vitro* ou *in vivo* expriment le TLR4 (Bes-Houtmann, Roche et al. 2007; Poulain-Godefroy and Froguel 2007). Les pré-adipocytes réagissent à la stimulation du TLR4 par le LPS entraînant ainsi la sécrétion de médiateurs pro-inflammatoires comme l'IL-6, le TNF-α et le MCP-1 (Kopp, Buechler et al. 2009). De plus, le maintien d'un état inflammatoire par une stimulation chronique au LPS inhibe la différenciation adipocytaire ainsi que l'expression des marqueurs adipogèniques, entraînant une accumulation de pré-adipocytes (Chung, Lapoint et al. 2006; Poulain-Godefroy and Froguel 2007).

De nombreuses évidences *in vitro et in vivo* montrent le rôle majeur du TLR4 dans l'inflammation du tissu adipeux. En effet, des souris invalidées pour le TLR4 ou possédant une mutation rendant le TLR4 non fonctionnel ne présentent pas, au cours d'un régime riche en graisse, d'augmentation d'infiltration macrophagique. Par ailleurs ces souris ne présentent ni inflammation dans le tissu adipeux, ni désordres métaboliques associés (Shi, Kokoeva et al. 2006; Poggi, Bastelica et al. 2007; Suganami, Mieda et al. 2007). Une délétion spécifique du TLR4 dans les cellules d'origine hématopoïétique confère la même protection vis-à-vis de l'inflammation et des désordres métaboliques montrant un rôle essentiel du TLR4 immun dans ces processus

(Saberi, Woods et al. 2009). Ces résultats prouvent un rôle important de ce récepteur dans la signalisation précoce de l'inflammation du TA.

2.2.2) Signalisation du TLR4

2.2.2.1) Signalisation du TLR4 Myd88 dépendante

Le TLR4 est le principal récepteur de l'endotoxine bactérienne appelée LPS. Ce composant des parois bactériennes gram négatives contient une partie lipidique A qui est reconnue par le TLR4. Au niveau systémique le LPS est d'abord reconnu par la protéine d'origine hépatocytaire LBP (*LPS Binding Protein*) (Chaby 2004). Le complexe LBP/LPS se lie de manière stable au co-récepteur du TLR4 le CD14 puis le tout s'associe au complexe TLR4/MD-2 (Kornbluth, Oh et al. 1989). La liaison du LPS au TLR4 induit le recrutement de la protéine Myd88 (*Myeloid differentiation 88*) sur la partie TIR (*Toll/Interleukine 1 Receptor*) du domaine intracellulaire du TLR4 (Kawai and Akira 2005). Myd88 possédant également un domaine TIR (Burns, Martinon et al. 1998), l'association TIR-TIR induit le recrutement de la protéine IRAK4 (*IL-1 receptor associated kinase*). Cette protéine phosphoryle IRAK1 ce qui lui permet de s'associer à TRAF6 (*TNF receptor activating factor*). Le duo IRAK1/TRAF6 permet de libérer NF-kB d'IkB (*inhibitor kappa B*) qui le séquestre dans le cytoplasme. Une fois NF-kB libéré de son inhibiteur, ce facteur de transcription est transloqué dans le noyau de la cellule afin d'induire la synthèse de cytokines (figure 11).

2.2.2.2) Signalisation du TLR4 Myd88 indépendante

Le TLR4 présente également une voie de signalisation indépendante de Myd88 (figure 11). La protéine TRIF (*TIR domain containing adaptator interferon beta*) possédant également un domaine TIR remplace Myd88. La protéine TRIF possède trois domaines de liaisons à TRAF6 et peut donc induire son recrutement directement (Akira and Takeda 2004). Celui-ci amène à l'activation de NF-kB de manière similaire à la voie Myd88 dépendante mais également à l'activation de la voie «interferon regulatory transcription factor 3» (IRF3) induisant la synthèse de différents interférons. La stimulation de la voie TLR4 Myd88 indépendante induit une réponse plus tardive que la voie Myd88 dépendante (Kawai, Adachi et al. 1999).

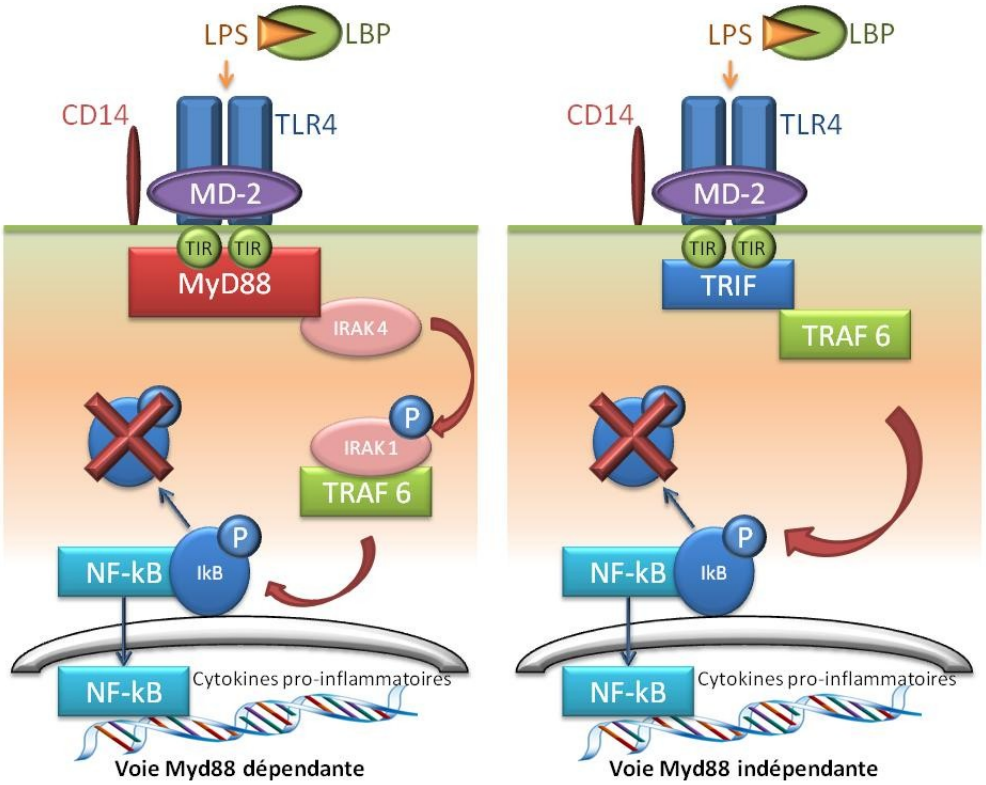

Figure 11: Voies de signalisation du TLR4

IkB: inhibitor kappa B; IRAK: IL-1 receptor associated kinase; LBP: LPS binding protein; LPS: lipopolysaccharide; MD2: Myeloid differentiation protein-2; MyD88: Myeloid differentiation 88; NF-kB: nuclear factor-kappa B; TIR: Toll/Interleukine 1 Receptor; TLR4: Toll-like receptor 4; TNFα: tumor necrosis factor alpha; TRAF: TNF receptor activating factor.

2.2.3) Stimulation du TLR4

2.2.3.1) Le LPS, principal ligand du TLR4

Un des facteurs qui pourrait être responsable de l'apparition et du maintien d'une inflammation *via* l'activation du TLR4 lors de la consommation d'un régime hyperlipidique est le LPS. Le LPS endogène est un facteur continuellement produit par le tractus intestinal. Il est transporté jusqu'aux organes cibles *via* les lipoprotéines, en particulier les chylomicrons synthétisés en période post-prandiale. Le LPS est par ailleurs un agent «inflammatogène», *via* sa partie lipidique A, qui entraîne la sécrétion de cytokines pro-inflammatoires quand il se lie au complexe CD14/TLR4 présent à la surface des cellules de l'immunité innée (Neal, Leaphart et al. 2006). De façon intéressante, il a été montré que la consommation de régimes hyperlipidiques pouvait moduler la composition du microbiote intestinal induisant une hausse de la concentration plasmatique en LPS à long terme. A plus court terme, l'ingestion d'un

repas riche en lipides induit également une augmentation du LPS plasmatique en postprandial (Erridge, Attina et al. 2007; Clemente-Postigo, Queipo-Ortuno et al. 2012). Tout ceci a pour conséquence l'apparition d'une endotoxémie métabolique chez l'obèse (Cani, Bibiloni et al. 2008).

2.2.3.2) Autres ligands ou coactivateurs endogènes du TLR4

Certaines études ont montré *in vitro* la capacité des AG à induire l'activation du TLR4, interaction pouvant expliquer l'inflammation du TA (Lee, Sohn et al. 2001; Kim 2006; Suganami, Tanimoto-Koyama et al. 2007). Une étude récente indique que la fétuine-a, protéine d'origine hépatique, pourrait être le lien entre AG et activation du TLR4. En effet elle agirait comme un adaptateur physique entre les deux (Heinrichsdorff and Olefsky 2012; Pal, Dasgupta et al. 2012). Ceci pourrait expliquer les résultats contradictoires obtenus dans certaines études *in vitro* où les AG, en absence de sérum, n'étaient pas capables d'activer le TLR4 (Erridge and Samani 2009; Schaeffler, Gross et al. 2009). D'après Erridge, il existe une vingtaine de molécules endogènes pouvant être ligands du TLR4 (Erridge 2010). Ces ligands peuvent être des protéines originaires de la MEC, être des protéines normalement intracellulaires ou encore des lipides .Par exemple la ténascine C, protéine de la matrice extracellulaire (MEC), a été montré *in vitro* et *in vivo* comme ligand direct du TLR4 (Midwood, Sacre et al. 2009; Erridge 2010). Cette protéine de la matrice extracellulaire est spécifiquement induite pendant une lésion ou une infection. *In vitro* l'activation du TLR4 par le LPS induit l'expression de cette protéine dans des cellules myéloïdes humaines (Goh, Piccinini et al. 2010). De manière très intéressante les animaux invalidés pour cette protéine montrent une moins bonne activation de la voie TLR4 par le LPS notamment dans les macrophages, ceux-ci produisant moins de TNF-α lors d'un traitement avec une forte dose de LPS. Cette étude montre un rôle important de cette protéine dans la genèse d'une réponse immune complète vis-à-vis du LPS (Piccinini and Midwood 2012). La ténascine C est donc également un coactivateur important du TLR4. La fibronectine possédant un domaine ED-A, transcrit alternatif de la fibronectine classique, largement impliquée dans le processus de fibrogenèse, est également un ligand du TLR4 (Okamura, Watari et al. 2001). D'autres protéines endogènes sont également connues pour potentialiser la liaison TLR4/LPS. Par exemple le lumican est capable de s'associer au CD14 co-récepteur du TLR4 à la surface des macrophages et favorise ainsi la réponse du TLR4 au LPS. (Wu, Vij et al. 2007; Lohr, Sardana et al. 2012).

III La matrice extracellulaire (MEC)

3.1) La matrice extracellulaire et ses constituants

3.1.1) Rôle de la matrice extracellulaire

La MEC est un réseau complexe de macromolécules entourant les cellules dans les tissus des mammifères. Cette matrice est composée de quatre familles de macromolécules (figure 12). Les collagènes et l'élastine forment une trame de protéines fibreuses qui lui confèrent respectivement ses propriétés de rigidité et d'élasticité. Les interstices de cette trame sont comblés par les protéoglycanes qui servent de renfort aux protéines fibreuses. Enfin, les glycoprotéines de structure assurent la cohésion entre cellules et matrice. La MEC n'est pas seulement un échafaudage dans lequel s'insèreraient les cellules, mais il s'agit aussi d'une structure active qui joue un grand rôle dans l'interaction cellule/cellule. Elle peut également, servir à stocker des protéines et des facteurs de croissance pour les libérer en cas de besoin (Taipale and Keski-Oja 1997) ou encore servir de guide aux cellules mobiles (Condeelis and Segall 2003).

3.1.2) Les protéines fibreuses

Le collagène est de loin la protéine la plus abondante chez les mammifères ; elle représente plus du quart des protéines du corps (Di Lullo, Sweeney et al. 2002). Mais en réalité, il ne faudrait pas parler du collagène, mais des collagènes. Il existe, en effet, toute une famille de molécules nommées collagènes, qui possèdent différentes structures moléculaires, différentes organisations macromoléculaires et différentes fonctions. On a découvert jusqu'à présent 23 types de collagènes, assemblés à partir de 41 chaînes α génétiquement distinctes (Ricard-Blum and Ruggiero 2005). Leur point commun est la présence d'un domaine en triple hélice qui leur donne un caractère inextensible et leur permet de résister à la traction. L'élastine, produite par les fibroblastes, est sécrétée dans l'espace extracellulaire notamment durant la croissance. La forte teneur en acides aminés hydrophobes confère à l'élastine ses propriétés élastiques.

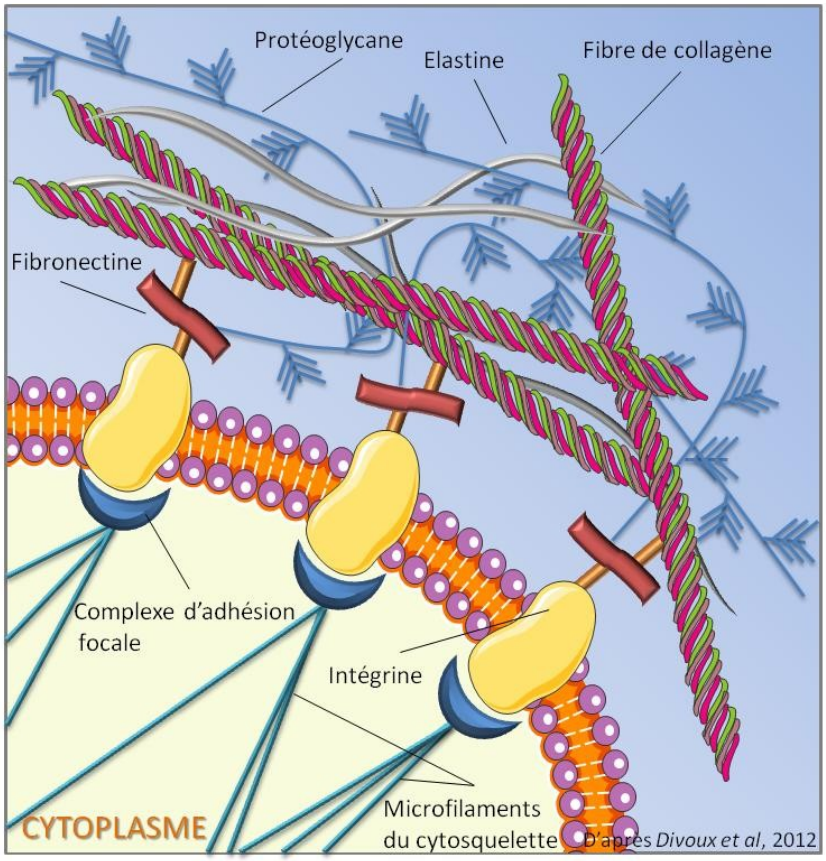

Figure 12: La MEC un réseau de macromolécules

3.1.3) Les protéoglycanes et glycoprotéines

Les glycosaminoglycanes se fixent de manière covalente avec des protéines porteuses, appelées «core-protéines», pour former des protéoglycanes. Ces protéoglycanes forment une sorte de gel où vont pouvoir se fixer les protéines fibreuses telles que les collagènes. Elles constituent également un réservoir de molécules comme les facteurs de croissance et les métalloprotéases matricielles (MMPs) (Christiaens and Lijnen 2006).

Les glycoprotéines (fibronectine ou la ténascine C) jouent un rôle important dans l'adhérence des cellules. Par exemple la fibronectine possède des domaines de fixation pour la fibrine, les collagènes et les intégrines. Ces glycoprotéines jouent un rôle de liaison entre la MEC et les cellules. Les changements de la MEC sont communiqués *via* ces intégrines aux cellules qui répondent en modifiant leur réseau microfilamentaire du cytosquelette.

3.2) Synthèse de la MEC: du fibroblaste au myofibroblaste

La matrice extracellulaire est extrêmement dynamique, se renouvelle souvent et alterne donc synthèse et dégradation. Les constituants de la MEC sont synthétisés et sécrétés par des cellules d'origine mésenchymateuse. Selon le tissu il s'agit des fibroblastes, des ostéoblastes ou des chondrocytes (Kerrigan, Mansell et al. 2000).

3.2.1) Le macrophage principal activateur du fibroblaste

Les macrophages M2, classiquement décrit comme anti-inflammatoires, semblent largement impliqués dans la réparation tissulaire et la fibrogenèse de nombreux tissus (Wynn 2004; Xiao, Hong et al. 2008). Ils antagonisent les effets des macrophages M1 et permettent de restaurer l'homéostasie du tissu après la réparation tissulaire (Sindrilaru, Peters et al. 2011). Des études récentes ont montré une conversion possible de certains macrophages M1 en M2 possédant alors un phénotype de «réparation tissulaire» (Arnold, Henry et al. 2007). Les macrophages M2 sont des producteurs de facteurs de croissance tels que le TGFβ (*Transforming Growth Factor Beta*) ou le PDGF (*Platelet-Derived Growth Factor*) (Barron and Wynn 2011). Ces facteurs de croissance sont largement impliqués dans la réparation tissulaire *via* leurs effets activateurs sur les fibroblastes (Shimokado, Raines et al. 1985; Roberts, Sporn et al. 1986; Sunderkotter, Steinbrink et al. 1994)

3.2.2) Les fibroblastes

Les fibroblastes sont les spécialistes de la production de MEC et sont grandement responsables de l'architecture de notre corps. On les retrouve en grande quantité dans tous les tissus et organes (Sartore, Chiavegato et al. 2001). Lors d'une lésion ils migrent, prolifèrent, produisent de la matrice afin de réparer le tissu. La réparation tissulaire d'une plaie ouverte a permis de comprendre les différentes étapes de l'activation des fibroblastes (Tomasek, Gabbiani et al. 2002). Le fibroblaste recruté sur un site de lésion produit de la fibronectine ED-A, une protéine plus longue que la fibronectine normalement produite, importante pour son activation et sa migration (Muro, Moretti et al. 2008). La migration des fibroblastes effectue une tension sur la matrice extracellulaire perçue par les autres fibroblastes. Ils réorganisent leurs

cytosquelettes le long de cette tension. Ils génèrent des fibres de stress intracellulaires et deviennent ainsi des proto-fibroblastes.

3.2.3) Les myofibroblastes

Le TGFβ produit initialement par les macrophages présents sur le site lésé puis de manière autocrine par le fibroblaste, induit la transformation de proto-fibroblastes en myofibroblastes exprimant l'actine musculaire αSMA caractéristique de ce type de fibroblaste (figure 13) (Desmouliere, Rubbia-Brandt et al. 1992). Cette production autocrine de TGFβ par les fibroblastes est un facteur important dans la préservation de l'activité fibrogénique du myofibroblaste même après le retrait du stimulus inflammatoire (Kim, Angel et al. 1990; Schmid, Itin et al. 1998). Il a également été démontré que l'administration d'IL-4 *in vitro* ou de GM-CSF *in vivo*, deux cytokines libérées par les cellules endommagées et les macrophages, sont en mesure d'induire la différenciation myofibroblastique chez les fibroblastes (Rubbia-Brandt, Sappino et al. 1991; Mattey, Dawes et al. 1997). Les microfilaments d'actine permettent de relier la membrane plasmique du myofibroblaste aux fibres extracellulaires de fibronectine *via* un complexe d'adhésion utilisant des intégrines transmembranaires (Singer, Kawka et al. 1984; Burridge and Chrzanowska-Wodnicka 1996). Grâce aux fibres d'actine, les myofibroblastes ont la capacité de générer une force contractile lors de la fermeture d'une plaie. De plus les myofibroblastes auraient pour mission de sécréter de la MEC en vue de la réparation tissulaire. En effet ces myofibroblastes, en plus d'exprimer fortement l'αSMA, expriment également certains collagènes notamment le collagène de type I. Dans le cas de la sclérose systémique (Ssc) caractérisée par une fibrose vasculaire généralisée, les myofibroblastes impliqués dans ce type de fibrose expriment fortement le collagène de types I et III (LeRoy 1974).

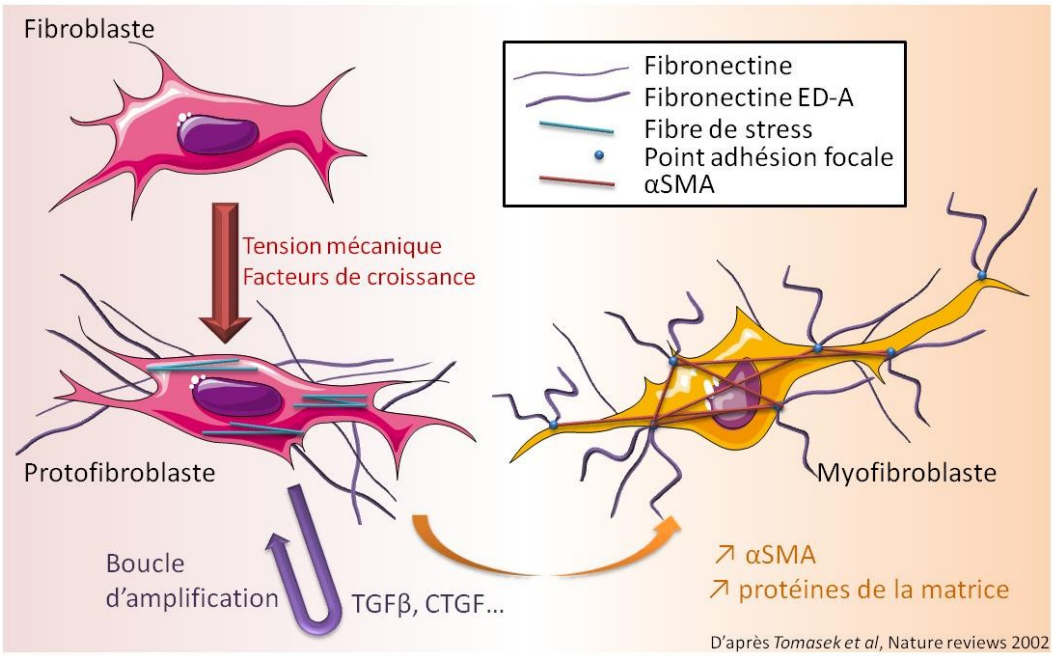

Figure 13: Activation du fibroblaste lors du remodelage de la MEC

αSMA: Alpha smooth muscle actin; CTGF: Connective tissue growth factor; TGFB: Tranforming growth factor.

3.3) Régulateurs de la matrice extracellulaire

3.3.1) Les métalloprotéases matricielles (MMPs) et leurs inhibiteurs (TIMPS)

La dégradation des collagènes, ou d'autres molécules de la MEC, est causée essentiellement par une famille d'enzymes : les métalloprotéases matricielles (Kerrigan, Mansell et al. 2000). Les MMPs sont des endopeptidases zinc-dépendantes synthétisées par les CSM, les fibroblastes mais également par un grand nombre de cellules d'origine hématopoïétique (Murphy and Willenbrock 1995). Les MMPs sont peu exprimées dans les cellules *in vivo* à l'état normal. En revanche, on en trouve des quantités importantes dans la MEC au cours des lésions, de l'inflammation ou des diffusions métastatiques de cellules cancéreuses, car elles sont induites en réponse à des cytokines, des facteurs de croissance ou à des hormones (l'IL-1β, le TNF- α, le PDGF…). A ce jour 24 MMPs ont été identifiées. Selon leur spécificité et leur substrat préférentiel, les MMPs peuvent être classées au moins en 5 groupes distincts: collagénases, gélatinases, stromélysines, métallo-élastases et MMPs membranaires.

Les MMPs sont inhibées spécifiquement par les TIMPs (Murphy and Willenbrock 1995). Tout comme les MMPs, les TIMPs peuvent provenir de différents types cellulaires

comme les fibroblastes ou les cellules endothéliales. Cette famille comprend 4 membres: TIMP1 à TIMP4. L'expression de TIMP1 et TIMP3 peut être induite par des cytokines alors que TIMP2 est constitutivement exprimée (Leco, Khokha et al. 1994; Wick, Burger et al. 1994; Sun, Hegamyer et al. 1995). TIMP1, 2 et 4 sont des protéines solubles sécrétées alors que TIMP3 est insoluble et est associé à la MEC (Leco, Khokha et al. 1994). La liaison de TIMP au niveau du site catalytique d'une MMP permet d'inhiber son activité (Willenbrock and Murphy 1994).

3.3.2) Relation cytokines/MMPs

Comme décrit auparavant, les cytokines peuvent augmenter l'expression des MMPs et donc favoriser l'obtention de MMPs actives. Cependant ces mêmes cytokines peuvent également être substrats de ces MMPs. Par exemple IL-1β peut être clivée et être inactivée par plusieurs MMPs (Ito, Mukaiyama et al. 1996). Il-1β étant un stimulant conduisant à la production de MMPs ceci pourrait être un rétrocontrôle négatif. Le même phénomène a été décrit pour le TNF-α (Gearing, Beckett et al. 1994). A l'inverse les MMPs peuvent activer certaines cytokines. Par exemple MMP2 est capable de cliver le TGFβ afin de le rendre actif (ten Dijke and Arthur 2007). Enfin la MEC étant un réservoir de protéines, sa dégradation régulée par les MMPs, induit la libération de facteurs de croissance. Par exemple le TGFβ normalement séquestré par la MEC peut être libéré sous l'action des MMPs (Imai, Hiramatsu et al. 1997).

3.3.3) Les facteurs jouant sur la synthèse de MEC

3.3.3.1) Le TGFβ

Le TGFβ sécrété notamment par les cellules immunes et les fibroblastes, joue un rôle pléiotrope dans l'organisme (Javelaud and Mauviel 2004). Il est en effet impliqué dans différents processus biologiques tel que le développement embryonnaire, la réparation tissulaire ou la croissance cellulaire (Bottner, Krieglstein et al. 2000; Govinden and Bhoola 2003). Cependant il est communément admis que le TGFβ est largement impliqué dans de nombreuses pathologies fibrosantes (Border and Noble 1994). *In vitro* il stimule la différenciation des fibroblastes en myofibroblastes (Hinz 2007), et induit un phénotype anti-apoptotique chez ces myofibroblastes (Zhang and Phan 1999). *In vivo* son administration induit le développement de la fibrose (Mori, Kawara et al. 1999; Zeisberg, Strutz et al. 2001). Il existe 3 isoformes de TGFβ issus de 3 gènes différents. Les réponses tissulaires au TGFβ se font *via* un récepteur sérine-thréonine kinase

membranaire puis par une voie de signalisation Smads dépendante (Javelaud and Mauviel 2004). Le TGFβ1, TGFβ majoritaire, semble être très impliqué dans les processus post-lésionnels (Krieglstein, Strelau et al. 2002). Le TGFβ est synthétisé sous forme de précurseur composé du domaine actif en C-terminal et du prodomaine LAP (*Latency Associated Peptide*) en N-terminal. Dès la fin de sa synthèse cette pro-protéine est modifiée par la furine convertase. En effet elle clive le TGFβ mature de son domaine LAP. LAP et TGFβ restent associés de manière covalente, deux complexes se dimérisent, cette forme est obligatoire afin d'être sécrétée. Sous cette forme inactive, la matrice devient un réservoir de TGFβ facilement activable par dissociation du LAP par exemple par l'action de la MMP2. Le TGFβ une fois libre peut alors induire une réponse cellulaire *via* ses récepteurs TβRI/TβRII. La liaison du TGFβ à TβRII induit le recrutement et la phosphorylation de TβRI. Ce complexe active alors la voie de transduction du signal intracellulaire Smads dépendante (Govinden and Bhoola 2003). Le complexe Smads établi se lie alors à l'ADN pour activer la transcription du gène cible. (Figure 14). Il existe également des voies de signalisation alternatives Smad indépendantes: voie ERK1/2, voie PI3K/Akt, voie RhoA-GTPase et JNKp38MAPK. Ces différentes voies d'activation permettent la modulation des effets du TGFβ en fonction de ses différents effets cellulaires (Zhang 2009).

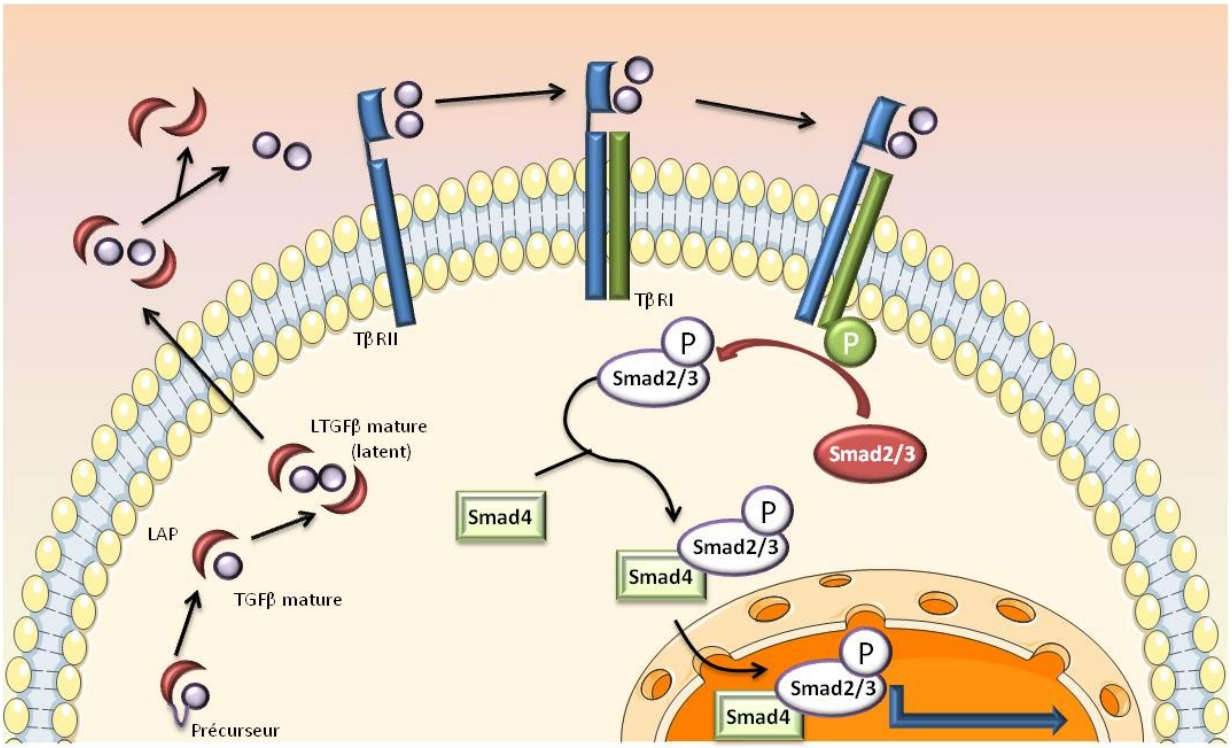

Figure 14: Voie de signalisation classique du TGFβ

3.3.3.2) Le CTGF

Le «*Connective Tissue Growth Factor*» (CTGF) est une protéine sécrétée majoritairement par les cellules endothéliales, elle est impliquée dans de nombreux processus biologiques tels que la chondrogenèse, l'angiogenèse ou la réparation tissulaire. Le CTGF est également impliqué dans certains processus pathologiques tel que la fibrose ou le cancer (Shi-Wen, Leask et al. 2008). L'expression du CTGF peut être augmentée par différents facteurs tels qu'une forte concentration en glucose, des produits terminaux de glycation avancée (Abdel Wahab and Mason 2004) ou encore le TGFβ, le TNF-α ou l'hypoxie (Rimon, Chen et al. 2008). Des études menées *in vitro* et *in vivo* montrent la capacité du CTGF à stimuler la production de cytokines pro-inflammtoires par les cellules endothéliales, le recrutement de macrophages, l'activation des fibroblastes ainsi que l'accumulation de MEC (Grotendorst, Rahmanie et al. 2004; Zhang, Meng et al. 2004). Aucun récepteur spécifique du CTGF n'est connu, cependant celui-ci peut se lier et activer différentes classes de récepteurs non spécifiques (Wahab, Weston et al. 2005; Mason 2009). De manière très intéressante le CTGF possède un domaine potentialisant la liaison du TGFβ au TβRII (Abreu, Ketpura et al. 2002).

3.3.3.3) TGFβ/CTGF

Il existe un phénomène d'interaction croisée entre CTGF et TGFβ. En effet le TGFβ stimule l'expression du CTGF dans de nombreux types cellulaires *via* la signalisation intracellulaire Smads dépendante. Le CTGF possède un élément de réponse au Smads et un élément de réponse au TGFβ dans son promoteur suggérant une boucle d'amplification pro-fibrotique (Abdel Wahab and Mason 2004). La voie de stimulation ERK-dépendante permet également au TGFβ de stimuler la production de CTGF (Phanish, Wahab et al. 2005). Mais le CTGF peut aussi réguler l'action du TGFβ en favorisant sa liaison à son récepteur ou augmenter son activation en favorisant le clivage du domaine LAP. Ces deux facteurs agissent donc ensemble afin d'induire la prolifération et l'activation des fibroblastes menant à l'accumulation de MEC. En effet ces facteurs sont étroitement liés puisque l'utilisation d'un anticorps neutralisant dirigé contre le CTGF permet d'inhiber l'effet activateur de TGFβ sur les fibroblastes (Frazier, Williams et al. 1996).

3.3.3.4) Le HGF

L'«*Hepatocyte Growth Factor*» (HGF) est produit par les CSM et stimule la prolifération, la motilité, la morphogenèse des cellules épithéliales et l'angiogenèse dans divers

organes par phosphorylation de la tyrosine de son récepteur HGFR (Birchmeier and Gherardi 1998). Le HGF possède des propriétés antifibrosantes notamment en bloquant la translocation nucléaire de Smad2/3 inhibant ainsi la voie du TGFβ et l'activation des fibroblastes (Yang, Dai et al. 2003). HGF induit également l'expression de certaines protéases dégradant la MEC dont les métalloprotéases telles que MMP1, MMP2, MMP3 et MMP9 (Hamasuna, Kataoka et al. 1999; Hanzawa, Shindoh et al. 2000). Cependant le HGF est potentiellement peu actif dans le tissu adipeux au vu de la forte présence d'un de ces inhibiteurs le «Plasminogen activator inhibitor-1» (PAI-1) (Shimizu, Hara et al. 2001) dans le tissu adipeux (Alessi, Peiretti et al. 1997).

IV De la réparation tissulaire à la fibrose

4.1) La réparation tissulaire

4.1.1) Réparation tissulaire ou fibrose: une question d'équilibre

La fibrose touche différents organes tels que le foie (cirrhose), le rein, le cœur, les poumons ou encore la peau. La fibrose découle d'un processus de réparation tissulaire infructueux activé suite à des lésions (figure 15). La réparation des tissus est un processus fondamental qui permet de remplacer les cellules mortes ou endommagées suite à une lésion. Ce mécanisme est nécessaire à la survie, la réparation tissulaire est un équilibre entre synthèse et dégradation de MEC. Initialement bénéfique, ce processus devient pathologique s'il est mal régulé ou si les lésions deviennent chroniques (Wynn 2007). L'accumulation de MEC induite par cette mauvaise régulation peut entraîner une dysfonction de l'organe (Wynn 2007). Les différentes atteintes fibrotiques citées plus haut ont des particularités communes: une lésion persistante induit une production de facteurs de croissance, de protéases, de facteurs angiogéniques ainsi que des cytokines profibrotiques. Ensemble, ces protéines conduisent à un remodelage du tissu et à une accumulation de MEC menant à une destruction de l'architecture initiale du tissu (Tomasek, Gabbiani et al. 2002; Friedman 2004).

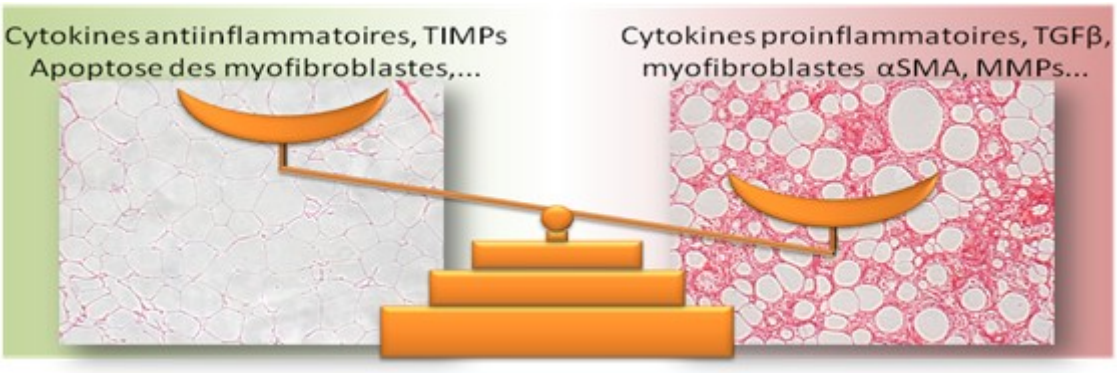

Figure 15: Réparation tissulaire ou fibrose; une question d'équilibre

αSMA: Alpha smooth muscle actin; MMP: métalloprotéase matricielle;TIMP: inhibiteur de métalloprotéase matricielle; TGFB: Tranforming growth factor beta.

4.1.2) Processus de réparation tissulaire

La réparation tissulaire, comme par exemple la cicatrisation d'une plaie, s'établit suite à une lésion tissulaire qui a conduit à une apoptose épithéliale ou endothéliale. Cette apoptose induit la production de médiateurs pro-inflammatoires qui provoque une cascade de coagulation, la formation d'un caillot et d'une matrice provisoire. Les cellules épithéliales et/ou endothéliales sécrètent également des MMPs qui dégradent la membrane basale. Ceci va permettre un meilleur recrutement des cellules immunes sur le site de la lésion et la libération de facteurs de croissance séquestrés. Les neutrophiles sont les premières cellules recrutées, celles-ci dégranulent puis meurent, recrutant ainsi les macrophages afin d'éliminer les débris cellulaires. Les macrophages actifs sécrètent ensuite du PDGF et du TGFβ afin de stimuler la migration de fibroblastes puis leur prolifération. Sur le site de lésion les fibroblastes deviennent des myofibroblastes exprimant ainsi l'αSMA nécessaire à la formation de fibres de stress et à la réparation tissulaire. Les fibroblastes et myofibroblastes sécrètent un grand nombre de protéines de la MEC tels que les collagènes, la fibronectine ou les protéoglycanes afin de remplacer la matrice provisoire. La réparation tissulaire se termine par l'apoptose des myofibroblastes (Tomasek, Gabbiani et al. 2002; Jun and Lau 2010). La fibrose s'établit lorsque la lésion se répète entraînant une accumulation excessive de MEC et de fibroblastes activés (Wynn 2007).

4.2) Implication de la voie TLR4 dans la fibrose de divers tissus

4.2.1) Implication dans la fibrose hépatique

Comme dans d'autres tissus, la fibrogenèse hépatique est un processus de réparation tissulaire exagéré suite à une inflammation induite par des lésions répétées. Ces lésions peuvent être dues à des toxines, à l'abus d'alcool ou encore à une infection virale. La fibrose hépatique est également une des nombreuses complications de l'obésité (Wanless and Lentz 1990). La lésion initiale touche généralement l'hépatocyte et induit une réaction inflammatoire, suivie d'une régénération cellulaire et d'une synthèse de composants matriciels. Lorsque l'atteinte hépatique est aiguë, ce processus permet la cicatrisation de la lésion en rétablissant une architecture hépatique normale. En revanche, si la maladie causale se prolonge, l'inflammation devient chronique, la synthèse de composants matriciels devient excessive et une fibrose hépatique se développe. La fibrose hépatique se caractérise par l'accumulation d'une

MEC riche en fibres de collagène. Elle s'étend progressivement à partir des zones lésées, formant de larges bandes à travers le lobule, unité fonctionnelle du foie, pour finalement se rejoindre, isolant des nodules d'hépatocytes (cirrhose). Le LPS d'origine intestinal a été impliqué dans la fibrogenèse hépatique d'origine alcoolique chez l'Homme (figure 16). En effet la perméabilité intestinale est augmentée chez les patients consommant de l'alcool et leur taux de LPS sanguin est plus élevé. Chez l'animal, l'administration d'un cocktail d'antibiotiques permet de réduire la flore intestinale et induit une diminution du niveau de LPS plasmatique et, en conséquence, supprime le développement de la fibrose hépatique (Rakoff-Nahoum, Paglino et al. 2004; Seki, De Minicis et al. 2007). Ceci suggère une forte implication du LPS circulant dans la fibrogenèse hépatique. En effet plusieurs études sur l'animal ont montré un rôle central du TLR4, récepteur du LPS, dans la mise en place de cette fibrose. Les animaux mutés pour le TLR4, pour son co-récepteur CD14 ou pour ses adaptateurs Myd88 et TRIF ou encore le transporteur plasmatique du LPS, la LBP, montrent tous une diminution de la fibrose hépatique induite par le LPS (Isayama, Hines et al. 2006; Jagavelu, Routray et al. 2010; Teratani, Tomita et al. 2012; Zhu, Zou et al. 2012).

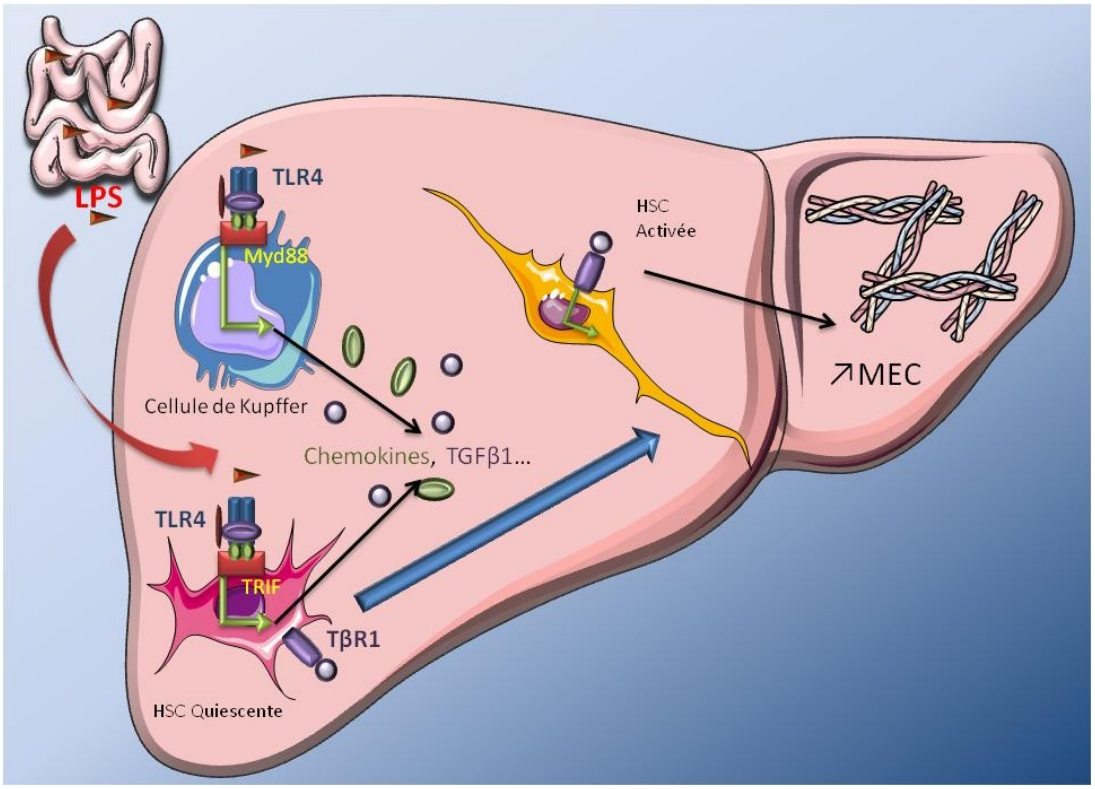

Figure 16: Axe LPS/TLR4 dans la fibrose hépatique

HSC: Hepatic stellate cells; LPS: lipopolisaccharide; MEC: matrice extracellulaire; TGFB: Tranforming growth factor; TLR4: Toll-like receptor 4.

Les cellules HSC quiescentes, dites cellules étoilées, forme de fibroblastes hépatiques, sensibles à de faible dose de LPS, sécrètent un grand nombre de cytokines *via* l'activation de la voie TLR4. Ces cytokines induisent le recrutement des cellules de Kupffer (macrophages hépatiques) ainsi que de monocytes circulants. Certaines cytokines telles que MCP-1 activent directement les HSC (Marra, Romanelli et al. 1999; Schwabe, Bataller et al. 2003). L'activation de la voie TLR4 induit une production de TGFβ également activateur des HSC ainsi que la production de fibronectine initiatrice de fibrose (Zhu, Zou et al. 2012).

4.2.2) Implication dans la fibrose rénale

L'implication de la voie TLR4 a également été montrée au niveau de la fibrose rénale. Cette voie contribue à augmenter l'inflammation dans des modèles d'ischémie-reperfusion. Dans ce modèle, les souris $TLR4^{-/-}$ ont beaucoup moins de fibrogenèse rénale que les souris sauvages (Wu, Chen et al. 2007). *In vitro* les myofibroblastes de rein de souris $TLR4^{-/-}$ sous stimulation du TGFβ produisent moins de mARN codant pour le collagène de type I. En comparaison à des souris TLR4 mutées, les souris sauvages présentent après le même type de lésion que précédemment, une augmentation de l'expression de TLR4, une augmentation de l'expression de l'αSMA, une accumulation de fibroblastes ainsi qu'une accumulation de collagènes (Campbell, Hile et al. 2011).

V MEC et remodelage du tissu adipeux

5.1) La MEC du tissu adipeux

5.1.1) Le rôle de la MEC pendant l'adipogenèse: processus physiologique

La MEC a un rôle très important au cours de l'adipogenèse (Napolitano 1963). En effet le bon déroulement de celle-ci nécessite un réseau de collagène (Cinti, Cigolini et al. 1984). Des études *in vitro* ont montré qu'un remaniement du collagène était nécessaire au cours de la différenciation adipocytaire, ce collagène devenant plus épais et cohésif. Le TA produit différents types de collagènes, notamment le collagène de type I (Ibrahimi, Bertrand et al. 1993) mais également le collagène de type VI. Ces deux collagènes sont les plus abondamment exprimés par les adipocytes matures (Nakajima, Yamaguchi et al. 1998; Scherer, Bickel et al. 1998).

5.1.2) Remodelage excessif du TA: vers un processus pathologique

Le TA est un tissu métaboliquement très flexible répondant rapidement à un besoin de libération ou de stockage d'énergie. Le remodelage du TA sera donc nécessaire au cours de l'obésité pour permettre l'hypertrophie et l'hyperplasie des adipocytes au cours de la prise de poids. Lorsque le remodelage du TA devient pathologique, celui ci s'accompagne d'une augmentation de l'expression des MMPs (Chavey, Mari et al. 2003), d'une accumulation de MEC ainsi que d'une infiltration de cellules immunes notamment des macrophages (Halberg, Wernstedt-Asterholm et al. 2008; Spencer, Yao-Borengasser et al. 2010).

5.2) Rôle du macrophage dans la synthèse de la MEC du TA

5.2.1) Importance de la communication Pré-adipocyte/Macrophage

Plusieurs études *in vitro* ont montré un effet des facteurs sécrétés par les macrophages sur les pré-adipocytes. En effet des cultures de pré-adipocytes en milieux conditionnés provenant de macrophages de sujets obèses, montrent l'action des facteurs sécrétés par ces macrophages sur le phénotype des pré-adipocytes. Ces pré-adipocytes surexpriment alors des gènes de la MEC tels que la fibronectine, le collagène de type I,

la ténascine C et des cytokines pro-inflammatoires comme l'IL6, IL8 et le TNF-α. Ces pré-adipocytes prennent donc un phénotype «profibrotique». L'utilisation de milieux conditionnés de macrophages augmente également la prolifération des pré-adipocytes en culture (Keophiphath, Achard et al. 2009).

Il a également été montré chez l'Homme que les pré-adipocytes étaient des cibles directes du TGFβ1 produit par les macrophages du TA. L'exposition des pré-adipocytes aux sécrétions macrophagiques induit l'apparition du marqueur spécifique du myofibroblaste le αSMA. L'utilisation d'un anticorps neutralisant dirigé contre le principal facteur profibrosant le TGFβ1 diminue cette activation induite par le milieu conditionné de macrophages (Bourlier, Sengenes et al. 2012).

5.2.2) Mécanismes initiateurs de l'infiltration macrophagique

5.2.2.1) Taille et mort adipocytaires

L'hypertrophie adipocytaire provoque la sécrétion de facteurs chimioattractants. En effet la taille adipocytaire est un déterminant de la sécrétion de nombreuses cytokines par l'adipocyte tel que MCP-1 (Cancello, Henegar et al. 2005).

En plus de l'hypertrophie adipocytaire, l'expansion de la masse adipeuse engendre l'apparition d'adipocytes nécrotiques. Leur perte de fonctionnalité est révélée par la perte de l'expression de la périlipine-1 en immunohistochimie (Cinti, Mitchell et al. 2005; Murano, Barbatelli et al. 2008). Les macrophages ont un rôle très important dans la prise en charge des adipocytes nécrotiques. Ceci induit chez les macrophages un phénotype pro-inflammatoire faisant d'eux une source importante de cytokines en particulier de TNF-α (Lumeng, Bodzin et al. 2007; Fujisaka, Usui et al. 2009). Les macrophages s'organisent en couronnes autour de ces cellules (également appelées «*crown like structure*» (CLS)) afin de prendre en charge les dérivés cellulaires potentiellement toxiques (Cinti, Mitchell et al. 2005). Ces macrophages se chargent notamment en lipides de la gouttelette comme le font les cellules spumeuses (Shapiro, Pecht et al. 2013). Le nettoyage des cellules nécrotiques par les macrophages a été proposé comme un élément initiateur de la réponse de réparation tissulaire (Duffield 2003; Strissel, Stancheva et al. 2007). L'apoptose, bien que rare dans les adipocytes, est également un événement déclencheur du recrutement macrophagique (Alkhouri, Gornicka et al. 2010).

5.2.2.2) L'hypoxie

L'hypoxie, dont les effets géniques sont relayés par le facteur de transcription HIF-1α (*hypoxia inducible factor 1 alpha*), contribue selon certains à l'attraction des macrophages dans le tissu adipeux et jouerait un rôle important dans les désordres métaboliques associés à l'obésité (Trayhurn 2013). HIF-1α ainsi que plusieurs de ses gènes cibles ont été montrés comme surexprimés dans le TA de l'obèse et diminués en réponse à la perte de poids (Cancello, Henegar et al. 2005). L'hypoxie tissulaire est une cause classique d'attraction et de maintien des macrophages dans certaines tumeurs et dans la plaque d'athérome. Ces observations suggèrent que si le tissu adipeux de l'obèse présente des zones hypoxiques cela pourrait favoriser localement l'expression de facteurs attractants (Guerre-Millo, Grosfeld et al. 2002). Cependant la présence d'hypoxie dans le tissu adipeux, au cours de l'obésité, est un sujet encore débattu. En effet Goosens et al ont montré que le tissu adipeux d'obèse était au contraire en hyperoxie due à une diminution de la consommation d'oxygène par les adipocytes (Goossens, Bizzarri et al. 2011; Goossens and Blaak 2012).

5.2.2.3) La sécrétion de leptine

L'adipocyte hypertrophié est un gros sécréteur de leptine (de Heredia, Gomez-Martinez et al. 2012) or, l'augmentation de la sécrétion de leptine semble favoriser le recrutement des macrophages dans le TA des personnes obèses. La leptine exerce un effet sur l'expression des molécules d'adhésion et l'adhésion des macrophages dans les cellules endothéliales du TA (Curat, Miranville et al. 2004). Gruen et al. ont également démontré dans une étude *in vitro* que la leptine pourrait agir comme une molécule chimioattractante pour les monocytes et les macrophages (Gruen, Hao et al. 2007).

5.2.2.4) Les acides gras

Les AG libérés par les adipocytes lors de la lipolyse pourraient être également impliqués dans le recrutement des macrophages (Suganami, Nishida et al. 2005; Kosteli, Sugaru et al. 2010). Kosteli et al. ont récemment démontré qu'une augmentation des acides gras libres induite par la lipolyse du tissu adipeux engendre un recrutement des macrophages dans les tissus adipeux de souris. En effet, ces données chez la souris suggèrent qu'une augmentation du flux lipidique local, plus spécifiquement de la lipolyse, pourrait agir comme régulateur du recrutement des macrophages dans le tissu adipeux.

5.3) Fibrose du TA et conséquences

5.3.1) Contrainte physique du TA et lipotoxicité

La mise en place d'une fibrose provoque une rigidification de l'architecture du TA. Ceci induit une contrainte physique empêchant l'expansion de ce tissu par une restriction de taille des adipocytes. Une étude a montré que l'administration d'un inhibiteur synthétique de MMPs durant un régime hyperlipidique chez la souris induit une augmentation du contenu en collagène dans le TA accompagné d'une diminution de la taille des adipocytes (Demeulemeester, Collen et al. 2005). Cette diminution de la taille adipocytaire dans les zones fibrotiques du TA a également été démontrée chez l'Homme (Divoux, Tordjman et al. 2010). Ceci montre une corrélation directe entre contenu en collagènes et diminution de la taille adipocytaire. Lorsque le TA n'est plus en capacité de tamponner les acides gras provenant de l'alimentation, ces AG vont alors se déposer dans des organes dont la fonction première n'est pas de stocker des lipides. Le foie et le muscle sont les tissus principalement touchés (Samuel and Shulman 2012), cette accumulation d'AG va induire une lipotoxicité entraînant un dysfonctionnement de ces tissus. En effet l'accumulation de lipides dans ces deux organes insulinosensibles de l'organisme va entraîner des troubles de la sensibilité à l'insuline (figure 17).

5.3.2) Expansion du TA: un effet protecteur

L'expansion du TA permettrait donc de tamponner le flux d'AG et d'éviter le dépôt de lipides ectopiques dans les tissus insulinosensibles. Ce processus aurait donc un effet protecteur et limiterait l'apparition de la lipotoxicité sur les tissus périphériques. Depuis quelques années s'est développée l'idée qu'une meilleure expansion du TA pourrait avoir un effet protecteur vis-à-vis d'un régime riche en graisses. Plusieurs modèles de souris transgéniques ont validé cette hypothèse.

Chez la souris obèse ob/ob, une délétion génique du collagène de type VI entraîne une amélioration des paramètres inflammatoires et métaboliques malgré la prise de poids (Khan, Iyengar et al. 2007). Il y a, dans ce modèle, une meilleure expansion du TA car la contrainte physique due à la MEC qu'il subit est diminuée. Chez ces souris les adipocytes sont plus gros, ils stockent plus de lipides et limitent de ce fait les dépôts de

lipides ectopiques. Tout cela conduit a une amélioration de la sensibilité périphérique au glucose chez ces souris malgré l'augmentation du poids corporel.

Dans une autre étude, le gène codant pour la protéine MitoNEET, élément clé de la bêta-oxydation mitochondriale, a été surexprimé chez des souris. Cette surexpression augmente la captation des lipides et leur stockage par les adipocytes, ce qui conduit à une expansion de la masse du TA. Malgré l'obésité massive qui en résulte, dans cette expérience les souris massivement obèses qui peuvent peser jusqu'à 130 grammes, cette expansion du TA a des effets bénins et la sensibilité à l'insuline est préservée. Ces souris présentent également moins d'infiltration macrophagique et moins de dépôt de collagène au niveau du TA (Kusminski, Holland et al. 2012).

Au contraire, la création de souris invalidées pour le facteur de transcription PPARγ, favorisant l'adipogenèse, a donné naissance à des souris ayant une diminution drastique de la masse adipeuse. De part l'incapacité de stockage des AG dans le TA, ces souris présentent une insulinorésistance sévére ainsi qu'une dyslipidémie. Ces résultats montrent, encore une fois, le rôle important de l'expansion du tissu adipeux dans la prise en charge des lipides afin d'éviter l'accumulation de lipides ectopiques (Medina-Gomez, Gray et al. 2007; Virtue and Vidal-Puig 2008).

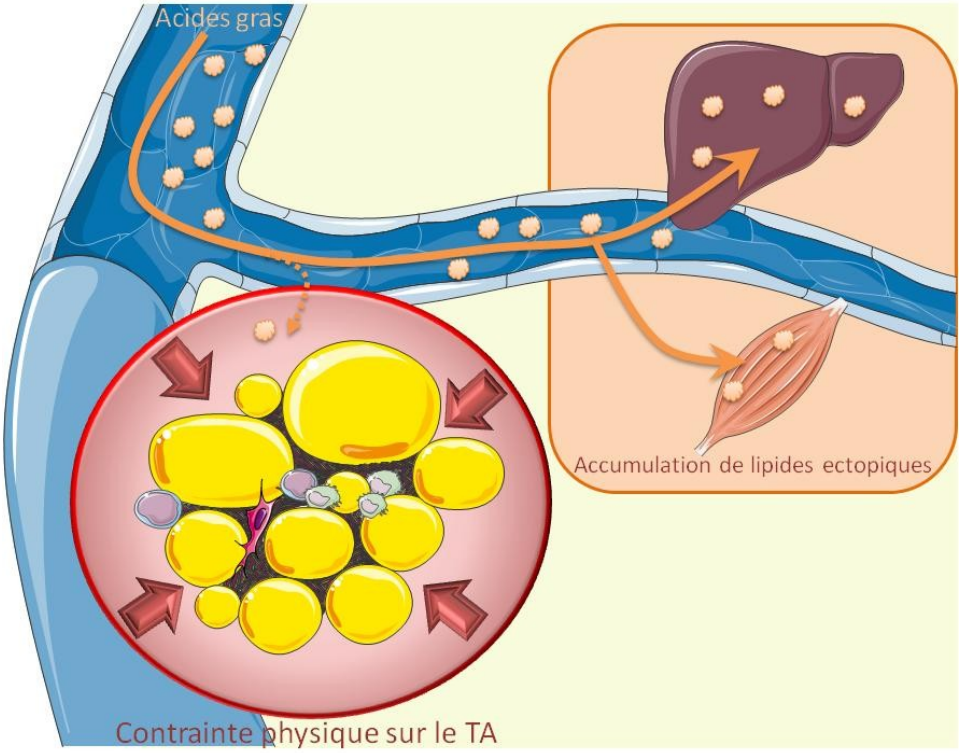

Figure 17: Fibrose du TA et lipotoxicité: importance des AG

OBJECTIFS

Suite à une étude conduite chez l'homme, où nous avons mis en évidence la surexpression de gènes de la fibrose avec l'obésité et le syndrome métabolique, nous avons recherché un modèle murin pouvant servir à étudier la fibrose adipeuse.

Pour cela nous avons utilisé un modèle de souris C3H/HeOuJ (WT), classiquement utilisé dans de nombreuses études de fibroses induites (par lésions ou traitements pharmacologiques). Connaissant le rôle clé du TLR4 dans la fibrose de nombreux autres organes, nous nous sommes demandé si ce récepteur se trouvait également impliqué dans la mise en place de la fibrose du TA. Nous avons donc utilisé des souris C3H/HeJ, souris possédant un TLR4 non fonctionnel ($TLR4^{mut}$).

L'objectif de ce travail a ensuite été d'étudier la mise en place de la fibrose du TA au cours d'une obésité induite chez la souris.

Le premier objectif de ma thèse a été de valider la mise en place de la fibrose adipeuse dans un modèle murin lors d'un régime hyperlipidique. Le deuxième objectif a été de déterminer l'importance du TLR4 immun dans ce processus de fibrogenèse.

ARTICLE 1

Immune Cell Toll-like Receptor 4 Mediates the Development of Obesity-associated Adipose Tissue Fibrosis

Isabelle K. Vila[1,2,3], Pierre-Marie Badin[1,2,3], Marie-Adeline Marques[1,2,3], Laurent Monbrun[1,2,3], Corinne Lefort[1,2,3], Balbine Roussel[1,2,3], Philippe Gui[2,3], Jacques Grober[4], Vladimír Štich[1,5], Lenka Rossmeislová[1,5], Alexia Zakaroff-Girard [3,6], Anne Bouloumié[3,6], Nathalie Viguerie[1,2,3], Cedric Moro[1,2,3], Geneviève Tavernier[1,2,3], Dominique Langin[1,2,3,7]

[1]Franco-Czech Laboratory for Clinical Research on Obesity, Third Faculty of Medicine, Prague, and Inserm, Toulouse

[2]INSERM, UMR1048, Obesity Research Laboratory, Institute of Metabolic and Cardiovascular Diseases, Toulouse, France;

[3]University of Toulouse, UMR1048, Paul Sabatier University, France;

[4]Centre de Recherche INSERM UMR866, Université de Bourgogne, Dijon, France;

[5]Department of Sport Medicine, Third Faculty of Medicine, Charles University in Prague, CZ-100 00 Czech Republic;

[6]INSERM, UMR1048, Team 1, Institute of Metabolic and Cardiovascular Diseases, Toulouse, France;

[7]Toulouse University Hospitals, Department of Clinical Biochemistry, Toulouse, France

Immune Cell Toll-like Receptor 4 Mediates the Development of Obesity-associated Adipose Tissue Fibrosis

Isabelle K. Vila[1,2,3], Pierre-Marie Badin[1,2,3], Marie-Adeline Marques[1,2,3], Laurent Monbrun[1,2,3], Corinne Lefort[1,2,3],Balbine Roussel[1,2,3], Philippe Gui[2,3], Jacques Grober[4], Vladimír Štich[1,5], Lenka Rossmeislová[1,5], Alexia Zakaroff-Girard [3,6], Anne Bouloumié[3,6], Nathalie Viguerie[1,2,3], Cedric Moro[1,2,3], Geneviève Tavernier[1,2,3], Dominique Langin[1,2,3,7]

[1]Franco-Czech Laboratory for Clinical Research on Obesity, Third Faculty of Medicine, Prague, and Inserm, Toulouse

[2]INSERM, UMR1048, Obesity Research Laboratory, Institute of Metabolic and Cardiovascular Diseases, Toulouse, France;

[3]University of Toulouse, UMR1048, Paul Sabatier University, France;

[4]Centre de Recherche INSERM UMR866, Université de Bourgogne, Dijon, France;

[5]Department of Sport Medicine, Third Faculty of Medicine, Charles University in Prague, CZ-100 00 Czech Republic;

[6]INSERM, UMR1048, Team 1, Institute of Metabolic and Cardiovascular Diseases, Toulouse, France;

[7]Toulouse University Hospitals, Department of Clinical Biochemistry, Toulouse, France

Running title: Macrophage TLR4 and Fibrosis in Adipose Tissue

Correspondence to: dominique.langin@inserm.fr

Summary

Adipose tissue expansion is a protective phenomenon against ectopic lipid accumulation. As it blocks adipocyte hypertrophy, the development of adipose tissue fibrosis is deleterious. Here we show that adipose tissue fibrosis is associated to obesity and insulin resistance in humans and mice. Kinetic studies in C3H mice fed high fat diet show progression of adipose tissue fibrosis and inflammation with fat cell dysregulation of metabolism, notably lipolysis, and adipocyte death. Toll-like-receptor 4 mutation or inhibition of Toll-like-receptor 4 signaling protected mice from obesity-induced fibrosis. Chronic low dose infusion of the Toll-like-receptor 4 ligand, lipopolysaccharide, promoted adipose tissue fibrosis. Bone marrow transplantation revealed that the presence of a functional Toll-like-receptor 4 on adipose tissue hematopoietic cells is necessary for adipose tissue fibrogenesis. Together, these results indicate that obesity and endotoxemia promote adipose tissue fibrosis, a condition associated with insulin resistance, through immune cell Toll-like-receptor 4.

Highlights

- Adipose tissue fibrosis develops during human and mouse obesity
- Insulin resistance is associated with adipose tissue fibrosis in both species
- Immune cell Toll-like receptor 4 is required for adipose tissue fibrosis
- Chronic low dose infusion of the Toll-like receptor 4 ligand, lipopolysaccharide, induces adipose tissue fibrosis
- High fat diet and endotoxemia promote fibrosis through adipose tissue immune cell Toll-like receptor 4

Introduction

Adipose tissue (AT) serves as a long-term reserve of energy which can be mobilized during food deprivation. In situations of excess of energy, AT expands through storage of fatty acids as triglycerides. AT expansion protects other organs against chronic lipid overload leading to metabolic disorders. Indeed, facilitated AT expansion is associated in transgenic mouse models with a better metabolic state (Kim et al., 2007; Kusminski et al., 2012; Medina-Gomez et al., 2007; Virtue and Vidal-Puig, 2008). On the opposite, the lack of AT seen in lipodystrophy leads to severe metabolic abnormalities (Gandotra et al., 2011; Pajvani et al., 2005; Rubio-Cabezas et al., 2009). During AT expansion in mice fed high fat diet, there is a strong remodeling of the tissue to accommodate adipocyte growth (Strissel et al., 2007). AT remodeling is a complex and dynamic process pathologically accelerated in the obese state by inflammatory cell infiltration, cytokine release and production of extracellular matrix. Mice lacking collagen VI, a collagen species found in human and mouse AT, show increased expansion of AT and improvements in whole-body energy homeostasis (Divoux et al., 2010; Khan et al., 2009). Therefore, excessive accumulation of collagen and development of fibrosis could limit AT expandability resulting in ectopic lipid accumulation and development of metabolic syndrome.

Obesity in humans and mice is characterized by systemic and AT inflammation (Cancello et al., 2005; Klimcakova et al., 2011a; Weisberg et al., 2003; Wellen and Hotamisligil, 2003; Xu et al., 2003). This state of low-grade inflammation results in an increased production of cytokines and chemiokines primarily by macrophages (Horng and Hotamisligil, 2011; Hotamisligil et al., 1993). In liver and kidney, there is a close link between inflammation, production of the extracellular matrix and development of fibrosis. In these organs, there is mounting evidence that the immune Toll-like receptor 4 (TLR4) acts as a key regulator in fibrogenesis (Aoyama et al., 2010; Campbell et al., 2011; Seki et al., 2007). A role for TLR4

in AT inflammation has been shown but its direct contribution to AT fibrosis remains elusive (Poggi et al., 2007; Saberi et al., 2009; Shi et al., 2006).

Despite its importance in the dynamics of AT remodeling and consequences on metabolic status, the mechanisms controlling AT fibrosis remain poorly known. One of the limitations has been the lack of suitable mouse models. Here, we characterized AT fibrosis in humans and mice to determine whether they share similar features. Unlike the commonly used C57Bl/6 mice, mice on C3H background develop AT fibrosis when obesity is induced by high fat feeding. This prompted us to investigate the role of TLR4 in C3H/HeJ mice which carry a spontaneous loss of function mutation of TLR4 and in control C3H/HeOuJ mice treated with an inhibitor of TLR4 signaling (Hoshino et al., 1999; Li et al., 2006). To determine whether immune cells expressing TLR4 are instrumental in promoting AT fibrosis, bone marrow transplantation was performed. The role of the prototypical TLR4 ligand, lipopolysaccharide, was investigated using chronic low dose infusion of the endotoxin.

Results

Identification of a mouse model of human obesity adipose tissue fibrosis

In human subcutaneous AT, expression of genes involved in fibrosis showed a progression from lean to obese individuals to reach the highest levels in obese patients with metabolic syndrome (Figure 1A, Table S1). Similar pattern was observed in human visceral adipose tissue (Figure S1A). Genes encoding extracellular matrix proteins such as collagen type I alpha 1 (*COL1A1*), collagen type VI alpha 3 (*COL6A3*), lumican (*LUM*) and tenascin C (*TNC*) were all upregulated in obese patients with metabolic syndrome compared to lean and healthy individuals (Figure 1B). These genes showed higher expression in stromavascular fraction cells compared to mature fat cells (Figure 1C). Accordingly, levels of gene expression were much higher in preadipocytes than in mature fat cells, revealing a downregulation of fibrosis gene expression during human adipocyte differentiation (Figure 1D).

In search for a model of progressive AT fibrosis during the development of obesity, we selected the C3H/HeOuJ mouse strain which has been shown to develop fibrosis in other organs such as kidney and liver (Campbell et al., 2011; Seki et al., 2007). Compared to mice fed chow diet, obese mice fed high fat diet for 4 weeks showed a higher body weight (27.9±0.4g *vs* 35.5±0.5g, $p<0.001$) due to a robust increase of fat mass (2.6±0.3g *vs* 9.1±0.3g, $p<0.001$). The obese mice also showed an upregulation of genes involved in fibrosis notably those encoding extracellular matrix proteins (*Col1a1*, *Col6a3*, *Lum* and *Tnc*) which are upregulated in obese humans (Figures 1E and F). In C3H mice, the fibrotic genes *Col1a1*, *Col6a3*, *Lum* and *Tnc* were, as in human AT, preferentially expressed in stromavascular cells compared to mature adipocytes (Figure 1G). In the commonly used C57Bl/6J mouse strain, the upregulation of fibrosis genes in AT was moderate and observed only after high fat diet of extended duration (15 weeks) (Figure 1H). The fibrotic genes were

preferentially expressed in stromavascular cells compared to mature adipocytes as in C3H mice (Figure S1B). Compared to mice fed chow diet, the difference in weight gain (27.7g±1.1g *vs* 37.6±1.2g, $p<0.001$) and fat mass (2.8±0.5g *vs* 10.8±0.7g, $p<0.001$) was similar to those observed in C3H mice fed high fat diet for 4 weeks. Thus, C3H mice represent a proper model for studying AT fibrosis during the development of obesity.

Mutation of TLR4 protects mice from high fat diet-induced adipose tissue fibrosis and inflammation

Next, we investigated the molecular mechanisms of high fat diet-induced AT fibrosis in C3H mice. The endotoxin receptor, TLR4, is involved in the development of fibrosis in liver and kidney (Campbell et al., 2011; Seki et al., 2007). To determine whether it was involved in AT fibrogenesis, we compared the expression of genes involved in tissue remodeling in C3H/HeJ mice carrying an inactivating mutation in the TLR4 gene ($TLR4^{mut}$ mice) with C3H/HeOuJ wild type (WT) mice during a 12 week time course of high fat feeding. In WT mice, mRNA levels of *Col6a3*, a matrix metalloprotease (*Mmp2*), and the major profibrotic factor, transforming growth factor beta 1 (*Tgfβ1*) were up-regulated after 4 weeks of high fat diet feeding (Figure 2A). Similar pattern of expression was seen for other genes involved in fibrosis (Figure S2A). There was strong positive correlations between *Tgfβ1* and *Col1a1* or *Col6a3* mRNA expression ($r=0.74$ $p<0.001$; $r=0.43$, $p<0.01$) (Figure S2B). In $TLR4^{mut}$ mice, AT expression of all genes investigated was lower than in WT mice and showed little progression, if any, during the 12 weeks of high fat diet (Figure 2A). Interestingly, fibrosis gene expression was comparable in AT from WT and $TLR4^{mut}$ mice fed 8 weeks on normal chow diet showing the requirement of, and interaction between, TLR4 and high fat diet-induced expansion of fat mass to induce AT fibrosis (Figure S2C). To confirm that an inactive TLR4 protects from high fat diet-induced AT fibrosis, the amount of collagens was

assessed by picrosirius staining. Staining quantification showed a dramatic increase of fibrotic areas in WT mice from 6 weeks of high fat diet while TLR4^{mut} mice were totally protected (Figure 2B). We also performed chronic perfusion of a specific inhibitor of TLR4 signaling (TAK242) in high fat diet-fed WT mice. Inhibition of TLR4 signaling with TAK242 limited AT fibrosis (Figure 2C). Therefore, genetic as well as pharmacological impairment of TLR4 signaling prevents the development of AT fibrosis.

During the development of high fat diet-induced obesity, expression of inflammatory genes was increased in WT mice whereas TLR4^{mut} mice were protected (Figure S2D). Gene expression of *Emr1* encoding the specific marker of macrophages, F4/80, was significantly upregulated in AT of WT mice from 4 weeks of high fat diet (Figure 2D). In TLR4^{mut} mice, the level of expression was much lower and the increase during high fat feeding was moderate. Consistently, flow cytometry analysis performed at 8 weeks of high fat diet revealed a higher number of AT macrophages in WT mice (2.2-fold, $P< 0.001$) compared to TLR4^{mut} mice (Figure 2E). F4/80 immunohistochemistry staining showed a much higher number of crown-like structures in AT of WT mice compared to TLR4^{mut} mice (Figure 2F). The relationship between AT inflammation and fibrosis was shown by the strong positive correlation between mRNA expression of *Emr1* and *Col6a3* ($r=0.62$, $p<0.001$) (Figure 2G).

As mast cells accumulate in inflamed and fibrotic human fat depots (Divoux et al., 2012), we investigated number and location of these cells in AT from TLR4^{mut} and WT mice. Mast cells were more numerous in WT compared to TLR4^{mut} mice (Figure S2E). Nevertheless, the number was very low in comparison to AT macrophages (F4/80 positive cells in crown-like structures per mm² 224 ± 50 *vs* mast cells per mm² 1.66 ± 0.33, $p<0.001$). Unlike F4/80 positive macrophages, the few mast cells were located outside fibrotic areas.

Fibrosis is associated with adipocyte metabolic dysfunction and death

We also explored the consequences of AT fibrosis on adipocyte metabolism through comparison of fibrosis-prone WT and fibrosis-protected TLR4^{mut} mice. High fat diet was associated with a strong down-regulation of genes involved in lipid metabolism in AT from WT mice whereas no change was observed in AT from TLR4^{mut} mice (Figure 3A, Figures S3). Notably, mRNA levels of genes encoding proteins involved in lipolysis began to be down regulated after 4 to 6 weeks of high fat diet in WT mice. Such down regulation was confirmed at protein level for hormone-sensitive and adipose triglyceride lipases (Figure 3B). TLR4^{mut} mice were protected from these changes. After 8 weeks of high fat diet, *in vitro* lipolysis experiments on isolated adipocytes showed that basal and stimulated glycerol release was significantly lower in WT compared to TLR4^{mut} mice (Figure 3C). Further emphasizing the role of fibrosis in altering adipocyte function, *Col6a3* mRNA expression was negatively correlated to mRNA levels of lipolytic genes in WT mice ($r=-0.6$, $p<0.001$; $r=-0.72$, $p<0.001$; $r=-0.66$, $p<0.001$) (Figure 3D). Together these data suggest a negative association between fibrosis and major proteins involved in AT metabolic functions.

We next investigated the consequence of AT fibrosis on adipocyte morphology and death. WT mice fed high fat diet for 12 weeks were characterized by a higher percentage of small fat cells between 500 and 3000 µm² and a lower percentage of large fat cells over 5000 µm² in WT mice (Figure 3E). Necrotic fat cells are characterized by a lack of perilipin 1, a protein coating the lipid droplet (Cinti et al., 2005). Perilipin 1 immunostaining was performed on AT sections to count the number of perilipin-negative fat cells. AT from WT mice had numerous dead adipocytes whereas those cells were rare in TLR4^{mut} mouse AT (Figure 3F). The shift of pattern in cell size distribution and the increase in the number of perilipin-negative cells both suggested increased adipocyte death in WT mice compared to TLR4^{mut} mice. The higher rate of adipocyte death was associated at 12 weeks of high fat diet with lower weight of epididymal fat pad in WT mice (Figure 3G) and higher plasma level of

FABP4, a cytosolic fatty acid binding protein released during adipocyte death, in WT mice compared to TLR4^{mut} mice (Figure 3H).

High fat diet-induced adipose tissue fibrosis is dependent on immune cell Toll-like receptor 4

In order to investigate the involvement of immune cells in the genesis of AT fibrosis, TLR4^{mut} mice were irradiated. Bone marrow transplantation of control or mutated mouse donor cells was performed into irradiated recipient mice (BMT-TLR4^{mut}/TLR4^{mut} and BMT-WT/TLR4^{mut} mice). The experiment did not alter hematopoietic cell lineage distribution. Monocyte, lymphocyte and neutrophil counts were similar in the two types of chimeric mice (Figure S4A). In BMT-WT/TLR4^{mut} mice, an intact TLR4 gene was detected in blood hematopoietic-derived cells and in AT macrophages (Figure S4B).

TLR4^{mut} mice reconstituted with WT bone marrow had higher AT expression of *Tgfβ1*, *Col6a3* and vimentin (*Vim)* genes compared to BMT-TLR4^{mut}/TLR4^{mut} mice (Figure 4A). Picrosirius staining showed more collagen deposition in AT from BMT-WT/TLR4^{mut} mice compared to BMT-TLR4^{mut}/TLR4^{mut} mice (Figure 4B). Associated to fibrosis, there was higher AT expression of inflammatory *Mrc1*, *Tnfα* and *Mcp1* genes (Figure 4C) and a tendency towards a greater number of AT macrophages in BMT-WT/TLR4^{mut} mice compared to BMT-TLR4^{mut}/TLR4^{mut} (Figure 4D).

Insulin resistance is associated with immune TLR4-mediated adipose tissue fibrosis

The relationship between insulin resistance and AT fibrosis was investigated in humans and in mice. The quantitative insulin sensitivity check index (QUICKI) decreased from lean to obese individuals to reach the lowest levels in obese patients with metabolic syndrome (Figure 5A). QUICKI values were negatively correlated with fibrosis gene expression ($r = -0.8$, $p<0.001$) (Figure 5B).

Insulin tolerance was investigated in WT and TLR4^{mut} mice. The TLR4 mutation prevented the high fat diet-induced decrease in insulin tolerance (Figure 5C). This improvement was not related to difference in weight gain during high fat diet between WT and TLR4^{mut} mice. The results were confirmed by QUICKI determination. WT mice were more insulin-resistant, i.e., had lower QUICKI values, than TLR4^{mut} mice (0.28± 0.01 vs 0.42± 0.01, $p<0.001$). QUICKI values were negatively correlated to the extent of AT fibrosis ($r= -0.75$, $p<0.01$) (Figure 5D).

In BMT-WT and BMT-TLR4^{mut} mice, an intraperitoneal glucose tolerance test was performed (Figure 5E). BMT-WT mice lost the protection against the development of glucose intolerance induced by high fat diet observed on TLR4^{mut} background. Plasma insulin and glucose levels were determined at 15 minutes after glucose injection. The insulin x glucose product was correlated to the extent of AT fibrosis ($r= 0.6$, $p<0.01$) (Figure 5F).

The TLR4 ligand, lipopolysaccharide, induces adipose tissue fibrosis

To assess if lipopolysaccharide, the endotoxin activating TLR4, induced AT fibrosis, we performed chronic perfusion of lipopolysaccharide for 4 weeks in normal chow diet-fed WT mice. This treatment induced a 2 fold increase in lipopolysaccharide plasma level (Figure 6A) with no change in body weight (Figure 6B). The higher circulating level of the TLR4 natural ligand produced overexpression of several fibrotic genes in AT (Figure 6C) and a marked increase of fibrotic areas in AT from lipopolysaccharide-treated compared to NaCl-treated mice (Figure 6D). AT expression of macrophage marker and inflammation-related genes was also higher (Figure 6E) together with the number of AT macrophages (+4.1 fold, $p<0.01$) and lymphocytes (Figure 6F).

Discussion

In humans, AT expression of fibrosis-related genes was increased in obesity and further elevated when obesity and metabolic syndrome are combined. We identified C3H mice fed high fat diet as a suitable model of human obesity-induced AT fibrosis. In both humans and mice, the extent of AT fibrosis was linked to the worsening of insulin resistance. Time-course studies in C3H mice revealed that AT expansion was associated with collagen overproduction, macrophage-related inflammation and, adipocyte metabolic dysfunction and death. Investigation of mice with genetic and pharmacological inhibition of TLR4 signaling showed that the endotoxin receptor is essential in mediating the development of AT fibrosis. Bone marrow transplantation experiments and chronic lipopolysaccharide infusion demonstrated that lipopolysaccharide activation of immune cell TLR4 is central in AT fibrogenesis.

The C57BL/6J strain, classically used in obesity research, appears, at first glance, as the model of choice to study AT fibrosis in mice. However, when fed high fat diet, the mice presented a late and modest modulation of profibrotic gene expression (Kwon et al., 2012). This moderate development of AT fibrosis may be related to lower immune cell infiltration on high fat diet compared to C3H mice (Nguyen et al., 2007; Spencer et al., 2010). The C3H mouse strain, on the other hand, could represent a more interesting model as they develop tubulointerstitial fibrosis in kidney following injury and hepatic fibrosis induced by lipopolysaccharide (Campbell et al., 2011; Seki et al., 2007). In preliminary studies, we observed that C3H mice rapidly gain fat mass when fed high fat diet. When comparing high fat diet-fed and chow diet-fed mice, we found an up regulation in AT of the same genes encoding extracellular matrix proteins as in the comparison between obese and lean individuals. In both obese individuals and obese C3H mice, expression of genes related to fibrosis were preferentially expressed in AT stromavascular fraction. Time-course studies revealed an early and prolonged collagen accumulation in AT associated to increased gene

expression of two major collagen species of AT, *Col1a1* and *Col6a3*. Fibrosis gene expression was not increased in C3H mice fed chow diet indicating that AT expansion and consequent remodeling is a necessary prerequisite for the development of AT fibrosis. In wound healing, there is an intimate link between fibrosis and inflammation (Stramer et al., 2007). Kinetic studies revealed that this is also the case in AT. Flow cytometry and immunohistochemistry analyses showed a higher amount of immune cells, notably macrophages, and enhanced inflammation-related gene expression (Weisberg et al., 2003). Macrophages are seen in several organs as master regulators of fibrosis (Wynn and Barron, 2011). Gene expression of the macrophage marker *Emr1* (F4/80) strongly correlated with *Col1a1* and *Col6a3* mRNA levels as observed in human AT (Spencer et al., 2010). Moreover, macrophages in crown-like structures were localized in fibrotic areas. Gene expression of *Mmp2* and *Mmp9* encoding macrophage matrix metalloproteases and the established profibrotic factor *Tgfβ1* were up regulated during high fat feeding. Among other functions in tissue remodelling, matrix metalloproteases activate cathepsin-based proteolytic pathways to generate an active TGFβ1. TGFβ family members produced by macrophages mediate a fibrotic reaction in human AT progenitor cells *in vitro* (Bourlier et al., 2012; Keophiphath et al., 2009). Our data are a further illustration of the role of TGFβ1 and matrix metalloproteases in fibrogenesis *in vivo* (Biernacka et al., 2011; Pardo and Selman, 2006). Mast cells have recently been shown to be present in human fat depots with inflammation and fibrosis (Divoux et al., 2012). Genetic deficiency of these cells is associated with reduced levels of inflammatory cytokines in mouse AT (Liu et al., 2009). Cell staining showed the presence of mast cells in AT of C3H mice fed high fat diet. However, the number was very low compared to macrophages. Mast cells were found outside of fibrotic areas. These results suggest an unlikely participation of mast cells in fibrogenesis in our mouse model. Although our data

point to macrophages as central players in AT fibrosis development, we cannot rule out that other immune cells are involved in high fat diet-induced AT fibrosis.

The detrimental effect of fibrosis in liver, lung and kidney is well established (Bataller and Brenner, 2005; Wynn, 2008). Few data are available on AT. Patterns of gene expression showed gradual metabolic dysfunction of fat cells with the progression of AT fibrosis. Notably, mRNA levels of lipases and other lipolytic factors were down regulated and showed inverse correlations with collagen gene expression. The lower protein levels of the two rate-limiting lipases, adipose triglyceride lipase and hormone-sensitive lipase, led to impaired basal and stimulated lipolysis (Bezaire et al., 2009). The alteration in fat cell metabolism was the prelude to adipocyte death by necrosis. At whole tissue level, there was a decrease of fat pad weight and fat cell size at 12 weeks of high fat diet in WT mice. Accordingly, a negative correlation has been reported between the extent of fibrosis and adipocyte size in human AT (Divoux et al., 2010). Adipocyte death by necrosis is characterized by negative perilipin staining and surrounding macrophage crowns (Cinti et al., 2005; Strissel et al., 2007). We found a much higher proportion of dead adipocytes in fibrotic AT. The increase in plasma FABP4 levels may be considered as a systemic consequence of adipocyte necrosis. This abundant fat cell cytosolic fatty acid protein is released upon adipocyte death (unpublished data). As further *in vivo* proof, we find an elevation of plasma FABP4 levels in hormone-sensitive lipase null mice, a model of pronounced large fat cell necrosis (unpublished data) (Cinti et al., 2005). These results suggest that AT fibrosis has a negative impact on adipocyte metabolic pathways and favors fat cell death by necrosis. Moreover, it reveals an intricate combination constituted of AT fibrosis, inflammation and, adipocyte dysfunction and death, that may contribute to the metabolic complications of obesity. The strongest signature of genes encoding extracellular matrix proteins was found in obese patients with metabolic syndrome, as also observed in morbidly obese patients,

indicating a link between AT fibrosis and worsening of the metabolic status (Henegar et al., 2008). This was corroborated by the positive association between AT fibrosis and insulin resistance found both in mice and humans. Insulin resistant obese patients are therefore characterized by AT fibrosis, increased macrophage immune response and decreased adipocyte metabolism (Klimcakova et al., 2011b; Spencer et al., 2010).

TLR4 is a key initiator of inflammatory responses in macrophages. Mice carrying an inactivating mutation of TLR4 are protected against AT inflammation (Suganami et al., 2007). Here, we show that $TLR4^{mut}$ mice fed high fat diet are also protected from AT fibrosis and, fat cell metabolic dysfunction and death. Moreover, studies of irradiated $TLR4^{mut}$ mice transplanted with WT bone marrow reveal that TLR4 competent immune cells in AT restore the high fat diet-mediated induction of collagen accumulation and up regulation of inflammatory markers, extracellular matrix and profibrotic genes. Of note, irradiated WT mice transplanted with bone marrow of TLR4-null mice show markedly reduced AT inflammation (Saberi et al., 2009). Furthermore, treatment with a TLR4 signaling inhibitor protected mice against fibrosis during high fat diet. Together, these results show that AT hematopoietic cell TLR4 is essential for recruitment and activation of macrophages leading to AT fibrogenesis. Furthermore, the innate immune receptor modulates systemic insulin sensitivity (Saberi et al., 2009; Tsukumo et al., 2007).

Obesity has been linked to metabolic endotoxemia with an elevation of circulating lipopolysaccharide level in rodents and in humans (Cani et al., 2007; Pussinen et al., 2011). Lipopolysaccharide is a membrane component of Gram-negative bacteria considered as the most potent inducer of inflammation through TLR4, its main receptor. We show that a chronic moderate increase in lipopolysaccharide plasma levels is sufficient to induce AT inflammation and fibrosis. Lipopolysaccharide is the best candidate of TLR4 activation but a potential role for other ligands and cofactors cannot be excluded (Erridge, 2010). Four weeks

of high fat feeding were sufficient to induce upregulation of two extracellular matrix genes, tenascin-C which is an endogenous ligand of the TLR4 (Midwood et al., 2009) and lumican which helps the presentation of lipopolysaccharide to TLR4 (Wu et al., 2007).

Fibrosis, inflammation and metabolic dysfunction constitute a detrimental triptych in AT. We found that these intricate processes are dependent on TLR4 expressed in AT immune cells, especially macrophages. Lipopolysaccharide, the main TLR4 ligand, which plasma levels are increased during obesity-associated metabolic endotoxemia, is a likely trigger of AT fibrogenesis. The TLR4-dependent AT remodeling leads to limited fat expansion and fibrosis, low metabolic capacity and necrotic death of fat cells, as well as marked inflammation which all concur to the metabolic complications of obesity.

Experimental Procedures

Expression of human fibrosis genes in human adipose tissue

Subcutaneous and visceral AT biopsies were performed in carefully phenotyped lean, obese and obese with metabolic syndrome individuals (Klimcakova et al., 2011a; Klimcakova et al., 2011b). Adipocytes and stromavascular fraction were isolated from abdominal subcutaneous AT by collagenase digestion (Klimcakova et al., 2011a). Progenitor cells from the stromavascular fraction were differentiated as previously reported (Rossmeislova et al., 2013). Gene expression profiling was performed using whole genome 44k oligonucleotide arrays (Agilent Technologies).

Animals

Animal protocols were performed according to Institut National de la Santé et de la Recherche Médicale and Institut des Maladies Métaboliques et Cardiovasculaires Animal Care Facility guidelines. Five week male C3H/HeJ which carry a missense mutation in the TLR4 gene and the wild-type C3H/HeOuJ were purchased from the Jackson Laboratory. C57BL/6J (Elevage Janvier) and C3H mice were housed four per cage at 20°C with a 12 h light–dark cycle.

Diets

After weaning, C3H/HeJ and C3H/HeOuJ mice were fed with high-fat diet (45% energy as fat, Research Diets D12451) for 2 to 12 weeks. In some experiments, C3H/HeOuJ mice were fed with a normal chow diet (10% energy as fat, Research Diets D12450B) for 4 weeks. C57BL/6J mice were fed normal chow and high-fat diets for 15 weeks.

Body composition

Mouse body composition was evaluated by quantitative nuclear magnetic resonance imaging (EchoMRI 3-in-1 system; Echo Medical Systems, Houston, Texas).

Glucose and insulin tolerance tests Mice were fasted for 6 h with free access to drinking water. Glucose was administered intraperitoneally (1g/kg) and blood glucose levels were monitored from the tip of the tail with a glucometer (Accucheck, Roche). At 15 minutes after glucose injection, blood was collected for insulin quantitation. For insulin tolerance tests, insulin was administered intraperitoneally (0.6 mU/g) and blood glucose was measured at various times after injection.

Generation of bone marrow chimeras

C3H/HeJ mice at 10 weeks of age received a sublethal dose of whole-body irradiation (9 Gy). The day after irradiation, donor C3H/HeJ or C3H/HeOuJ mice were killed and their femurs and tibias removed aseptically. Marrow cavities were flushed, and single-cell suspensions were prepared. The irradiated recipients received 1×10^7 bone marrow cells in 0.1 ml of phosphate-buffered saline by retro-orbital injection. During 4 weeks after the bone marrow transplantation, Bactrim (sulfamethoxazole 200 mg/ml, trimethoprim 48 mg/ml, Roche) was added to drinking water. After 2 additional weeks, all mice were switched to high-fat diet. Mice were sacrificed 8 weeks later when blood and tissues were collected.

Lipopolysaccharide and TAK242 chronic infusions

For lipopolysaccharide infusion, 5 week old mice fed normal chow diet were implanted intraperitoneally with an osmotic minipump (Alzet Model 1004; Alza). Pumps were filled either with NaCl (0.9%) or lipopolysaccharide (from *Escherichia coli* 055:B5; Sigma) to infuse 300 μg kg^{-1}·$day^{-1}$for 4 weeks.

For TAK242 infusion, mice were fed high-fat diet for 4 weeks and then implanted intraperitoneally with osmotic minipumps filled either with a solution of DMSO/Ethanol/H_2O (5/1.5/3.5) or TAK242 (Invivogen) to infuse 350 μg kg^{-1}·day^{-1} for 4 weeks with continuous feeding of high-fat diet.

Analysis of blood parameters

Plasma glucose levels were measured by enzymatic assay kit (Glucose RTU, Biomerieux). Serum insulin concentration was determined by the respective enzyme-linked immunosorbent assay kits (Mouse Ultrasensitive insulin ELISA, ALPCO Diagnostics). Plasma lipopolysaccharide levels were measured by the direct quantitation of 3-hydroxymyristic acid by gas chromatography-mass spectrometry (Gautier et al., 2008). Plasma FABP4 concentration was determined by enzyme immunoassay kit (BioVendor, R&D).

In vitro lipolysis experiments.

Isolated packed adipocytes were diluted to $1/20^{th}$ and incubated in Krebs-Ringer bicarbonate buffer with 2% free fatty acid albumin and 1g/l glucose containing forskolin (10^{-5} M) for maximal lipolysis determination. Incubations were carried out for 90 min. Glycerol was measured by free glycerol reagent (Sigma). Total lipid content was determined gravimetrically after organic extraction.

Flow cytometry analysis

One epididymal fat pad was digested by a cocktail of collagenases. Digested tissues were filtered through a 225 μm pore filter. The stromavascular fraction was separated from remaining fibrous material and floating adipocytes by centrifugation at 300g. The infranatant containing the collagenase solution was carefully removed using a long needle and syringe to pick up stromavascular fraction cells. Stromavascular fraction cells were then filtered through a 70 μm pore filter, followed by an incubation step in an erythrocyte lysing buffer. 10^6 cells were incubated 10 minutes at room temperature with Fcblock (BD Biosciences) in FACS buffer (PBS, 0.2% BSA, 2mM EDTA). Pools of specific fluorescent-labeled antibodies (PerCP-CD45, FITC-F4/80, APC-Cy7-CD11b, PE-Cy7-CD11c, APC-CD31, PE-CD34, FITC-Ly-6A/E, PE-CD3, FITC-CD4, APC-CD8 from BD Biosciences) were prepared and added to the stromavascular cell solution. After an incubation of 30 min on ice in the dark,

cells were washed with 2 mL of PBS and centrifuge at 300×g, 10 min at 4°C. Supernatant was discarded and the cell pellet was resuspended in 0.5ml of PBS.

RNA extraction and real-time PCR

Total RNA was extracted from epididymal white adipose pad using RNeasy kit (Qiagen) and quantified by Nanodrop spectrophotometer (ND-1000, Nanodrop Technologies). RNA (1 μg) was reverse-transcribed using the Multi-reverse Transcriptase (InVitrogen). Taqman probes for adipose triglyceride lipase (*Pnpla2*), collagen 1A1 (*Col1a1*), collagen 6A3 (*Col6a3*), EGF-like module receptor 1 (*Emr1;* F4/80), lumican (*Lum*), lysyl oxydase like 2 (*Loxl2*), mannose receptor C type1 (*Mrc1*), transforming growth factor β 1 (*Tgfβ1*), tumor necrosis factor alpha (*Tnfα*), vimentin (*Vim*) and *18S* were provided by Applied Biosystems (Assays-on-Demand Applied Biosystems). SYBR Green primers are listed in Table S2. The PCR mixtures were prepared with SYBR Green and TaqMan Universal PCR Master Mixes (Applied Biosystems). All amplification reactions were performed in duplicate from 5, 10 or 25 ng cDNA. Real-time PCR was run on an Applied Biosystems StepOne.

Western blot analysis

Epididymal AT were homogenized using the Precellys 24 apparatus (Bertin) in a buffer containing 50 mM Tris-HCl (pH 8.0), 150 mM NaCl, 1% NP40, 0.5% Sodium deoxycholate, 0.1% SDS, 10 μl/ml protease inhibitor, 10 μl/ml phosphatase I inhibitor and 10 μl/ml phosphatase II inhibitor. Tissue lysates were centrifuged at 14,000g for 30 min at 4°C, and supernatants were stored at -80°C. 30μg of solubilized proteins from AT were run on a 4-12% gradient SDS-PolyAcrylamide Gel Electrophoresis PAGE (Biorad) transferred onto nitrocellulose membrane (Hybond ECL, Amersham Biosciences) and incubated with primary antibodies for ATGL and HSL (Cell Signaling Technology) for lipases. Subsequently, immunoreactive proteins were determined by enhanced chemiluminescence reagent (SuperSignal West Dura Thermo Scientific) and visualized by exposure in the apparatus

Chemidoc (Biorad). For loading controls, proteins were detected directly with the Criterion Stain Free Gel imaging system (BioRad)

Histological analysis

The epididymal white AT was fixed with neutral-buffered formalin 10% for 24 h, embedded in paraffin, sectioned and stained with picrosirius dye. Fibrosis quantification was done after picrosirius staining using the software ImageJ.

For mast cells staining, slides were stained in toluidine blue solution (Sigma). Mast cells were counted on the basis of metachromatic staining of their cytoplasmic granules by toluidine blue.

Immunohistochemistry and immunofluorescence

For immunofluorescence, epididymal adipose fat serial sections were incubated overnight at room temperature in a humid chamber with anti-perilipin antiboby (GP 29 Progen) diluted at 1:200 in a solution containing 0.1% of BSA and 0.05% of Tween 20. After three washes in phosphate-buffered saline (PBS), immunofluorescence was revealed by incubation for 1h in the appropriate secondary antibody: Alexa Fluor568 anti-guinea pig diluted at 1:200. For nucleus staining, Hoechst 33342 (5 µg/ml) was added to section and stained for 5 min at room temperature. Slides were mounted and processed for microscope observation.

For immunohistochemistry, epididymal adipose fat serial sections were incubated overnight at room temperature in a humid chamber with anti-F4/80 antibody (AbD serotec) diluted at 10ng/µl. After three washes in TBS buffer, incubation for 1h in the appropriate secondary biotinylated antibody was performed. Staining was revealed with diaminobenzidine (DAB 1%).

Statistical analysis

All statistical analyses were performed using GraphPad Prism 5.0 for Windows (GraphPad Software Inc). Normal distribution of the data was tested with Kolmogorov-Smirnov tests.

Paired or Unpaired Student's t-tests were performed to determine differences between groups. Two-way ANOVA followed by Bonferonni's post hoc tests was applied when appropriate. Pearson correlations were applied when data were normally distributed and Spearman correlations for non-parametric data. All values in figures and tables are presented as mean ± SEM. Statistical significance was set at $p<0.05$.

SUPPLEMENTAL INFORMATION

Supplemental Information includes 4 figures and 2 Tables and can be found with this article online at

ACKNOWLEDGMENTS

We thank K. Louche, L. Mir, V. Bourlier and E. Mouisel (Institut National de la Santé et de la Recherche Médicale INSERM, Unité Mixte de Recherche UMR 1048) for outstanding help and critical reading of the manuscript.

I.K.V. was supported by fellowships from Inserm and Région Midi-Pyrénées. Grants to D.L. from Agence Nationale de la Recherche (LIPOB and OBELIP projects), Région Midi-Pyrénées, Fondation pour la Recherche Médicale, and the Commission of the European Communities (Projects HEPADIP and ADAPT). Grant to C.M. from Société Francophone du Diabète. We gratefully acknowledge the GenoToul Animal Care, Anexplo, Imagery-TRI and Quantitative Transcriptomics facilities.

References

Aoyama, T., Paik, Y.H., and Seki, E. (2010). Toll-like receptor signaling and liver fibrosis. Gastroenterol Res Pract *2010*.

Bataller, R., and Brenner, D.A. (2005). Liver fibrosis. J Clin Invest *115*, 209-218.

Bezaire, V., Mairal, A., Ribet, C., Lefort, C., Girousse, A., Jocken, J., Laurencikiene, J., Anesia, R., Rodriguez, A.M., Ryden, M., et al. (2009). Contribution of adipose triglyceride lipase and hormone-sensitive lipase to lipolysis in hMADS adipocytes. J Biol Chem *284*, 18282-18291.

Biernacka, A., Dobaczewski, M., and Frangogiannis, N.G. (2011). TGF-beta signaling in fibrosis. Growth Factors *29*, 196-202.

Bourlier, V., Sengenes, C., Zakaroff-Girard, A., Decaunes, P., Wdziekonski, B., Galitzky, J., Villageois, P., Esteve, D., Chiotasso, P., Dani, C., et al. (2012). TGFbeta family members are key mediators in the induction of myofibroblast phenotype of human adipose tissue progenitor cells by macrophages. PloS one *7*, e31274.

Campbell, M.T., Hile, K.L., Zhang, H., Asanuma, H., Vanderbrink, B.A., Rink, R.R., and Meldrum, K.K. (2011). Toll-like receptor 4: a novel signaling pathway during renal fibrogenesis. J Surg Res *168*, e61-69.

Cancello, R., Henegar, C., Viguerie, N., Taleb, S., Poitou, C., Rouault, C., Coupaye, M., Pelloux, V., Hugol, D., Bouillot, J.L., et al. (2005). Reduction of macrophage infiltration and chemoattractant gene expression changes in white adipose tissue of morbidly obese subjects after surgery-induced weight loss. Diabetes *54*, 2277-2286.

Cani, P.D., Amar, J., Iglesias, M.A., Poggi, M., Knauf, C., Bastelica, D., Neyrinck, A.M., Fava, F., Tuohy, K.M., Chabo, C., et al. (2007). Metabolic endotoxemia initiates obesity and insulin resistance. Diabetes *56*, 1761-1772.

Cinti, S., Mitchell, G., Barbatelli, G., Murano, I., Ceresi, E., Faloia, E., Wang, S., Fortier, M., Greenberg, A.S., and Obin, M.S. (2005). Adipocyte death defines macrophage localization and function in adipose tissue of obese mice and humans. Journal of lipid research *46*, 2347-2355.

Divoux, A., Moutel, S., Poitou, C., Lacasa, D., Veyrie, N., Aissat, A., Arock, M., Guerre-Millo, M., and Clement, K. (2012). Mast cells in human adipose tissue: link with morbid obesity, inflammatory status, and diabetes. J Clin Endocrinol Metab *97*, E1677-1685.

Divoux, A., Tordjman, J., Lacasa, D., Veyrie, N., Hugol, D., Aissat, A., Basdevant, A., Guerre-Millo, M., Poitou, C., Zucker, J.D., et al. (2010). Fibrosis in human adipose tissue: composition, distribution, and link with lipid metabolism and fat mass loss. Diabetes *59*, 2817-2825.

Erridge, C. (2010). Endogenous ligands of TLR2 and TLR4: agonists or assistants? J Leukoc Biol *87*, 989-999.

Gandotra, S., Le Dour, C., Bottomley, W., Cervera, P., Giral, P., Reznik, Y., Charpentier, G., Auclair, M., Delepine, M., Barroso, I., et al. (2011). Perilipin deficiency and autosomal dominant partial lipodystrophy. N Engl J Med *364*, 740-748.

Gautier, T., Klein, A., Deckert, V., Desrumaux, C., Ogier, N., Sberna, A.L., Paul, C., Le Guern, N., Athias, A., Montange, T., et al. (2008). Effect of plasma phospholipid transfer protein deficiency on lethal endotoxemia in mice. J Biol Chem *283*, 18702-18710.

Henegar, C., Tordjman, J., Achard, V., Lacasa, D., Cremer, I., Guerre-Millo, M., Poitou, C., Basdevant, A., Stich, V., Viguerie, N., et al. (2008). Adipose tissue transcriptomic signature highlights the pathological relevance of extracellular matrix in human obesity. Genome Biol *9*, R14.

Horng, T., and Hotamisligil, G.S. (2011). Linking the inflammasome to obesity-related disease. Nat Med *17*, 164-165.

Hoshino, K., Takeuchi, O., Kawai, T., Sanjo, H., Ogawa, T., Takeda, Y., Takeda, K., and Akira, S. (1999). Cutting edge: Toll-like receptor 4 (TLR4)-deficient mice are hyporesponsive to lipopolysaccharide: evidence for TLR4 as the Lps gene product. J Immunol *162*, 3749-3752.

Hotamisligil, G.S., Shargill, N.S., and Spiegelman, B.M. (1993). Adipose expression of tumor necrosis factor-alpha: direct role in obesity-linked insulin resistance. Science *259*, 87-91.

Keophiphath, M., Achard, V., Henegar, C., Rouault, C., Clement, K., and Lacasa, D. (2009). Macrophage-secreted factors promote a profibrotic phenotype in human preadipocytes. Mol Endocrinol *23*, 11-24.

Khan, T., Muise, E.S., Iyengar, P., Wang, Z.V., Chandalia, M., Abate, N., Zhang, B.B., Bonaldo, P., Chua, S., and Scherer, P.E. (2009). Metabolic Dysregulation and Adipose Tissue Fibrosis: Role of Collagen VI. Molecular and Cellular Biology *29*, 1575-1591.

Kim, J.Y., van de Wall, E., Laplante, M., Azzara, A., Trujillo, M.E., Hofmann, S.M., Schraw, T., Durand, J.L., Li, H., Li, G., et al. (2007). Obesity-associated improvements in metabolic profile through expansion of adipose tissue. J Clin Invest *117*, 2621-2637.

Klimcakova, E., Roussel, B., Kovacova, Z., Kovacikova, M., Siklova-Vitkova, M., Combes, M., Hejnova, J., Decaunes, P., Maoret, J.J., Vedral, T., et al. (2011a). Macrophage gene expression is related to obesity and the metabolic syndrome in human subcutaneous fat as well as in visceral fat. Diabetologia *54*, 876-887.

Klimcakova, E., Roussel, B., Marquez-Quinones, A., Kovacova, Z., Kovacikova, M., Combes, M., Siklova-Vitkova, M., Hejnova, J., Sramkova, P., Bouloumie, A., et al. (2011b). Worsening of obesity and metabolic status yields similar molecular adaptations in human subcutaneous and visceral adipose tissue: decreased metabolism and increased immune response. J Clin Endocrinol Metab *96*, E73-82.

Kusminski, C.M., Holland, W.L., Sun, K., Park, J., Spurgin, S.B., Lin, Y., Askew, G.R., Simcox, J.A., McClain, D.A., Li, C., et al. (2012). MitoNEET-driven alterations in adipocyte mitochondrial activity reveal a crucial adaptive process that preserves insulin sensitivity in obesity. Nat Med *18*, 1539-1549.

Kwon, E.Y., Shin, S.K., Cho, Y.Y., Jung, U.J., Kim, E., Park, T., Park, J.H., Yun, J.W., McGregor, R.A., Park, Y.B., et al. (2012). Time-course microarrays reveal early activation of the immune transcriptome and adipokine dysregulation leads to fibrosis in visceral adipose depots during diet-induced obesity. BMC Genomics *13*, 450.

Li, M., Matsunaga, N., Hazeki, K., Nakamura, K., Takashima, K., Seya, T., Hazeki, O., Kitazaki, T., and Iizawa, Y. (2006). A novel cyclohexene derivative, ethyl (6R)-6-[N-(2-Chloro-4-fluorophenyl)sulfamoyl]cyclohex-1-ene-1-carboxylate (TAK-242), selectively inhibits toll-like receptor 4-mediated cytokine production through suppression of intracellular signaling. Mol Pharmacol *69*, 1288-1295.

Liu, J., Divoux, A., Sun, J., Zhang, J., Clement, K., Glickman, J.N., Sukhova, G.K., Wolters, P.J., Du, J., Gorgun, C.Z., et al. (2009). Genetic deficiency and pharmacological stabilization of mast cells reduce diet-induced obesity and diabetes in mice. Nat Med *15*, 940-945.

Medina-Gomez, G., Gray, S.L., Yetukuri, L., Shimomura, K., Virtue, S., Campbell, M., Curtis, R.K., Jimenez-Linan, M., Blount, M., Yeo, G.S., et al. (2007). PPAR gamma 2 prevents lipotoxicity by controlling adipose tissue expandability and peripheral lipid metabolism. PLoS Genet *3*, e64.

Midwood, K., Sacre, S., Piccinini, A.M., Inglis, J., Trebaul, A., Chan, E., Drexler, S., Sofat, N., Kashiwagi, M., Orend, G., et al. (2009). Tenascin-C is an endogenous activator of Toll-like receptor 4 that is essential for maintaining inflammation in arthritic joint disease. Nat Med *15*, 774-780.

Nguyen, M.T., Favelyukis, S., Nguyen, A.K., Reichart, D., Scott, P.A., Jenn, A., Liu-Bryan, R., Glass, C.K., Neels, J.G., and Olefsky, J.M. (2007). A subpopulation of macrophages infiltrates hypertrophic adipose tissue and is activated by free fatty acids via Toll-like receptors 2 and 4 and JNK-dependent pathways. J Biol Chem *282*, 35279-35292.

Pajvani, U.B., Trujillo, M.E., Combs, T.P., Iyengar, P., Jelicks, L., Roth, K.A., Kitsis, R.N., and Scherer, P.E. (2005). Fat apoptosis through targeted activation of caspase 8: a new mouse model of inducible and reversible lipoatrophy. Nat Med *11*, 797-803.

Pardo, A., and Selman, M. (2006). Matrix metalloproteases in aberrant fibrotic tissue remodeling. Proc Am Thorac Soc *3*, 383-388.

Poggi, M., Bastelica, D., Gual, P., Iglesias, M.A., Gremeaux, T., Knauf, C., Peiretti, F., Verdier, M., Juhan-Vague, I., Tanti, J.F., et al. (2007). C3H/HeJ mice carrying a toll-like receptor 4 mutation are protected against the development of insulin resistance in white adipose tissue in response to a high-fat diet. Diabetologia *50*, 1267-1276.

Pussinen, P.J., Havulinna, A.S., Lehto, M., Sundvall, J., and Salomaa, V. (2011). Endotoxemia is associated with an increased risk of incident diabetes. Diabetes Care *34*, 392-397.

Rossmeislova, L., Malisova, L., Kracmerova, J., Tencerova, M., Kovacova, Z., Koc, M., M, S.I.-V., Viquerie, N., Langin, D., and Stich, V. (2013). Weight loss improves adipogenic capacity of human preadipocytes and modulates their secretory profile. Diabetes.

Rubio-Cabezas, O., Puri, V., Murano, I., Saudek, V., Semple, R.K., Dash, S., Hyden, C.S., Bottomley, W., Vigouroux, C., Magre, J., et al. (2009). Partial lipodystrophy and insulin resistant diabetes in a patient with a homozygous nonsense mutation in CIDEC. EMBO Mol Med *1*, 280-287.

Saberi, M., Woods, N.B., de Luca, C., Schenk, S., Lu, J.C., Bandyopadhyay, G., Verma, I.M., and Olefsky, J.M. (2009). Hematopoietic Cell-Specific Deletion of Toll-like Receptor 4

Ameliorates Hepatic and Adipose Tissue Insulin Resistance in High-Fat-Fed Mice. Cell Metabolism *10*, 419-429.

Seki, E., De Minicis, S., Osterreicher, C.H., Kluwe, J., Osawa, Y., Brenner, D.A., and Schwabe, R.F. (2007). TLR4 enhances TGF-beta signaling and hepatic fibrosis. Nat Med *13*, 1324-1332.

Shi, H., Kokoeva, M.V., Inouye, K., Tzameli, I., Yin, H., and Flier, J.S. (2006). TLR4 links innate immunity and fatty acid-induced insulin resistance. J Clin Invest *116*, 3015-3025.

Spencer, M., Yao-Borengasser, A., Unal, R., Rasouli, N., Gurley, C.M., Zhu, B., Peterson, C.A., and Kern, P.A. (2010). Adipose tissue macrophages in insulin-resistant subjects are associated with collagen VI and fibrosis and demonstrate alternative activation. American journal of physiology *299*, E1016-1027.

Stramer, B.M., Mori, R., and Martin, P. (2007). The inflammation-fibrosis link? A Jekyll and Hyde role for blood cells during wound repair. J Invest Dermatol *127*, 1009-1017.

Strissel, K.J., Stancheva, Z., Miyoshi, H., Perfield, J.W., 2nd, DeFuria, J., Jick, Z., Greenberg, A.S., and Obin, M.S. (2007). Adipocyte death, adipose tissue remodeling, and obesity complications. Diabetes *56*, 2910-2918.

Suganami, T., Mieda, T., Itoh, M., Shimoda, Y., Kamei, Y., and Ogawa, Y. (2007). Attenuation of obesity-induced adipose tissue inflammation in C3H/HeJ mice carrying a Toll-like receptor 4 mutation. Biochem Biophys Res Commun *354*, 45-49.

Tsukumo, D.M., Carvalho-Filho, M.A., Carvalheira, J.B., Prada, P.O., Hirabara, S.M., Schenka, A.A., Araujo, E.P., Vassallo, J., Curi, R., Velloso, L.A., et al. (2007). Loss-of-function mutation in Toll-like receptor 4 prevents diet-induced obesity and insulin resistance. Diabetes *56*, 1986-1998.

Virtue, S., and Vidal-Puig, A. (2008). It's not how fat you are, it's what you do with it that counts. PLoS Biol *6*, e237.

Weisberg, S.P., McCann, D., Desai, M., Rosenbaum, M., Leibel, R.L., and Ferrante, A.W. (2003). Obesity is associated with macrophage accumulation in adipose tissue. Journal of Clinical Investigation *112*, 1796-1808.

Wellen, K.E., and Hotamisligil, G.S. (2003). Obesity-induced inflammatory changes in adipose tissue. J Clin Invest *112*, 1785-1788.

Wu, F., Vij, N., Roberts, L., Lopez-Briones, S., Joyce, S., and Chakravarti, S. (2007). A novel role of the lumican core protein in bacterial lipopolysaccharide-induced innate immune response. J Biol Chem *282*, 26409-26417.

Wynn, T.A. (2008). Cellular and molecular mechanisms of fibrosis. J Pathol *214*, 199-210.

Wynn, T.A., and Barron, L. (2011). Macrophages: master regulators of inflammation and fibrosis. Semin Liver Dis *30*, 245-257.

Xu, H., Barnes, G.T., Yang, Q., Tan, G., Yang, D., Chou, C.J., Sole, J., Nichols, A., Ross, J.S., Tartaglia, L.A., et al. (2003). Chronic inflammation in fat plays a crucial role in the development of obesity-related insulin resistance. J Clin Invest *112*, 1821-1830.

Figure Legends

Figure 1. Fibrosis Appearance during Obesity in Human (A-D) and Mouse Adipose Tissues (E-H)

(A) Centroid analysis of 18 fibrosis pathway genes in subcutaneous adipose tissue from lean (LE), obese (OB) and obese with metabolic syndrome (OB/MS) individuals (n=8 per group).

(B) mRNA levels of fibrosis genes in human adipose tissue (n=8 per group).

(C) Expression of fibrosis genes in adipocytes and stromavascular fraction (SVF) of human adipose tissue (n=5 per group).

(D) Changes during human preadipocyte differentiation of extracellular matrix gene expression (n=9).

(E) Centroid analysis of 9 fibrosis pathway genes in mouse adipose tissue (n=6 per group).

(F) mRNA levels of fibrosis genes in adipose tissue of C3H/HeOuJ mice fed normal chow diet (NCD) and high fat diet (HFD) for 4 weeks (n=6 per group).

(G) Expression of fibrosis genes in adipocytes and stromavascular fraction (SVF) of C3H/HeOuJ mouse adipose tissue (n=6 per group).

(H) mRNA levels of fibrosis genes in adipose tissue of C57BL/6J mice fed NCD or HFD for 15 weeks (n=7 per group).

Values represent mean ± SEM *$p<0.05$, ** $p<0.01$, *** $p<0.001$.

Figure 2. Time Course Study Shows Development of Fibrosis and Inflammation in Wild Type (WT) but not in TLR4^{mut} Mouse Adipose Tissue During High Fat Diet (HFD)

(A) mRNA levels of fibrosis genes (n=8 per group).

(B) Representative picrosirius red slides (x100) showing collagen fiber deposition at 12 weeks of HFD and quantitation of fibrosis area at different time points (n=8 per group).

(C) Representative picrosirius red slides (x100) after chronic treatment with TAK242 or vehicle (DMSO) in WT mice and quantitation of fibrosis area at 8 weeks of HFD (n=10 per group).

(D) mRNA levels of the macrophage marker *Emr1* (F4/80) (n=8 per group).

(E) Quantitation of stromavascular fraction cell types by flow cytometry at 8 weeks of HFD (n=8 per group).

(F) Representative staining (x1000) and quantitation of F4/80 positive crown-like structures (n=8 per group).

(G) Correlation between *Emr1* and *Col6a3* mRNA levels.

Values represent mean ± SEM. *$p<0.05$, ** $p<0.01$, *** $p<0.001$.

Figure 3. High Fat Diet (HFD) Induces Progressive Metabolic and Morphological Alterations in Adipocytes from Wild Type (WT) but not TLR4^{mut} Mice

(A) mRNA levels of metabolic genes (n=8 per group).

(B) Representative Western blot and quantitation of hormone-sensitive lipase (HSL) and adipose triglyceride lipase (ATGL) (n=8 per group).

(C) Glycerol release during *in vitro* lipolysis experiments on isolated adipocytes at 8 weeks of HFD (n=6 per group).

(D) Correlation between *Col6a3* and metabolic gene mRNA levels.

(E) Frequency of adipocyte diameter observed at 12 weeks of HFD (n=8 per group).

(F) Representative immunofluorescence of perilipin 1 staining (x200) and quantitation of perilipin-negative cells at 12 weeks of HFD (n=8 per group).

(G) Epididymal fat pad weight at 8 and 12 weeks of HFD (n=8 per group).

(H) Plasma FABP4 level after 12 weeks of HFD (n=8 per group).

Values represent mean ± SEM. *p<0.05, ** p<0.01, *** p<0.001.

Figure 4. Hematopoietic Cell-Competent TLR4 Induces Fibrosis and Inflammation in TLR4^{mut} Mouse Adipose Tissue Fed High Fat Diet (HFD). Bone marrow transplantation (BMT) of donor cells from wild type (WT) or mutated TLR4 (TLR4^{mut}) mouse was performed into irradiated recipient TLR4^{mut} mice (BMT-TLR4^{mut}/TLR4^{mut} and BMT-WT/TLR4^{mut} mice).

(A) mRNA levels of fibrosis genes.

(B) Representative picrosirius red slides (x100) showing collagen fiber deposition and quantitation of fibrosis area at 8 weeks of HFD.

(C) mRNA levels of inflammatory genes.

(D) Quantitation of stromavascular fraction cell types by flow cytometry at 8 weeks of HFD.

Values represent mean ± SEM (n=8 per group). $^{\$}$p<0.06, *p<0.05 ,** p<0.01, *** p<0.001. BMT-WT/TLR4^{mut} *vs*. BMT-TLR4^{mut}/TLR4^{mut}.

Figure 5. Insulin sensitivity is associated with adipose tissue fibrosis in humans and mice

(A) QUICKI values in lean (LE), obese (OB) and obese with metabolic syndrome (OB/MS) individuals (n=8 per group).

(B) Correlation between QUICKI and mean centroid of 18 fibrosis pathway genes (n=24).

(C) Insulin tolerance test and weight gain after 8 weeks of high fat diet (n=8 per group)

(D) Correlation between QUICKI and quantitation of fibrosis area by picrosirius staining (n=16).

(E) Glucose tolerance test and body weight after 8 weeks of high fat diet (n=8 per group)

(F) Correlation between insulin x glucose levels and quantitation of fibrosis area by picrosirius staining (n=16).

Values represent mean ± SEM. *p<0.05, ** p<0.01, *** p<0.001

Figure 6. Chronic Lipopolysaccharide Infusion Promotes Adipose Tissue Fibrosis

(A) Fasting plasma lipopolysaccharide (LPS) levels after 4 weeks of saline or LPS infusion.

(B) Body weight after 4 weeks of LPS infusion.

(C) mRNA levels of fibrosis genes.

(D) Representative picrosirius red slides (x100) showing collagen fiber deposition and quantitation of fibrosis area.

(E) mRNA levels of inflammatory genes.

(F) Quantitation of stromavascular fraction cell types by flow cytometry.

Values represent mean ± SEM (n=8 per group). *p<0.05, ** p<0.01, *** p<0.001.

SUPPLEMENTAL INFORMATION

Immune Cell Toll-like Receptor 4 Mediates the Development of Obesity-associated Adipose Tissue Fibrosis

Isabelle K. Vila, Pierre-Marie Badin, Marie-Adeline Marques, Laurent Monbrun, Corinne Lefort, Balbine Roussel, Philippe Gui, Jacques Grober, Vladimír Štich, Lenka Rossmeislová, Alexia Zakaroff-Girard, Anne Bouloumié, Cedric Moro, Geneviève Tavernier, Dominique Langin

SUPPLEMENTAL TABLE

Supplemental Table 1.

Human	*COL1A2, COL3A1, COL5A2, COL6A1, COL6A2, COL6A3, COL8A2, COL12A1, COL16A1; FN1, LOX, LOXL1, LOXL2, LUM, MMP2, MMP9, TGFβ1, TIMP1*

Mouse	*Col1a1, Col6a3, Ctgf, Decorin, Loxl2, Lum, Tnc, Tgfβ1, Vim*

List of fibrosis genes used in centroid analyses.

Supplemental Table 2.

Gene	FW	Rev
Lipe	5'-ACT CAA CAG CCT GGC AAA AT-3'	5'-AGG TCA CAG TGC TTG ACA GC-3'
Mcp-1	5'-ACT GAA GCC AGC TCT CTC TTC CTC-3'	5'-TTC CTT CTT GGG GTC AGC ACA GAC-3'
Mmp2	5'-GCT GAT ACT GAC ACT GGT ACT G-3'	5'-CAA TCT TTT CTG GGA GCT C-3'
Mmp9	5'-CGT CGT GAT CCC CAC TTA CT-3'	5'-AGA GTA CTG CTT GCC CAG GA-3'
Pparα	5'-AGT TCA CGC ATG TGA AGG CTG-3'	5'-TGT TCC GGT TCT TCT TCT GAA TC-3'
Pparγ	5'-CAT AAA GTC CTT CCC GCT GA-3'	5'-GAA ACT GGC ACC CTT GAA AA-3'
Tnc	5'-CAG ACT CAG CCA TCA CCA AC-3'	5'-CAG TTA ACG CCC TGA CTG TG-3'

Oligonucleotides sequences used in real-time PCR analysis

SUPPLEMENTAL FIGURE LEGENDS

Figure S1. Expression of Fibrosis Genes in Visceral Human Adipose Tissue and C57Bl/6J Mouse Adipose Tissue

(A) Centroid analysis of 18 fibrosis pathway genes in visceral adipose tissue from lean (LE), obese (OB) and obese with metabolic syndrome (OB/MS) individuals (n=8 per group).

(B) Expression of fibrosis genes in adipocytes and stromavascular fraction (SVF) of C57Bl/6J mouse adipose tissue (n=8 per group).

Values represent mean ± SEM $<0.1, *p<0.05, ** p<0.01, *** p<0.001.

Figure S2. Development of Fibrosis and Inflammation in Wild Type (WT) and TLR4^{mut} Mouse Adipose Tissue

(A) mRNA levels of fibrosis genes during high fat diet (HFD) (n=8 per group).

(B) Correlation between *Tfgβ1* and fibrosis genes mRNA levels.

(C) mRNA levels of fibrosis genes on normal chow diet (n=6).

(D) mRNA levels of inflammatory genes during HFD (n=8 per group).

(E) Representative toluidine blue slides showing mast cells and quantitation mast cells per mm² at 8 weeks of HFD (n=8 per group).

Values represent mean ± SEM *p<0.05, ** p<0.01, *** p<0.001.

Figure S3. mRNA Levels of Metabolic Genes in Wild Type (WT) and TLR4^{mut} Mouse Adipose Tissue during High Fat Diet (HFD)

Values represent mean ± SEM (n=8 per group). *p<0.05, ** p<0.01, *** p<0.001.

Figure S4. Effect of Bone Marrow Transplantation (BMT) of Wild Type (WT) and TLR4^{mut} Hematopoietic Cells in TLR4^{mut} Mice

(A) Hematopoietic cell lineage distribution.

(B) Agarose gel (2%) showing amplification of specific TLR4 PCR products from blood cells (left panel) and adipose tissue macrophages (right panel).

SUPPLEMENTAL EXPERIMENTAL PROCEDURES

TLR4 expression in blood cells and adipose tissue macrophages

Total DNA was extracted from blood cells of BMT mice (DNeasy Blood and tissue kit, Qiagen). Stromavascular fraction cells were isolated from epididymal AT after collagenase digestion. Progenitor cells were first removed (EasySep Mouse Sca1-PE, STEM CELL) then AT macrophages were selected (EasySep Mouse CD11b-PE, STEM CELL). Total DNA was extracted from AT macrophages. Designed sequences were used to amplify TLR4 area of interest containing the point mutation: TLR4 FW- GGG TCA AGG AAC AGA AGC AG, Rev- TGT CCT CCC ATT CCA GGT AG. We obtained an amplicon of 623bp where the point mutation unmasks a recognition site for the restriction enzyme NlaIII (New England biolabs). Overnight enzyme digestion on PCR products permitted to obtained two differents profiles: 3 fragments (447-128-48 bp) for WT and 4 fragments (320-128-127-48 bp) for TLR^{mut} .

Figure 1

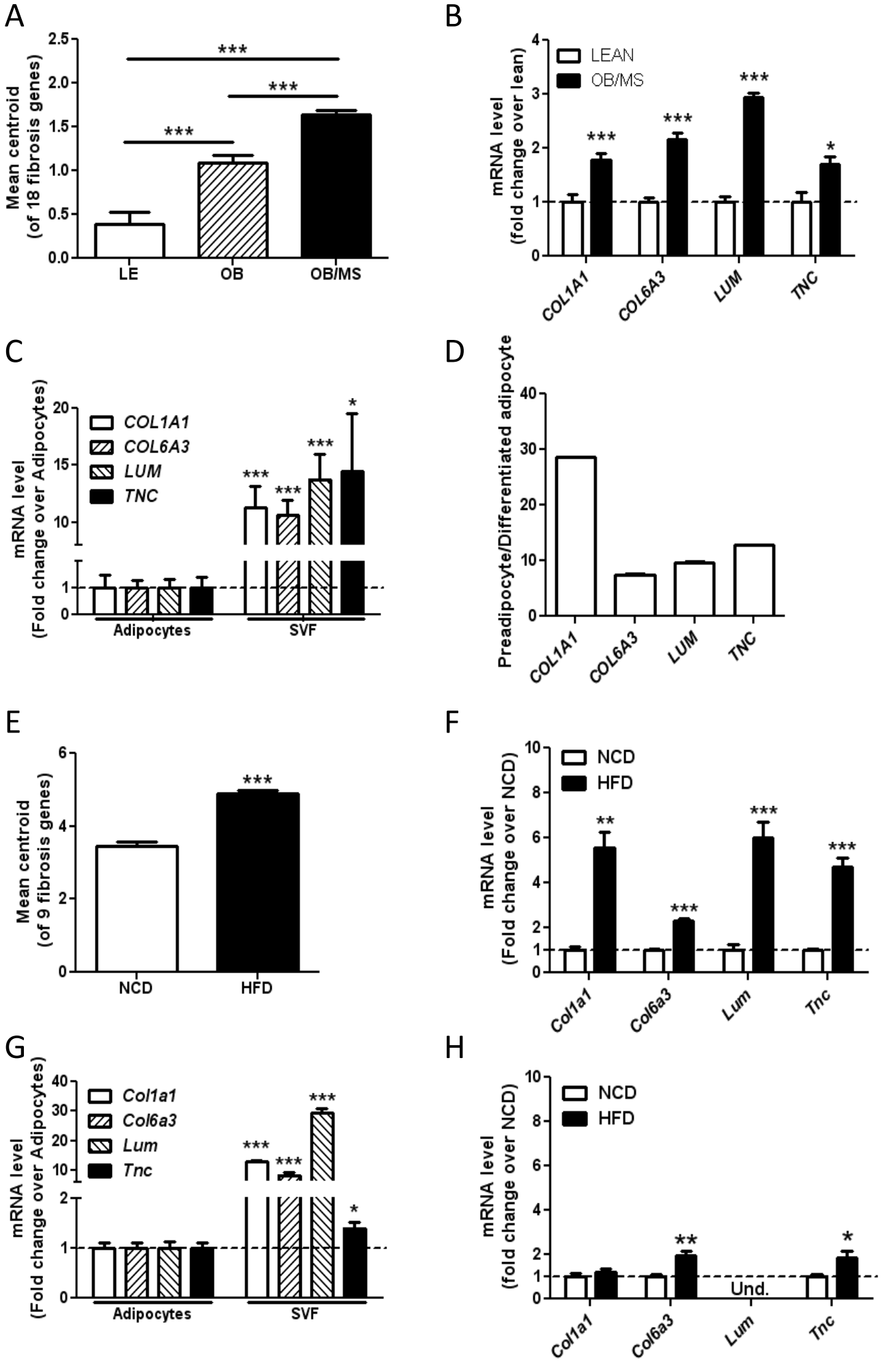
A
Mean centroid (of 18 fibrosis genes)
LE
OB
OB/MS
B
LEAN
OB/MS
mRNA level (fold change over lean)
COL1A1
COL6A3
LUM
TNC
C
mRNA level (Fold change over Adipocytes)
COL1A1
COL6A3
LUM
TNC
Adipocytes
SVF
D
Preadipocyte/Differentiated adipocyte
COL1A1
COL6A3
LUM
TNC
E
Mean centroid (of 9 fibrosis genes)
NCD
HFD
F
NCD
HFD
mRNA level (Fold change over NCD)
Col1a1
Col6a3
Lum
Tnc
G
mRNA level (Fold change over Adipocytes)
Col1a1
Col6a3
Lum
Tnc
Adipocytes
SVF
H
NCD
HFD
mRNA level (fold change over NCD)
Und.
Col1a1
Col6a3
Lum
Tnc

Figure 2

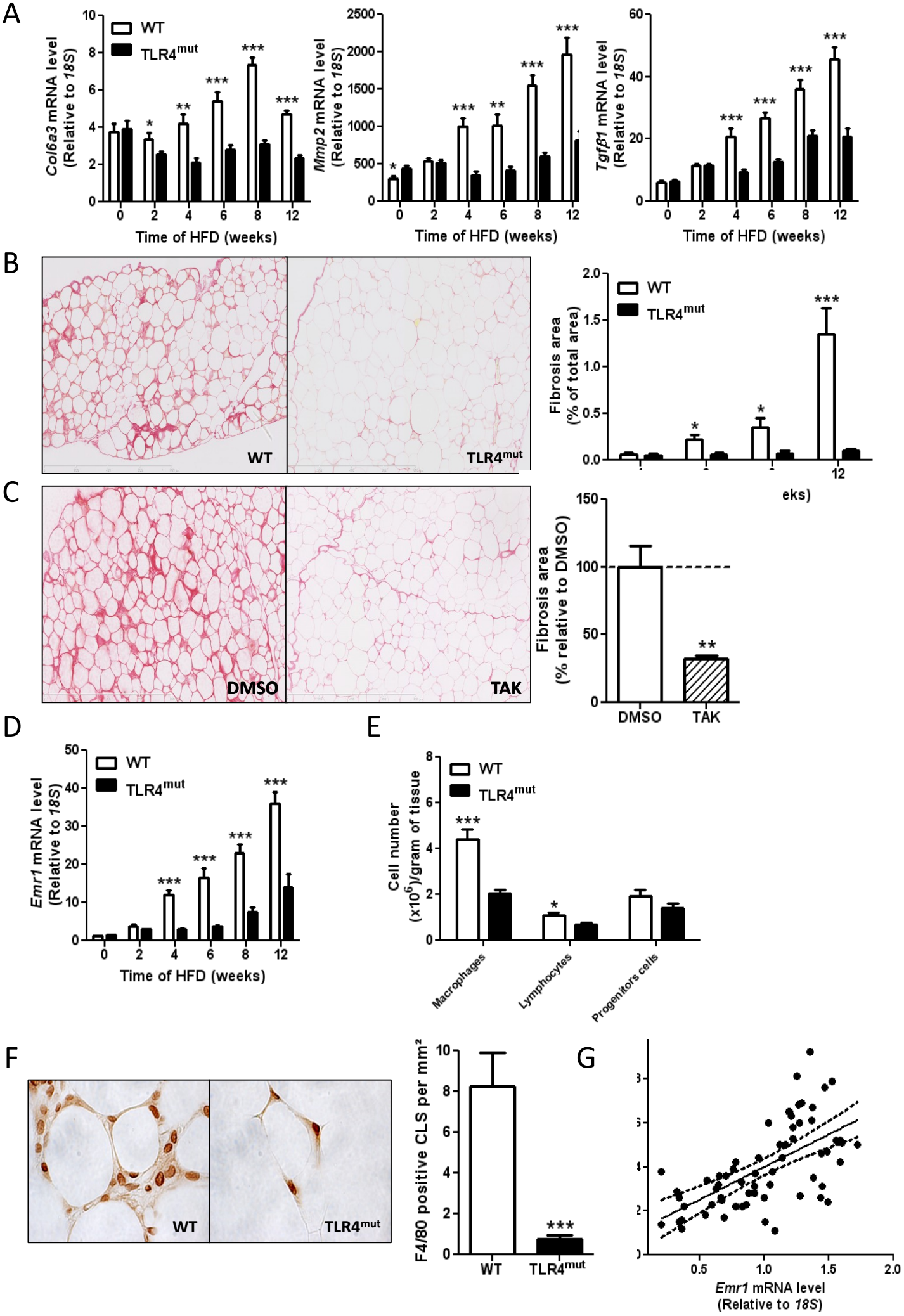
A
WT
TLR4mut
Col6a3 mRNA level (Relative to 18S)
Mmp2 mRNA level (Relative to 18S)
Tgfβ1 mRNA level (Relative to 18S)
Time of HFD (weeks)
B
WT
TLR4mut
Fibrosis area (% of total area)
C
DMSO
TAK
Fibrosis area (% relative to DMSO)
D
Emr1 mRNA level (Relative to 18S)
Time of HFD (weeks)
E
Cell number (x10^6)/gram of tissue
Macrophages
Lymphocytes
Progenitors cells
F
F4/80 positive CLS per mm²
G
Emr1 mRNA level (Relative to 18S)

Figure 3

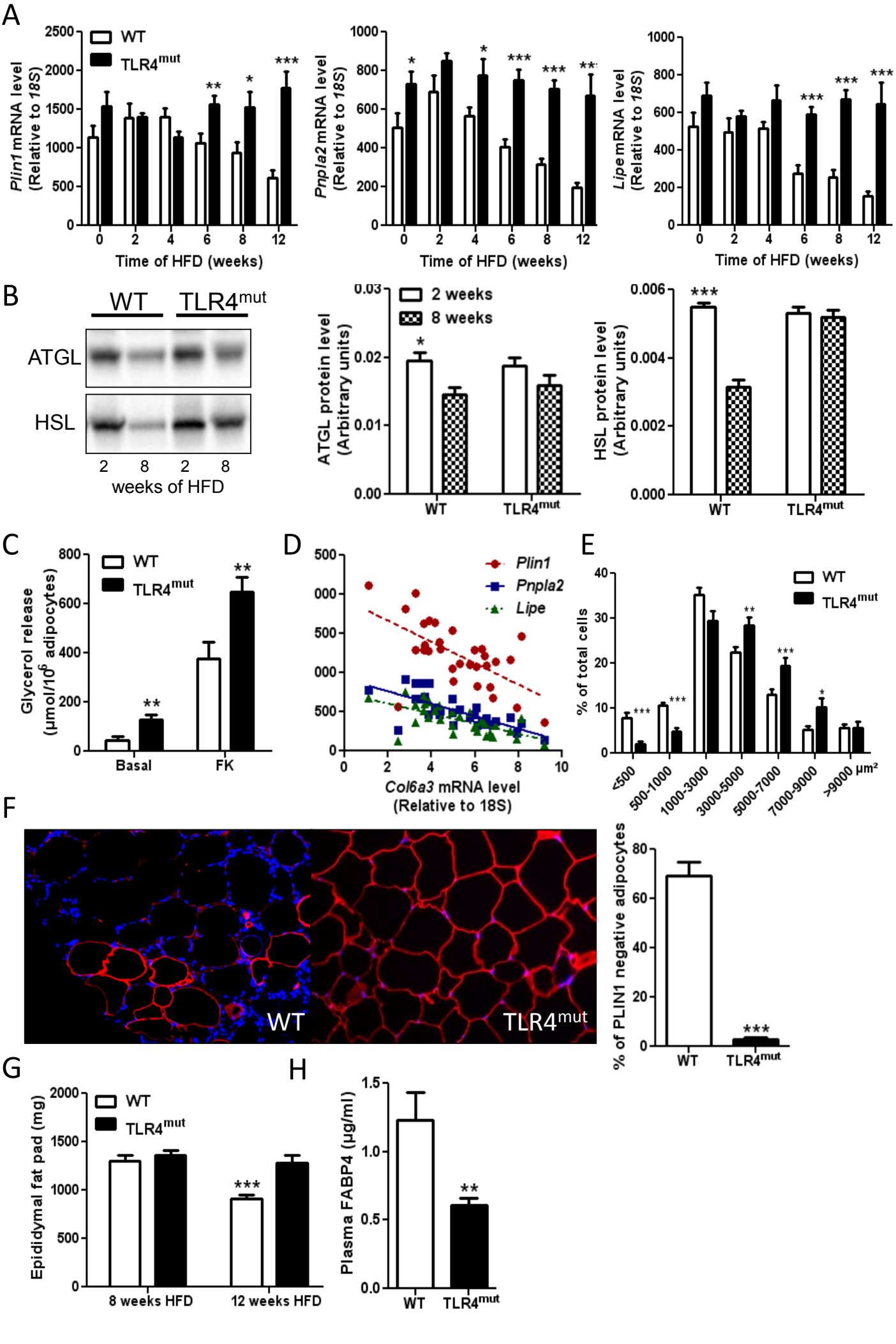
A
WT
TLR4mut
Plin1 mRNA level (Relative to 18S)
Pnpla2 mRNA level (Relative to 18S)
Lipe mRNA level (Relative to 18S)
Time of HFD (weeks)
B
WT
TLR4mut
ATGL
HSL
2 8 2 8
weeks of HFD
2 weeks
8 weeks
ATGL protein level (Arbitrary units)
HSL protein level (Arbitrary units)
C
Glycerol release (µmol/10^6 adipocytes)
Basal
FK
D
Plin1
Pnpla2
Lipe
Col6a3 mRNA level (Relative to 18S)
E
% of total cells
<500
500-1000
1000-3000
3000-5000
5000-7000
7000-9000
>9000 µm²
F
WT
TLR4mut
% of PLIN1 negative adipocytes
G
Epididymal fat pad (mg)
8 weeks HFD
12 weeks HFD
H
Plasma FABP4 (µg/ml)

Figure 4

A

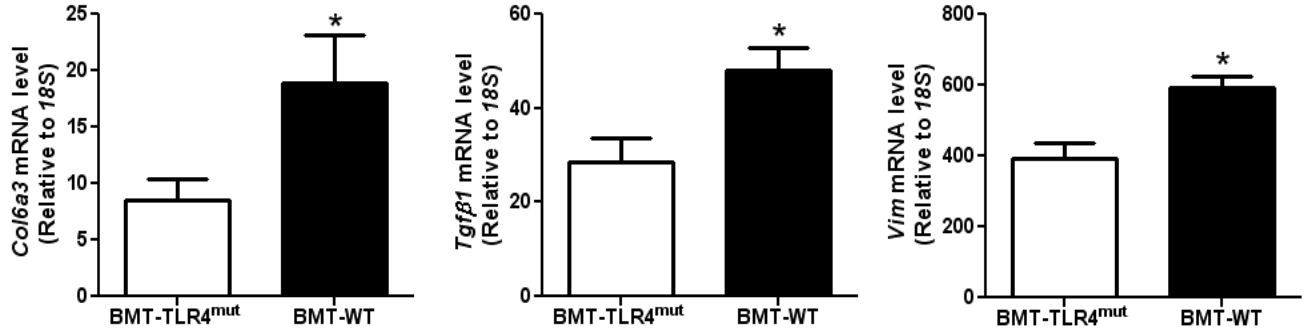

B

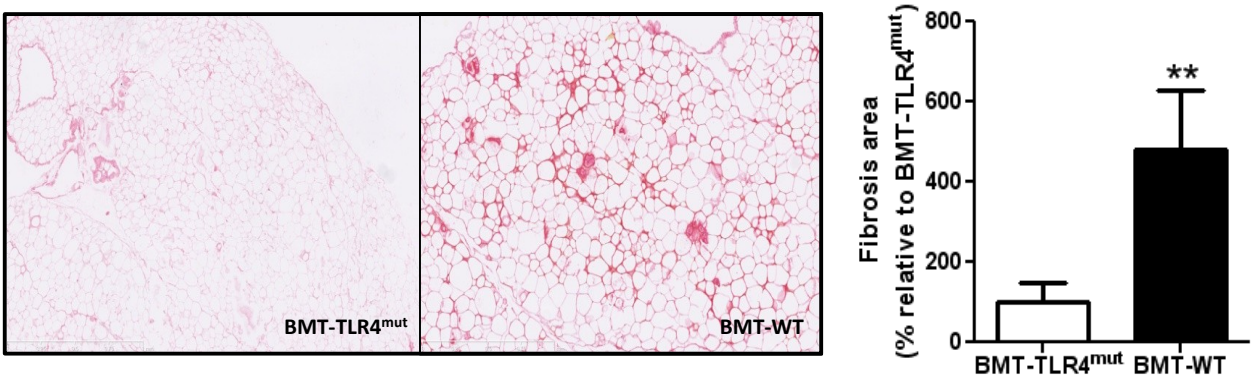

C

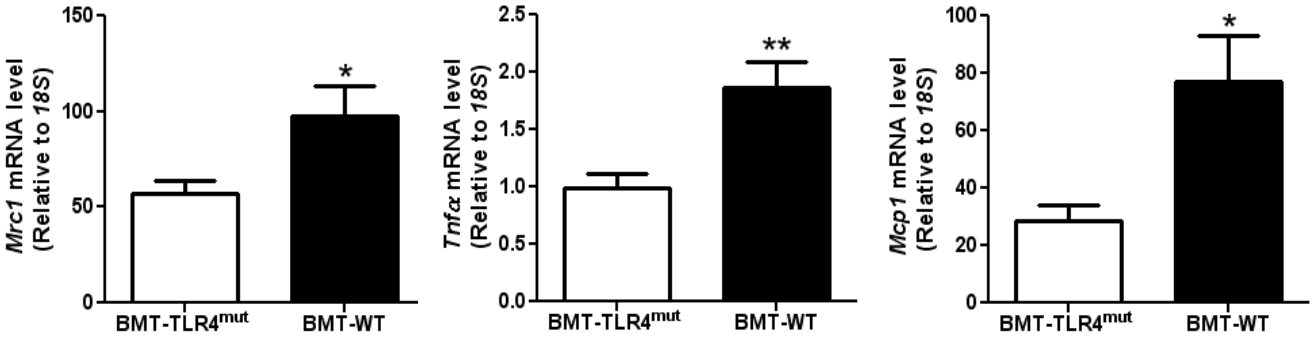

D

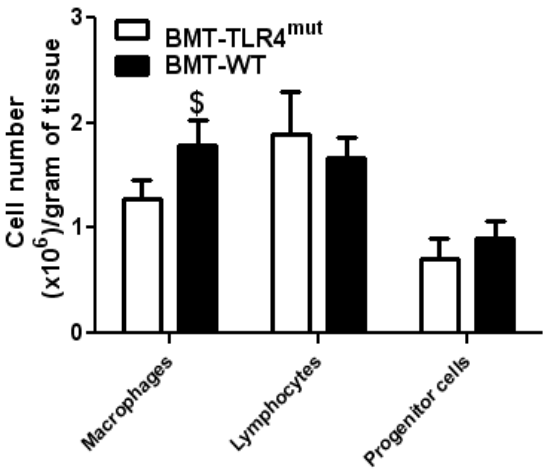

Figure 5

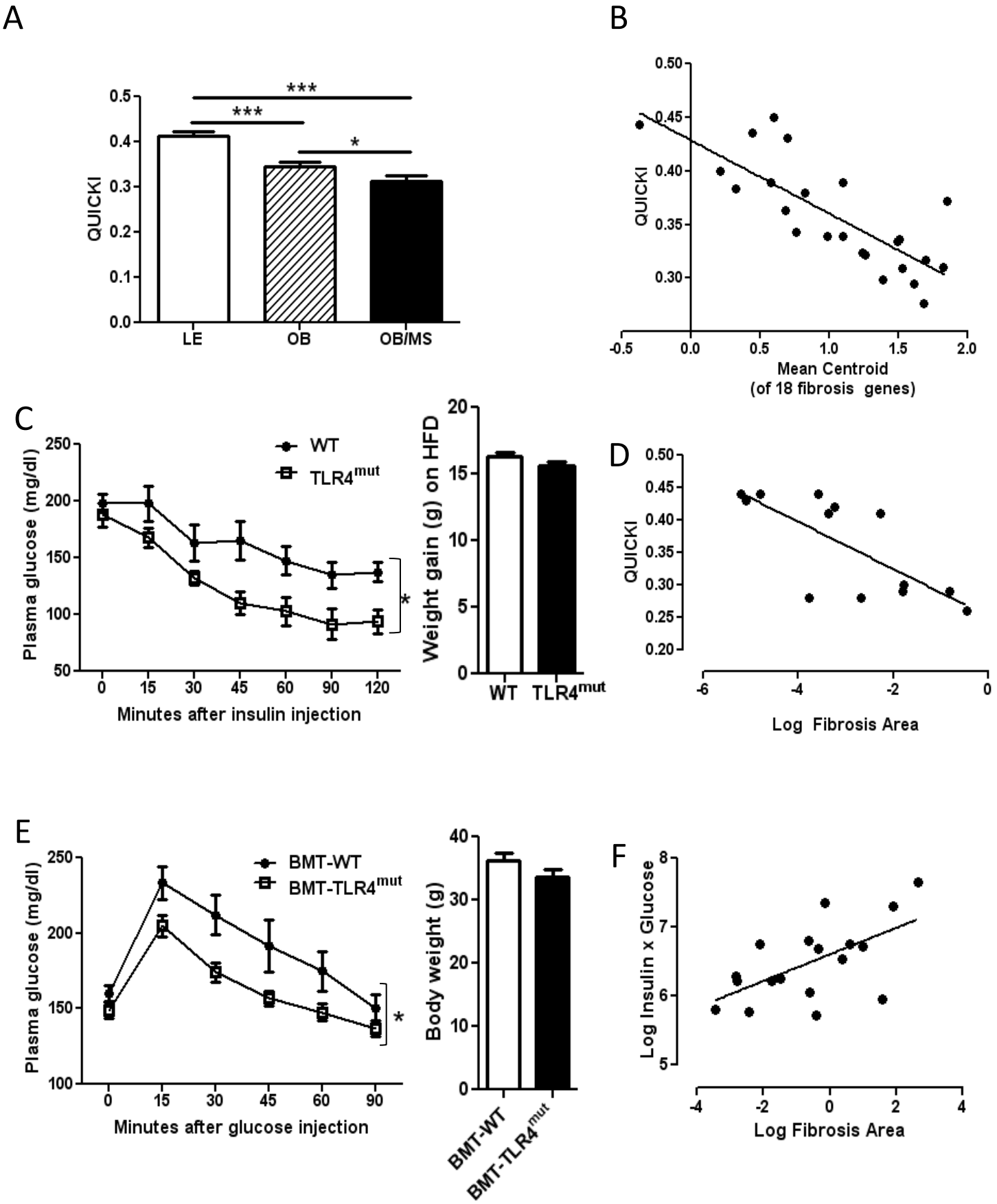
A
B
C
D
E
F
QUICKI
LE
OB
OB/MS
***
***
*
Mean Centroid
(of 18 fibrosis genes)
Plasma glucose (mg/dl)
WT
TLR4mut
Minutes after insulin injection
Weight gain (g) on HFD
Log Fibrosis Area
BMT-WT
BMT-TLR4mut
Minutes after glucose injection
Body weight (g)
Log Insulin x Glucose

Figure 6

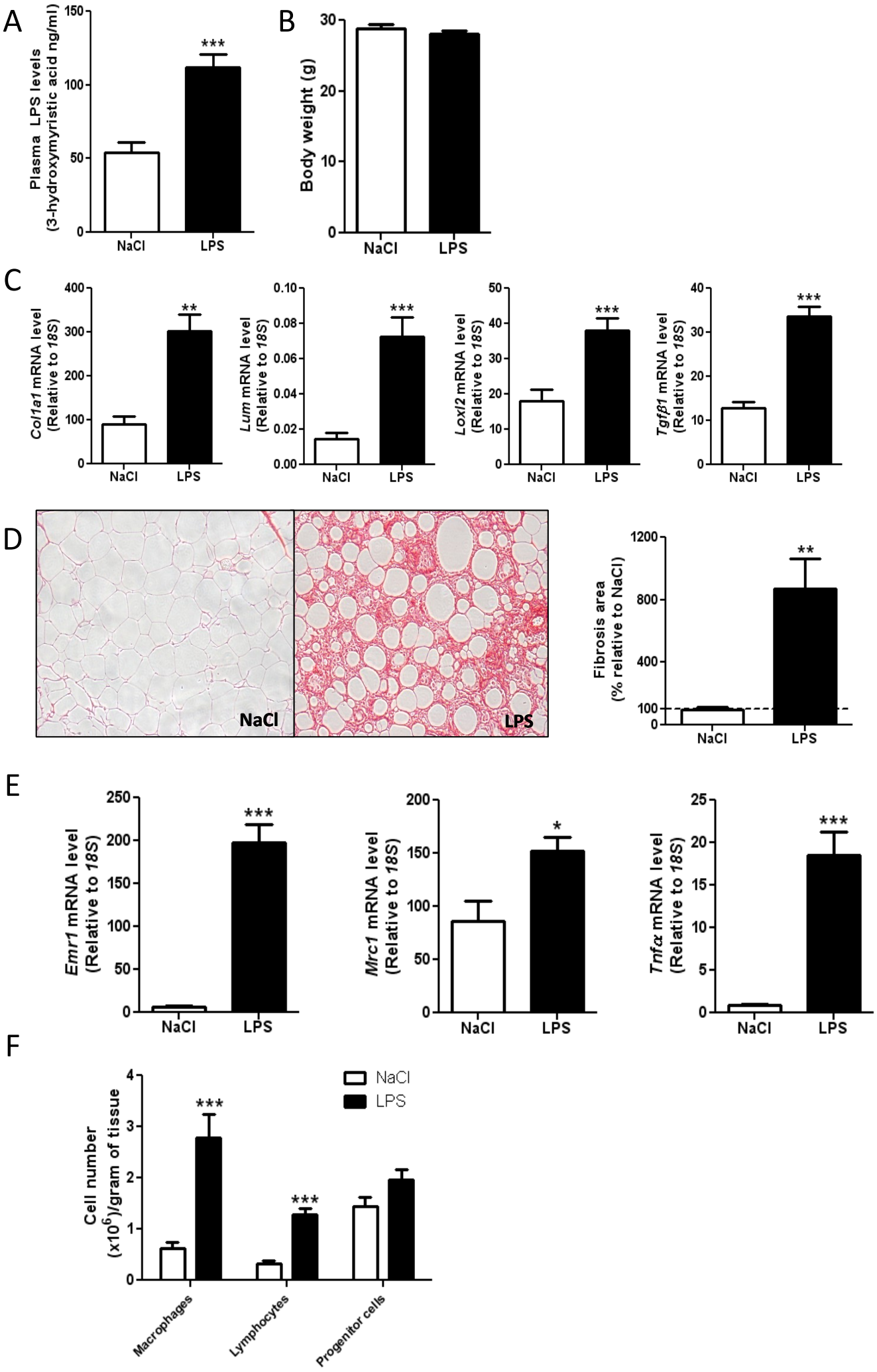
A
Plasma LPS levels (3-hydroxymyristic acid ng/ml)
150
100
50
0
***
NaCl
LPS
B
Body weight (g)
30
20
10
0
NaCl
LPS
C
Col1a1 mRNA level (Relative to 18S)
400
300
200
100
0
**
NaCl
LPS
Lum mRNA level (Relative to 18S)
0.10
0.08
0.06
0.04
0.02
0.00
***
NaCl
LPS
Loxl2 mRNA level (Relative to 18S)
50
40
30
20
10
0
***
NaCl
LPS
Tgfβ1 mRNA level (Relative to 18S)
40
30
20
10
0
***
NaCl
LPS
D
NaCl
LPS
Fibrosis area (% relative to NaCl)
1200
800
400
100
0
**
NaCl
LPS
E
Emr1 mRNA level (Relative to 18S)
250
200
150
100
50
0
***
NaCl
LPS
Mrc1 mRNA level (Relative to 18S)
200
150
100
50
0
*
NaCl
LPS
Tnfα mRNA level (Relative to 18S)
25
20
15
10
5
0
***
NaCl
LPS
F
Cell number (x10^6)/gram of tissue
4
3
2
1
0
NaCl
LPS
***
***
Macrophages
Lymphocytes
Progenitor cells

Figure S1

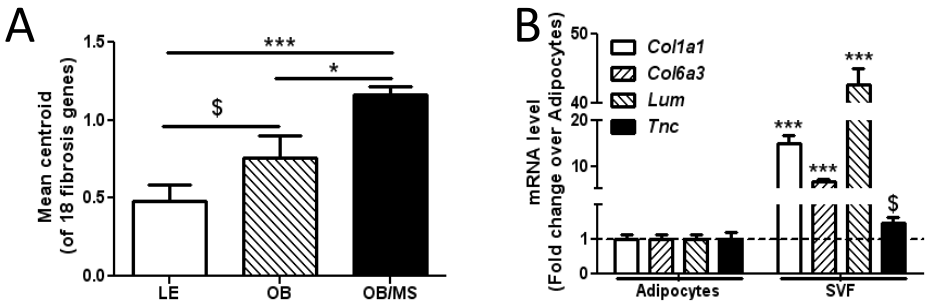

Figure S2

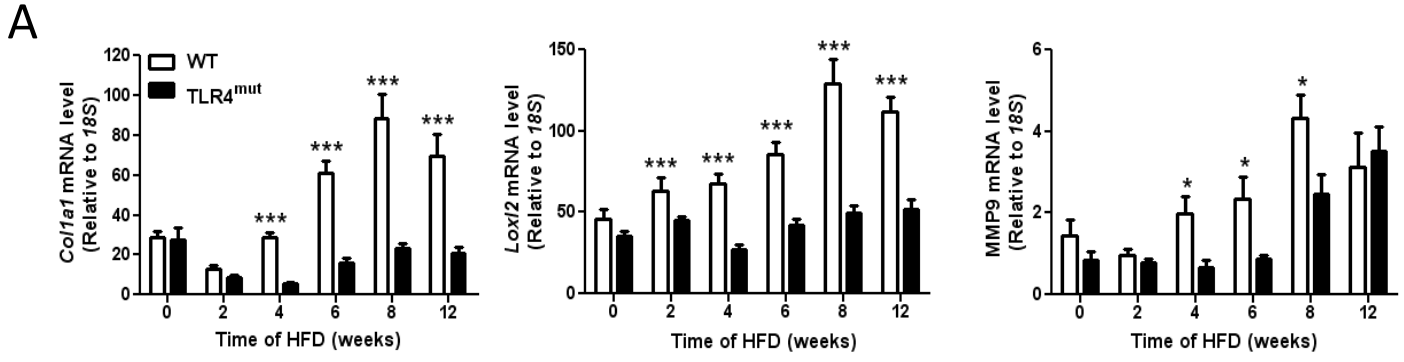

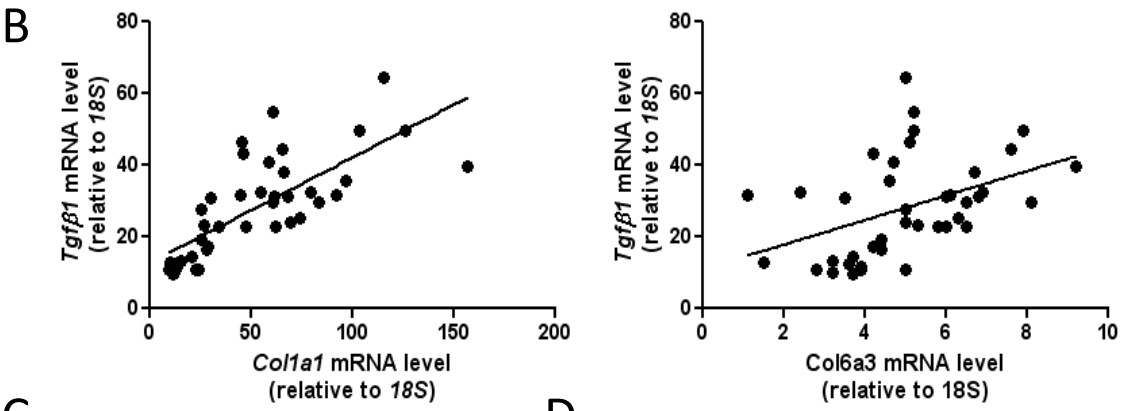

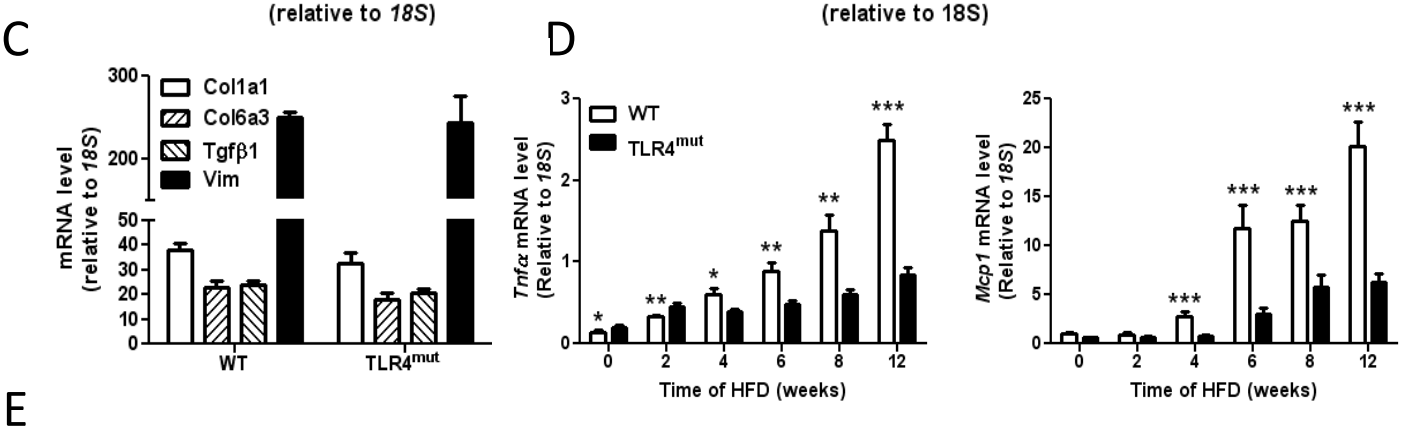

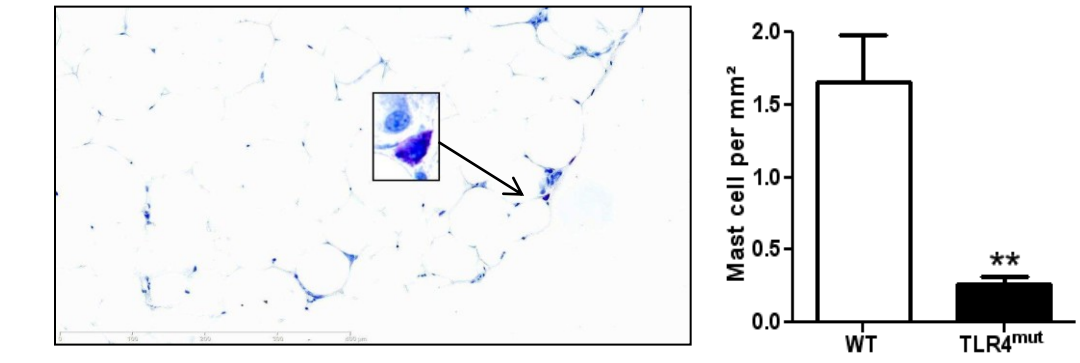

Figure S3

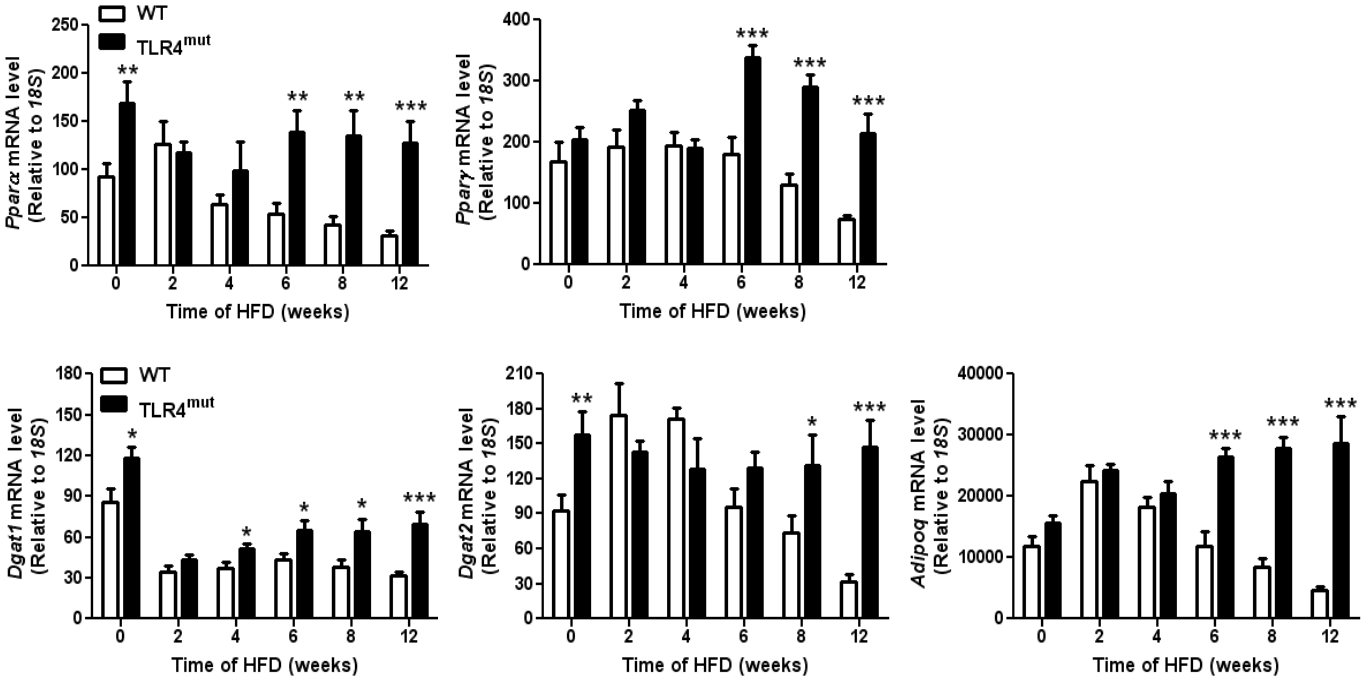

Figure S4

A

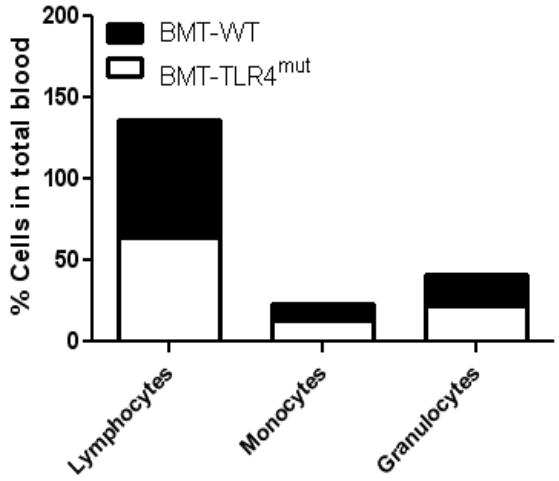

B

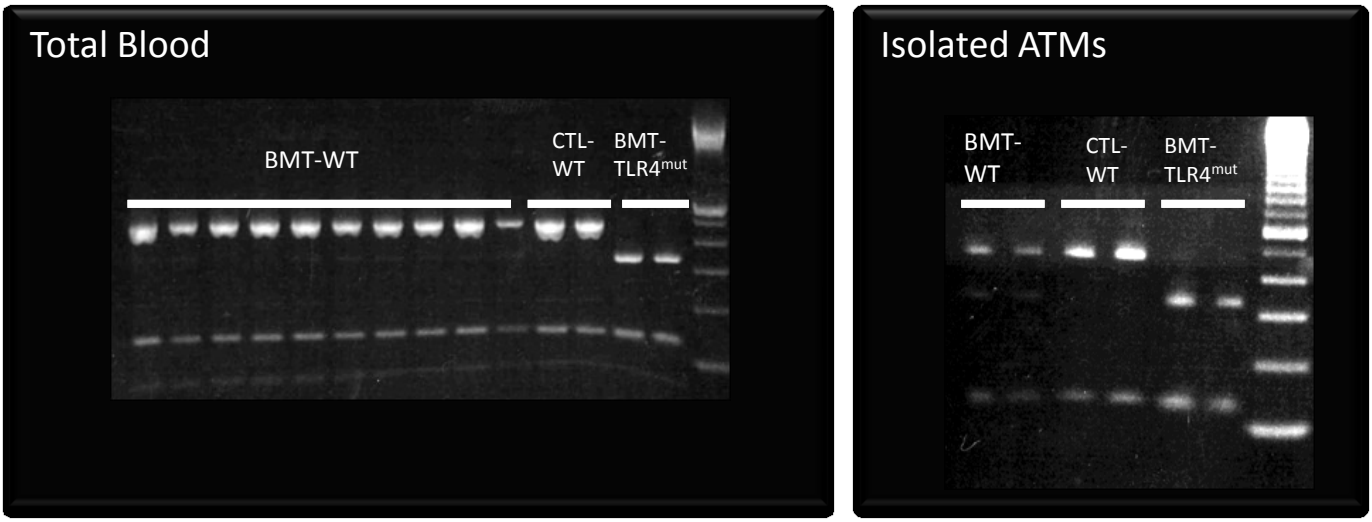

DISCUSSION

Ces travaux ont montré le rôle clé du TLR4 des cellules immunes dans le développement de la fibrose du tissu adipeux murin.

Lors de nos premières expériences nous avons constaté que les animaux WT avaient, au bout de 8 semaines de régime hyperlipidique, un TA épididymaire fibrosé contrairement aux animaux mutés pour le TLR4. Le modèle murin C3H demeure couramment utilisé pour l'étude de la fibrose induite dans différents organes (Seki, De Minicis et al. 2007; Campbell, Hile et al. 2011). Sans lésion ces animaux ne présentent pas de fibrose évidente. Nous avons donc voulu confirmer que le régime hyperlipidique pouvait être, dans nos expériences, le déclencheur de la fibrose adipeuse. Pour étudier cela, nous avons effectué une cinétique de régime hyperlipidique durant laquelle nous avons analysé toutes les deux semaines des animaux afin de déterminer la fenêtre d'apparition de la fibrose. En parallèle, nous avons maintenu des animaux en régime normal et nous avons pu confirmer que la mise en régime hyperlipidique était bien le déclencheur de cette fibrose.

Nos résultats de cinétique nous ont montré une apparition précoce des marqueurs de la fibrose tels que les collagènes de type I et VI ou encore le TGFβ1 dans le TA dès 4 semaines de régime riche en graisses chez les animaux WT. Cette apparition précoce de la fibrose fait de cette souche murine un excellent modèle d'étude de la fibrose du TA. En effet des temps de régime bien supérieurs sont nécessaires dans d'autres fonds génétiques, comme la souche C57/Bl6 qui est communément utilisée dans les recherches sur l'obésité, avant de constater les premiers signes de fibrose (Kwon, Shin et al. 2012). Nous avons retrouvé, chez ces animaux WT en régime gras, la surexpression des mêmes gènes liés à la fibrose que ceux augmentés chez l'homme entre patient normopondéré, obèse et obèse avec syndrome métabolique. L'apparition des marqueurs de la fibrose, chez nos animaux WT soumis à un régime hyperlipidique à 45%, était étroitement liée à une importante infiltration macrophagique dans le tissu adipeux ainsi qu'à une augmentation des gènes de l'inflammation, signe d'un état inflammatoire important du tissu adipeux. Le marquage spécifique du collagène en

histologie indiquait une apparition macroscopique de la fibrose à partir de 6 semaines de régime hyperlipidique. Nous avons également montré une forte corrélation entre diminution de la taille des adipocytes et fibrose ce qui confirme les observations faites chez l'Homme (Divoux, Tordjman et al. 2010). En parallèle les souris mutées pour le récepteur TLR4 au cours du régime hyperlipidique n'ont montré ni apparition de fibrose ni augmentation de macrophages ou de l'inflammation dans le tissu adipeux (Suganami, Mieda et al. 2007). De plus ces souris mutées ne présentaient ni dysfonctions du tissu adipeux ni mort adipocytaire contrairement aux souris WT. La fonction principale de l'adipocyte, la lipolyse, quelle soit basale ou stimulée, était altérée au sein du tissu fibrosé.

L'ensemble de ces résultats montre une forte implication du TLR4 et des macrophages dans la fibrogenèse du TA. Afin de confirmer que ce sont les TLR4 immuns qui sont impliqués dans la fibrose du TA, une irradiation/reconstitution de moelle osseuse a été effectuée sur des souris mutées. Ceci nous a permis d'obtenir des souris mutées pour le TLR4 dans l'ensemble de l'organisme mais ayant des cellules immunes possédant un TLR4 compétent. Les résultats de cytométrie ont indiqué une augmentation du recrutement de macrophages chez les animaux mutés exprimant un TLR4 compétent par rapport à ceux exprimant un TLR4 muté. Ces résultats étaient accompagnés d'une augmentation significative des gènes de la voie de la fibrose ainsi que de l'inflammation chez les animaux mutés ayant un TLR4 compétent. Tout cela a mis en avant le rôle clé du récepteur TLR4 immun dans l'initiation de la fibrose du TA. En effet lorsque celui-ci est fonctionnel, cela suffit à initier la fibrose chez des animaux normalement protégés. L'ensemble de ces résultats montrent un lien fort entre inflammation, fibrose et dysfonction métabolique; tryptique étroitement contrôlé, dans notre modèle, par le TLR4 des cellules immunes.

Lors d'un régime riche en lipides, il existe une augmentation des niveaux circulants de LPS issu des bactéries intestinales (Cani, Amar et al. 2007). Celui-ci étant un ligand activateur du TLR4, nous avons voulu savoir si l'élévation de ces concentrations plasmatiques suffisait à induire une fibrose du TA. Pour cela nous avons installé dans deux groupes de souris WT (LPS et véhicule) des minipompes «ALZET» en localisation intrapéritonéale. Le LPS a été diffusé en faible quantité, mimant ainsi l'inflammation de bas niveau observée au cours de l'obésité (Cani, Bibiloni et al. 2008; Cani, Possemiers et al. 2009). Le traitement, d'une durée de 4 semaines, a été administré à des souris

sous un régime standard qui n'entraîne pas à lui seul de fibrose du TA. Nous avons ainsi pu montrer qu'une administration de LPS était suffisante pour induire de la fibrose du TA. En utilisant le même type d'administration, nous avons infusé du TAK-242, inhibiteur spécifique de la voie du TLR4 (Kawamoto, Ii et al. 2008). Des animaux contrôles ont été placés durant 8 semaines en régime riche en graisses. L'administration de l'inhibiteur a commencé après 4 semaines de régime, moment où les premiers marqueurs de fibrose apparaissent. Nous avons ainsi pu voir que ce traitement permettait de ralentir la fibrose du TA.

L'ensemble de ces résultats a permis d'apporter des informations nouvelles sur les relations entre fibrose du TA et inflammation en démontrant le rôle clé du récepteur TLR4 immun.

Autres résultats

Lien entre insulinorésistance et fibrose du TA ?

Au cours de notre première étude de cinétique de régime gras, nous avons également mesuré, à chaque temps, la tolérance des animaux à l'insuline (Figure A). Plusieurs études ont montré que les animaux C3H/HeJ avaient une meilleure tolérance à l'insuline que leurs contrôles pour un temps de régime gras donné (Poggi, Bastelica et al. 2007; Tsukumo, Carvalho-Filho et al. 2007). Nos résultats confirment ces données publiées. Ils apportent également des informations complémentaires. En effet nous montrons pour la première fois que la différence de tolérance apparait après 4 semaines de régime entre WT et $TLR4^{mut}$.

La dégradation de la tolérance arrive relativement rapidement après la mise en régime gras cependant elle semble déjà en partie dépendante de l'inflammation. En effet les animaux $TLR4^{mut}$ sont protégés de la dégradation observée entre 2 et 4 semaines. Il existe différents mécanismes de l'insulinorésistance à court et long terme. Le mécanisme rapide d'installation est dû directement aux surplus de lipides comme ce qui peut être observé au cours d'une infusion de lipides (Nowotny, Zahiragic et al. 2013) puis on observe une implication de l'inflammation de manière plus tardive (Lee, Li et al. 2012). Dans notre expérience de cinétique d'ITTs il est possible que nous ayons manqué la dégradation à très court terme «lipide dépendante» qui a pu se produire avant 2 semaines de régime chez nos animaux WT et $TLR4^{mut}$. A 4 semaines de régime nous observons entre WT et $TLR4^{mut}$ plutôt une dégradation «inflammation dépendante». Cependant au vu des nos résultats, nous ne pouvons pas exclure un rôle de la dysfonction métabolique du TA dans cette perte de tolérance à l'insuline.

A

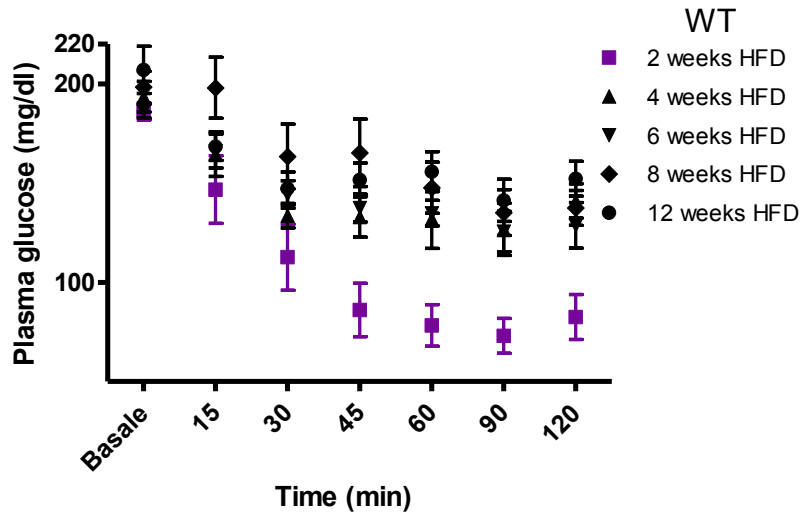

B

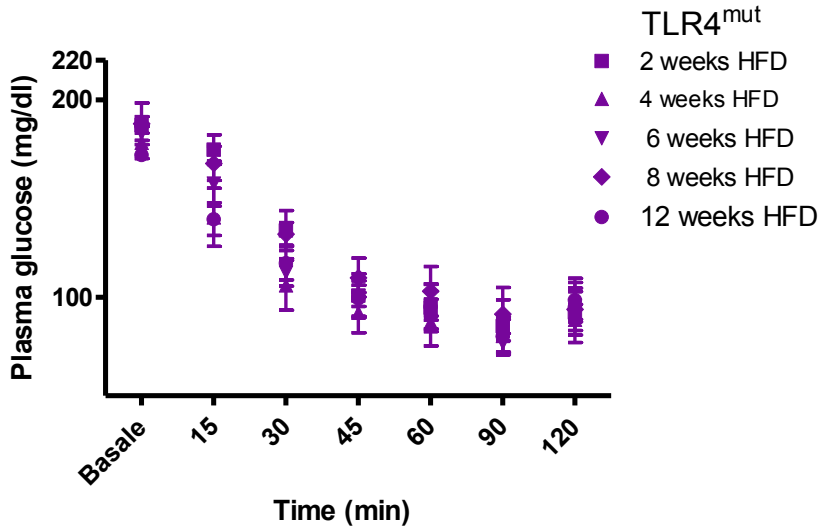

<u>Figure A:</u>Cinétique de tests de tolérance à l'insuline (0,6 U/Kg) (A) animaux C3H/HeOuJ (WT) (B) animaux C3H/HeJ (TLR4^{mut})

Les animaux WT présentent une augmentation des gènes de la fibrose et une fibrose macroscopique (picrosirius) graduelle entre 6 et 12 semaines. Ceci rappelle l'expression graduelle des gènes de la fibrose retrouvée entre patients normo-pondérés

et patients obèses présentant un syndrome métabolique. Contrairement aux résultats chez l'Homme, ces animaux ne montrent pas en parallèle de l'apparition de fibrose adipeuse une détérioration de leur métabolisme glucidique (supérieure à celle observée à 4 semaines). En effet nos résultats d'ITTs obtenus chez les souris WT et $TLR4^{mut}$ ne nous permettent pas d'identifier un potentiel rôle de la fibrose du TA dans le développement de l'insulinorésistance.

Plusieurs hypothèses peuvent expliquer l'absence de lien entre la fibrose et la dégradation de la tolérance à l'insuline dans nos expériences.

Premièrement, il est possible que ce modèle ne soit pas adéquat pour répondre à cette question. En effet, si dès 6 semaines le poids du TA épididymaire n'augmente plus chez les souris WT (Figure B), freiné par le développement de la fibrose, le TA sous cutané semble alors compenser l'atrophie du TA viscéral. En effet à masse grasse égale, on voit à 12 semaines de régime lipidique, que les souris WT ont plus développé leur TA sous cutané (Figure C). Il est donc probable que les animaux WT arrivent encore à tamponner le surplus de lipides après 12 semaines de régime. Cependant il est possible que l'allongement des temps de régime permette, à terme, de voir l'effet néfaste de la fibrose sur la sensibilité à l'insuline.

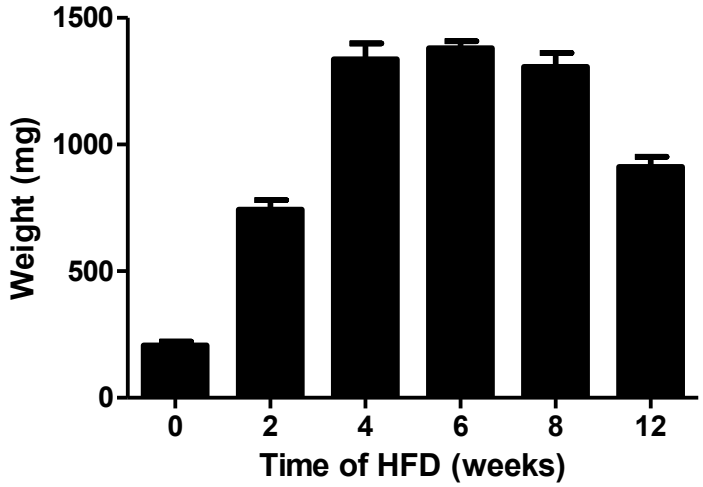

<u>Figure B:</u> Evolution du poids en milligrammes du dépôt adipeux épididymaire des animaux C3H/HeOuJ (WT)

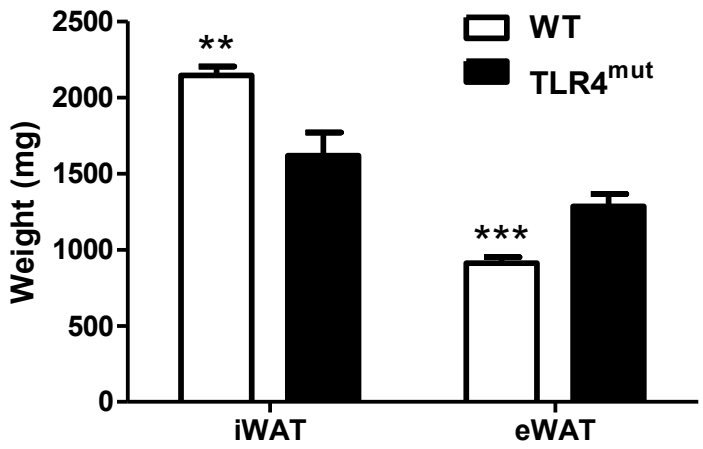

<u>Figure C:</u> Poids en milligrammes des dépots adipeux sous-cutané (iWAT) et épididymaire (eWAT) à 12 semaines de régime gras (blanc) animaux C3H/HeOuJ (WT) (noir) animaux C3H/HeJ (TLR4^{mut})

Deuxièmement, il est possible que les tests d'ITTs utilisés dans ces temps courts de régime ne soient pas suffisamment sensibles pour révéler de faibles modifications de la tolérance à l'insuline. Ainsi nous pensons qu'il serait nécessaire de reproduire ces expériences de cinétique en utilisant d'autres modes d'évaluations de la sensibilité à l'insuline. Nous pensons qu'il serait, par exemple, intéressant de réaliser des clamps hyperinsulinémiques/euglycémiques couplés à une administration de 2-déoxyglucose radiomarqué. Cela nous permettrait d'évaluer de façon très précise et plus physiologique l'évolution de la sensibilité à l'insuline des deux génotypes au cours du régime. Cela nous donnerait également des indications sur les tissus périphériques les plus touchés lors de la fibrose du TA.

Les acides gras issus de la lipolyse, potentiels inducteurs de fibrose ?

Nous avons également réalisé des expériences complémentaires pour déterminer si les AG issus de la lipolyse pouvaient être, comme le LPS, des ligands potentiels du TLR4 et initier la fibrose. Nous avons pour cela traité des animaux WT, sous régime gras, avec un inhibiteur de la LHS (BAY à 2 x 70 mg/Kg/jour) pendant 7 semaines.

Comme le montrent les expressions géniques des marqueurs de fibrose que sont les collagènes (*Col1a1* et *Col6a3*) et le *Tgfß1* de la figure D, le traitement n'a pas permis de ralentir l'apparition de ces marqueurs. Cette expérience écarte un potentiel rôle des acides gras issus de la lipolyse dans l'activation du TLR4 et l'initiation de la fibrose dans notre modèle.

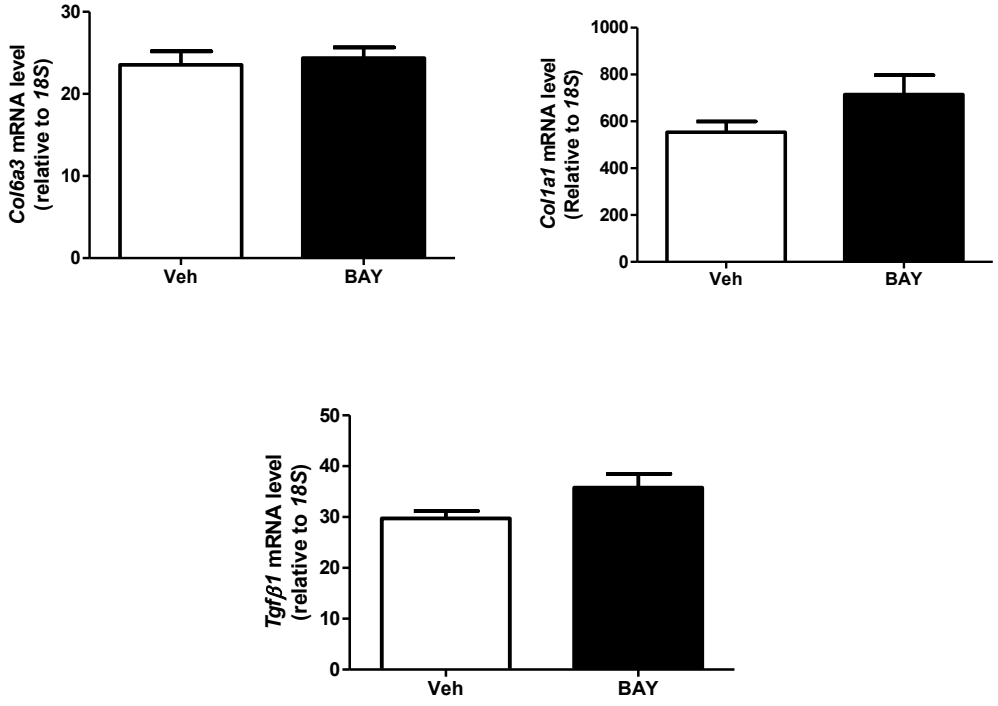

<u>Figure D:</u> Niveau d'expression génique de 3 marqueurs de la fibrose dans le dépôt adipeux épididymaire d'animaux C3H/HeOuJ (WT) soumis ou non à traitement pharmacologique inhibant la lipolyse

Résultats associés à d'autres études

Nous avons également utilisé notre fond C3H (WT et TLR4^{mut}) afin de tester un inhibiteur de la LHS et de rechercher un éventuel lien entre acides gras issus de la lipolyse et inflammation *via* le TLR4. Ces expériences m'ont permis de participer à deux études (cf: annexes).

Les acides gras issus de la lipolyse, potentiels activateurs du TLR4 macrophagique ?

La première étude, récemment soumise pour publication, montre l'incapacité des acides gras issus de la lipolyse à activer les macrophages *via* le TLR4 (Catherine-Ines Kolditz et al, pour publication).

Cette étude repose sur l'utilisation de milieux conditionnés d'adipocytes (HMADS) ou d'un cocktail d'acides gras reflétant les acides gras libérés par les adipocytes *in vitro* lors de la lipolyse (acides gras issus de la lipogenèse *de novo*). Par la suite, des THP1 (macrophages) ont été traités par les milieux conditionnés d'adipocytes ou un cocktail d'acides gras, en présence ou non d'un inhibiteur de TLR4 (TAK242). Aucun de ces traitements n'a permis d'induire l'expression ou la sécrétion de cytokines, chimiokines ou interleukines. Ces résultats *in vitro* montrent l'incapacité des acides gras issus de la lipolyse adipocytaire à activer le TLR4 macrophagique afin d'induire une réponse inflammatoire. Afin de compléter ces résultats, j'ai étudié *in vivo* sur les animaux C3H (WT et TLR4^{mut}) l'interaction entre acides gras issus de la lipolyse et l'inflammation TLR4 dépendante.

Afin d'induire une réponse inflammatoire, les animaux ont été nourris 6 semaines en régime hyperlipidique avant le traitement. Le BAY a été administré en parallèle du régime gras durant 2 semaines supplémentaires. Nos résultats ont montré une diminution significative du niveau de glycérol circulant, reflet de la diminution de la lipolyse par le BAY (TLR4^{mut}: 732±50 µM vs. 455±69 µM, $p<0.005$, n=12) (WT: 1029±55 µM vs. 635±57 µM, $p<0.0001$, n=12).

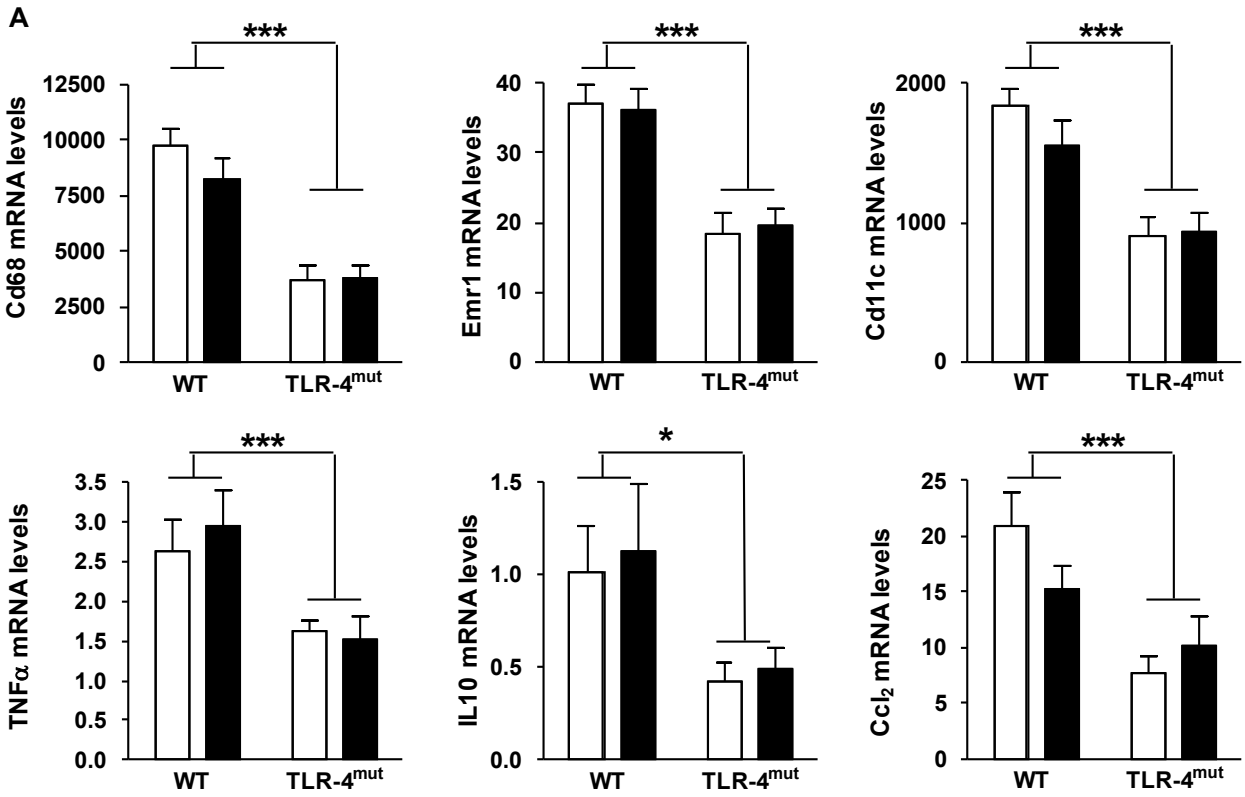

<u>Figure E</u>: Niveau d'expression génique dans le TA épididymaire de différents médiateurs de l'inflammation chez des souris C3H/HeOuJ (WT) et C3H/HeJ (TLR4^{mut}) après 8 semaines de régime HFD et 15 jours de traitement au BAY (70mg/Kg/jr)(blanc: véhicule) (noir: BAY)

Cependant comme le montre la figure E, la diminution de la lipolyse n'est pas accompagnée d'une diminution des marqueurs géniques de l'inflammation du tissu adipeux. En effet l'expression génique de *Cd68, Emr1 (*plus connu sous le nom de F4/80*), CD11c, Tnf-α, Il-10* et *Ccl2 (ou* Mcp-1*)* n'est pas modifiée par le traitement au BAY (Figure E). La différence d'état inflammatoire entre les souris WT et TLR4^{mut}, comme précédemment décrit dans l'article portant sur la fibrose du tissu adipeux, a été confirmé dans cette expérience. Ces résultats *in vivo* confirment les résultats *in vitro* et tendent à montrer une dissociation entre acides gras issus de la lipolyse et inflammation du tissu adipeux *via* le récepteur TLR4.

La deuxième étude a permis de montrer qu'une diminution partielle et chronique de la lipolyse provoquait une réduction du flux d'acides gras dans l'organisme. Cette diminution s'accompagnait d'une amélioration de l'action de l'insuline sur le métabolisme du glucose dans le foie et le muscle. Ceci a été confirmé sur des souris hétérozygotes pour le gène de la LHS ainsi que sur des souris de différents fonds génétiques traitées avec un agent pharmacologique, inhibiteur de la LHS (BAY) (Girousse, Tavernier et al. 2013).

Dans le cadre de cette étude, j'ai pu montrer que l'inhibition de la LHS par le BAY améliorait la réponse à l'insuline des animaux C3H/HeJ sans modification de la masse grasse ou du poids corporel. Ces résultats vont dans le même sens que ceux obtenus sur le fond B6D2. (Figure F)

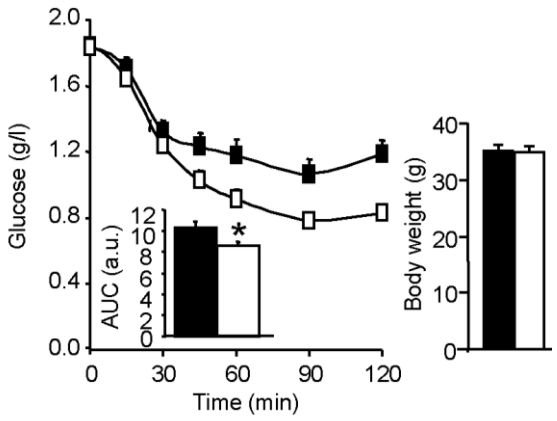

<u>Figure F:</u> Test de tolérance à l'insuline après 7 semaines de régime HFD chez des souris C3H/HeJ après 7 jours de traitement au BAY (70mg/Kg/jr)(noir: véhicule) (blanc: BAY)

CONCLUSION ET PERSPECTIVES

Nos résultats ont permis d'apporter certaines réponses quant aux facteurs impliqués dans l'initiation de la fibrose du tissu adipeux, notamment l'importance du TLR4 immun dans ce processus. Cependant d'autres questions se posent encore à nous. En effet dans cette étude nous avons montré une forte augmentation des macrophages dans le tissu adipeux fibrosé mais il nous reste encore à confirmer leur implication directe. Dans notre modèle, les mastocytes semblent peu impliqués car très peu présents, ce qui est également le cas des lymphocytes. Cependant ces types cellulaires sont augmentés chez nos animaux WT, nous ne pouvons donc pas exclure un rôle de ces cellules dans la mise en place de la fibrose du tissu adipeux.

L'utilisation d'une technique d'irradiation/reconstitution de moelle osseuse nous a permis d'incriminer les cellules immunes mais pas un type particulier. Des expériences complémentaires permettraient de confirmer le rôle clé des macrophages spécifiquement soit 1) par l'étude de souris transgéniques lysM-cre/ TLR4-flox/flox qui permettrait d'obtenir des souris invalidées pour le TLR4 spécifiquement dans les macrophages (Clausen, Burkhardt et al. 1999) 2) par l'administration orale dans un fond C3H de siRNA-TLR4 encapsulés et phagocytés par les macrophages, ce qui permet de cibler les macrophages *in vivo* (Aouadi, Tesz et al. 2009), 3) par la destruction des macrophages chez des souris C3H par un traitement au dichloro-méthylène-biphosphate induisant l'apoptose des macrophages (Naito, Nagai et al. 1996).

Le tissu adipeux des animaux WT a montré de fortes altérations fonctionnelles, en effet la lipolyse basale et stimulée est altérée ainsi que l'expression génique des lipases. L'impact de la fibrose sur le métabolisme du tissu adipeux n'a pas été étudié et il serait intéressant de regarder les interactions matrice/adipocyte impliquées dans la régulation des gènes et des protéines de la lipolyse. L'impact de la fibrose adipeuse sur le métabolisme de l'organisme entier n'a pas non plus été étudié. La mort des adipocytes doit être à l'origine d'un déversement au niveau circulant de nombreux médiateurs pouvant induire des modifications métaboliques dans d'autres tissus.

Dans le tissu adipeux, il est suggéré que les pré-adipocytes joueraient le rôle des myofibroblastes. En effet, il a été démontré qu'en présence d'un environnement inflammatoire, notamment sous l'effet de facteurs sécrétés par les macrophages, les pré-adipocytes produisent des molécules profibrosantes comme les collagènes, la fibronectine, ainsi que des protéines de la famille du TGFβ (Keophiphath, Achard et al. 2009; Bourlier, Sengenes et al. 2012). L'implication du TLR4 dans cette communication macrophage/pré-adipocyte reste encore à éclaircir. Pour cela, nous pourrions partir directement d'une biopsie de TA, digéré ce TA puis mettre en culture des macrophages et des pré-adipocytes après un tri cellulaire. Pour déterminer le rôle du TLR4 macrophagique dans cette communication, nous utiliserions les milieux conditionnées des macrophages traités avec du LPS en présence ou non d'un inhibiteur du TLR4, mis ensuite en contact avec les pré-adipocytes. Cette expérience nous permettrait de voir l'effet de la stimulation du TLR4 macrophagique sur le phénotype et l'expression des gènes profibrotiques des pré-adipocytes exposés à ces milieux conditionnés.

Les souris invalidées pour le collagène de type VI ont montré une meilleure expansion de leur tissu adipeux accompagnée d'une amélioration de leur métabolisme glucidique (Khan, Iyengar et al. 2007). Ces souris ont également une diminution de l'inflammation dans leur tissu adipeux. Il serait intéressant de parvenir à dissocier l'inflammation de la fibrose. Ceci afin de regarder l'impact direct de la fibrose sur le métabolisme glucidique et la sensibilité à l'insuline de l'organisme. La dissociation des deux phénomènes présente des difficultés. La meilleure solution serait d'intervenir en amont de la fibrose et en aval de l'inflammation en agissant sur la voie du TGF par exemple, par l'utilisation d'anticorps neutralisants (Shah, Foreman et al. 1994) ou en utilisant un système de surexpression d'un récepteur TGF soluble inactif (TβRII) rentrant en compétition avec les récepteurs actifs endogènes (Qi, Atsuchi et al. 1999).

Nous avons montré que le LPS, augmenté durant l'obésité (Cani, Bibiloni et al. 2008), était capable d'induire une fibrose adipeuse en quelques semaines alors que les acides gras issus de la lipolyse ne semblent pas impliqués. Cette expérience nous a permis de déterminer que le LPS était capable d'induire de la fibrose, cependant dans notre modèle nous ne pouvons pas affirmer que le LPS est le responsable. Pour cela nous pourrions créer une colonie de souris axéniques WT et nous pourrions regarder si il y a apparition ou pas de fibrose adipeuse chez ces WT en régime gras.

En plus du LPS, d'autres ligands endogènes, notamment des protéines de la matrice sont également des ligands du TLR4 (Erridge 2010) et pourraient participer à l'initiation ou au maintien du processus de réparation tissulaire pathologique. L'effet de protéines candidates, comme la ténascine C ou la fibronectine EDA, pourrait être testé *in vitro via* des milieux conditionnés de macrophages. L'utilisation de ces milieux conditionnés sur des pré-adipocytes permettrait de voir si l'activation du TLR4 macrophagique par ces protéines permet de changer le phénotype de pré-adipocytes.

LIPOLYSE MUSCULAIRE ET INSULINORESISTANCE

PARTIE II: LIPOLYSE MUSCULAIRE ET INSULINORESISTANCE

I Muscle squelettique et insulinorésistance

1.1) Muscle squelettique et régulation de la glycémie

1.1.1) Homéostasie glucidique

La glycémie oscille en permanence autour d'une valeur physiologique voisine de 0.9g/L. Les muscles sont les principaux tissus utilisateurs de glucose. Lors du repas, les cellules musculaires capturent ~60-70% du glucose atteignant la circulation sanguine (Kelley, Mitrakou et al. 1988). Au cours des clamps hyperinsulinémiques et euglycémiques, 80-90% du glucose injecté par voie intraveineuse est capté par les tissus périphériques et pour une majeure partie par les muscles squelettiques (DeFronzo, Jacot et al. 1981). Ce tissu joue donc un rôle clé dans la régulation de l'homéostasie glucidique

1.1.2) Le récepteur à l'insuline

Le récepteur de l'insuline est un récepteur ubiquitaire tyrosine kinase transmembranaire. La liaison de l'insuline induit un changement de conformation du récepteur qui libère son activité catalytique par une autophosphorylation. Plusieurs sites tyrosine sur la sous unité β sont phosphorylés; la phosphorylation sur un résidu tyrosine en position 960 ou 972 selon la source, chez l'Homme et la souris, crée un motif de reconnaissance pour l'ancrage des effecteurs cellulaires protéiques, IRS-1 et IRS-2 (Le Roith and Zick 2001). Les IRS sont ancrées à la membrane plasmique à proximité du récepteur. Leur interaction avec le récepteur de l'insuline activé induit la phosphorylation de plusieurs résidus tyrosine de leur région C-terminale permettant la fixation de protéines possédant un domaine SH2 (*Scr Homology 2 domain*) comme l'unité p85 du complexe p85/p110 de la PI3-K (*Phosphatidyl Inositol 3-Kinase*) et le Grb2 (*growth factor receptor binding protein 2*). Ces deux protéines sont les médiateurs

des fonctions de l'insuline respectivement sur le métabolisme et la croissance cellulaire.

1.1.3) La voie de signalisation de l'insuline

La voie de signalisation de l'insuline sur le métabolisme (Le Roith and Zick 2001) implique la voie de la PI-3 kinase (figure 18). Après son activation par les IRS, la PI3- K induit la production de PIP3 (*Phosphatidylinositol 3, 4, 5 Phosphate*) qui se lie aux domaines PH (*Pleckstrin Homology domain*) de la PDK-1 (*PIP3 dependent kinase 1*). A son tour celle-ci phosphoryle et active la sérine/thréonine kinase B ou AKT qui va phosphoryler ensuite AS160. AS160 non phosphorylé empêche GLUT4 d'être transloqué à la membrane, une fois phosphorylée le frein est levé et GLUT4 peut être transloqué. Lors du repas, l'insuline active la capture du glucose dans les cellules musculaires en stimulant la translocation du transporteur au glucose GLUT4 (Guma, Zierath et al. 1995; Goodyear, Hirshman et al. 1996). Ce transporteur est présent dans le cytosol au sein de vésicules cytoplasmiques qui sont mobilisées vers la membrane de la cellule en réponse à l'action de l'insuline.

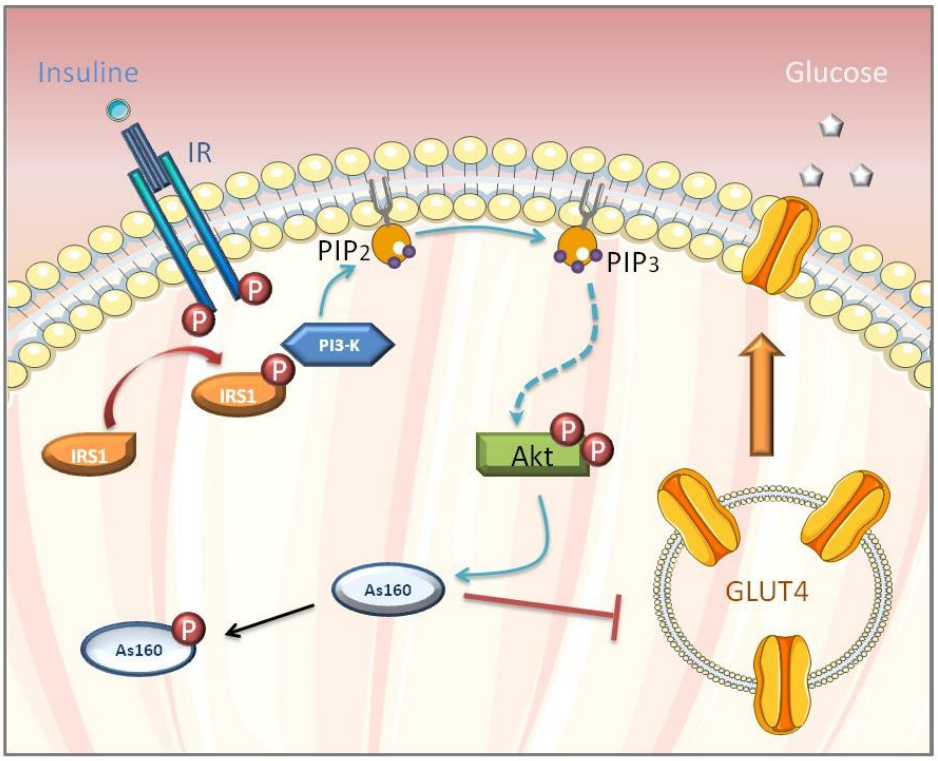

Figure 18: Signalisation de l'insuline

Akt:sérine/thréonine kinase B; GLUT4: transporteur du glucose; IR: insulin receptor; IRS1: insulin receptor substrat; PI3-K: phosphatidyl inositol 3-kinase; PIP: Phosphatidyl inositol phosphate.

1.2) Obésité et Insulinorésistance musculaire

1.2.1) Inflammation

L'obésité s'accompagne d'une inflammation chronique de bas grade, caractérisée par une augmentation sérique de la CRP et de cytokines inflammatoires tels que le TNF-α et l'IL-6. De plus, dans le tissu adipeux de patients obèses, l'expression de l'IL-6 et du TNF-α est augmentée proportionnellement à la masse grasse et corrélée avec les marqueurs sériques de l'inflammation comme la CRP (Yudkin, Stehouwer et al. 1999).

Or, on sait actuellement que ces cytokines TNF-α et IL-6 ont un effet inhibiteur sur la voie de signalisation de l'insuline (Marette 2002). La perfusion de TNF-α induit une insulinorésistance musculaire. L'IL-6 diminue la signalisation de l'insuline dans les hépatocytes et le transport du glucose dans les adipocytes. Le TNF-α et l'IL-6 induisent l'expression des protéines «*Suppressor Of Cytokine Signaling*» (SOCS), qui interrompent la signalisation de l'insuline en empêchant le récepteur de l'insuline d'activer ses différents substrats (Kawazoe, Naka et al. 2001; Rieusset, Bouzakri et al. 2004).

De plus une étude récente chez l'Homme d'infusion de LPS, endotoxine d'origine bactérienne fortement inflammatogène, a montré une induction par ce LPS d'une insulinorésistance musculaire médiée par des cytokines proinflammatoires (Nowotny, Zahiragic et al. 2013).

1.2.2) Lipotoxicité

1.2.2.1) Les TAG

De nombreuses études ont montré une forte accumulation de TAG au sein du muscle de personnes obèses par rapport à des personnes minces (Goodpaster et al., 1997; Jacob et al., 1999; Krssak et al., 1999; Pan et al., 1997). Sur la base de ces études associatives, dans un premier temps il a été envisagé que les TAG pourraient être à l'origine de l'insulinorésistance de ces personnes obèses. Cependant les travaux de Goodpaster et al ont permis d'établir pour la première fois en 2001, qu'une augmentation comparable des TAG musculaires était également retrouvée dans des populations d'athlètes en endurance par rapport à des personnes sédentaires normo-pondérés. Les athlètes possédaient cependant une sensibilité à l'insuline accrue. Ce

paradoxe est depuis connu sous le nom de «paradoxe des athlètes» (Goodpaster, He et al. 2001). Associé à ces résultats, des études d'entrainement en endurance de plusieurs semaines améliorent la sensibilité de patients normo-pondérés comme de patients obèses et augmente parallèlement le contenu en TAG (Schrauwen-Hinderling, Schrauwen et al. 2003; Schrauwen-Hinderling, van Loon et al. 2003; Dube, Amati et al. 2008; Dube, Amati et al. 2011; Shepherd, Cocks et al. 2013). Il semble maintenant établi, sur la base de ces résultats, que l'accumulation de TAG musculaire n'est pas responsable de l'insulinorésistance chez l'obèse.

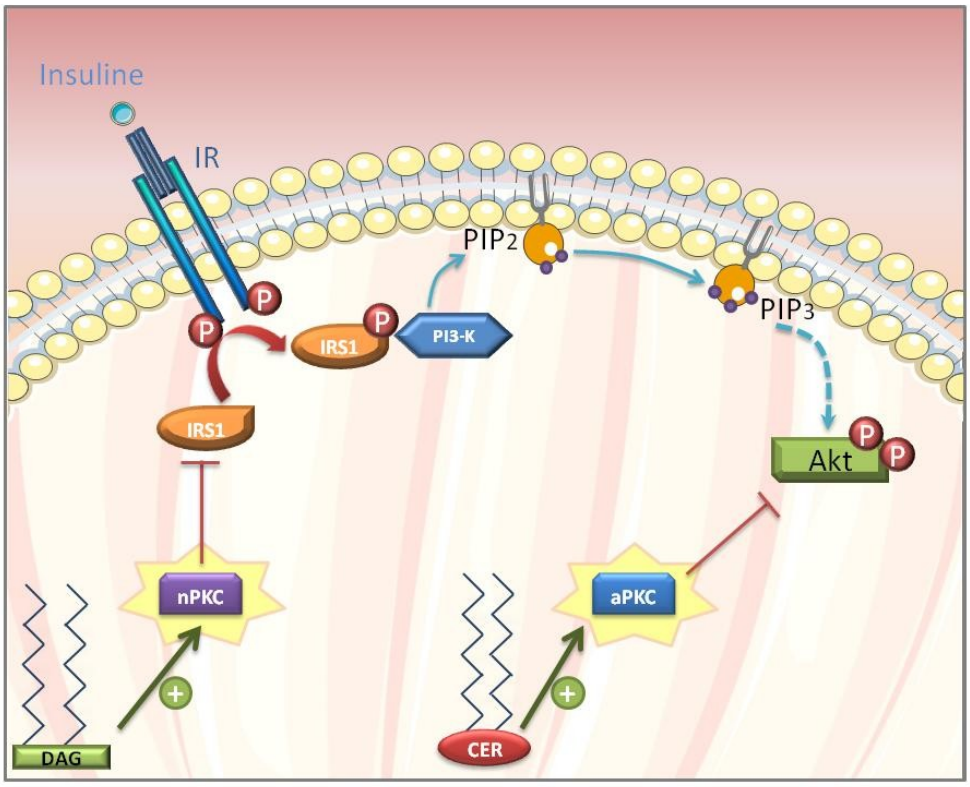

Figure 19 : Inhibiteurs lipidiques de la voie de l'insuline

Akt: Sérine/thréonine kinase B; CER: Céramide; DAG: Diacylglycerol; IR: insulin receptor; IRS1: insulin receptor substrat; PI3-K: phosphatidyl inositol 3-kinase; PKC: Protéine kinase C; PIP: Phosphatidyl inositol phosphate

1.2.2.2) Les DAG

De nombreuses études de cohortes chez l'Homme montrent des concentrations de DAG supérieures dans le muscle de patients obèses insulinorésistants par rapport à des personnes de poids normal insulinosensibles (Moro et al., 2009; Straczkowski et al., 2007). Une élévation des DAG a également été décrite dans le muscle de rongeur soumis à un régime riche en lipides (Chibalin et al., 2008; Timmers et al., 2011). De

plus des études d'infusion de lipides ont montré une forte association entre l'augmentation des DAG et l'insulinorésistance. Les effets toxiques des DAG étant reliés à une augmentation de l'activité de certaines PKC (notamment PKCθ) et une diminution de la phosphorylation et de «l'activité d'IRS1» et de PI3-K (figure 19) (Griffin, Marcucci et al. 1999; Itani, Ruderman et al. 2002).

De plus de nombreux modèles murins transgéniques ont établit un lien fort entre la voie DAG/PKC dans le muscle et l'insulinorésistance. La surexpression de la DGAT1, dans le muscle squelettique (MCK-DGAT1) induit une accumulation de TAG intramusculaires. Ces souris transgéniques ont un faible contenu en DAG et sont protégées de l'insulinorésistance induite par les lipides (Liu, Zhang et al. 2007). De plus des souris invalidées pour le gène de la PKCθ au niveau muscle spécifique présentent une forte amélioration de leur sensibilité à l'insuline. Favoriser le stockage sous forme de TAG et diminuer le contenu intramusculaire de DAG pourraient donc être bénéfique pour préserver l'insulinosensibilité du muscle.

1.2.2.3) Les céramides (CER)

D'autres dérivés lipidiques musculaires tels que les céramides ont été associés à l'insulinorésistance chez l'Homme. En effets plusieurs études ont trouvé de plus fortes concentrations de céramides chez des patients obèses et diabétiques que chez des patients sains et de poids normal (Straczkowski, Kowalska et al. 2007; Moro, Galgani et al. 2009). Des études sur myocytes en culture ont permis de montrer que l'effet des céramides passe par l'activation de la protéine phosphatase 2A (PP2A) connue pour déphosphoryler Akt sur son résidu activateur serine 473 (chez l'Homme et chez la souris) (Chavez and Summers 2003).

Des études menées sur rongeur ont de plus permis de montrer le lien causal existant entre céramides et insulinorésistance. Chez des rongeurs diabétiques, l'implication des céramides dans l'insulinorésistance a été montrée par l'inhibition de leur synthèse *via* un traitement par la myriosine (Holland, Brozinick et al. 2007; Ussher, Koves et al. 2010). Cette expérience a permis de restaurer un contenu en céramides équivalent aux animaux non diabétiques améliorant ainsi la sensibilité à l'insuline. De plus la surexpression musculaire d'une enzyme stimulant la dégradation des céramides, la sphingosine kinase conduit également à une protection contre l'insulinorésistance induite par le régime hyperlipidique (Bruce, Risis et al. 2012).

II Les différentes voies d'accumulation de lipides intermédiaires

2.1) Augmentation du flux d'acides gras

L'étude de la clairance d'acides gras radiomarqués a permis de mettre en évidence une augmentation de l'entrée des acides gras dans le muscle de rats insulinorésistants. Cette augmentation du flux d'acides gras pourrait être responsable de l'accumulation excessive de lipides dans le muscle (Hegarty, Cooney et al. 2002). Ces résultats ont été confirmés *ex vivo* sur muscle de sujets obèses et diabétiques (Bonen, Parolin et al. 2004; Aguer, Mercier et al. 2010) et dans des modèles d'obésité chez le rongeur (Luiken, Arumugam et al. 2001). Plusieurs hypothèses ont été proposées afin d'expliquer l'augmentation de l'entrée d'acides gras dans le muscle des obèses. En plus de l'augmentation du flux d'acides gras plasmatiques, une augmentation du nombre de transporteurs aux acides gras à la membrane du muscle squelettique de sujets obèses a été montrée (Aguer, Mercier et al. 2010; Aguer, Foretz et al. 2011). L'augmentation du flux lipidique au sein du muscle squelettique est associée à une augmentation du stockage des acides gras sous forme de TAG. Par effet masse, chez l'obèse l'augmentation du stockage des TAG induit une augmentation des intermédiaires lipotoxiques tels que les DAG (Moro, Galgani et al. 2009).

2.2) Dysfonction mitochondriale

De nombreuses études chez l'Homme et le rongeur ont remis en cause le lien entre le dysfonctionnement mitochondrial et l'insulinorésistance. L'exemple le plus probant étant que l'oxydation des AG n'est pas modifiée voire augmentée chez l'obèse (Holloway, Thrush et al. 2007). D'autres études ont montré chez des animaux nourris par un régime riche en graisses une augmentation de leur capacité oxydative mitochondriale associée à une insulinorésistance (Turner, Bruce et al. 2007). Cependant certaines études ont montré qu'une surcharge mitochondriale pouvait entrainer une accumulation de dérivés d'oxydation incomplète des acides gras tels que les acylcarnitines. Plusieurs études ont montré des niveaux élevés de ce dérivé chez le rat obèse (An, Muoio et al. 2004; Koves, Li et al. 2005). Il a été suggéré que ces acylcarnitines pourraient activer

des protéines kinases telles que PKC, IKK-β et JNK entrainant l'inhibition d'IRS-1 (Muoio and Newgard 2008).

2.3) Lipolyse musculaire

Les connaissances sur la régulation de la lipolyse musculaire sont moins vastes que dans le tissu adipeux cependant elles ont permis d'établir qu'il existait certains points communs et quelques divergences cruciales entre les deux tissus. Tout d'abord comme dans le tissu adipeux, la lipolyse musculaire est un processus catabolique en trois étapes faisant intervenir l'ATGL, la LHS et la MGL. Comme dans l'adipocyte, l'activité de l'ATGL est dans le la cellule musculaire humaine fortement augmentée par son co-activateur CGI-58 (Badin, Loubiere et al. 2012). Il est intéressant de noter que lors de stimulations électriques sur fibres musculaire isolées, afin de mimer l'exercice, on note une hausse de l'interaction entre CGI-58 et l'ATGL (Macpherson, Ramos et al. 2013). A l'inverse de CGI-58, le rôle musculaire de G0S2 reste à étudier.

Comme pour l'ATGL, la régulation de l'activité musculaire de la LHS présente des similitudes avec celle du tissu adipeux. Par exemple, l'activité de la LHS est dans le muscle augmenté par des agonistes β adrénergiques (épinéphrine) qui phosphorylent la LHS sur son résidu activateur ser660 chez la souris (ser650 chez l'Homme). Dans le muscle squelettique il a également été montré que la contraction seule pouvait également augmenter l'activité de la LHS et ce de manière indépendante de l'élévation des taux d'épinéphrine à l'exercice. Ces mécanismes semblent passer par l'activation calcium-dépendante des PKCs et par l'activation des protéines ERK (Donsmark, Langfort et al. 2003; Watt, Heigenhauser et al. 2003). Cependant à l'inverse du tissu adipeux, il semble que l'activité de la LHS ne soit pas diminuée par l'insuline dans le muscle (Moberg, Sjoberg et al. 2002).

La différence majeure entre la lipolyse du tissu adipeux et la lipolyse musculaire est l'absence totale d'expression de la périlipine 1 (PLIN1) dans le muscle squelettique. En l'absence de cette protéine qui est dans le TA au cœur du controle de la lipolyse, il est par conséquence impossible d'imaginer un controle de la lipolyse musculaire similaire à celui de l'adipocyte. Depuis quelques années les études se sont multipliées pour essayer de comprendre comment est contrôlé l'accès des lipases musculaires à la gouttelette lipidique. Il semble probable que d'autres protéines de la famille des perillipines jouent, dans le muscle, un rôle similaire à la PLIN1 dans l'adipocyte. Il

pourrait s'agir de la PLIN5 ou de la PLIN2 toutes deux très exprimées dans les tissus oxydatifs. De plus l'absence de l'une ou de l'autre de ces PLIN dans le cœur ou le muscle engendre une forte diminution de l'hydrolyse des TAG (Bosma, Minnaard et al. 2012) s'expliquant sans doute par une plus forte inhibition de la lipolyse (Wang, Sreenevasan et al. 2011; Pollak, Schweiger et al. 2013; Wang, Sreenivasan et al. 2013). Un papier récent de MacPherson montre également que l'augmentation de l'activité des lipases à l'exercice pourrait s'expliquer par une baisse de la séquestration de l'ATGL et de CGI-58 par PLIN5 et/ou PLIN2 (Macpherson, Ramos et al. 2013).

Récemment des papiers de notre laboratoire ont montré un possible lien chez l'Homme entre la dérégulation de l'activité lipolytique musculaire et l'insulinorésistance. En effet il a été montré chez l'obèse une augmentation de l'expression de l'ATGL ainsi qu'une diminution de l'expression de la LHS dans le muscle (Jocken, Roepstorff et al. 2008; Badin, Louche et al. 2011). Ces modifications d'expression entrainent une perturbation de la lipolyse musculaire avec un déséquilibre entre l'hydrolyse des TAG et celle des DAG menant à une accumulation de DAG intramusculaires. De la même manière la surexpression de l'ATGL ou l'utilisation d'un inhibiteur de la LHS entrainent dans des myotubes en culture une accumulation de DAG accompagnée d'une moins bonne activation par l'insuline de sa voie de signalisation.

OBJECTIFS

En collaboration avec des collègues de l'équipe dont le projet est ciblé sur le muscle, nous avons regardé la régulation des lipases du muscle squelettique au cours d'un régime gras *in vivo*. En effet dans une précédente publication, ceux-ci ont montré qu'une dérégulation de l'expression des deux principales lipases de la lipolyse (ATGL et LHS), dans des myotubes humains, entrainait une accumulation de diacylglycérols (DAG), néfaste pour le signal insulinique. **Nous avons voulu confirmer *in vivo* le lien physiopathologique entre dérégulation de la lipolyse, lipotoxicité, et insulinorésistance dans le muscle squelettique de souris soumises à un régime gras.**

ARTICLE 2

High fat diet-mediated lipotoxicity and insulin resistance is related to impaired lipase expression in mouse skeletal muscle

Pierre-Marie Badin[1,2*], Isabelle K. Vila[1,2*], Katie Louche[1,2], Aline Mairal[1,2], Virginie Bourlier[1,2], Geneviève Tavernier[1,2], Dominique Langin[1,2,3] and Cedric Moro[1,2#]

[1]Inserm, UMR 1048, Obesity Research Laboratory, Institute of Metabolic and Cardiovascular Diseases, Toulouse, France

[2]University of Toulouse, Paul Sabatier University, France

[3]Toulouse University Hospitals, Department of Clinical Biochemistry, France

*The authors equally contributed to this work

High-Fat Diet-Mediated Lipotoxicity and Insulin Resistance Is Related to Impaired Lipase Expression in Mouse Skeletal Muscle

Pierre-Marie Badin,* Isabelle K. Vila,* Katie Louche, Aline Mairal, Marie-Adeline Marques, Virginie Bourlier, Geneviève Tavernier, Dominique Langin, and Cedric Moro

Institut National de la Santé et de la Recherche Médicale (P.-M.B., I.K.V., K.L., A.M., M.-A.M., V.B., G.T., D.L., C.M.), Unité Mixte de Recherche 1048, Obesity Research Laboratory, Institute of Metabolic and Cardiovascular Diseases, 31432 Toulouse Cedex 4, France; University of Toulouse (P.-M.B., I.K.V., K.L., A.M., M.-A.M., V.B., G.T., D.L., C.M.), Paul Sabatier University, 31062 Toulouse Cedex 9, France; and Department of Clinical Biochemistry (D.L.), Toulouse University Hospitals, 31059 Toulouse Cedex 9, France

Elevated expression/activity of adipose triglyceride lipase (ATGL) and/or reduced activity of hormone-sensitive lipase (HSL) in skeletal muscle are causally linked to insulin resistance in vitro. We investigated here the effect of high-fat feeding on skeletal muscle lipolytic proteins, lipotoxicity, and insulin signaling in vivo. Five-week-old C3H mice were fed normal chow diet (NCD) or 45% kcal high-fat diet (HFD) for 4 weeks. Wild-type and HSL knockout mice fed NCD were also studied. Whole-body and muscle insulin sensitivity, as well as lipolytic protein expression, lipid levels, and insulin signaling in skeletal muscle, were measured. HFD induced whole-body insulin resistance and glucose intolerance and reduced skeletal muscle glucose uptake compared with NCD. HFD increased skeletal muscle total diacylglycerol (DAG) content, protein kinase Cθ and protein kinase Cϵ membrane translocation, and impaired insulin signaling as reflected by a robust increase of basal Ser1101 insulin receptor substrate 1 phosphorylation (2.8-fold, $P < .05$) and a decrease of insulin-stimulated v-Akt murine thymoma viral oncogene homolog Ser473 (-37%, $P < .05$) and AS160 Thr642 (-47%, $P < .01$) phosphorylation. We next showed that HFD strongly reduced HSL phosphorylation at Ser660. HFD significantly up-regulated the muscle protein content of the ATGL coactivator comparative gene identification 58 and triacylglycerol hydrolase activity, despite a lower ATGL protein content. We further show a defective skeletal muscle insulin signaling and DAG accumulation in HSL knockout compared with wild-type mice. Together, these data suggest a pathophysiological link between altered skeletal muscle lipase expression and DAG-mediated insulin resistance in mice. **(*Endocrinology* 154: 1444–1453, 2013)**

Obesity has become a major health problem worldwide. It constitutes a strong risk factor for other diseases, such as type 2 diabetes mellitus and cardiovascular diseases (1, 2). Obesity has been associated with ectopic fat deposition, and in sedentary populations, the level of intramyocellular triacylglycerol (TAG) (IMTG) is negatively correlated with insulin sensitivity (3, 4). However, studies on endurance athletes revealed a paradoxically elevated IMTG content in highly insulin sensitive subjects (5). It is now well established that skeletal muscle insulin resistance is mechanistically linked to accumulation of lipotoxic lipid species. Several studies show the detrimental

ISSN Print 0013-7227 ISSN Online 1945-7170
Printed in U.S.A.

Received October 8, 2012. Accepted February 12, 2013.
First Published Online March 7, 2013

* P.-M.B. and I.K.V. contributed equally to this work.

Abbreviations: AAC, area above the curve; AMPK, 5′-AMP protein kinase; Akt, v-Akt murine thymoma viral oncogene homolog; ATGL, adipose triglyceride lipase; AU, arbitrary unit; AUC, area under the curve; CGI58, comparative gene identification 58; DAG, diacylglycerol; GTT, glucose tolerance test; HFD, high-fat diet; HSL, hormone-sensitive lipase; IMTG, intramyocellular TAG; IRS1, insulin receptor substrate-1; ITT, insulin tolerance test; NCD, normal chow diet; PKC, protein kinase C; PLIN, perilipin; TAG, triacylglycerol; TAGH, TAG hydrolase.

role of diacylglycerols (DAGs) and ceramides in cultured myotubes (6, 7), as well as in vivo in mice and human skeletal muscle (8–11).

DAG, a byproduct of lipolysis, is derived from TAG hydrolysis by adipose triglyceride lipase (ATGL) and is further hydrolyzed by the DAG hydrolase hormone-sensitive lipase (HSL) (12). Thus, HSL knockout mice accumulate DAG in several organs, such as skeletal muscle (13), whereas ATGL null mice appear more glucose tolerant (14). We recently demonstrated a causal relationship between defective lipolysis, lipotoxicity, and insulin resistance in human primary myotubes. Up-regulation of ATGL expression and/or inhibition of HSL activity both promoted DAG accumulation and impaired insulin signaling (7). Besides lipases, lipid droplet-associated proteins of the perilipin (PLIN) family (PLIN1–PLIN5) have been shown to play a major role in the control of TAG hydrolysis and lipolysis in multiple tissues (15, 16). It is still unclear whether skeletal muscle PLIN protein expression is disturbed in obesity and insulin-resistance states.

The aim of the present study was to test in vivo in mice the pathophysiological relevance of altered skeletal muscle lipolytic protein expression. We investigated here the impact of a high-fat diet (HFD) on the expression of lipases and PLIN proteins and its relationship with lipotoxicity and insulin resistance in skeletal muscle of C3H mice. This model has been previously used as a relevant model of diet-induced obesity and diabetes (17). We further examined this relationship in HSL knockout mice.

Materials and Methods

Animals

Animal protocols were performed according to Institut National de la Santé et de la Recherche Médicale and Institut des Maladies Métaboliques et Cardiovasculaires Animal Care Facility guidelines. All protocols were reviewed and approved by an Institutional Animal Care and Use Committee. Wild-type males C3H/HeOuJ and females B6D2 HSL null mice (kindly provided by Dr Cecilia Holm) were used and maintained on a 12-hour light, 12-hour dark cycle. They were housed 4 per cage, with ad libitum water and food. HFD (45% fat, Research Diets D12451; Research Diets, Inc, New Brunswick, New Jersey) or normal chow diet (NCD) (10% fat, D12450B) were initiated for 4 weeks right after weaning (5 wk of age) in C3H mice. HSL null mice were fed for 7 weeks under NCD.

Body mass and body composition

Body weight was measured weekly. For C3H mice, body composition was evaluated by quantitative nuclear magnetic resonance imaging (EchoMRI 3-in-1 system; Echo Medical Systems, Houston, Texas) before and at 4 weeks of each diet.

Glucose tolerance test (GTT) and insulin tolerance test (ITT)

For ip ITT and GTT, a bolus of insulin 0.5 mU/g of lean mass (Insuman Rapid, Sanofi Aventis, France) and D-glucose 2 mg/g of lean mass (Sigma-Aldrich, Saint-Quentin Fallavier, France) was injected to 6-hour-fasted mice, respectively. Blood glucose levels were monitored from the tip of the tail with a glucometer (Accucheck; Roche, Meylan, France) at 0, 15, 30, 45, 60, and 90 minutes after injection. Fasting insulin was measured using an ultrasensitive ELISA (ALPCO Diagnostics, Salem, New Hampshire). For ITTs, area above the curve (AAC) was calculated to account for differences in baseline fasting blood glucose concentrations as previously suggested (18).

Tissue-specific [2-^{3}H]deoxyglucose uptake during the GTT

To determine muscle-specific glucose uptake, [2-^{3}H]deoxyglucose (PerkinElmer, Boston, Massachusetts) (12 μCi/mouse) was mixed with 20% D-glucose to obtain a fixed specific activity before ip injection (2-mg/g lean body mass) as previously described with slight modifications (19). Animals were killed by cervical dislocation 45 minutes after injection, and soleus and gastrocnemius muscles were snap frozen in liquid nitrogen. Tissue-specific accumulation of 2-deoxyglucose-6-phosphate was determined as previously described, with minor modifications (20). The total of the [^{3}H]-radioactivity found in 2-deoxyglucose-6-phosphate was divided by the mean specific activity of glucose at 45 minutes to obtain the tissue-specific clearance index (Kg) (milliliter per 100 g of tissue per minute) as described elsewhere (21).

Tissue collection and preparation

After an overnight fast, mice were killed by cervical dislocation, and tissues were rapidly extracted and freeze clamped in liquid nitrogen before being stored at −80°C. For insulin signaling experiments, fresh tissues of C3H mice were incubated at 37°C for 20 minutes in Krebs-Henseleit buffer with or without 100nM insulin. After incubation, tissues were freeze clamped in liquid nitrogen and stored at −80°C. B6D2 wild-type and HSL null mice were injected ip with 10 mU/g of insulin 10 minutes before being killed.

Tissue fractionation

Plasma membrane and cytosol fractions were prepared as previously described with slight modifications (22, 23). Briefly, 50 mg of gastrocnemius muscles were extracted in buffer A (50mM Tris [pH 8.0] and 0.5mM dithiothreitol) containing 10-μL/mL protease inhibitor (Sigma-Aldrich), 10-μL/mL phosphatase I inhibitor (Sigma-Aldrich), and 10-μL/mL phosphatase II inhibitor (Sigma-Aldrich). Tissues were homogenized using a polytron and centrifuged at 1000*g* for 10 minutes at 4°C. The supernatant 1 was collected and kept on ice. The pellet was rinsed once in buffer A, centrifuged at 1000*g* for 10 minutes at 4°C, and the new pellet was resuspended in buffer B (buffer A plus Nonidet P-40 1%) and stood on ice for 1 hour with occasional mixing. The tube was then centrifuged at 16 000*g* for 20 minutes at 4°C, and the supernatant was used as the crude membrane fraction. The supernatant 1 was centrifuged at 16 000*g* for 20 minutes at 4°C, and the new supernatant was used as the cytosol fraction. A representative blot of 1 tissue fractionation experiment is shown in Supplemental Figure 1, published on The

Endocrine Society's Journals Online web site at http://endo.endojournals.org.

Western blot analysis

Soleus muscles were homogenized during 2 cycles of 30 seconds, 5500 rpm, 4°C using the Precellys 24 apparatus (Bertin Technologies, Montigny-le-Bretonneux, France) in a buffer containing 50mM Tris-HCl (pH 8.0), 150mM NaCl, 1% Nonidet P-40, 0.5% sodium deoxycholate, 0.1% sodium dodecyl sulfate, 10-μL/mL protease inhibitor, 10-μL/mL phosphatase I inhibitor, and 10-μL/mL phosphatase II inhibitor. Tissue lysates were centrifuged at 14 000*g* for 25 minutes, and supernatants were stored at −80°C. A total of 40 μg of solubilized proteins from muscle tissue were run on a 4%–20% gradient SDS-PAGE (Bio-Rad, Hercules, California), transferred onto nitrocellulose membrane (Hybond ECL; Amersham Biosciences, Piscataway, New Jersey), and incubated with the primary antibodies: ATGL, HSL, pSer660-HSL, and pSer*565*-HSL (Cell Signaling Technology, Beverly, Massachusetts) and comparative gene identification 58 (CGI58) (Abnova Corp, Tapei, Taiwan) for lipases; pSer473-Akt, v-Akt murine thymoma viral oncogene homolog (Akt), pSer1101-insulin receptor substrate-1 (IRS1), pTyr612-IRS1, IRS1, pThr642-AS160, and AS160 for insulin signaling (Cell Signaling Technology). For protein kinase C (PKC) translocation assays, PKCpan, PKCθ, and PKCϵ primary antibodies were from Santa Cruz Biotechnology, Inc (Santa Cruz, California). α-Tubulin (Sigma-Aldrich) was used as cytosolic marker, and caveolin1 (Cell Signaling Technology) was used as plasma membrane marker. Gels were loaded with equal amount of membrane and cytosol proteins. For detection of PLIN, membranes were also probed with PLIN2 and PLIN3 (Thermo Scientific, Illkirch, France) and PLIN5 (Progen, Heidelberg, Germany) antibodies. Subsequently, immunoreactive proteins were determined by enhanced chemiluminescence reagent (SuperSignal West Dura or SuperSignal West Femto; Thermo Scientific) and visualized by exposure to Hyperfilm ECL (GE Healthcare, Princeton, New Jersey). Glyceraldehyde-3-phosphate dehydrogenase (Cell Signaling Technology) was used as internal control.

Lipase activity assays

TAG hydrolase (TAGH) activity was measured on soleus lysates as previously described (24). Briefly, muscles were extracted in a lysis buffer containing 0.25M sucrose, 1mM EDTA, 1mM dithiothreitol, 20-μg/mL leupeptin, and 20-μg/mL antipain. [9, 10-^{3}H(N)]triolein (PerkinElmer) and cold triolein were emulsified with phospholipids by sonication. The data are expressed in nanomoles of oleic acid released per hour per milligram of protein.

Neutral lipid molecular species analysis

Soleus muscles were homogenized in 1 mL of methanol/5mM EGTA (2:1, vol/vol) with FAST-PREP (MP Biochemicals, Solon, Ohio). Lipids corresponding to 2 mg of tissue were extracted according to Bligh and Dyer (25) in methanol/water/dichloromethane (1.5:1.5:2, vol/vol/vol), in the presence of internal standards: 3 μg of stigmasterol, 3 μg of 1,3-dimyristine, 3 μg of cholesteryl heptadecanoate, and 20 μg of glyceryl trinonadecanoate. Dichloromethane phase was evaporated to dryness. Neutral lipid were separated on solid phase extraction columns (Macherey Nagel glass Chromabond pure silice, 200 mg) after washing cartridge with 2 mL of chloroform, crude extract was applied on the cartridge in 40 μL of chloroform, and neutral lipids were eluted in 2 mL of chloroform:methanol (9:1, vol/vol). The organic phase was evaporated to dryness and dissolved in 20 μL of ethyl acetate. One microliter of the lipid extract was analyzed by gas-liquid chromatography on a FOCUS Thermo Electron system using an Zebron-1 Phenomenex fused silica capillary columns (5 m × 0,32 mm inner diameter, 0.50 μm of film thickness) (26). Oven temperature was programmed from 200°C to 350°C at a rate of 5°C per minute, and the carrier gas was hydrogen (0.5 bar). The injector and the detector were at 315°C and 345°C, respectively. The equivalent of 0.3 mg of tissue was evaporated under nitrogen, the dry pellets were dissolved overnight in 0.2 mL of NaOH (0.1M), and proteins were measured with the Bio-Rad protein assay.

[1-^{14}C]palmitate incorporation

Whole solei were incubated for 2 hours in a modified sucrose-EDTA medium (250mM sucrose, 1mM EDTA, and 10mM Tris-HCl [pH 7.4]) with a combination of [1-^{14}C]palmitate (1 μCi/ml; PerkinElmer) and unlabeled palmitate (200μM final concentration). At the end of incubation, total lipids were extracted in chloroform/methanol (2volume/1volume) and separated by thin layer chromatography as previously described (27). Incorporation rates were normalized to wet tissue weight.

Statistics

All statistical analyses were performed using GraphPad Prism 5.0 for Windows (GraphPad Software, Inc, San Diego, California). Normal distribution of the data was tested with Kolmogorov-Smirnov tests. Unpaired Student's *t* tests were performed to determine differences between groups. Two-way ANOVA followed by Bonferonni's post hoc tests was applied when appropriate. Pearson correlations were applied when data were normally distributed and Spearman correlations for nonparametric data. All values in figures and tables are presented as mean ± SEM. Statistical significance was set at $P < .05$.

Results

Short-term HFD induces rapid weight gain and whole-body insulin resistance in C3H mice

As expected, 4 weeks of HFD 45% kcal from fat induced greater weight gain compared with NCD in C3H mice (NCD +25%, $P < .001$; HFD +60%, $P < .001$) mainly because of a robust increase in fat mass (NCD +61%, $P < .01$; HFD +382%, $P < .001$), whereas lean body mass was not significantly changed between NCD and HFD (Table 1). Importantly, 4 weeks of HFD in C3H mice were sufficient to induce a comparable body weight gain (about 60%) as is typically observed in C57Bl/6 mice after 8 weeks under the same diet (data not shown). In addition, HFD increased fasting blood glucose (+18%, $P < .001$) and fasting blood insulin (4.5-fold, $P < .001$) compared with NCD in C3H mice (Table 1). Whole-body insulin and glucose tolerance were measured (Figure 1, A

Table 1. Body Composition and Metabolic Variables in Fasted C3H Mice

	NCD	HFD	*P* value
Weight (g)	27.9 ± 0.38	35.5 ± 0.50	<.001
Fat mass (g)	2.6 ± 0.28	9.1 ± 0.33	<.001
Lean mass (g)	19.5 ± 0.20	19.7 ± 0.22	N.S.
Fasting insulin (ng/mL)	0.47 ± 0.08	2.1 ± 0.30	<.001
Fasting glucose (mg/dL)	140 ± 3.87	166 ± 4.21	<.001

N.S., not significant.

and B). The ITT AAC was reduced by −44% ($P < .01$) (Figure 1A), whereas the GTT area under the curve (AUC) was significantly increased in HFD-fed mice (3-fold, $P < .01$) (Figure 1B). Interestingly, plasma insulin concentration at 15 minutes during the GTT was significantly elevated in HFD-fed mice (2.8-fold, $P < .001$) (Figure 1C). Thus, C3H mice were strongly insulin resistant after 4 weeks of HFD and represent an interesting model to study the effect of short-term high-fat feeding on the mechanisms of fat-induced insulin resistance.

Short-term HFD promotes lipotoxicity and impairs insulin signaling in skeletal muscle

Because skeletal muscle is an important site of glucose disposal in the body, we examined the effects of short-term HFD on skeletal muscle glucose uptake, lipotoxicity, and insulin signaling. We first showed a reduced glucose uptake in both oxidative soleus and glycolytic gastrocnemius muscles of HFD-fed mice in vivo (Figure 2A). Of interest, glucose uptake in soleus was inversely correlated to the log(AUC) of the GTT ($r = -0.73$, $P = .01$). The reduced glucose uptake was associated with significant disturbances in muscle insulin signaling. Indeed, we noticed an increased basal Ser1101 phosphorylation of the IRS1 (2.8-fold, $P < .05$) (Figure 2, B and F), associated with an expected decrease of its activating phosphorylation on Tyr612 upon insulin stimulation (−68% $P < .01$) (Figure 2, C and F). Consistently, downstream insulin-stimulated phosphorylation of Akt at Ser473 residue (−37%, $P < .01$) (Figure 2, D and F) and AS160 at Thr642 (−88%, $P < .01$) (Figure 2, E and F) was reduced in HFD-fed mice, whereas their basal phosphorylation remained unaffected by the diet (Supplemental Figure 2). IRS1 phosphorylation at Ser1101 inhibits IRS1 function and is a primary target for DAG-activated PKC (28). This prompted us to examine PKC translocation to the plasma membrane and skeletal muscle lipid content. We found a higher membrane to cytosol ratio of all PKC isoforms (PKCpan) as well as of the main novel PKC isoforms, PKCθ and PKCϵ, in the muscle of HFD-fed compared with NCD-fed mice (Figure 3, A and B, and Supplemental Figure 3). As expected, the higher novel PKC membrane translocation was associated

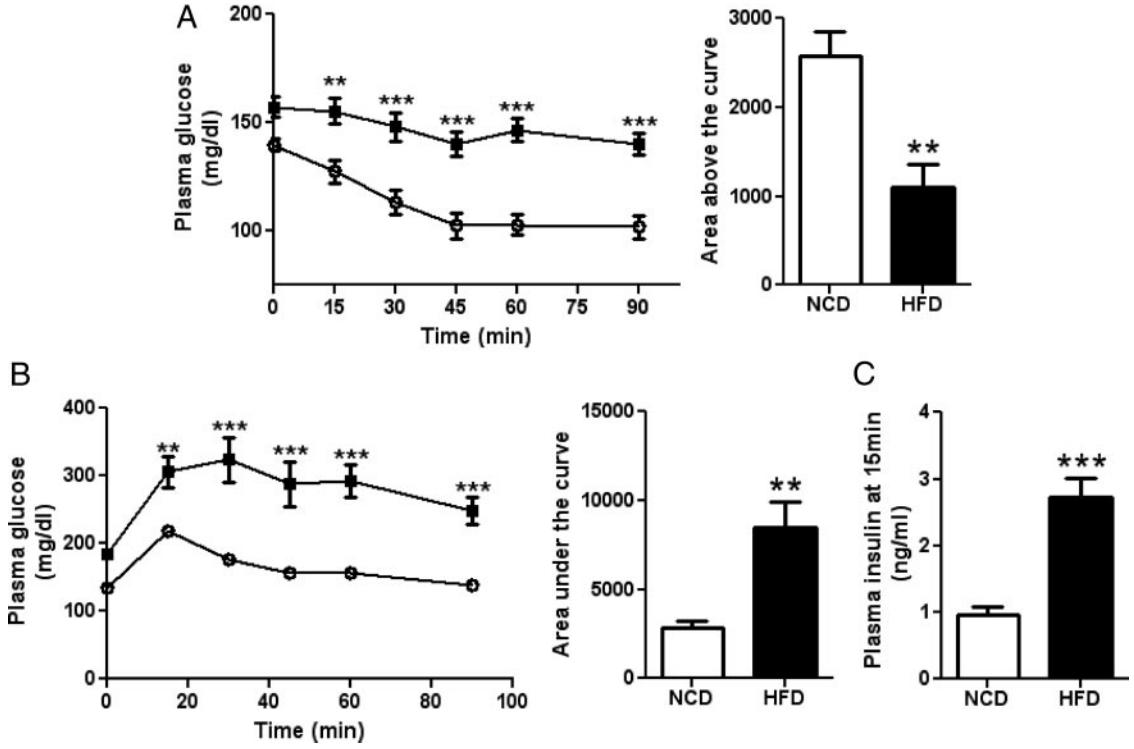

Figure 1. Short-term HFD induces whole-body insulin resistance in C3H mice. (A) (left panel) ITT in mice at 4 weeks of HFD (black square) or NCD (open circle); (right panel) AAC during the ITT. (B) (left panel) GTT in mice at 4 weeks of HFD or NCD; (right panel) AUC during the GTT. (C) Plasma insulin concentration measured 15 minutes after glucose injection. n = 8; $^{**}P < .01$, $^{***}P < .001$ vs NCD.

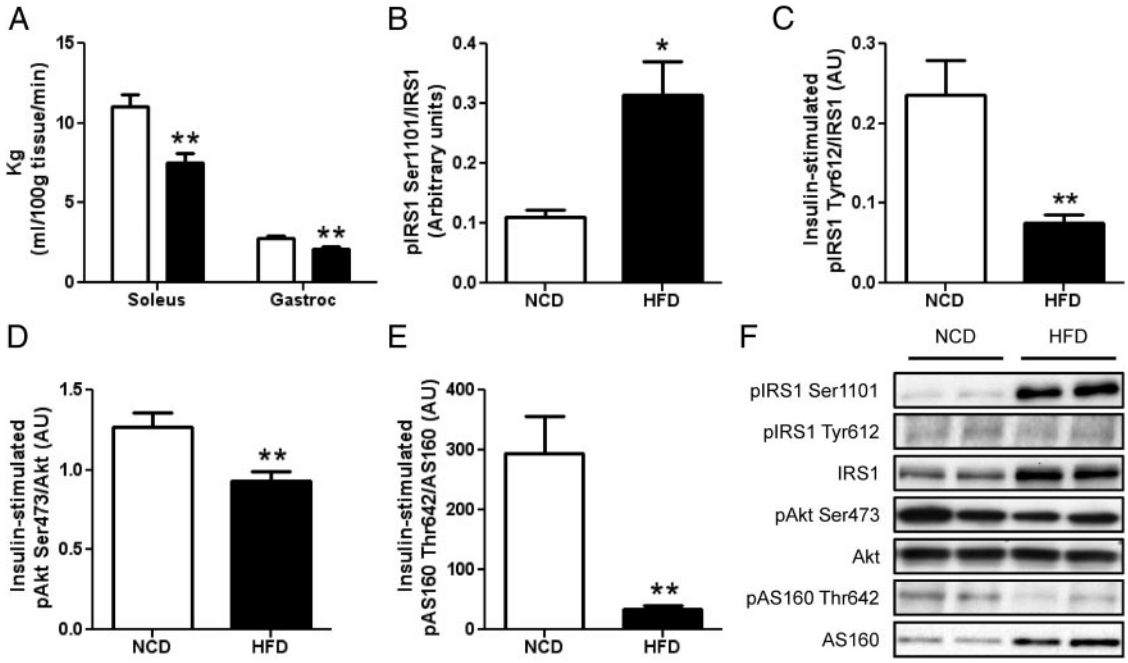

Figure 2. Impaired skeletal muscle insulin signaling after 4 weeks of HFD. (A) Tissue-specific glucose uptake in soleus and gastrocnemius muscles after 4 weeks of NCD or HFD (n = 6–8). (B) Quantitative bar graph of basal pIRS1 Ser1101 in mice soleus after 4 weeks of NCD or HFD (n = 4–5). (C) Quantitative bar graph of insulin-stimulated pIRS1 Tyr612 phosphorylation in mice soleus after 4 weeks of NCD or HFD (n = 8). (D) Quantitative bar graph of insulin-stimulated pAkt Ser473 phosphorylation in mice soleus after 4 weeks of NCD or HFD (n = 8). (E) Quantitative bar graph of insulin-stimulated pAS160 Thr642 phosphorylation in mice soleus after 4 weeks of NCD or HFD (n = 8). (F) Representative blots of 2 NCD- and 2 HFD-fed mice. $*P < .05$, $**P < .01$ vs NCD.

with a significantly elevated total DAG content (+39%, $P < .05$) (Figure 3C), whereas a trend for higher IMTG content (+35%, $P = .12$) (Figure 3D) was observed in HFD-fed mice. Interestingly, we noted a strong relationship between skeletal muscle DAG content and fasting blood insulin ($r = 0.60$, $P = .01$), as well as a negative correlation between muscle plasma membrane PKCpan and whole-body insulin sensitivity as measured by the ITT AAC ($r = -0.57$, $P = .03$). Additionally, IRS1 serine phosphorylation occurred without any significant change in c-Jun N-terminal kinase-1 phosphorylation (Supplemental Figure 4A), whereas 5′-AMP protein kinase (AMPK) Thr172 phosphorylation was significantly reduced in HFD-fed mice (Supplemental Figure 4B).

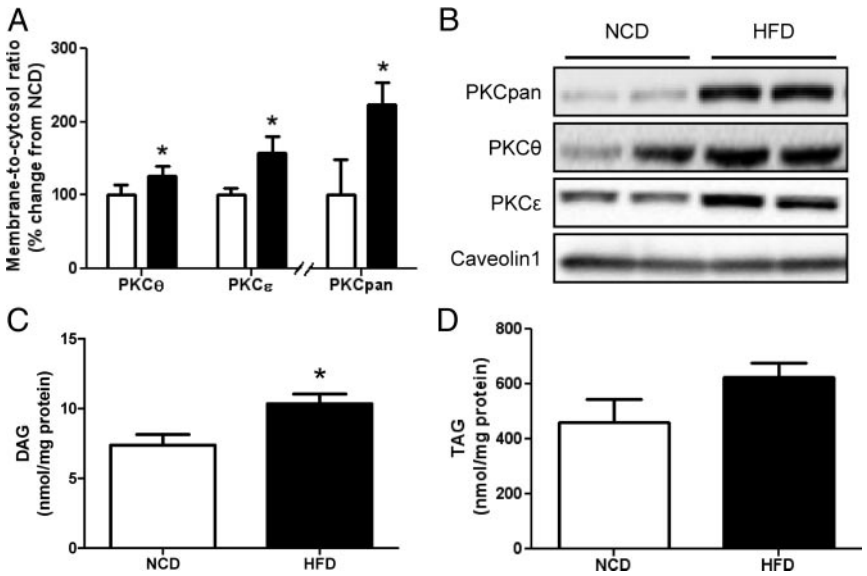

Figure 3. HFD-induced lipotoxicity in skeletal muscle. (A) Gastrocnemius muscle PKCs membrane to cytosol ratio of mice fed NCD (white bars) or HFD (black bars) during 4 weeks. (B) Representative blots of membrane PKCs (n = 6–8). (C and D) Neutral lipid content in soleus of mice after 4 weeks of NCD or HFD. (C) Total DAG content. (D) TAG content (n = 8). $*P < .05$ vs NCD.

Short-term HFD alters skeletal muscle lipolytic proteins

To gain further insight into the mechanisms of HFD-induced lipotoxicity, we examined lipase and PLIN protein expression in skeletal muscle. Interestingly, compared with NCD, HFD up-regulated the expression of the ATGL coactivator CGI58 both in soleus and gastrocnemius muscles (Figure 4B and Supplemental Figure 5B), whereas ATGL protein tended to decrease (Figure 4A and Supplemental Figure 5A). CGI58 protein level progressively

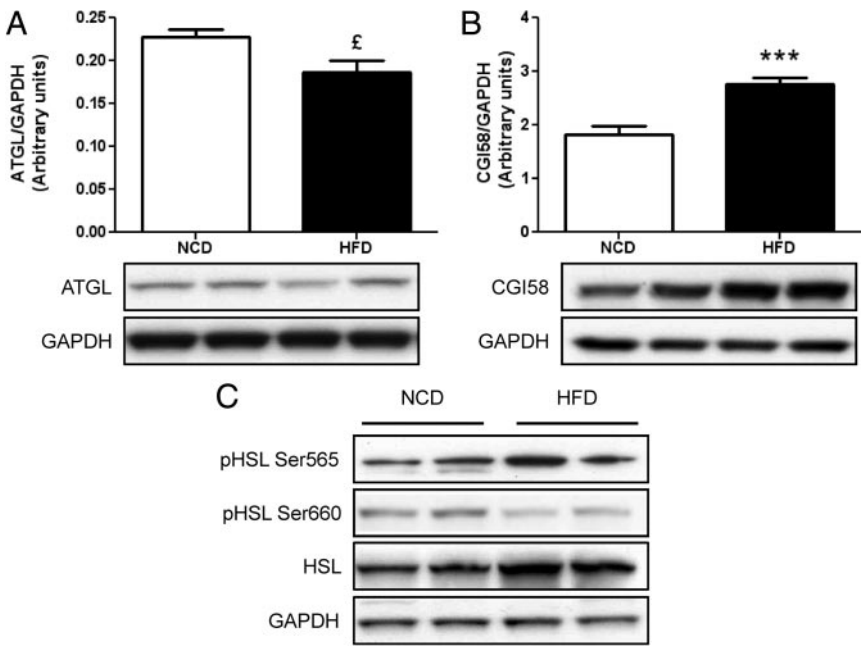

Figure 4. Altered skeletal muscle lipases expression in soleus of HFD-fed mice. (A–C) Lipase protein expression in mice fed with NCD or HFD for 4 weeks. (A) ATGL protein expression (n = 4–5). (B) CGI58 protein expression (n = 12–13). Insets show a representative blot of 2 NCD- and 2 HFD-fed mice. £ = 0.06, ***$P < .001$ vs NCD. (C) Representative blots of pHSL Ser660, pHSL Ser565, and total HSL protein. GAPDH, glyceraldehyde-3-phosphate dehydrogenase.

rose from the beginning of the HFD until 4 weeks, whereas ATGL expression was not significantly changed (Supplemental Figure 6). Importantly, we observed a very strong decrease in Ser660-HSL phosphorylation (NCD, 0.16 ± 0.02 arbitrary units [AU] vs HFD, 0.08 ± 0.01 AU, $P < .01$) (Figure 4C and Supplemental Figure 5C), whereas Ser565-HSL phosphorylation was not altered when adjusted to total HSL (NCD, 3.73 ± 0.76 AU vs HFD, 2.28 ± 0.62 AU, $P = .18$) (Figure 4C). The decrease in Ser660-HSL phosphorylation occurred despite a significant increase of total HSL protein (NCD, 0.90 ± 0.03 AU vs HFD, 1.21 ± 0.05 AU, $P < .01$) (Figure 4C). We also measured the protein content of PLINs that are lipid droplet related proteins involved in the control of lipid droplet dynamics and metabolism. PLIN2 and PLIN3 proteins were not affected by HFD (Figure 5, A and B), whereas PLIN5 was strongly up-regulated in HFD-fed mice compared with NCD (+86%, $P < .01$) (Figure 5C and Supplemental Figure 5D). Moreover, PLIN5 expression paralleled the increase of CGI58 protein during the time course of high-fat feeding (Supplemental Figure 7). In a larger cohort of mice, we found a very strong positive relationship between PLIN5 expression and total body weight (Figure 5D), as well as fat mass ($r = 0.81$, $P < .001$). Skeletal muscle lipase and PLIN protein expression responded similarly in B6D2 mice fed the same HFD for a longer period of 14 weeks (data not shown). These changes in lipolytic proteins were associated with a trend for increased TAGH activity (+53%) (NCD, 1.64 ± 0.24 nmol/h^{-1}·mg^{-1} vs HFD, 2.51 ± 0.41 nmol/h^{-1}·mg^{-1}, $P = .09$).

Increased DAG and disrupted insulin signaling in skeletal muscle of HSL knockout mice

To examine the link between reduced HSL activity in skeletal muscle and insulin resistance, we also studied HSL null mice on NCD (Figure 6A). We performed ex vivo studies in whole-soleus muscle and showed a higher incorporation rate of palmitate into DAG (+93%, $P < .05$) (Figure 6B), whereas the rate of incorporation of palmitate into TAG was not significantly affected (Figure 6C). This was accompanied by a reduced insulin activation of Akt on its Ser473 residue (−19%, $P < .05$) (Figure 6D), whereas basal Akt phosphorylation remained unaffected (data not shown). Thus, HSL deficiency in skeletal muscle promotes DAG accumulation and impairs insulin signaling.

Discussion

It is now well established that insulin resistance is related to accumulation of DAG and ceramides in skeletal muscle (6, 29). However, the mechanisms underlying their accumulation during the development of obesity are still discussed. In this study, we show that short-term HFD impairs skeletal muscle lipases and PLIN proteins and concomitantly promotes DAG accumulation, PKC membrane translocation, and insulin resistance in skeletal muscle. These findings are consistent with recent in vitro data, where we demonstrated a causal relationship between altered lipase expression, DAG accumulation, and insulin resistance in human primary myotubes (7).

In the present study, we used C3H mice, which represent an interesting model to study the effect of short-term high-fat feeding on skeletal muscle lipotoxicity and insulin resistance (17). A robust and fast body weight gain is observed in C3H mice within 4 weeks of HFD. Under the same diet, 8 weeks are required for C57Bl/6 mice to reach the same level of weight gain. We observed a strong deterioration of whole-body insulin sensitivity, glucose tolerance, and skeletal muscle glucose uptake in C3H mice

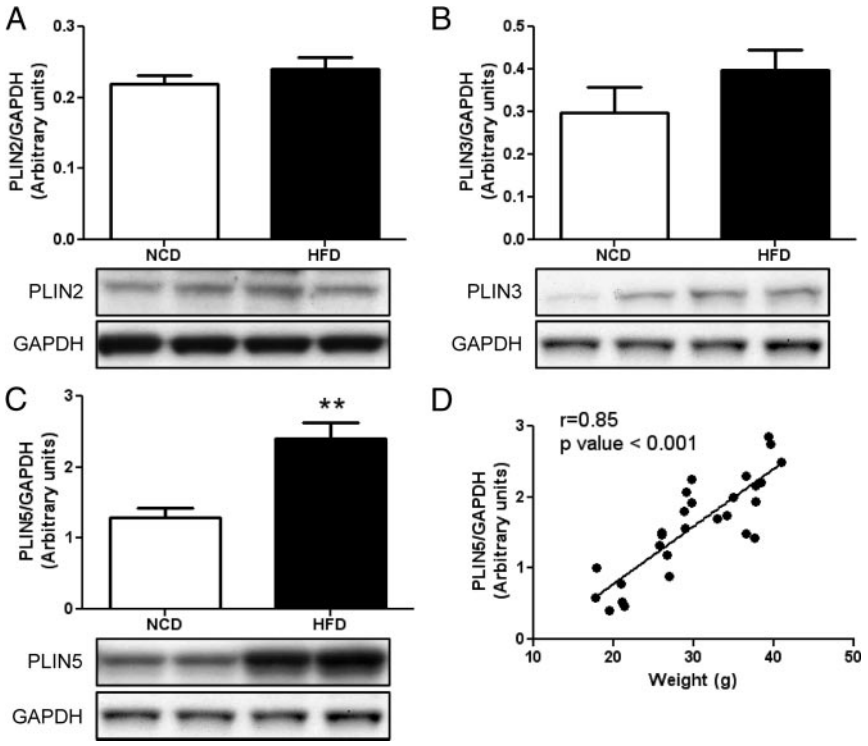

Figure 5. HFD-induced modulation of skeletal muscle PLINs. (A–C) PLIN protein expression in mice fed with NCD or HFD for 4 weeks. (A) PLIN2 protein expression. (B) PLIN3 protein expression. (C) PLIN5 protein expression (n = 4–5). Insets show a representative blot of 2 NCD- and 2 HFD-fed mice. $^{**}P < .01$ vs NCD. (D) Pearson correlation between body weight and PLIN5 protein expression (n = 28). GAPDH, glyceraldehyde-3-phosphate dehydrogenase.

within 4 weeks of HFD. Importantly, skeletal muscle insulin signaling was impaired in HFD-fed mice as reflected by an increased Ser1101-IRS1 phosphorylation and a decrease of Tyr612-IRS1 phosphorylation despite a significant increase of IRS1 protein. The higher expression of IRS1 protein could be explained by relatively higher fasting plasma insulin in HFD-fed mice. Insulin was shown to acutely induce IRS1 expression in mouse and human skeletal muscle to compensate for serine phosphorylation-induced IRS1 proteasomal degradation (30). As expected, downstream IRS1 signaling was strongly impaired as evidenced by reduced insulin-stimulated Ser473-Akt and Thr642-AS160 phosphorylation. We also showed impaired muscle AMPK activation, which could, together with reduced Akt activity, contribute to reduced AS160 activation, which is a downstream target of both Akt and AMPK signaling (31). These alterations of insulin signaling are consistent with other reports and confirm that skeletal muscle is a primary site of glucose disposal and insulin action (32). Increased Ser1101 phosphorylation of IRS1 has been shown to inhibit IRS1 function and could be a specific target of PKCθ (28). We thus show a higher translocation of both PKCθ and PKCϵ at the plasma membrane of skeletal muscle in HFD-fed mice. DAGs are involved in activation of conventional PKC (α, βI, βII, γ) and novel PKC (δ, ϵ, η, θ), and DAG accumulation is known to be strongly associated with obesity and insulin resistance in humans (9, 24, 33) and mice (34). Interestingly, we noted that in parallel to insulin resistance, HFD-fed mice had elevated levels of DAG in skeletal muscle as previously described (35). HFD-induced impairments in skeletal muscle IRS1 function and insulin signaling were also independent of changes in c-Jun N-terminal kinase-1 activation in agreement with recent studies (36, 37). Our data are consistent with the view that HFD induces muscle insulin resistance through DAG-mediated novel PKC activation (9, 38).

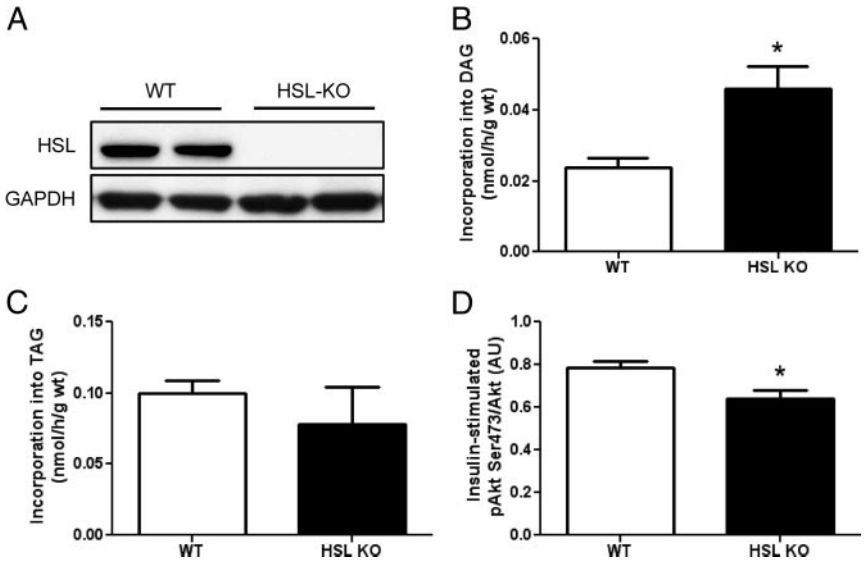

Figure 6. Elevated DAG and impaired insulin signaling in skeletal muscle of HSL null mice. (A) Representative blots of HSL protein and loading control in 2 wild-type (WT) and 2 HSL-knockout (KO) mice. (B and C) Incorporation of [1-^{14}C]palmitate in neutral lipid pools in soleus of WT and HSL-KO mice. (B) Incorporation rate into the DAG pool. (C) Incorporation rate into the TAG pool. (D) Insulin-stimulated Akt Ser473 phosphorylation in soleus of WT and HSL-KO mice (n = 5–6). $^{*}P < .05$ vs WT. GAPDH, glyceraldehyde-3-phosphate dehydrogenase.

Because DAG and TAG availability is highly regulated by lipolytic proteins (12), and that defective expression/activity of skeletal muscle lipases may promote DAG accumulation, we next investigated the influence of HFD on lipolytic proteins. This hypothesis is based on previous work, which demonstrate a strong association between obesity and defective skeletal muscle TAG and DAG hydrolysis (24) and related lipases in humans (7, 39). Although sn-1,2-DAG has been the most studied DAG in mammalian cells, it was shown that sn-1,3-DAG can promote PKCα binding to pure palmitoyl-2-oleoyl-sn-glycero-3-phosphoserine membrane vesicles (40). Thus, both sn-1,3-DAG and sn-1,2-DAG could activate PKC translocation to plasma membrane. In addition, we and others have recently shown that DAG produced from TAGHs, such as ATGL, can enter the pathway of phospholipid synthesis in normal human fibroblasts (41) and primary human myotubes (42). This suggests that ATGL-mediated TAG hydrolysis can provide sn-1,2-DAG capable of activating PKC. Of interest, ATGL protein content tended to be down-regulated, whereas its coactivator CGI58 was significantly up-regulated in skeletal muscle of HFD-fed mice. This inverse relationship has been previously observed in human myotubes (42) and in a human adipocyte cell line (43) and suggests that CGI58 and ATGL are reciprocally regulated in skeletal muscle and possibly in other tissues. Up-regulation of CGI58 despite the decrease of ATGL was sufficient to increase TAGH activity and lipolysis. This result confirms in vivo the central and limiting role of CGI58 in the regulation of skeletal muscle lipolysis (42).

An important finding of this study is that HSL Ser660 phosphorylation was dramatically reduced in the muscle of HFD-fed mice. No change in the phosphorylation level of the inhibitory HSL Ser565 residue was observed. Interestingly, HSL Ser660 phosphorylation is closely related to HSL activity in vitro (44). This serine residue is activated by cAMP-dependent protein kinase A (44). A similar down-regulation of HSL phosphorylation has been observed in adipose tissue during high-fat feeding (45). This may be explained by a reduction of protein kinase A activity through a down-regulation of its α-subunit in the obese state (46). Moreover, a reduced HSL Ser660 phosphorylation and partial resistance to catecholamine-induced lipolysis have been observed in skeletal muscle of obese insulin-resistant subjects (39, 47). Together, these data suggest that obesity and high-fat feeding may be associated with a low HSL activity in skeletal muscle.

We further investigated HSL null mice to understand the mechanistic link between low HSL activity and insulin resistance in skeletal muscle. We could show that HSL deficiency increases the rate of DAG accumulation without significant changes in skeletal muscle TAG dynamics. This finding is in agreement with a previous report (13). The higher DAG accumulation was associated with a lower insulin-stimulated activation of Akt on its Ser473 residue in the muscle of HSL null mice. Our data are in agreement with other reports showing a reduced insulin-mediated glucose transport in skeletal muscle of chow diet-fed HSL null mice (48, 49). It is important to note here that whole-body HSL deficiency may give a more complex phenotype than muscle-specific HSL deficiency. Thus, several phenotypic discrepancies have been observed in HSL knockout mice under different backgrounds and diet (48–50). This is also in line with recent findings showing an increased DAG accumulation and mild insulin resistance in human primary myotubes treated with a selective HSL inhibitor (7). Thus, the observed changes in DAG and insulin signaling were muscle autonomous. Together, these data suggest a causal link between low HSL activity, DAG accumulation, and insulin resistance in skeletal muscle.

The access of lipases to lipid droplets is partly controlled by PLIN proteins. In adipose tissue, PLIN1 is strongly expressed, and its role in lipolysis has been well studied (51, 52). Recent studies highlight the role of another member of the PLIN family, PLIN5, especially in oxidative tissues where PLIN1 is virtually not expressed (53). Wang et al (54, 55) and Granneman et al (56) showed that PLIN5 regulates negatively lipolysis and can link ATGL and CGI58 (54–56). PLIN5 protein expression increases in parallel of body fat mass during the HFD. This may be seen as an adaptive response to buffer excess dietary lipids into lipid droplets. This could be driven by increased FA flux and activation of peroxisome proliferator activated receptor signaling within the skeletal muscle (57, 58), because PLIN5 is a well-known target of peroxisome proliferator activated receptor α (16, 59). Futures studies will be necessary to understand the physiological role of PLIN5 in skeletal muscle in vivo and its association with insulin resistance.

One study limitation is that besides DAG, we cannot exclude a role of ceramides in fat-induced insulin resistance. Several studies have shown that ceramides contribute to the development of insulin resistance in palmitate-treated myocytes (6) and in mice fed lard diet and/or during saturated oil infusions (8, 35, 60). However, to the best of our knowledge, a direct effect of ceramide-activated Ser/Thr kinases on IRS1 serine phosphorylation has never been reported. We cannot dismiss either that other mechanisms might contribute to skeletal muscle DAG accumulation in obesity and diabetes, such as reduced DAG kinase activity and/or DAG-acyl-transferase-1 activity (34, 61).

In summary, our data show a pathophysiological link between altered lipase expression, lipotoxicity, and insulin resistance in skeletal muscle in vivo. These findings strengthen the relevance of in vitro results showing a causal association between altered lipase expression and insulin resistance in myotubes. Restoring a proper lipolytic control in skeletal muscle may alleviate obesity-related lipotoxicity and insulin resistance.

Acknowledgments

We thank M. Coonen, A. Girousse and A. Besse-Patin (Institut National de la Santé et de la Recherche Médicale [INSERM], Unité Mixte de Recherche [UMR] 1048) for outstanding help; J. Bertrand-Michel and V. Roques (Lipidomic Core Facility, INSERM, UMR 1048, part of Toulouse Metatoul Platform) for lipidomic analysis, advice, and technical assistance; and the Anexplo Mouse Phenotyping and Animal Care facility cores.

Address all correspondence and requests for reprints to: Cedric Moro, PhD, Institut National de la Santé et de la Recherche Médicale, Unité Mixte de Recherche 1048, Institut des Maladies Métaboliques et Cardiovasculaires, CHU Rangueil, BP 84225, 1 Avenue Jean Poulhès, 31432 Toulouse Cedex 4, France. E-mail: cedric.moro@inserm.fr.

This work was supported by grants from the European Foundation for the Study of Diabetes/Novo Nordisk, the National Research Agency Grant ANR-09-JCJC-0019-01, and the Société Francophone du Diabète (C.M.) and by the Fondation pour la Recherche Médicale (D.L.). I.K.V. was supported by a fellowship from the Midi-Pyrénées region.

Disclosure Summary: The authors have nothing to disclose.

References

1. **DeFronzo RA.** Pathogenesis of type 2 diabetes mellitus. *Med Clin North Am*. 2004;88:787–835, ix.
2. **McGarry JD.** Banting lecture 2001: dysregulation of fatty acid metabolism in the etiology of type 2 diabetes. *Diabetes*. 2002;51:7–18.
3. **Szczepaniak LS, Babcock EE, Schick F, et al.** Measurement of intracellular triglyceride stores by H spectroscopy: validation in vivo. *Am J Physiol*. 1999;276:E977–E989.
4. **Kelley DE, Goodpaster BH, Storlien L.** Muscle triglyceride and insulin resistance. *Annu Rev Nutr*. 2002;22:325–346.
5. **Moro C, Bajpeyi S, Smith SR.** Determinants of intramyocellular triglyceride turnover: implications for insulin sensitivity. *Am J Physiol*. 2008;294:E203–E213.
6. **Pickersgill L, Litherland GJ, Greenberg AS, Walker M, Yeaman SJ.** Key role for ceramides in mediating insulin resistance in human muscle cells. *J Biol Chem*. 2007;282:12583–12589.
7. **Badin PM, Louche K, Mairal A, et al.** Altered skeletal muscle lipase expression and activity contribute to insulin resistance in humans. *Diabetes*. 2011;60:1734–1742.
8. **Holland WL, Brozinick JT, Wang LP, et al.** Inhibition of ceramide synthesis ameliorates glucocorticoid-, saturated-fat-, and obesity-induced insulin resistance. *Cell Metab*. 2007;5:167–179.
9. **Itani SI, Ruderman NB, Schmieder F, Boden G.** Lipid-induced insulin resistance in human muscle is associated with changes in diacylglycerol, protein kinase C, and IκB-α. *Diabetes*. 2002;51:2005–2011.
10. **Dresner A, Laurent D, Marcucci M, et al.** Effects of free fatty acids on glucose transport and IRS-1-associated phosphatidylinositol 3-kinase activity. *J Clin Invest*. 1999;103:253–259.
11. **Adams JM 2nd, Pratipanawatr T, Berria R, et al.** Ceramide content is increased in skeletal muscle from obese insulin-resistant humans. *Diabetes*. 2004;53:25–31.
12. **Zechner R, Zimmermann R, Eichmann TO, et al.** FAT SIGNALS—lipases and lipolysis in lipid metabolism and signaling. *Cell Metab*. 2012;15:279–291.
13. **Haemmerle G, Zimmermann R, Hayn M, et al.** Hormone-sensitive lipase deficiency in mice causes diglyceride accumulation in adipose tissue, muscle, and testis. *J Biol Chem*. 2002;277:4806–4815.
14. **Haemmerle G, Lass A, Zimmermann R, et al.** Defective lipolysis and altered energy metabolism in mice lacking adipose triglyceride lipase. *Science*. 2006;312:734–737.
15. **Prats C, Donsmark M, Qvortrup K, et al.** Decrease in intramuscular lipid droplets and translocation of HSL in response to muscle contraction and epinephrine. *J Lipid Res*. 2006;47:2392–2399.
16. **Wolins NE, Quaynor BK, Skinner JR, et al.** OXPAT/PAT-1 is a PPAR-induced lipid droplet protein that promotes fatty acid utilization. *Diabetes*. 2006;55:3418–3428.
17. **Toye AA, Lippiat JD, Proks P, et al.** A genetic and physiological study of impaired glucose homeostasis control in C57BL/6J mice. *Diabetologia*. 2005;48:675–686.
18. **Ayala JE, Samuel VT, Morton GJ, et al.** Standard operating procedures for describing and performing metabolic tests of glucose homeostasis in mice. *Dis Model Mech*. 2010;3:525–534.
19. **Mauvais-Jarvis F, Virkamaki A, Michael MD, et al.** A model to explore the interaction between muscle insulin resistance and β-cell dysfunction in the development of type 2 diabetes. *Diabetes*. 2000;49:2126–2134.
20. **Virkamaki A, Rissanen E, Hamalainen S, Utriainen T, Yki-Jarvinen H.** Incorporation of [3–3H]glucose and 2-[1-14C]deoxyglucose into glycogen in heart and skeletal muscle in vivo: implications for the quantitation of tissue glucose uptake. *Diabetes*. 1997;46:1106–1110.
21. **Kraegen EW, James DE, Jenkins AB, Chisholm DJ.** Dose-response curves for in vivo insulin sensitivity in individual tissues in rats. *Am J Physiol*. 1985;248:E353–E362.
22. **Nishiumi S, Ashida H.** Rapid preparation of a plasma membrane fraction from adipocytes and muscle cells: application to detection of translocated glucose transporter 4 on the plasma membrane. *Biosci Biotechnol Biochem*. 2007;71:2343–2346.
23. **Bostrom P, Andersson L, Vind B, et al.** The SNARE protein SNAP23 and the SNARE-interacting protein Munc18c in human skeletal muscle are implicated in insulin resistance/type 2 diabetes. *Diabetes*. 2010;59:1870–1878.
24. **Moro C, Galgani JE, Luu L, et al.** Influence of gender, obesity, and muscle lipase activity on intramyocellular lipids in sedentary individuals. *J Clin Endocrinol Metab*. 2009;94:3440–3447.
25. **Bligh EG, Dyer WJ.** A rapid method of total lipid extraction and purification. *Can J Biochem Physiol*. 1959;37:911–917.
26. **Barrans A, Collet X, Barbaras R, et al.** Hepatic lipase induces the formation of pre-β 1 high density lipoprotein (HDL) from triacylglycerol-rich HDL2. A study comparing liver perfusion to in vitro incubation with lipases. *J Biol Chem*. 1994;269:11572–11577.
27. **Hessvik NP, Bakke SS, Fredriksson K, et al.** Metabolic switching of human myotubes is improved by n-3 fatty acids. *J Lipid Res*. 2010;51:2090–2104.
28. **Li Y, Soos TJ, Li X, et al.** Protein kinase Cθ inhibits insulin signaling by phosphorylating IRS1 at Ser(1101). *J Biol Chem*. 2004;279:45304–45307.
29. **Yu C, Chen Y, Cline GW, et al.** Mechanism by which fatty acids inhibit insulin activation of insulin receptor substrate-1 (IRS-1)-as-

sociated phosphatidylinositol 3-kinase activity in muscle. *J Biol Chem*. 2002;277:50230–50236.
30. **Ruiz-Alcaraz AJ, Liu HK, Cuthbertson DJ, et al.** A novel regulation of IRS1 (insulin receptor substrate-1) expression following short term insulin administration. *Biochem J*. 2005;392:345–352.
31. **Deshmukh AS, Hawley JA, Zierath JR.** Exercise-induced phosphoproteins in skeletal muscle. *Int J Obes (Lond)*. 2008;4(suppl 32): S18–S23.
32. **DeFronzo RA, Tripathy D.** Skeletal muscle insulin resistance is the primary defect in type 2 diabetes. *Diabetes Care*. 2009;2(suppl 32): S157–S163.
33. **Samuel VT, Shulman GI.** Mechanisms for insulin resistance: common threads and missing links. *Cell*. 2012;148:852–871.
34. **Chibalin AV, Leng Y, Vieira E, et al.** Downregulation of diacylglycerol kinase δ contributes to hyperglycemia-induced insulin resistance. *Cell*. 2008;132:375–386.
35. **Ussher JR, Koves TR, Cadete VJ, et al.** Inhibition of de novo ceramide synthesis reverses diet-induced insulin resistance and enhances whole-body oxygen consumption. *Diabetes*. 2010;59:2453–2464.
36. **Hage Hassan R, Hainault I, Vilquin JT, et al.** Endoplasmic reticulum stress does not mediate palmitate-induced insulin resistance in mouse and human muscle cells. *Diabetologia*. 2012;55:204–214.
37. **Rieusset J, Chauvin MA, Durand A, et al.** Reduction of endoplasmic reticulum stress using chemical chaperones or Grp78 overexpression does not protect muscle cells from palmitate-induced insulin resistance. *Biochem Biophys Res Commun*. 2012;417:439–445.
38. **Itani SI, Zhou Q, Pories WJ, MacDonald KG, Dohm GL.** Involvement of protein kinase C in human skeletal muscle insulin resistance and obesity. *Diabetes*. 2000;49:1353–1358.
39. **Jocken JW, Roepstorff C, Goossens GH, et al.** Hormone-sensitive lipase serine phosphorylation and glycerol exchange across skeletal muscle in lean and obese subjects: effect of β-adrenergic stimulation. *Diabetes*. 2008;57:1834–1841.
40. **Sanchez-Pinera P, Micol V, Corbalan-Garcia S, Gomez-Fernandez JC.** A comparative study of the activation of protein kinase Cα by different diacylglycerol isomers. *Biochem J*. 1999;337(pt 3):387–395.
41. **Igal RA, Coleman RA.** Acylglycerol recycling from triacylglycerol to phospholipid, not lipase activity, is defective in neutral lipid storage disease fibroblasts. *J Biol Chem*. 1996;271:16644–16651.
42. **Badin PM, Loubiere C, Coonen M, et al.** Regulation of skeletal muscle lipolysis and oxidative metabolism by the co-lipase CGI-58. *J Lipid Res*. 2012;53:839–848.
43. **Bezaire V, Mairal A, Ribet C, et al.** Contribution of adipose triglyceride lipase and hormone-sensitive lipase to lipolysis in hMADS adipocytes. *J Biol Chem*. 2009;284:18282–18291.
44. **Anthonsen MW, Ronnstrand L, Wernstedt C, Degerman E, Holm C.** Identification of novel phosphorylation sites in hormone-sensitive lipase that are phosphorylated in response to isoproterenol and govern activation properties in vitro. *J Biol Chem*. 1998;273:215–221.
45. **Gaidhu MP, Anthony NM, Patel P, Hawke TJ, Ceddia RB.** Dysregulation of lipolysis and lipid metabolism in visceral and subcutaneous adipocytes by high-fat diet: role of ATGL, HSL, and AMPK. *Am J Physiol Cell Physiol*. 2010;298:C961–C971.
46. **Rodriguez-Cuenca S, Carobbio S, Velagapudi VR, et al.** Peroxisome proliferator-activated receptor γ-dependent regulation of lipolytic nodes and metabolic flexibility. *Mol Cell Biol*. 2012;32:1555–1565.
47. **Blaak EE, Schiffelers SL, Saris WH, Mensink M, Kooi ME.** Impaired β-adrenergically mediated lipolysis in skeletal muscle of obese subjects. *Diabetologia*. 2004;47:1462–1468.
48. **Mulder H, Sorhede-Winzell M, Contreras JA, et al.** Hormone-sensitive lipase null mice exhibit signs of impaired insulin sensitivity whereas insulin secretion is intact. *J Biol Chem*. 2003;278:36380–36388.
49. **Park SY, Kim HJ, Wang S, et al.** Hormone-sensitive lipase knockout mice have increased hepatic insulin sensitivity and are protected from short-term diet-induced insulin resistance in skeletal muscle and heart. *Am J Physiol*. 2005;289:E30–E39.
50. **Harada K, Shen WJ, Patel S, et al.** Resistance to high-fat diet-induced obesity and altered expression of adipose-specific genes in HSL-deficient mice. *Am J Physiol*. 2003;285:E1182–E1195.
51. **Brasaemle DL, Rubin B, Harten IA, Gruia-Gray J, Kimmel AR, Londos C.** Perilipin A increases triacylglycerol storage by decreasing the rate of triacylglycerol hydrolysis. *J Biol Chem*. 2000;275:38486–38493.
52. **Subramanian V, Rothenberg A, Gomez C, et al.** Perilipin A mediates the reversible binding of CGI-58 to lipid droplets in 3T3-L1 adipocytes. *J Biol Chem*. 2004;279:42062–42071.
53. **Bosma M, Minnaard R, Sparks LM, et al.** The lipid droplet coat protein perilipin 5 also localizes to muscle mitochondria. *Histochem Cell Biol*. 2012;137:205–216.
54. **Wang H, Bell M, Sreenevasan U, et al.** Unique regulation of adipose triglyceride lipase (ATGL) by perilipin 5, a lipid droplet-associated protein. *J Biol Chem*. 2011;286:15707–15715.
55. **Wang H, Sreenevasan U, Hu H, et al.** Perilipin 5, a lipid droplet-associated protein, provides physical and metabolic linkage to mitochondria. *J Lipid Res*. 2011;52:2159–2168.
56. **Granneman JG, Moore HP, Mottillo EP, Zhu Z, Zhou L.** Interactions of perilipin-5 (Plin5) with adipose triglyceride lipase. *J Biol Chem*. 2011;286:5126–5135.
57. **Schmidt A, Endo N, Rutledge SJ, Vogel R, Shinar D, Rodan GA.** Identification of a new member of the steroid hormone receptor superfamily that is activated by a peroxisome proliferator and fatty acids. *Mol Endocrinol*. 1992;6:1634–1641.
58. **Garcia-Roves P, Huss JM, Han DH, et al.** Raising plasma fatty acid concentration induces increased biogenesis of mitochondria in skeletal muscle. *Proc Natl Acad Sci USA*. 2007;104:10709–10713.
59. **Dalen KT, Dahl T, Holter E, et al.** LSDP5 is a PAT protein specifically expressed in fatty acid oxidizing tissues. *Biochim Biophys Acta*. 2007;1771:210–227.
60. **Frangioudakis G, Garrard J, Raddatz K, Nadler JL, Mitchell TW, Schmitz-Peiffer C.** Saturated- and n-6 polyunsaturated-fat diets each induce ceramide accumulation in mouse skeletal muscle: reversal and improvement of glucose tolerance by lipid metabolism inhibitors. *Endocrinology*. 2010;151:4187–4196.
61. **Liu L, Zhang Y, Chen N, Shi X, Tsang B, Yu YH.** Upregulation of myocellular DGAT1 augments triglyceride synthesis in skeletal muscle and protects against fat-induced insulin resistance. *J Clin Invest*. 2007;117:1679–1689.

Supplemental Figure 1: Validation of skeletal muscle tissue fractionation. Representative blots of α-Tubulin (markers of cytosol), and caveolin1 (marker of membrane) on cytosol and membrane fractions of *gactrocnemius* extracts from two different mice.

Supplemental Figure 2: No change in basal phosphorylation of key insulin signaling proteins. This Figure is companion to Figure 2. A. Quantitative bar graph of basal pIRS1 Tyr612 phosphorylation in mice *soleus* after 4 weeks of NCD or HFD. B. Quantitative bar graph of basal pAkt Ser473 phosphorylation in mice *soleus* after 4 weeks of NCD or HFD. C. Quantitative bar graph of basal pAS160 Thr642 phosphorylation in mice *soleus* after 4 weeks of NCD or HFD. Insets show a representative blot of 2 NCD and 2 HFD fed mice. n=8; £=0.06

Supplemental Figure 3: Representative blots of cytosol PKC proteins. This figure is companion to Figure 3B and shows cytosolic PKCs from *gastrocnemius* muscle of C3H mice fed NCD and HFD during 4 weeks (n=6-8).

Supplemental Figure 4: No change in JNK1 phosphorylation in muscle of HFD-fed mice. A. Quantitative bar graph of pJNK1 and total JNK1 in *soleus* muscle of C3H mice fed NCD and HFD during 4 weeks. B. Quantitative bar graph of pAMPK and total AMPK in *soleus* muscle of C3H mice fed NCD and HFD during 4 weeks. Insets show a representative blot of 2 NCD and 2 HFD fed mice. n=4-5; *$p<0.05$.

Supplemental Figure 5: Altered skeletal muscle lipases and PLIN5 expression in *gastrocnemius* of HFD fed mice. A. ATGL protein expression. B. CGI58 protein expression. C. HSL Ser660 phosphorylation. D. PLIN5 protein expression. Insets show a representative blot of 2 NCD and 2 HFD fed mice. n=8 *$p<0.05$, **$p<0.01$ vs NCD. 2

Supplemental Figure 6: Time-course of ATGL and CGI-58 protein expression in skeletal muscle during 4 weeks of HFD. ATGL (black circle) and CGI58 protein (open square) at different time points during HFD on the top panel. A representative blot is shown on the bottom panel. n=6; ** $p<0.01$, ***$p<0.001$ vs 0 time point.

Supplemental Figure 7: Time-course of PLIN5 protein expression in skeletal muscle during 4 weeks of HFD in C3H mice. Western blot of PLIN5 protein on C3H mice at different time points during HFD on the top panel. A representative blot is shown on the bottom panel. n=6; ***$p<0.001$ vs 0 time point.

Supplemental Figure 1

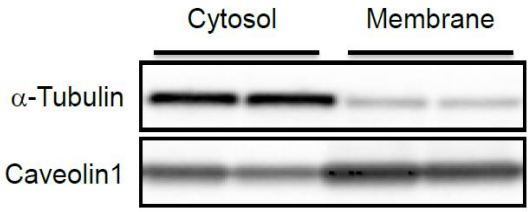

Supplemental Figure 2

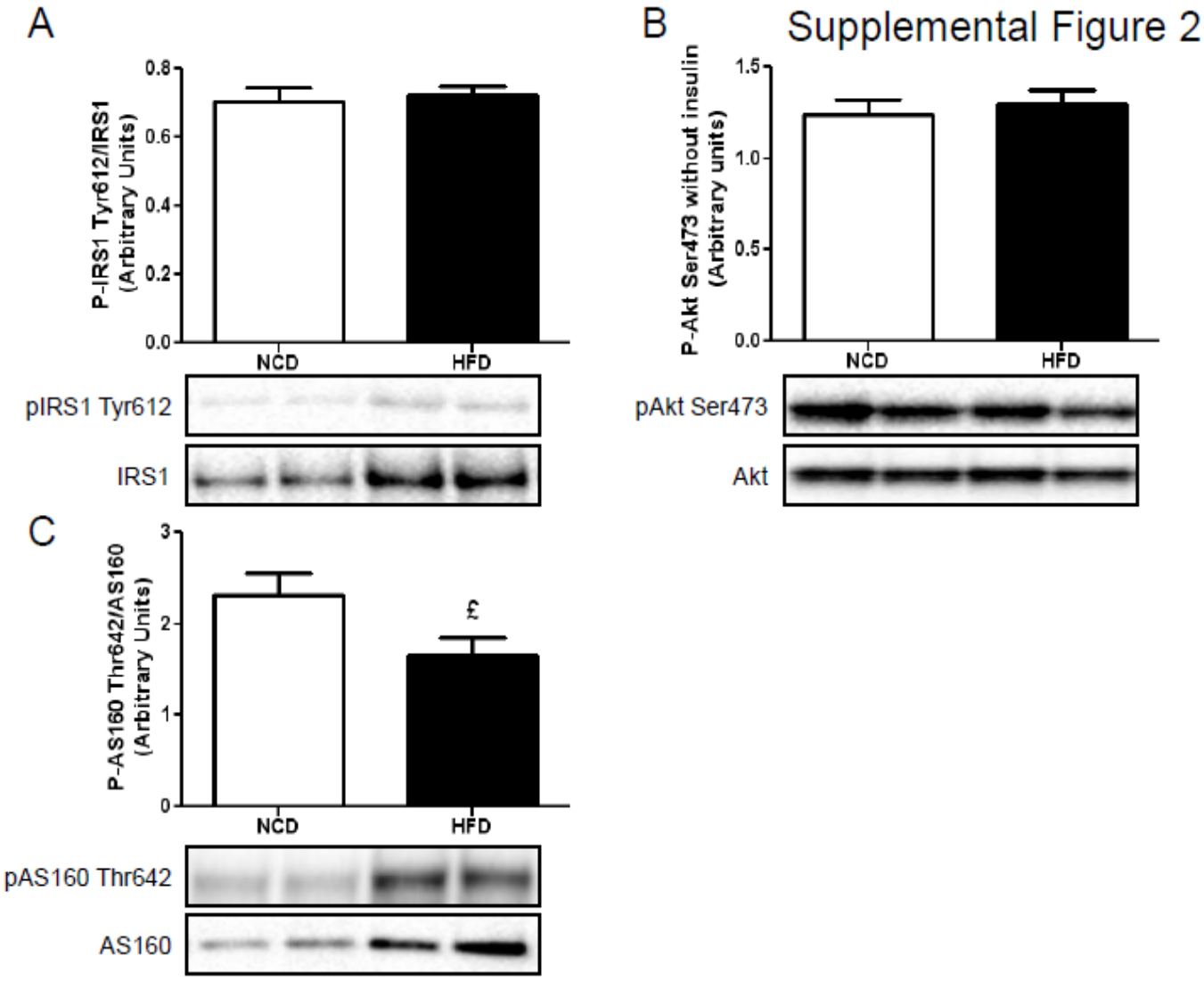

Supplemental Figure 3

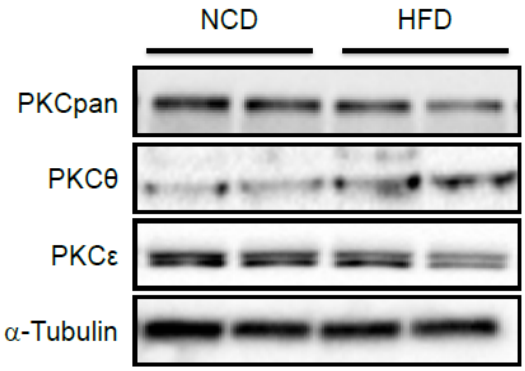

Supplemental Figure 4

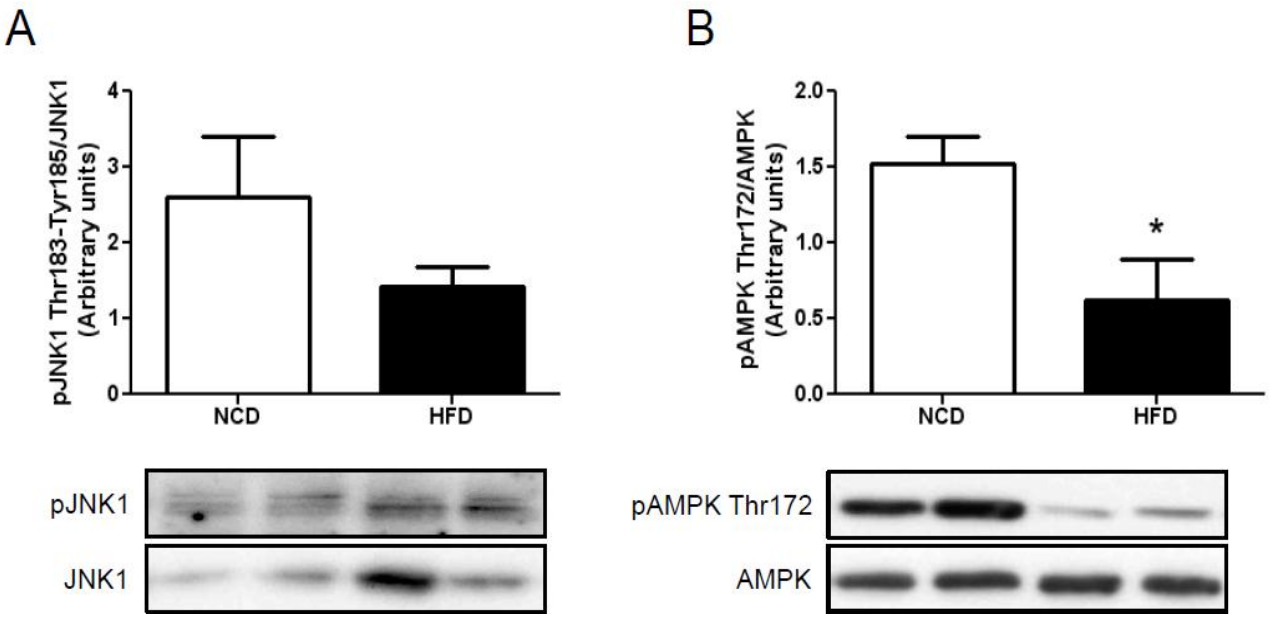

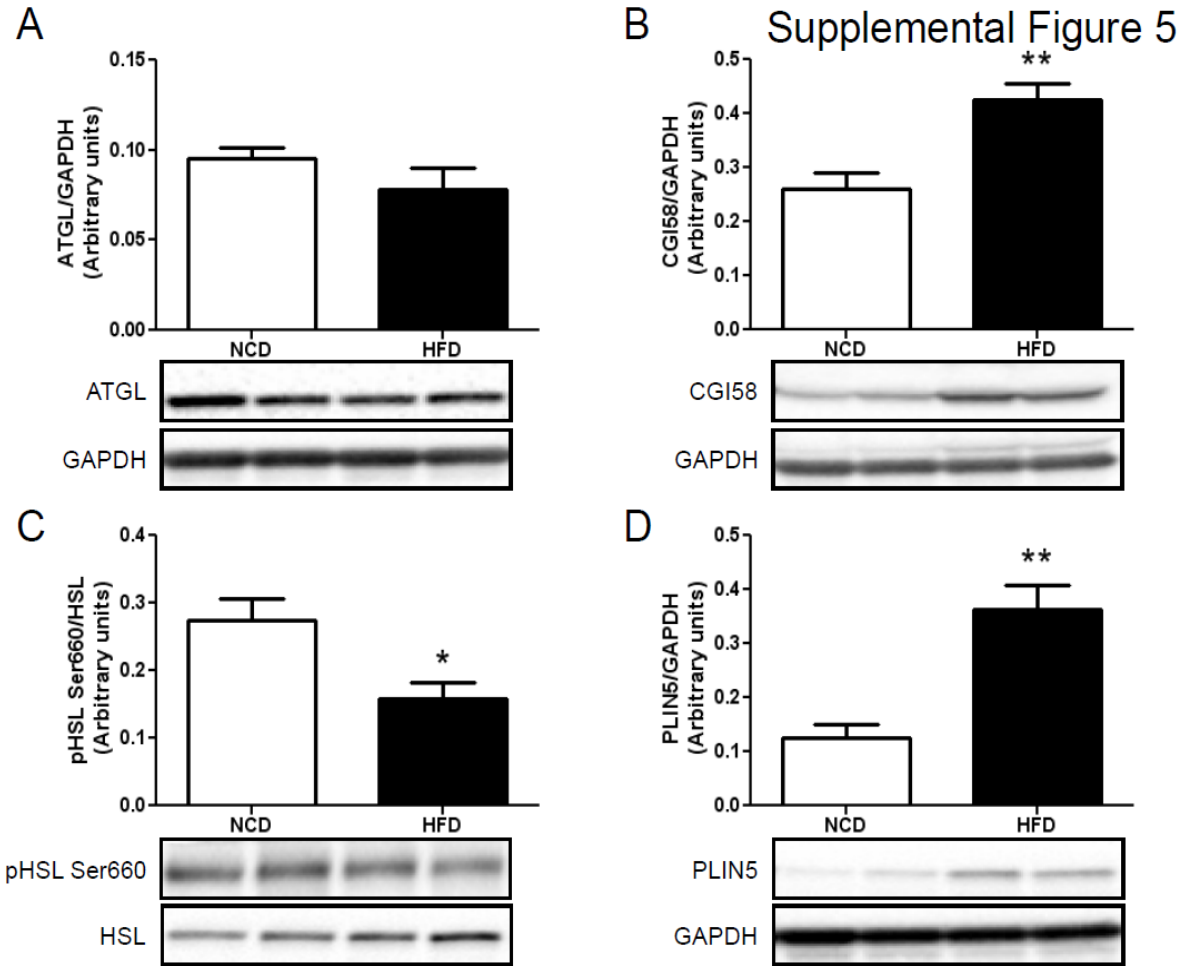

Supplemental Figure 5

Supplemental Figure 6

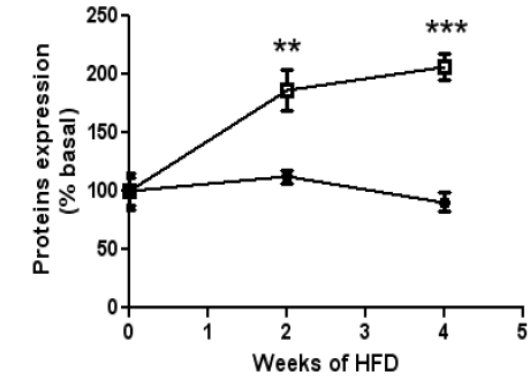

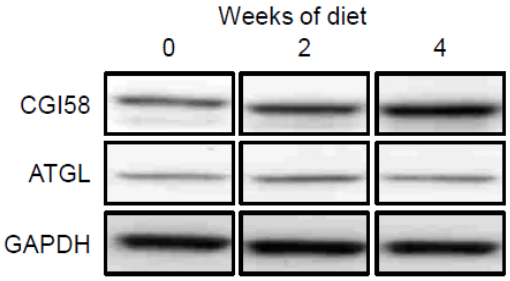

Supplemental Figure 7

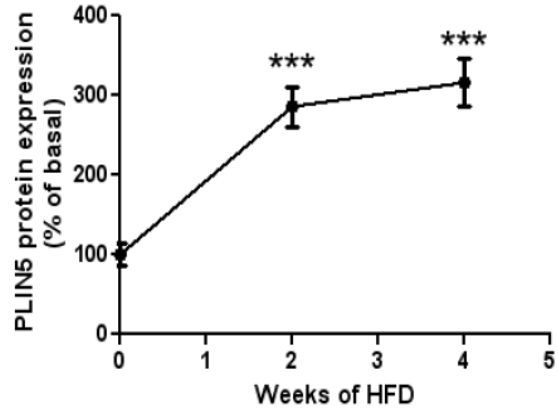

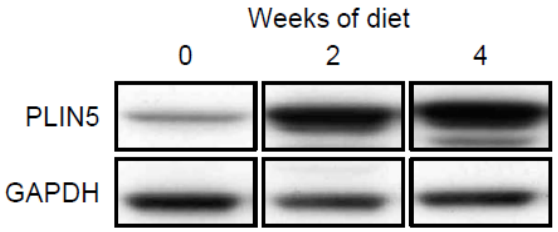

DISCUSSION

Ce travail a été réalisé en parallèle de mon sujet principal sur la fibrose du tissu adipeux. Les animaux C3H/HeOuJ (WT) ont montré la particularité de prendre très rapidement du poids. En effet nous avons évalué qu'à 4 semaines de régime gras 45% de nos souris WT avaient pris autant de poids que des souris C57BL/6 à 8 semaines du même régime. Cela en fait un modèle particulièrement adapté à l'étude des troubles métaboliques induit par un régime riche en graisses. De plus ces souris ont montré des dérégulations importantes de la sensibilité à l'insuline et de la tolérance au glucose dès 4 semaines de régime hyperlipidique. Cette détérioration du métabolisme lipidique s'explique en partie par une forte perte de la sensibilité musculaire à l'insuline et notamment d'une augmentation de la phosphorylation d'IRS1 sur le résidu inhibiteur sérine 1101.

Dans le muscle, le résidu serine 1101 d'IRS1 a été décrit comme pouvant être phosphorylé par c-Jun N-terminal kinase (JNK) et certaines PKC (Yu, Chen et al. 2002; Gual, Le Marchand-Brustel et al. 2005). Nous avons mesuré le niveau de phosphorylation de JNK et réalisé des études de fractionnement cytosol/membrane afin d'évaluer le niveau d'activité des PKC et de JNK. De façon intéressante nous n'avons pas retrouvé de modification de la phosphorylation de JNK dans le groupe de souris nourries en régime hyperlipidique. Ce résultat montre que dans ce modèle, le stress du réticulum (Rieusset, Chauvin et al. 2012) ainsi que la signalisation inflammatoire JNK dépendante ne semble pas être impliqué dans l'insulinorésistance musculaire. A l'inverse, nous avons retrouvé chez les souris soumises à un régime hyperlipidique une augmentation du contenu en PKC-θ et -ε à la membrane, localisation révélatrice d'une plus grande activité de ces dernières. Ceci peut expliquer l'augmentation de la phosphorylation du résidu sérine 1101 d'IRS1.

Nous avons ensuite dosé les DAG, dérivés lipidiques très bien décrits comme activateurs des PKC (Schmitz-Peiffer and Biden 2008; Schmitz-Peiffer 2010). Comme attendu nous avons trouvé une augmentation du contenu en DAG musculaire chez les

souris en régime hyperlipidique comparées aux souris soumises au régime standard. Nous avons ensuite cherché à comprendre comment pouvaient s'accumuler les DAG. Pour cela et en s'appuyant sur des résultats précédemment obtenus au laboratoire nous avons étudié par western blot l'expression et les phosphorylations des lipases musculaires.

En effet une dérégulation de ces lipases pourrait participer à l'accumulation de DAG, accumulation menant à l'insulinorésistance musculaire (Badin, Louche et al. 2011; Badin, Loubiere et al. 2012). De façon intéressante nous avons observé une forte augmentation de l'expression de CGI-58 alors que l'expression de l'ATGL tend à diminuer. Il est intéressant de noter que l'augmentation de CGI-58 malgré la diminution de l'ATGL suffit à augmenter l'hydrolyse des TAG dans des myocytes (Badin, Loubiere et al. 2012). Comme dans cette étude la régulation croisée de l'ATGL et de CGI-58 avait déjà été observée dans des adipocytes, reflet sans doute d'une régulation commune des deux gènes (Bezaire, Mairal et al. 2009). Associé aux modifications d'expression de CGI-58 et ATGL, nous avons également noté une forte diminution de la phosphorylation activatrice de la LHS en serine 660.

Pour confirmer qu'un déséquilibre de la balance lipolytique peut conduire à une perturbation du signal insulinique musculaire, nous avons également utilisé des souris invalidées pour la LHS. Ces souris présentent une augmentation de la synthèse des DAG au niveau musculaire accompagné d'un signal insulinique altéré. Cette expérience réalisée en régime standard confirme une légère insulinorésistance musculaire de ces souris (Mulder, Sorhede-Winzell et al. 2003) sans doute dû à une augmentation de la synthèse des DAG (Haemmerle, Zimmermann et al. 2002). Cependant nous n'oublions pas le fait que certaines souches de souris invalidées et hétérozygotes pour la LHS sont protégées de l'insulinorésistance pendant un régime riche en lipides alors que leur prise de poids n'est pas différente de leurs contrôles (Park, Kim et al. 2005; Girousse, Tavernier et al. 2013). Ceci s'explique probablement par la diminution du flux d'acide gras en provenance du tissu adipeux.

Cet article montre pour la première fois *in vivo* chez le rongeur qu'il existe une association forte entre l'insulinorésistance induite par un régime hyperlipidique et la dérégulation des lipases musculaires.

Cette dérégulation de la lipolyse musculaire semble responsable de l'accumulation de DAGs et l'augmentation des PKC membranaires observées dans le muscle de ces souris, comme le montre l'étude du signal insulinique menée sur le modèle LHS knockout. Cette étude ouvre la voie à des travaux évaluant l'effet d'une extinction de l'ATGL ou de CGI-58 dans des souris nourries en régime hyperlipidique. Ceci permettrait d'évaluer de manière causale si la diminution de l'hydrolyse des TAG est suffisante pour reverser la dégradation de signal insulinique musculaire chez des souris obèses.

Mes travaux de thèse ont permis d'étudier chez la souris, la mise en place de la fibrose du TA durant un régime riche en lipides. Si les mécanismes de mise en place de cette pathologie sont très bien décrits dans d'autres organes comme le foie ou le rein (Seki, De Minicis et al. 2007), il y avait jusqu'à présent peu de données sur son développement dans le tissu adipeux murin. Nos résultats montrent donc pour la première fois *in vivo* le rôle clé des cellules de l'immunité et de leurs récepteurs TLR4 dans la mise en place de la fibrose du tissu adipeux. De plus sur la base de nos données, il semble que l'augmentation des concentrations de LPS (principal ligand du TLR4) due au régime hyperlipidique soit à l'origine de l'activation des cellules immunes du TA et de la fibrose. Ces résultats permettent de mieux comprendre la mise en place de la fibrose du TA et pourrait être dans les prochaines années d'un certain intérêt médical. En effet de nombreux faisceaux d'évidences commencent à montrer que la fibrose du TA engendre des complications métaboliques. Nous montrons par exemple qu'il existe une augmentation graduelle de l'expression des gènes de la fibrose entre normo-pondérés, obèses et obèses atteint de syndrome métabolique. De plus l'équipe de Scherer a montré, chez la souris, qu'une diminution du contenu en collagène du tissu adipeux permettait l'amélioration des paramètres métaboliques (Khan, Iyengar et al. 2007). Enfin des études très intéressantes ont établi chez l'homme que la fibrose du TA était limitante dans la perte de poids après chirurgie bariatrique (Divoux, Tordjman et al. 2010). D'autres études devront confirmer ces données préliminaires en s'intéressant par exemple au rôle potentiel de la fibrose dans la mise en place et l'aggravation de l'insulinorésistance chez l'homme et l'animal. Cependant il semble déjà clair que la mise en place de la fibrose soit associé à de nombreuses complications métaboliques.

De façon périphérique j'ai également, durant ma thèse, pu contribuer à plusieurs autres travaux de recherche. J'ai par exemple récemment été associé à un travail étudiant le rôle des acides gras issus de la lipolyse sur l'activation du TLR4 macrophagique. J'ai également été impliquée dans deux autres projets portant sur la lipolyse dont l'étude est un des centres d'intérêt du laboratoire depuis de nombreuses années. Ainsi j'ai contribué de façon mineure au projet de thèse d'A Girousse. Elle a montré chez la souris que la diminution d'expression de la LHS protégeait de la mise en place de

l'insulinorésistance en ralentissant le flux d'acides gras en provenance du tissu adipeux (Girousse, Tavernier et al. 2013). J'ai participé à démontrer dans un fond C3H que la diminution de la lipolyse lors d'un traitement pharmacologique améliorait la tolérance à l'insuline.

En parallèle de mon projet de thèse, ma principale implication a porté sur le lien entre la dérégulation de la lipolyse musculaire et insulinorésistance lors d'un régime hyperlipidique. Nous avons, ainsi pu montrer, dans des souris C3H que 4 semaines de régime hyperlipidique conduit à une forte insulinorésistance musculaire. Nous avons montré que cette insulinorésistance est associé à une plus forte accumulation de DAG et une activation des PKC θ et ε. Afin nos résultats associent l'augmentation des DAG à l'augmentation d'expression de CGI-58 et la baisse de la phosphorylation activatrice de la LHS en ser660. Nous pensons donc que le régime hyperlipidique est responsable d'une dérégulation de l'expression/activité des lipases musculaires conduisant à l'insulinorésistance (Badin, Vila et al. 2013).

REFERENCES

REFERENCES BIBLIOGRAPHIQUES

A

Abdel Wahab, N. and R. M. Mason (2004). "Connective tissue growth factor and renal diseases: some answers, more questions." Curr Opin Nephrol Hypertens **13**(1): 53-8.

Abreu, J. G., N. I. Ketpura, et al. (2002). "Connective-tissue growth factor (CTGF) modulates cell signalling by BMP and TGF-beta." Nat Cell Biol **4**(8): 599-604.

Abumrad, N., C. Coburn, et al. (1999). "Membrane proteins implicated in long-chain fatty acid uptake by mammalian cells: CD36, FATP and FABPm." Biochim Biophys Acta **1441**(1): 4-13.

Abumrad, N. A., M. R. el-Maghrabi, et al. (1993). "Cloning of a rat adipocyte membrane protein implicated in binding or transport of long-chain fatty acids that is induced during preadipocyte differentiation. Homology with human CD36." J Biol Chem **268**(24): 17665-8.

Aguer, C., M. Foretz, et al. (2011). "Increased FAT/CD36 cycling and lipid accumulation in myotubes derived from obese type 2 diabetic patients." PLoS One **6**(12): e28981.

Aguer, C., J. Mercier, et al. (2010). "Intramyocellular lipid accumulation is associated with permanent relocation ex vivo and in vitro of fatty acid translocase (FAT)/CD36 in obese patients." Diabetologia **53**(6): 1151-63.

Akira, S., T. Taga, et al. (1993). "Interleukin-6 in biology and medicine." Adv Immunol **54**: 1-78.

Akira, S. and K. Takeda (2004). "Functions of toll-like receptors: lessons from KO mice." C R Biol **327**(6): 581-9.

Alessi, M. C., F. Peiretti, et al. (1997). "Production of plasminogen activator inhibitor 1 by human adipose tissue: possible link between visceral fat accumulation and vascular disease." Diabetes **46**(5): 860-7.

Alkhouri, N., A. Gornicka, et al. (2010). "Adipocyte apoptosis, a link between obesity, insulin resistance, and hepatic steatosis." J Biol Chem **285**(5): 3428-38.

Altintas, M. M., A. Azad, et al. (2011). "Mast cells, macrophages, and crown-like structures distinguish subcutaneous from visceral fat in mice." J Lipid Res **52**(3): 480-8.

An, J., D. M. Muoio, et al. (2004). "Hepatic expression of malonyl-CoA decarboxylase reverses muscle, liver and whole-animal insulin resistance." Nat Med **10**(3): 268-74.

Aouadi, M., G. J. Tesz, et al. (2009). "Orally delivered siRNA targeting macrophage Map4k4 suppresses systemic inflammation." Nature **458**(7242): 1180-4.

Arner, P., S. Bernard, et al. (2011). "Dynamics of human adipose lipid turnover in health and metabolic disease." Nature **478**(7367): 110-3.

Arnold, L., A. Henry, et al. (2007). "Inflammatory monocytes recruited after skeletal muscle injury switch into antiinflammatory macrophages to support myogenesis." J Exp Med **204**(5): 1057-69.

Aron-Wisnewsky, J., J. Tordjman, et al. (2009). "Human adipose tissue macrophages: m1 and m2 cell surface markers in subcutaneous and omental depots and after weight loss." J Clin Endocrinol Metab **94**(11): 4619-23.

B

Badin, P. M., C. Loubiere, et al. (2012). "Regulation of skeletal muscle lipolysis and oxidative metabolism by the co-lipase CGI-58." J Lipid Res **53**(5): 839-48.

Badin, P. M., K. Louche, et al. (2011). "Altered skeletal muscle lipase expression and activity contribute to insulin resistance in humans." Diabetes **60**(6): 1734-42.

Badin, P. M., I. K. Vila, et al. (2013). "High-fat diet-mediated lipotoxicity and insulin resistance is related to impaired lipase expression in mouse skeletal muscle." Endocrinology **154**(4): 1444-53.
Banchereau, J. and R. M. Steinman (1998). "Dendritic cells and the control of immunity." Nature **392**(6673): 245-52.
Barron, L. and T. A. Wynn (2011). "Fibrosis is regulated by Th2 and Th17 responses and by dynamic interactions between fibroblasts and macrophages." Am J Physiol Gastrointest Liver Physiol **300**(5): G723-8.
Bastard, J. P., C. Jardel, et al. (2000). "Elevated levels of interleukin 6 are reduced in serum and subcutaneous adipose tissue of obese women after weight loss." J Clin Endocrinol Metab **85**(9): 3338-42.
Bertola, A., T. Ciucci, et al. (2012). "Identification of adipose tissue dendritic cells correlated with obesity-associated insulin-resistance and inducing Th17 responses in mice and patients." Diabetes **61**(9): 2238-47.
Bes-Houtmann, S., R. Roche, et al. (2007). "Presence of functional TLR2 and TLR4 on human adipocytes." Histochem Cell Biol **127**(2): 131-7.
Bezaire, V. and D. Langin (2009). "Regulation of adipose tissue lipolysis revisited." Proc Nutr Soc **68**(4): 350-60.
Bezaire, V., A. Mairal, et al. (2009). "Contribution of adipose triglyceride lipase and hormone-sensitive lipase to lipolysis in hMADS adipocytes." J Biol Chem **284**(27): 18282-91.
Birchmeier, C. and E. Gherardi (1998). "Developmental roles of HGF/SF and its receptor, the c-Met tyrosine kinase." Trends Cell Biol **8**(10): 404-10.
Bjorntorp, P., A. Gustafson, et al. (1971). "Adipose tissue fat cell size and number in relation to metabolism in endogenous hypertriglyceridemia." Acta Med Scand **190**(5): 363-7.
Bonen, A., M. L. Parolin, et al. (2004). "Triacylglycerol accumulation in human obesity and type 2 diabetes is associated with increased rates of skeletal muscle fatty acid transport and increased sarcolemmal FAT/CD36." Faseb J **18**(10): 1144-6.
Border, W. A. and N. A. Noble (1994). "Transforming growth factor beta in tissue fibrosis." N Engl J Med **331**(19): 1286-92.
Bosma, M., R. Minnaard, et al. (2012). "The lipid droplet coat protein perilipin 5 also localizes to muscle mitochondria." Histochem Cell Biol **137**(2): 205-16.
Bottner, M., K. Krieglstein, et al. (2000). "The transforming growth factor-betas: structure, signaling, and roles in nervous system development and functions." J Neurochem **75**(6): 2227-40.
Bourlier, V., C. Sengenes, et al. (2012). "TGFbeta family members are key mediators in the induction of myofibroblast phenotype of human adipose tissue progenitor cells by macrophages." PLoS One **7**(2): e31274.
Bourlier, V., A. Zakaroff-Girard, et al. (2008). "Remodeling phenotype of human subcutaneous adipose tissue macrophages." Circulation **117**(6): 806-15.
Brakenhielm, E., R. Cao, et al. (2004). "Angiogenesis inhibitor, TNP-470, prevents diet-induced and genetic obesity in mice." Circ Res **94**(12): 1579-88.
Bruce, C. R., S. Risis, et al. (2012). "Overexpression of sphingosine kinase 1 prevents ceramide accumulation and ameliorates muscle insulin resistance in high-fat diet-fed mice." Diabetes **61**(12): 3148-55.
Burns, K., F. Martinon, et al. (1998). "MyD88, an adapter protein involved in interleukin-1 signaling." J Biol Chem **273**(20): 12203-9.
Burridge, K. and M. Chrzanowska-Wodnicka (1996). "Focal adhesions, contractility, and signaling." Annu Rev Cell Dev Biol **12**: 463-518.

C

Campbell, M. T., K. L. Hile, et al. (2011). "Toll-like receptor 4: a novel signaling pathway during renal fibrogenesis." J Surg Res **168**(1): e61-9.

Cancello, R., C. Henegar, et al. (2005). "Reduction of macrophage infiltration and chemoattractant gene expression changes in white adipose tissue of morbidly obese subjects after surgery-induced weight loss." Diabetes **54**(8): 2277-86.

Cani, P. D., J. Amar, et al. (2007). "Metabolic endotoxemia initiates obesity and insulin resistance." Diabetes **56**(7): 1761-72.

Cani, P. D., R. Bibiloni, et al. (2008). "Changes in gut microbiota control metabolic endotoxemia-induced inflammation in high-fat diet-induced obesity and diabetes in mice." Diabetes **57**(6): 1470-1481.

Cani, P. D., S. Possemiers, et al. (2009). "Changes in gut microbiota control inflammation in obese mice through a mechanism involving GLP-2-driven improvement of gut permeability." Gut **58**(8): 1091-103.

Chaby, R. (2004). "Lipopolysaccharide-binding molecules: transporters, blockers and sensors." Cell Mol Life Sci **61**(14): 1697-713.

Chavey, C., B. Mari, et al. (2003). "Matrix metalloproteinases are differentially expressed in adipose tissue during obesity and modulate adipocyte differentiation." J Biol Chem **278**(14): 11888-96.

Chavez, J. A. and S. A. Summers (2003). "Characterizing the effects of saturated fatty acids on insulin signaling and ceramide and diacylglycerol accumulation in 3T3-L1 adipocytes and C2C12 myotubes." Arch Biochem Biophys **419**(2): 101-9.

Chen, X., S. W. Cushman, et al. (2005). "Quantitative proteomic analysis of the secretory proteins from rat adipose cells using a 2D liquid chromatography-MS/MS approach." J Proteome Res **4**(2): 570-7.

Christiaens, V. and H. R. Lijnen (2006). "Role of the fibrinolytic and matrix metalloproteinase systems in development of adipose tissue." Arch Physiol Biochem **112**(4-5): 254-9.

Christiansen, T., B. Richelsen, et al. (2005). "Monocyte chemoattractant protein-1 is produced in isolated adipocytes, associated with adiposity and reduced after weight loss in morbid obese subjects." Int J Obes (Lond) **29**(1): 146-50.

Chu, W. M. (2013). "Tumor necrosis factor." Cancer Lett **328**(2): 222-5.

Chung, S., K. Lapoint, et al. (2006). "Preadipocytes mediate lipopolysaccharide-induced inflammation and insulin resistance in primary cultures of newly differentiated human adipocytes." Endocrinology **147**(11): 5340-51.

Cinti, S., M. Cigolini, et al. (1984). "A morphological study of the adipocyte precursor." J Submicrosc Cytol **16**(2): 243-51.

Cinti, S., G. Mitchell, et al. (2005). "Adipocyte death defines macrophage localization and function in adipose tissue of obese mice and humans." J Lipid Res **46**(11): 2347-55.

Clausen, B. E., C. Burkhardt, et al. (1999). "Conditional gene targeting in macrophages and granulocytes using LysMcre mice." Transgenic Res **8**(4): 265-77.

Clement, K., N. Viguerie, et al. (2004). "Weight loss regulates inflammation-related genes in white adipose tissue of obese subjects." Faseb J **18**(14): 1657-69.

Clemente-Postigo, M., M. I. Queipo-Ortuno, et al. (2012). "Endotoxin increase after fat overload is related to postprandial hypertriglyceridemia in morbidly obese patients." J Lipid Res **53**(5): 973-8.

Collins, J. M., M. J. Neville, et al. (2011). "De novo lipogenesis in the differentiating human adipocyte can provide all fatty acids necessary for maturation." J Lipid Res **52**(9): 1683-92.

Condeelis, J. and J. E. Segall (2003). "Intravital imaging of cell movement in tumours." Nat Rev Cancer **3**(12): 921-30.

Cornaciu, I., A. Boeszoermenyi, et al. (2011). "The minimal domain of adipose triglyceride lipase (ATGL) ranges until leucine 254 and can be activated and inhibited by CGI-58 and G0S2, respectively." PLoS One **6**(10): e26349.
Cousin, B., S. Caspar-Bauguil, et al. (2006). "[Adipose tissue: a subtle and complex cell system]." J Soc Biol **200**(1): 51-7.
Curat, C. A., A. Miranville, et al. (2004). "From blood monocytes to adipose tissue-resident macrophages: induction of diapedesis by human mature adipocytes." Diabetes **53**(5): 1285-92.
Curat, C. A., V. Wegner, et al. (2006). "Macrophages in human visceral adipose tissue: increased accumulation in obesity and a source of resistin and visfatin." Diabetologia **49**(4): 744-7.

𝒟

Das, U. N. (2004). "Metabolic syndrome X: an inflammatory condition?" Curr Hypertens Rep **6**(1): 66-73.
de Heredia, F. P., S. Gomez-Martinez, et al. (2012). "Obesity, inflammation and the immune system." Proc Nutr Soc **71**(2): 332-8.
DeFronzo, R. A., E. Jacot, et al. (1981). "The effect of insulin on the disposal of intravenous glucose. Results from indirect calorimetry and hepatic and femoral venous catheterization." Diabetes **30**(12): 1000-7.
Demeulemeester, D., D. Collen, et al. (2005). "Effect of matrix metalloproteinase inhibition on adipose tissue development." Biochem Biophys Res Commun **329**(1): 105-10.
Desmouliere, A., L. Rubbia-Brandt, et al. (1992). "Heparin induces alpha-smooth muscle actin expression in cultured fibroblasts and in granulation tissue myofibroblasts." Lab Invest **67**(6): 716-26.
Di Lullo, G. A., S. M. Sweeney, et al. (2002). "Mapping the ligand-binding sites and disease-associated mutations on the most abundant protein in the human, type I collagen." J Biol Chem **277**(6): 4223-31.
Divoux, A., S. Moutel, et al. (2012). "Mast cells in human adipose tissue: link with morbid obesity, inflammatory status, and diabetes." J Clin Endocrinol Metab **97**(9): E1677-85.
Divoux, A., J. Tordjman, et al. (2010). "Fibrosis in human adipose tissue: composition, distribution, and link with lipid metabolism and fat mass loss." Diabetes **59**(11): 2817-25.
Donsmark, M., J. Langfort, et al. (2003). "Contractions activate hormone-sensitive lipase in rat muscle by protein kinase C and mitogen-activated protein kinase." J Physiol **550**(Pt 3): 845-54.
Dube, J. J., F. Amati, et al. (2008). "Exercise-induced alterations in intramyocellular lipids and insulin resistance: the athlete's paradox revisited." Am J Physiol Endocrinol Metab **294**(5): E882-8.
Dube, J. J., F. Amati, et al. (2011). "Effects of weight loss and exercise on insulin resistance, and intramyocellular triacylglycerol, diacylglycerol and ceramide." Diabetologia **54**(5): 1147-56.
Duffaut, C., A. Zakaroff-Girard, et al. (2009). "Interplay between human adipocytes and T lymphocytes in obesity: CCL20 as an adipochemokine and T lymphocytes as lipogenic modulators." Arterioscler Thromb Vasc Biol **29**(10): 1608-14.
Duffield, J. S. (2003). "The inflammatory macrophage: a story of Jekyll and Hyde." Clin Sci (Lond) **104**(1): 27-38.

ℰ

Erridge, C. (2010). "Endogenous ligands of TLR2 and TLR4: agonists or assistants?" J Leukoc Biol **87**(6): 989-99.
Erridge, C., T. Attina, et al. (2007). "A high-fat meal induces low-grade endotoxemia: evidence of a novel mechanism of postprandial inflammation." Am J Clin Nutr **86**(5): 1286-92.

Erridge, C. and N. J. Samani (2009). "Saturated fatty acids do not directly stimulate Toll-like receptor signaling." Arterioscler Thromb Vasc Biol **29**(11): 1944-9.

F

Fagarasan, S. and T. Honjo (2000). "T-Independent immune response: new aspects of B cell biology." Science **290**(5489): 89-92.

Fain, J. N. (2006). "Release of interleukins and other inflammatory cytokines by human adipose tissue is enhanced in obesity and primarily due to the nonfat cells." Vitam Horm **74**: 443-77.

Fain, J. N. and J. A. Garcija-Sainz (1983). "Adrenergic regulation of adipocyte metabolism." J Lipid Res **24**(8): 945-66.

Fain, J. N., A. K. Madan, et al. (2004). "Comparison of the release of adipokines by adipose tissue, adipose tissue matrix, and adipocytes from visceral and subcutaneous abdominal adipose tissues of obese humans." Endocrinology **145**(5): 2273-82.

Ford, E. S. (2003). "The metabolic syndrome and C-reactive protein, fibrinogen, and leukocyte count: findings from the Third National Health and Nutrition Examination Survey." Atherosclerosis **168**(2): 351-8.

Frazier, K., S. Williams, et al. (1996). "Stimulation of fibroblast cell growth, matrix production, and granulation tissue formation by connective tissue growth factor." J Invest Dermatol **107**(3): 404-11.

Frederich, R. C., A. Hamann, et al. (1995). "Leptin levels reflect body lipid content in mice: evidence for diet-induced resistance to leptin action." Nat Med **1**(12): 1311-4.

Fried, S. K., D. A. Bunkin, et al. (1998). "Omental and subcutaneous adipose tissues of obese subjects release interleukin-6: depot difference and regulation by glucocorticoid." J Clin Endocrinol Metab **83**(3): 847-50.

Friedman, S. L. (2004). "Mechanisms of disease: Mechanisms of hepatic fibrosis and therapeutic implications." Nat Clin Pract Gastroenterol Hepatol **1**(2): 98-105.

Fujisaka, S., I. Usui, et al. (2009). "Regulatory mechanisms for adipose tissue M1 and M2 macrophages in diet-induced obese mice." Diabetes **58**(11): 2574-82.

G

Gearing, A. J., P. Beckett, et al. (1994). "Processing of tumour necrosis factor-alpha precursor by metalloproteinases." Nature **370**(6490): 555-7.

Geloen, A., A. J. Collet, et al. (1989). "Insulin stimulates in vivo cell proliferation in white adipose tissue." Am J Physiol **256**(1 Pt 1): C190-6.

Gersh, I. and M. A. Still (1945). "Blood Vessels in Fat Tissue. Relation to Problems of Gas Exchange." J Exp Med **81**(2): 219-32.

Gesta, S., Y. H. Tseng, et al. (2007). "Developmental origin of fat: tracking obesity to its source." Cell **131**(2): 242-56.

Girousse, A., G. Tavernier, et al. (2013). "Partial inhibition of adipose tissue lipolysis improves glucose metabolism and insulin sensitivity without alteration of fat mass." PLoS Biol **11**(2): e1001485.

Goh, F. G., A. M. Piccinini, et al. (2010). "Transcriptional regulation of the endogenous danger signal tenascin-C: a novel autocrine loop in inflammation." J Immunol **184**(5): 2655-62.

Goldberg, I. J. (1996). "Lipoprotein lipase and lipolysis: central roles in lipoprotein metabolism and atherogenesis." J Lipid Res **37**(4): 693-707.

Goodpaster, B. H., J. He, et al. (2001). "Skeletal muscle lipid content and insulin resistance: evidence for a paradox in endurance-trained athletes." J Clin Endocrinol Metab **86**(12): 5755-61.

Goodyear, L. J., M. F. Hirshman, et al. (1996). "Glucose ingestion causes GLUT4 translocation in human skeletal muscle." Diabetes **45**(8): 1051-6.

Goossens, G. H., A. Bizzarri, et al. (2011). "Increased adipose tissue oxygen tension in obese compared with lean men is accompanied by insulin resistance, impaired adipose tissue capillarization, and inflammation." Circulation **124**(1): 67-76.
Goossens, G. H. and E. E. Blaak (2012). "Adipose tissue oxygen tension: implications for chronic metabolic and inflammatory diseases." Curr Opin Clin Nutr Metab Care **15**(6): 539-46.
Gordon, S. and P. R. Taylor (2005). "Monocyte and macrophage heterogeneity." Nat Rev Immunol **5**(12): 953-64.
Govinden, R. and K. D. Bhoola (2003). "Genealogy, expression, and cellular function of transforming growth factor-beta." Pharmacol Ther **98**(2): 257-65.
Granneman, J. G., H. P. Moore, et al. (2007). "Analysis of lipolytic protein trafficking and interactions in adipocytes." J Biol Chem **282**(8): 5726-35.
Griffin, M. E., M. J. Marcucci, et al. (1999). "Free fatty acid-induced insulin resistance is associated with activation of protein kinase C theta and alterations in the insulin signaling cascade." Diabetes **48**(6): 1270-4.
Grotendorst, G. R., H. Rahmanie, et al. (2004). "Combinatorial signaling pathways determine fibroblast proliferation and myofibroblast differentiation." Faseb J **18**(3): 469-79.
Gruen, M. L., M. Hao, et al. (2007). "Leptin requires canonical migratory signaling pathways for induction of monocyte and macrophage chemotaxis." Am J Physiol Cell Physiol **293**(5): C1481-8.
Grunfeld, C. and K. R. Feingold (1991). "The metabolic effects of tumor necrosis factor and other cytokines." Biotherapy **3**(2): 143-58.
Gual, P., Y. Le Marchand-Brustel, et al. (2005). "Positive and negative regulation of insulin signaling through IRS-1 phosphorylation." Biochimie **87**(1): 99-109.
Guerre-Millo, M., A. Grosfeld, et al. (2002). "Leptin is a hypoxia-inducible gene." Obes Res **10**(8): 856; author reply 857-8.
Guma, A., J. R. Zierath, et al. (1995). "Insulin induces translocation of GLUT-4 glucose transporters in human skeletal muscle." Am J Physiol **268**(4 Pt 1): E613-22.

H

Haemmerle, G., A. Lass, et al. (2006). "Defective lipolysis and altered energy metabolism in mice lacking adipose triglyceride lipase." Science **312**(5774): 734-7.
Haemmerle, G., R. Zimmermann, et al. (2002). "Hormone-sensitive lipase deficiency in mice causes diglyceride accumulation in adipose tissue, muscle, and testis." J Biol Chem **277**(7): 4806-15.
Halberg, N., I. Wernstedt-Asterholm, et al. (2008). "The adipocyte as an endocrine cell." Endocrinol Metab Clin North Am **37**(3): 753-68, x-xi.
Hamasuna, R., H. Kataoka, et al. (1999). "Regulation of matrix metalloproteinase-2 (MMP-2) by hepatocyte growth factor/scatter factor (HGF/SF) in human glioma cells: HGF/SF enhances MMP-2 expression and activation accompanying up-regulation of membrane type-1 MMP." Int J Cancer **82**(2): 274-81.
Hanzawa, M., M. Shindoh, et al. (2000). "Hepatocyte growth factor upregulates E1AF that induces oral squamous cell carcinoma cell invasion by activating matrix metalloproteinase genes." Carcinogenesis **21**(6): 1079-85.
Hausberger, F. X. and M. M. Widelitz (1963). "Distribution of labeled erythrocytes in adipose tissue and muscle in the rat." Am J Physiol **204**: 649-52.
Hausman, G. J. and R. L. Richardson (2004). "Adipose tissue angiogenesis." J Anim Sci **82**(3): 925-34.
Hegarty, B. D., G. J. Cooney, et al. (2002). "Increased efficiency of fatty acid uptake contributes to lipid accumulation in skeletal muscle of high fat-fed insulin-resistant rats." Diabetes **51**(5): 1477-84.

Heinrichsdorff, J. and J. M. Olefsky (2012). "Fetuin-A: the missing link in lipid-induced inflammation." Nat Med **18**(8): 1182-3.
Heymann, F., C. Meyer-Schwesinger, et al. (2009). "Kidney dendritic cell activation is required for progression of renal disease in a mouse model of glomerular injury." J Clin Invest **119**(5): 1286-97.
Hinz, B. (2007). "Formation and function of the myofibroblast during tissue repair." J Invest Dermatol **127**(3): 526-37.
Holland, W. L., J. T. Brozinick, et al. (2007). "Inhibition of ceramide synthesis ameliorates glucocorticoid-, saturated-fat-, and obesity-induced insulin resistance." Cell Metab **5**(3): 167-79.
Holloway, G. P., A. B. Thrush, et al. (2007). "Skeletal muscle mitochondrial FAT/CD36 content and palmitate oxidation are not decreased in obese women." Am J Physiol Endocrinol Metab **292**(6): E1782-9.
Holm, C., T. Osterlund, et al. (2000). "Molecular mechanisms regulating hormone-sensitive lipase and lipolysis." Annu Rev Nutr **20**: 365-93.
Horowitz, J. F. (2001). "Regulation of lipid mobilization and oxidation during exercise in obesity." Exerc Sport Sci Rev **29**(1): 42-6.
Hotamisligil, G. S., P. Peraldi, et al. (1996). "IRS-1-mediated inhibition of insulin receptor tyrosine kinase activity in TNF-alpha- and obesity-induced insulin resistance." Science **271**(5249): 665-8.
Hotamisligil, G. S., N. S. Shargill, et al. (1993). "Adipose expression of tumor necrosis factor-alpha: direct role in obesity-linked insulin resistance." Science **259**(5091): 87-91.

I

Ibrahimi, A., B. Bertrand, et al. (1993). "Cloning of alpha 2 chain of type VI collagen and expression during mouse development." Biochem J **289 (Pt 1)**: 141-7.
Imai, K., A. Hiramatsu, et al. (1997). "Degradation of decorin by matrix metalloproteinases: identification of the cleavage sites, kinetic analyses and transforming growth factor-beta1 release." Biochem J **322 (Pt 3)**: 809-14.
Isayama, F., I. N. Hines, et al. (2006). "LPS signaling enhances hepatic fibrogenesis caused by experimental cholestasis in mice." Am J Physiol Gastrointest Liver Physiol **290**(6): G1318-28.
Itani, S. I., N. B. Ruderman, et al. (2002). "Lipid-induced insulin resistance in human muscle is associated with changes in diacylglycerol, protein kinase C, and IkappaB-alpha." Diabetes **51**(7): 2005-11.
Ito, A., A. Mukaiyama, et al. (1996). "Degradation of interleukin 1beta by matrix metalloproteinases." J Biol Chem **271**(25): 14657-60.

J

Jagavelu, K., C. Routray, et al. (2010). "Endothelial cell toll-like receptor 4 regulates fibrosis-associated angiogenesis in the liver." Hepatology **52**(2): 590-601.
Javelaud, D. and A. Mauviel (2004). "Mammalian transforming growth factor-betas: Smad signaling and physio-pathological roles." Int J Biochem Cell Biol **36**(7): 1161-5.
Jenkins, C. M., D. J. Mancuso, et al. (2004). "Identification, cloning, expression, and purification of three novel human calcium-independent phospholipase A2 family members possessing triacylglycerol lipase and acylglycerol transacylase activities." J Biol Chem **279**(47): 48968-75.
Jocken, J. W., D. Langin, et al. (2007). "Adipose triglyceride lipase and hormone-sensitive lipase protein expression is decreased in the obese insulin-resistant state." J Clin Endocrinol Metab **92**(6): 2292-9.

Jocken, J. W., C. Roepstorff, et al. (2008). "Hormone-sensitive lipase serine phosphorylation and glycerol exchange across skeletal muscle in lean and obese subjects: effect of beta-adrenergic stimulation." Diabetes **57**(7): 1834-41.
Jun, J. I. and L. F. Lau (2010). "Cellular senescence controls fibrosis in wound healing." Aging (Albany NY) **2**(9): 627-31.

K

Kanda, H., S. Tateya, et al. (2006). "MCP-1 contributes to macrophage infiltration into adipose tissue, insulin resistance, and hepatic steatosis in obesity." J Clin Invest **116**(6): 1494-505.
Karlsson, M., J. A. Contreras, et al. (1997). "cDNA cloning, tissue distribution, and identification of the catalytic triad of monoglyceride lipase. Evolutionary relationship to esterases, lysophospholipases, and haloperoxidases." J Biol Chem **272**(43): 27218-23.
Kawai, T., O. Adachi, et al. (1999). "Unresponsiveness of MyD88-deficient mice to endotoxin." Immunity **11**(1): 115-22.
Kawai, T. and S. Akira (2005). "Toll-like receptor downstream signaling." Arthritis Res Ther **7**(1): 12-9.
Kawamoto, T., M. Ii, et al. (2008). "TAK-242 selectively suppresses Toll-like receptor 4-signaling mediated by the intracellular domain." Eur J Pharmacol **584**(1): 40-8.
Kawazoe, Y., T. Naka, et al. (2001). "Signal transducer and activator of transcription (STAT)-induced STAT inhibitor 1 (SSI-1)/suppressor of cytokine signaling 1 (SOCS1) inhibits insulin signal transduction pathway through modulating insulin receptor substrate 1 (IRS-1) phosphorylation." J Exp Med **193**(2): 263-9.
Kelley, D., A. Mitrakou, et al. (1988). "Skeletal muscle glycolysis, oxidation, and storage of an oral glucose load." J Clin Invest **81**(5): 1563-71.
Keophiphath, M., V. Achard, et al. (2009). "Macrophage-secreted factors promote a profibrotic phenotype in human preadipocytes." Mol Endocrinol **23**(1): 11-24.
Kerrigan, J. J., J. P. Mansell, et al. (2000). "Matrix turnover." J Orthod **27**(3): 227-33.
Khan, T., P. Iyengar, et al. (2007). "ob/ob mice lacking collagen VI have an improved metabolic phenotype: Larger adipocytes are associated with improvements in whole-body metabolism." Diabetes **56**: A459-A459.
Kim, J. K. (2006). "Fat uses a TOLL-road to connect inflammation and diabetes." Cell Metab **4**(6): 417-9.
Kim, S. J., P. Angel, et al. (1990). "Autoinduction of transforming growth factor beta 1 is mediated by the AP-1 complex." Mol Cell Biol **10**(4): 1492-7.
Kintscher, U., M. Hartge, et al. (2008). "T-lymphocyte infiltration in visceral adipose tissue: a primary event in adipose tissue inflammation and the development of obesity-mediated insulin resistance." Arterioscler Thromb Vasc Biol **28**(7): 1304-10.
Kolditz, C. I. and D. Langin (2010). "Adipose tissue lipolysis." Curr Opin Clin Nutr Metab Care **13**(4): 377-81.
Kopp, A., C. Buechler, et al. (2009). "Innate immunity and adipocyte function: ligand-specific activation of multiple Toll-like receptors modulates cytokine, adipokine, and chemokine secretion in adipocytes." Obesity (Silver Spring) **17**(4): 648-56.
Kornbluth, R. S., P. S. Oh, et al. (1989). "Interferons and bacterial lipopolysaccharide protect macrophages from productive infection by human immunodeficiency virus in vitro." J Exp Med **169**(3): 1137-51.
Kosteli, A., E. Sugaru, et al. (2010). "Weight loss and lipolysis promote a dynamic immune response in murine adipose tissue." J Clin Invest **120**(10): 3466-79.
Koutnikova, H. and J. Auwerx (2001). "Regulation of adipocyte differentiation." Ann Med **33**(8): 556-61.

Koves, T. R., P. Li, et al. (2005). "Peroxisome proliferator-activated receptor-gamma co-activator 1alpha-mediated metabolic remodeling of skeletal myocytes mimics exercise training and reverses lipid-induced mitochondrial inefficiency." J Biol Chem **280**(39): 33588-98.
Krieglstein, K., J. Strelau, et al. (2002). "TGF-beta and the regulation of neuron survival and death." J Physiol Paris **96**(1-2): 25-30.
Kusminski, C. M., W. L. Holland, et al. (2012). "MitoNEET-driven alterations in adipocyte mitochondrial activity reveal a crucial adaptive process that preserves insulin sensitivity in obesity." Nat Med **18**(10): 1539-49.
Kwon, E. Y., S. K. Shin, et al. (2012). "Time-course microarrays reveal early activation of the immune transcriptome and adipokine dysregulation leads to fibrosis in visceral adipose depots during diet-induced obesity." BMC Genomics **13**: 450.

$\mathcal{L}$

Lafontan, M. and M. Berlan (1993). "Fat cell adrenergic receptors and the control of white and brown fat cell function." J Lipid Res **34**(7): 1057-91.
Lafontan, M. and D. Langin (2009). "Lipolysis and lipid mobilization in human adipose tissue." Prog Lipid Res **48**(5): 275-97.
Lafontan, M., C. Moro, et al. (2008). "Control of lipolysis by natriuretic peptides and cyclic GMP." Trends Endocrinol Metab **19**(4): 130-7.
Lafontan, M., C. Moro, et al. (2005). "An unsuspected metabolic role for atrial natriuretic peptides: the control of lipolysis, lipid mobilization, and systemic nonesterified fatty acids levels in humans." Arterioscler Thromb Vasc Biol **25**(10): 2032-42.
Langin, D., A. Dicker, et al. (2005). "Adipocyte lipases and defect of lipolysis in human obesity." Diabetes **54**(11): 3190-7.
Large, V., S. Reynisdottir, et al. (1999). "Decreased expression and function of adipocyte hormone-sensitive lipase in subcutaneous fat cells of obese subjects." J Lipid Res **40**(11): 2059-66.
Lass, A., R. Zimmermann, et al. (2006). "Adipose triglyceride lipase-mediated lipolysis of cellular fat stores is activated by CGI-58 and defective in Chanarin-Dorfman Syndrome." Cell Metab **3**(5): 309-19.
Le Roith, D. and Y. Zick (2001). "Recent advances in our understanding of insulin action and insulin resistance." Diabetes Care **24**(3): 588-97.
Leco, K. J., R. Khokha, et al. (1994). "Tissue inhibitor of metalloproteinases-3 (TIMP-3) is an extracellular matrix-associated protein with a distinctive pattern of expression in mouse cells and tissues." J Biol Chem **269**(12): 9352-60.
Lee, J. Y., K. H. Sohn, et al. (2001). "Saturated fatty acids, but not unsaturated fatty acids, induce the expression of cyclooxygenase-2 mediated through Toll-like receptor 4." J Biol Chem **276**(20): 16683-9.
Lee, Y. S., P. Li, et al. (2012). "Inflammation is necessary for long-term but not short-term high-fat diet-induced insulin resistance." Diabetes **60**(10): 2474-83.
LeRoy, E. C. (1974). "Increased collagen synthesis by scleroderma skin fibroblasts in vitro: a possible defect in the regulation or activation of the scleroderma fibroblast." J Clin Invest **54**(4): 880-9.
Liu, J., A. Divoux, et al. (2009). "Genetic deficiency and pharmacological stabilization of mast cells reduce diet-induced obesity and diabetes in mice." Nat Med **15**(8): 940-5.
Liu, L., Y. Zhang, et al. (2007). "Upregulation of myocellular DGAT1 augments triglyceride synthesis in skeletal muscle and protects against fat-induced insulin resistance." J Clin Invest **117**(6): 1679-89.
Lodhi, I. J., X. Wei, et al. (2011). "Lipoexpediency: de novo lipogenesis as a metabolic signal transmitter." Trends Endocrinol Metab **22**(1): 1-8.

Lohr, K., H. Sardana, et al. (2012). "Extracellular matrix protein lumican regulates inflammation in a mouse model of colitis." Inflamm Bowel Dis **18**(1): 143-51.
Luiken, J. J., Y. Arumugam, et al. (2001). "Increased rates of fatty acid uptake and plasmalemmal fatty acid transporters in obese Zucker rats." J Biol Chem **276**(44): 40567-73.
Lumeng, C. N., J. L. Bodzin, et al. (2007). "Obesity induces a phenotypic switch in adipose tissue macrophage polarization." J Clin Invest **117**(1): 175-84.
Lumeng, C. N., S. M. Deyoung, et al. (2007). "Increased inflammatory properties of adipose tissue macrophages recruited during diet-induced obesity." Diabetes **56**(1): 16-23.
Lumeng, C. N., I. Maillard, et al. (2009). "T-ing up inflammation in fat." Nat Med **15**(8): 846-7.

M

MacDougald, O. A. and S. Mandrup (2002). "Adipogenesis: forces that tip the scales." Trends Endocrinol Metab **13**(1): 5-11.
Macpherson, R. E., S. V. Ramos, et al. (2013). "Skeletal muscle PLIN proteins, ATGL and CGI-58, interactions at rest and following stimulated contraction." Am J Physiol Regul Integr Comp Physiol **304**(8): R644-50.
Mantovani, A., A. Sica, et al. (2004). "The chemokine system in diverse forms of macrophage activation and polarization." Trends Immunol **25**(12): 677-86.
Marette, A. (2002). "Mediators of cytokine-induced insulin resistance in obesity and other inflammatory settings." Curr Opin Clin Nutr Metab Care **5**(4): 377-83.
Marra, F., R. G. Romanelli, et al. (1999). "Monocyte chemotactic protein-1 as a chemoattractant for human hepatic stellate cells." Hepatology **29**(1): 140-8.
Mason, R. M. (2009). "Connective tissue growth factor(CCN2), a pathogenic factor in diabetic nephropathy. What does it do? How does it do it?" J Cell Commun Signal **3**(2): 95-104.
Mattey, D. L., P. T. Dawes, et al. (1997). "Transforming growth factor beta 1 and interleukin 4 induced alpha smooth muscle actin expression and myofibroblast-like differentiation in human synovial fibroblasts in vitro: modulation by basic fibroblast growth factor." Ann Rheum Dis **56**(7): 426-31.
Mazurek, T., L. Zhang, et al. (2003). "Human epicardial adipose tissue is a source of inflammatory mediators." Circulation **108**(20): 2460-6.
Medina-Gomez, G., S. L. Gray, et al. (2007). "PPAR gamma 2 prevents lipotoxicity by controlling adipose tissue expandability and peripheral lipid metabolism." PLoS Genet **3**(4): e64.
Metcalfe, D. D., D. Baram, et al. (1997). "Mast cells." Physiol Rev **77**(4): 1033-79.
Midwood, K., S. Sacre, et al. (2009). "Tenascin-C is an endogenous activator of Toll-like receptor 4 that is essential for maintaining inflammation in arthritic joint disease." Nat Med **15**(7): 774-80.
Miranville, A., C. Heeschen, et al. (2004). "Improvement of postnatal neovascularization by human adipose tissue-derived stem cells." Circulation **110**(3): 349-55.
Miyoshi, H., S. C. Souza, et al. (2006). "Perilipin promotes hormone-sensitive lipase-mediated adipocyte lipolysis via phosphorylation-dependent and -independent mechanisms." J Biol Chem **281**(23): 15837-44.
Moberg, E., S. Sjoberg, et al. (2002). "No apparent suppression by insulin of in vivo skeletal muscle lipolysis in nonobese women." Am J Physiol Endocrinol Metab **283**(2): E295-301.
Moller, D. E. (2000). "Potential role of TNF-alpha in the pathogenesis of insulin resistance and type 2 diabetes." Trends Endocrinol Metab **11**(6): 212-7.
Mori, T., S. Kawara, et al. (1999). "Role and interaction of connective tissue growth factor with transforming growth factor-beta in persistent fibrosis: A mouse fibrosis model." J Cell Physiol **181**(1): 153-9.

Moro, C., J. E. Galgani, et al. (2009). "Influence of gender, obesity, and muscle lipase activity on intramyocellular lipids in sedentary individuals." J Clin Endocrinol Metab **94**(9): 3440-7.
Mosser, D. M. and J. P. Edwards (2008). "Exploring the full spectrum of macrophage activation." Nat Rev Immunol **8**(12): 958-69.
Mulder, H., M. Sorhede-Winzell, et al. (2003). "Hormone-sensitive lipase null mice exhibit signs of impaired insulin sensitivity whereas insulin secretion is intact." J Biol Chem **278**(38): 36380-8.
Munzberg, H., M. Bjornholm, et al. (2005). "Leptin receptor action and mechanisms of leptin resistance." Cell Mol Life Sci **62**(6): 642-52.
Muoio, D. M. and C. B. Newgard (2008). "Mechanisms of disease: molecular and metabolic mechanisms of insulin resistance and beta-cell failure in type 2 diabetes." Nat Rev Mol Cell Biol **9**(3): 193-205.
Murano, I., G. Barbatelli, et al. (2008). "Dead adipocytes, detected as crown-like structures, are prevalent in visceral fat depots of genetically obese mice." J Lipid Res **49**(7): 1562-8.
Muro, A. F., F. A. Moretti, et al. (2008). "An essential role for fibronectin extra type III domain A in pulmonary fibrosis." Am J Respir Crit Care Med **177**(6): 638-45.
Murphy, G. and F. Willenbrock (1995). "Tissue inhibitors of matrix metalloendopeptidases." Methods Enzymol **248**: 496-510.

N

Naito, M., H. Nagai, et al. (1996). "Liposome-encapsulated dichloromethylene diphosphonate induces macrophage apoptosis in vivo and in vitro." J Leukoc Biol **60**(3): 337-44.
Nakajima, I., T. Yamaguchi, et al. (1998). "Adipose tissue extracellular matrix: newly organized by adipocytes during differentiation." Differentiation **63**(4): 193-200.
Napolitano, L. (1963). "The Differentiation of White Adipose Cells. an Electron Microscope Study." J Cell Biol **18**: 663-79.
Neal, M. D., C. Leaphart, et al. (2006). "Enterocyte TLR4 mediates phagocytosis and translocation of bacteria across the intestinal barrier." J Immunol **176**(5): 3070-9.
Nguyen, M. T., S. Favelyukis, et al. (2007). "A subpopulation of macrophages infiltrates hypertrophic adipose tissue and is activated by free fatty acids via Toll-like receptors 2 and 4 and JNK-dependent pathways." J Biol Chem **282**(48): 35279-92.
Nishimura, S., I. Manabe, et al. (2009). "CD8+ effector T cells contribute to macrophage recruitment and adipose tissue inflammation in obesity." Nat Med **15**(8): 914-20.
Nowotny, B., L. Zahiragic, et al. (2013). "Mechanisms underlying the onset of oral lipid-induced skeletal muscle insulin resistance in humans." Diabetes.

O

Okamura, Y., M. Watari, et al. (2001). "The extra domain A of fibronectin activates Toll-like receptor 4." J Biol Chem **276**(13): 10229-33.
Olefsky, J. M. and C. K. Glass (2010). "Macrophages, inflammation, and insulin resistance." Annu Rev Physiol **72**: 219-46.

P

Pal, D., S. Dasgupta, et al. (2012). "Fetuin-A acts as an endogenous ligand of TLR4 to promote lipid-induced insulin resistance." Nat Med.
Park, S. Y., H. J. Kim, et al. (2005). "Hormone-sensitive lipase knockout mice have increased hepatic insulin sensitivity and are protected from short-term diet-induced insulin resistance in skeletal muscle and heart." Am J Physiol Endocrinol Metab **289**(1): E30-9.
Patsouris, D., P. P. Li, et al. (2008). "Ablation of CD11c-positive cells normalizes insulin sensitivity in obese insulin resistant animals." Cell Metab **8**(4): 301-9.

Phanish, M. K., N. A. Wahab, et al. (2005). "TGF-beta1-induced connective tissue growth factor (CCN2) expression in human renal proximal tubule epithelial cells requires Ras/MEK/ERK and Smad signalling." Nephron Exp Nephrol **100**(4): e156-65.
Piccinini, A. M. and K. S. Midwood (2012). "Endogenous control of immunity against infection: tenascin-C regulates TLR4-mediated inflammation via microRNA-155." Cell Rep **2**(4): 914-26.
Pittenger, M. F., A. M. Mackay, et al. (1999). "Multilineage potential of adult human mesenchymal stem cells." Science **284**(5411): 143-7.
Poggi, M., D. Bastelica, et al. (2007). "C3H/HeJ mice carrying a toll-like receptor 4 mutation are protected against the development of insulin resistance in white adipose tissue in response to a high-fat diet." Diabetologia **50**(6): 1267-76.
Pollak, N. M., M. Schweiger, et al. (2013). "Cardiac-specific overexpression of perilipin 5 provokes severe cardiac steatosis via the formation of a lipolytic barrier." J Lipid Res **54**(4): 1092-102.
Poulain-Godefroy, O. and P. Froguel (2007). "Preadipocyte response and impairment of differentiation in an inflammatory environment." Biochem Biophys Res Commun **356**(3): 662-7.
Prins, J. B. and S. O'Rahilly (1997). "Regulation of adipose cell number in man." Clin Sci (Lond) **92**(1): 3-11.

Q

Qi, Z., N. Atsuchi, et al. (1999). "Blockade of type beta transforming growth factor signaling prevents liver fibrosis and dysfunction in the rat." Proc Natl Acad Sci U S A **96**(5): 2345-9.

R

Raes, G., R. Van den Bergh, et al. (2005). "Arginase-1 and Ym1 are markers for murine, but not human, alternatively activated myeloid cells." J Immunol **174**(11): 6561; author reply 6561-2.
Rakoff-Nahoum, S., J. Paglino, et al. (2004). "Recognition of commensal microflora by toll-like receptors is required for intestinal homeostasis." Cell **118**(2): 229-41.
Ricard-Blum, S. and F. Ruggiero (2005). "The collagen superfamily: from the extracellular matrix to the cell membrane." Pathol Biol (Paris) **53**(7): 430-42.
Rieusset, J., K. Bouzakri, et al. (2004). "Suppressor of cytokine signaling 3 expression and insulin resistance in skeletal muscle of obese and type 2 diabetic patients." Diabetes **53**(9): 2232-41.
Rieusset, J., M. A. Chauvin, et al. (2012). "Reduction of endoplasmic reticulum stress using chemical chaperones or Grp78 overexpression does not protect muscle cells from palmitate-induced insulin resistance." Biochem Biophys Res Commun **417**(1): 439-45.
Rimon, E., B. Chen, et al. (2008). "Hypoxia in human trophoblasts stimulates the expression and secretion of connective tissue growth factor." Endocrinology **149**(6): 2952-8.
Roberts, A. B., M. B. Sporn, et al. (1986). "Transforming growth factor type beta: rapid induction of fibrosis and angiogenesis in vivo and stimulation of collagen formation in vitro." Proc Natl Acad Sci U S A **83**(12): 4167-71.
Rodbell, M. (1964). "Localization of Lipoprotein Lipase in Fat Cells of Rat Adipose Tissue." J Biol Chem **239**: 753-5.
Ross, R. (1999). "Atherosclerosis--an inflammatory disease." N Engl J Med **340**(2): 115-26.
Rubbia-Brandt, L., A. P. Sappino, et al. (1991). "Locally applied GM-CSF induces the accumulation of alpha-smooth muscle actin containing myofibroblasts." Virchows Arch B Cell Pathol Incl Mol Pathol **60**(2): 73-82.

Rupnick, M. A., D. Panigrahy, et al. (2002). "Adipose tissue mass can be regulated through the vasculature." Proc Natl Acad Sci U S A **99**(16): 10730-5.

S

Saberi, M., N. B. Woods, et al. (2009). "Hematopoietic Cell-Specific Deletion of Toll-like Receptor 4 Ameliorates Hepatic and Adipose Tissue Insulin Resistance in High-Fat-Fed Mice." Cell Metabolism **10**(5): 419-429.

Samad, F., K. Yamamoto, et al. (1997). "Elevated expression of transforming growth factor-beta in adipose tissue from obese mice." Mol Med **3**(1): 37-48.

Samuel, V. T. and G. I. Shulman (2012). "Mechanisms for insulin resistance: common threads and missing links." Cell **148**(5): 852-71.

Sartore, S., A. Chiavegato, et al. (2001). "Contribution of adventitial fibroblasts to neointima formation and vascular remodeling: from innocent bystander to active participant." Circ Res **89**(12): 1111-21.

Schaeffler, A., P. Gross, et al. (2009). "Fatty acid-induced induction of Toll-like receptor-4/nuclear factor-kappaB pathway in adipocytes links nutritional signalling with innate immunity." Immunology **126**(2): 233-45.

Schaffer, J. E. and H. F. Lodish (1994). "Expression cloning and characterization of a novel adipocyte long chain fatty acid transport protein." Cell **79**(3): 427-36.

Scherer, P. E., P. E. Bickel, et al. (1998). "Cloning of cell-specific secreted and surface proteins by subtractive antibody screening." Nature Biotechnology **16**(6): 581-586.

Scherer, P. E., S. Williams, et al. (1995). "A novel serum protein similar to C1q, produced exclusively in adipocytes." J Biol Chem **270**(45): 26746-9.

Schmid, P., P. Itin, et al. (1998). "Enhanced expression of transforming growth factor-beta type I and type II receptors in wound granulation tissue and hypertrophic scar." Am J Pathol **152**(2): 485-93.

Schmitz-Peiffer, C. (2010). "Targeting ceramide synthesis to reverse insulin resistance." Diabetes **59**(10): 2351-3.

Schmitz-Peiffer, C. and T. J. Biden (2008). "Protein kinase C function in muscle, liver, and beta-cells and its therapeutic implications for type 2 diabetes." Diabetes **57**(7): 1774-83.

Schrauwen-Hinderling, V. B., P. Schrauwen, et al. (2003). "The increase in intramyocellular lipid content is a very early response to training." J Clin Endocrinol Metab **88**(4): 1610-6.

Schrauwen-Hinderling, V. B., L. J. van Loon, et al. (2003). "Intramyocellular lipid content is increased after exercise in nonexercising human skeletal muscle." J Appl Physiol **95**(6): 2328-32.

Schwabe, R. F., R. Bataller, et al. (2003). "Human hepatic stellate cells express CCR5 and RANTES to induce proliferation and migration." Am J Physiol Gastrointest Liver Physiol **285**(5): G949-58.

Schwartz, M. W., R. J. Seeley, et al. (1996). "Identification of targets of leptin action in rat hypothalamus." J Clin Invest **98**(5): 1101-6.

Schweiger, M., M. Paar, et al. (2012). "G0/G1 switch gene-2 regulates human adipocyte lipolysis by affecting activity and localization of adipose triglyceride lipase." J Lipid Res **53**(11): 2307-17.

Seki, E., S. De Minicis, et al. (2007). "TLR4 enhances TGF-beta signaling and hepatic fibrosis." Nat Med **13**(11): 1324-32.

Sengenes, C., A. Bouloumie, et al. (2003). "Involvement of a cGMP-dependent pathway in the natriuretic peptide-mediated hormone-sensitive lipase phosphorylation in human adipocytes." J Biol Chem **278**(49): 48617-26.

Sengenes, C., K. Lolmede, et al. (2005). "Preadipocytes in the human subcutaneous adipose tissue display distinct features from the adult mesenchymal and hematopoietic stem cells." J Cell Physiol **205**(1): 114-22.

Sengenes, C., C. Moro, et al. (2005). "[Natriuretic peptides: a new lipolytic pathway in human fat cells]." Med Sci (Paris) **21 Spec No**: 29-33.
Senn, J. J., P. J. Klover, et al. (2002). "Interleukin-6 induces cellular insulin resistance in hepatocytes." Diabetes **51**(12): 3391-9.
Shah, M., D. M. Foreman, et al. (1994). "Neutralising antibody to TGF-beta 1,2 reduces cutaneous scarring in adult rodents." J Cell Sci **107 (Pt 5)**: 1137-57.
Shapiro, H., T. Pecht, et al. (2013). "Adipose tissue foam cells are present in human obesity." J Clin Endocrinol Metab **98**(3): 1173-81.
Shaul, M. E., G. Bennett, et al. (2010). "Dynamic, M2-like remodeling phenotypes of CD11c+ adipose tissue macrophages during high-fat diet--induced obesity in mice." Diabetes **59**(5): 1171-81.
Shepherd, S. O., M. Cocks, et al. (2013). "Sprint interval and traditional endurance training increase net intramuscular triglyceride breakdown and expression of perilipin 2 and 5." J Physiol **591**(Pt 3): 657-75.
Shi-Wen, X., A. Leask, et al. (2008). "Regulation and function of connective tissue growth factor/CCN2 in tissue repair, scarring and fibrosis." Cytokine Growth Factor Rev **19**(2): 133-44.
Shi, H., M. V. Kokoeva, et al. (2006). "TLR4 links innate immunity and fatty acid-induced insulin resistance." J Clin Invest **116**(11): 3015-25.
Shi, M. A. and G. P. Shi (2012). "Different roles of mast cells in obesity and diabetes: lessons from experimental animals and humans." Front Immunol **3**: 7.
Shimizu, M., A. Hara, et al. (2001). "Mechanism of retarded liver regeneration in plasminogen activator-deficient mice: impaired activation of hepatocyte growth factor after Fas-mediated massive hepatic apoptosis." Hepatology **33**(3): 569-76.
Shimokado, K., E. W. Raines, et al. (1985). "A significant part of macrophage-derived growth factor consists of at least two forms of PDGF." Cell **43**(1): 277-86.
Sindrilaru, A., T. Peters, et al. (2011). "An unrestrained proinflammatory M1 macrophage population induced by iron impairs wound healing in humans and mice." J Clin Invest **121**(3): 985-97.
Singer, II, D. W. Kawka, et al. (1984). "In vivo co-distribution of fibronectin and actin fibers in granulation tissue: immunofluorescence and electron microscope studies of the fibronexus at the myofibroblast surface." J Cell Biol **98**(6): 2091-106.
Smas, C. M. and H. S. Sul (1993). "Pref-1, a protein containing EGF-like repeats, inhibits adipocyte differentiation." Cell **73**(4): 725-34.
Spalding, K. L., E. Arner, et al. (2008). "Dynamics of fat cell turnover in humans." Nature **453**(7196): 783-7.
Spencer, M., A. Yao-Borengasser, et al. (2010). "Adipose tissue macrophages in insulin-resistant subjects are associated with collagen VI and fibrosis and demonstrate alternative activation." Am J Physiol Endocrinol Metab **299**(6): E1016-27.
Spiegelman, B. M. and G. S. Hotamisligil (1993). "Through thick and thin: wasting, obesity, and TNF alpha." Cell **73**(4): 625-7.
Stefanovic-Racic, M., X. Yang, et al. (2012). "Dendritic cells promote macrophage infiltration and comprise a substantial proportion of obesity-associated increases in CD11c+ cells in adipose tissue and liver." Diabetes **61**(9): 2330-9.
Stephens, J. M. and P. H. Pekala (1991). "Transcriptional repression of the GLUT4 and C/EBP genes in 3T3-L1 adipocytes by tumor necrosis factor-alpha." J Biol Chem **266**(32): 21839-45.
Stich, V., I. De Glisezinski, et al. (2000). "Activation of alpha(2)-adrenergic receptors impairs exercise-induced lipolysis in SCAT of obese subjects." Am J Physiol Regul Integr Comp Physiol **279**(2): R499-504.

Straczkowski, M., I. Kowalska, et al. (2007). "Increased skeletal muscle ceramide level in men at risk of developing type 2 diabetes." Diabetologia **50**(11): 2366-73.
Strissel, K. J., Z. Stancheva, et al. (2007). "Adipocyte death, adipose tissue remodeling, and obesity complications." Diabetes **56**(12): 2910-8.
Suganami, T., T. Mieda, et al. (2007). "Attenuation of obesity-induced adipose tissue inflammation in C3H/HeJ mice carrying a Toll-like receptor 4 mutation." Biochem Biophys Res Commun **354**(1): 45-9.
Suganami, T., J. Nishida, et al. (2005). "A paracrine loop between adipocytes and macrophages aggravates inflammatory changes: role of free fatty acids and tumor necrosis factor alpha." Arterioscler Thromb Vasc Biol **25**(10): 2062-8.
Suganami, T. and Y. Ogawa (2010). "Adipose tissue macrophages: their role in adipose tissue remodeling." J Leukoc Biol **88**(1): 33-9.
Suganami, T., K. Tanimoto-Koyama, et al. (2007). "Role of the Toll-like receptor 4/NF-kappaB pathway in saturated fatty acid-induced inflammatory changes in the interaction between adipocytes and macrophages." Arterioscler Thromb Vasc Biol **27**(1): 84-91.
Sun, Y., G. Hegamyer, et al. (1995). "Molecular cloning of mouse tissue inhibitor of metalloproteinases-3 and its promoter. Specific lack of expression in neoplastic JB6 cells may reflect altered gene methylation." J Biol Chem **270**(33): 19312-9.
Sunderkotter, C., K. Steinbrink, et al. (1994). "Macrophages and angiogenesis." J Leukoc Biol **55**(3): 410-22.

$\mathcal{T}$

Tacken, P. J., B. Teusink, et al. (2000). "LDL receptor deficiency unmasks altered VLDL triglyceride metabolism in VLDL receptor transgenic and knockout mice." J Lipid Res **41**(12): 2055-62.
Taipale, J. and J. Keski-Oja (1997). "Growth factors in the extracellular matrix." Faseb J **11**(1): 51-9.
Takahashi, K., S. Mizuarai, et al. (2003). "Adiposity elevates plasma MCP-1 levels leading to the increased CD11b-positive monocytes in mice." J Biol Chem **278**(47): 46654-60.
ten Dijke, P. and H. M. Arthur (2007). "Extracellular control of TGFbeta signalling in vascular development and disease." Nat Rev Mol Cell Biol **8**(11): 857-69.
Teratani, T., K. Tomita, et al. (2012). "A high-cholesterol diet exacerbates liver fibrosis in mice via accumulation of free cholesterol in hepatic stellate cells." Gastroenterology **142**(1): 152-164 e10.
Tomas, E., T. S. Tsao, et al. (2002). "Enhanced muscle fat oxidation and glucose transport by ACRP30 globular domain: acetyl-CoA carboxylase inhibition and AMP-activated protein kinase activation." Proc Natl Acad Sci U S A **99**(25): 16309-13.
Tomasek, J. J., G. Gabbiani, et al. (2002). "Myofibroblasts and mechano-regulation of connective tissue remodelling." Nat Rev Mol Cell Biol **3**(5): 349-63.
Trayhurn, P. (2013). "Hypoxia and adipose tissue function and dysfunction in obesity." Physiol Rev **93**(1): 1-21.
Tsukumo, D. M., M. A. Carvalho-Filho, et al. (2007). "Loss-of-function mutation in Toll-like receptor 4 prevents diet-induced obesity and insulin resistance." Diabetes **56**(8): 1986-98.
Turner, N., C. R. Bruce, et al. (2007). "Excess lipid availability increases mitochondrial fatty acid oxidative capacity in muscle: evidence against a role for reduced fatty acid oxidation in lipid-induced insulin resistance in rodents." Diabetes **56**(8): 2085-92.

$\mathcal{U}$

Ussher, J. R., T. R. Koves, et al. (2010). "Inhibition of de novo ceramide synthesis reverses diet-induced insulin resistance and enhances whole-body oxygen consumption." Diabetes **59**(10): 2453-64.

V

Virtue, S. and A. Vidal-Puig (2008). "It's not how fat you are, it's what you do with it that counts." PLoS Biol **6**(9): e237.

W

Wahab, N. A., B. S. Weston, et al. (2005). "Connective tissue growth factor CCN2 interacts with and activates the tyrosine kinase receptor TrkA." J Am Soc Nephrol **16**(2): 340-51.

Wallenius, V., K. Wallenius, et al. (2002). "Interleukin-6-deficient mice develop mature-onset obesity." Nat Med **8**(1): 75-9.

Wang, H., U. Sreenevasan, et al. (2011). "Perilipin 5, a lipid droplet-associated protein, provides physical and metabolic linkage to mitochondria." J Lipid Res **52**(12): 2159-68.

Wang, H., U. Sreenivasan, et al. (2013). "Cardiomyocyte-specific perilipin 5 overexpression leads to myocardial steatosis and modest cardiac dysfunction." J Lipid Res **54**(4): 953-65.

Wanless, I. R. and J. S. Lentz (1990). "Fatty liver hepatitis (steatohepatitis) and obesity: an autopsy study with analysis of risk factors." Hepatology **12**(5): 1106-10.

Watt, M. J., G. J. Heigenhauser, et al. (2003). "Hormone-sensitive lipase activity and fatty acyl-CoA content in human skeletal muscle during prolonged exercise." J Appl Physiol **95**(1): 314-21.

Weisberg, S. P., D. Hunter, et al. (2006). "CCR2 modulates inflammatory and metabolic effects of high-fat feeding." J Clin Invest **116**(1): 115-24.

Weisberg, S. P., D. McCann, et al. (2003). "Obesity is associated with macrophage accumulation in adipose tissue." Journal of Clinical Investigation **112**(12): 1796-1808.

Wellen, K. E. and G. S. Hotamisligil (2003). "Obesity-induced inflammatory changes in adipose tissue." J Clin Invest **112**(12): 1785-8.

Wick, M., C. Burger, et al. (1994). "A novel member of human tissue inhibitor of metalloproteinases (TIMP) gene family is regulated during G1 progression, mitogenic stimulation, differentiation, and senescence." J Biol Chem **269**(29): 18953-60.

Willenbrock, F. and G. Murphy (1994). "Structure-function relationships in the tissue inhibitors of metalloproteinases." Am J Respir Crit Care Med **150**(6 Pt 2): S165-70.

Wu, F., N. Vij, et al. (2007). "A novel role of the lumican core protein in bacterial lipopolysaccharide-induced innate immune response." J Biol Chem **282**(36): 26409-17.

Wu, H., G. Chen, et al. (2007). "TLR4 activation mediates kidney ischemia/reperfusion injury." J Clin Invest **117**(10): 2847-59.

Wu, L. and Y. J. Liu (2007). "Development of dendritic-cell lineages." Immunity **26**(6): 741-50.

Wynn, T. A. (2004). "Fibrotic disease and the T(H)1/T(H)2 paradigm." Nat Rev Immunol **4**(8): 583-94.

Wynn, T. A. (2007). "Common and unique mechanisms regulate fibrosis in various fibroproliferative diseases." J Clin Invest **117**(3): 524-9.

X

Xiao, W., H. Hong, et al. (2008). "Regulation of myeloproliferation and M2 macrophage programming in mice by Lyn/Hck, SHIP, and Stat5." J Clin Invest **118**(3): 924-34.

Xu, H., G. T. Barnes, et al. (2003). "Chronic inflammation in fat plays a crucial role in the development of obesity-related insulin resistance." J Clin Invest **112**(12): 1821-30.

Y

Yamauchi, T., J. Kamon, et al. (2003). "Cloning of adiponectin receptors that mediate antidiabetic metabolic effects." Nature **423**(6941): 762-9.

Yang, J., C. Dai, et al. (2003). "Hepatocyte growth factor suppresses renal interstitial myofibroblast activation and intercepts Smad signal transduction." Am J Pathol **163**(2): 621-32.

Yu, C., Y. Chen, et al. (2002). "Mechanism by which fatty acids inhibit insulin activation of insulin receptor substrate-1 (IRS-1)-associated phosphatidylinositol 3-kinase activity in muscle." J Biol Chem **277**(52): 50230-6.

Yudkin, J. S., C. D. Stehouwer, et al. (1999). "C-reactive protein in healthy subjects: associations with obesity, insulin resistance, and endothelial dysfunction: a potential role for cytokines originating from adipose tissue?" Arterioscler Thromb Vasc Biol **19**(4): 972-8.

Z

Zechner, R., P. C. Kienesberger, et al. (2009). "Adipose triglyceride lipase and the lipolytic catabolism of cellular fat stores." J Lipid Res **50**(1): 3-21.

Zeisberg, M., F. Strutz, et al. (2001). "Renal fibrosis: an update." Curr Opin Nephrol Hypertens **10**(3): 315-20.

Zeyda, M., D. Farmer, et al. (2007). "Human adipose tissue macrophages are of an anti-inflammatory phenotype but capable of excessive pro-inflammatory mediator production." Int J Obes (Lond) **31**(9): 1420-8.

Zeyda, M., K. Gollinger, et al. (2010). "Newly identified adipose tissue macrophage populations in obesity with distinct chemokine and chemokine receptor expression." Int J Obes (Lond) **34**(12): 1684-94.

Zhang, C., X. Meng, et al. (2004). "Role of connective tissue growth factor in renal tubular epithelial-myofibroblast transdifferentiation and extracellular matrix accumulation in vitro." Life Sci **75**(3): 367-79.

Zhang, H. H., M. Halbleib, et al. (2002). "Tumor necrosis factor-alpha stimulates lipolysis in differentiated human adipocytes through activation of extracellular signal-related kinase and elevation of intracellular cAMP." Diabetes **51**(10): 2929-35.

Zhang, H. Y. and S. H. Phan (1999). "Inhibition of myofibroblast apoptosis by transforming growth factor beta(1)." Am J Respir Cell Mol Biol **21**(6): 658-65.

Zhang, Y. E. (2009). "Non-Smad pathways in TGF-beta signaling." Cell Res **19**(1): 128-39.

Zhu, Q., L. Zou, et al. (2012). "Intestinal decontamination inhibits TLR4 dependent fibronectin-mediated cross-talk between stellate cells and endothelial cells in liver fibrosis in mice." J Hepatol **56**(4): 893-9.

Zimmermann, R., J. G. Strauss, et al. (2004). "Fat mobilization in adipose tissue is promoted by adipose triglyceride lipase." Science **306**(5700): 1383-6.

ANNEXES

ANNEXES 1 & 2

- **Partial inhibition of adipose tissue lipolysis improves glucose metabolism and insulin sensitivity without alteration of fat mass.** ***Girousse et al Plos Biology 2013***

- **De Novo Lipogenesis-Derived Fatty Acids Released during Human Adipocyte Lipolysis Promote Lipid Storage but not Macrophage Activation.** ***Kolditz et al en soumission***

OPEN ACCESS Freely available online

PLOS BIOLOGY

Partial Inhibition of Adipose Tissue Lipolysis Improves Glucose Metabolism and Insulin Sensitivity Without Alteration of Fat Mass

Amandine Girousse[1,2], Geneviève Tavernier[1,2], Carine Valle[1,2], Cedric Moro[1,2], Niklas Mejhert[3], Anne-Laure Dinel[1,2], Marianne Houssier[1,2], Balbine Roussel[1,2], Aurèle Besse-Patin[1,2], Marion Combes[1,2], Lucile Mir[1,2], Laurent Monbrun[1,2], Véronic Bézaire[1,2], Bénédicte Prunet-Marcassus[4], Aurélie Waget[2,5], Isabelle Vila[1,2], Sylvie Caspar-Bauguil[1,2,6], Katie Louche[1,2], Marie-Adeline Marques[1,2], Aline Mairal[1,2], Marie-Laure Renoud[2,7], Jean Galitzky[2,7], Cecilia Holm[8], Etienne Mouisel[1,2], Claire Thalamas[1,2,9], Nathalie Viguerie[1,2], Thierry Sulpice[4], Rémy Burcelin[2,5], Peter Arner[3], Dominique Langin[1,2,6]*

1 INSERM, UMR1048, Obesity Research Laboratory, Institute of Metabolic and Cardiovascular Diseases, Toulouse, France, **2** University of Toulouse, UMR1048, Paul Sabatier University, France, **3** Department of Medicine, Karolinska Institute at Karolinska Hospital, Huddinge, Stockholm, Sweden, **4** Physiogenex, Prologue Biotech, Labège-Innopole, France, **5** INSERM, UMR1048,Team 2, I2MC, Institute of Metabolic and Cardiovascular Diseases, Toulouse, France, **6** Toulouse University Hospitals, Laboratory of Clinical Biochemistry, Toulouse, France, **7** INSERM, UMR1048, Team 1, I2MC, Institute of Metabolic and Cardiovascular Diseases, Toulouse, France, **8** Department of Experimental Medical Science, Lund University, Lund, Sweden, **9** Toulouse University Hospitals, INSERM, Clinical Investigation Center, Toulouse, France

Abstract

When energy is needed, white adipose tissue (WAT) provides fatty acids (FAs) for use in peripheral tissues via stimulation of fat cell lipolysis. FAs have been postulated to play a critical role in the development of obesity-induced insulin resistance, a major risk factor for diabetes and cardiovascular disease. However, whether and how chronic inhibition of fat mobilization from WAT modulates insulin sensitivity remains elusive. Hormone-sensitive lipase (HSL) participates in the breakdown of WAT triacylglycerol into FAs. HSL haploinsufficiency and treatment with a HSL inhibitor resulted in improvement of insulin tolerance without impact on body weight, fat mass, and WAT inflammation in high-fat-diet–fed mice. In vivo palmitate turnover analysis revealed that blunted lipolytic capacity is associated with diminution in FA uptake and storage in peripheral tissues of obese HSL haploinsufficient mice. The reduction in FA turnover was accompanied by an improvement of glucose metabolism with a shift in respiratory quotient, increase of glucose uptake in WAT and skeletal muscle, and enhancement of de novo lipogenesis and insulin signalling in liver. In human adipocytes, HSL gene silencing led to improved insulin-stimulated glucose uptake, resulting in increased de novo lipogenesis and activation of cognate gene expression. In clinical studies, WAT lipolytic rate was positively and negatively correlated with indexes of insulin resistance and WAT de novo lipogenesis gene expression, respectively. In obese individuals, chronic inhibition of lipolysis resulted in induction of WAT de novo lipogenesis gene expression. Thus, reduction in WAT lipolysis reshapes FA fluxes without increase of fat mass and improves glucose metabolism through cell-autonomous induction of fat cell de novo lipogenesis, which contributes to improved insulin sensitivity.

Citation: Girousse A, Tavernier G, Valle C, Moro C, Mejhert N, et al. (2013) Partial Inhibition of Adipose Tissue Lipolysis Improves Glucose Metabolism and Insulin Sensitivity Without Alteration of Fat Mass. PLoS Biol 11(2): e1001485. doi:10.1371/journal.pbio.1001485

Academic Editor: Stephen O'Rahilly, University of Cambridge, United Kingdom

Received July 10, 2012; **Accepted** January 8, 2013; **Published** February 19, 2013

Funding: A.G. was supported by Inserm and Fondation pour la Recherche Médicale. Grants to D.L. from Agence Nationale de la Recherche (LIPOB and OBELIP projects), Région Midi-Pyrénées, GlaxoSmithKline, Inserm/DHOS, CHU de Toulouse, Fondation pour la Recherche Médicale, and the Commission of the European Communities (Projects HEPADIP, ADAPT and DIABAT). Grants to P.A. from the Swedish Research Council, the Swedish Diabetes Foundation, The Strategic Research Programme in Diabetes at Karolinska Institute, the Novo Nordisk Foundation, and the European Foundation for the Study of Diabetes/Lilly Programme. The funders had no role in study design, data collection and analysis, decision to publish, or preparation of the manuscript.

Competing Interests: The authors have declared that no competing interests exist.

Abbreviations: ATGL, adipose triglyceride lipase; BMI, body mass index; ChREBP, carbohydrate responsive element-binding protein; DG, diacylglycerol; FA, fatty acid; GFP, green fluorescent protein; GLUT4, glucose transporter 4; HFD, high fat diet; hMADS, human multipotent adipose-derived stem cells; HSL, hormone-sensitive lipase; HOMA-IR, homeostatic model assessment–insulin resistance; NEFA, nonesterified fatty acid; QUICKI, quantitative insulin sensitivity check index; RBP4, retinol binding protein 4; TG, triacylglycerol; WAT, white adipose tissue; WT, wild type

* E-mail: dominique.langin@inserm.fr

Introduction

White adipose tissue (WAT) is the main energy store of the body in mammals. In the fed state, under the influence of insulin, WAT stores excess energy as triacylglycerols (TGs) in the lipid droplet of adipocytes. When energy is needed between meals or during physical exercise, WAT delivers fatty acids (FAs) to be oxidized in peripheral tissues. Lipolysis is the process by which stored TGs are released as nonesterified FA (NEFA) [1]. It involves different regulators such as lipases, co-lipases, and proteins that coat the lipid droplet. It is now largely accepted that the enzymatic breakdown of TG is initiated by adipose triglyceride lipase

Author Summary

In periods of energy demand, mobilization of fat stores in mammals (i.e., adipose tissue lipolysis) is essential to provide energy in the form of fatty acids. In excess, however, fatty acids induce resistance to the action of insulin, which serves to regulate glucose metabolism in skeletal muscle and liver. Insulin resistance (or low insulin sensitivity) is believed to be a cornerstone of the complications of obesity such as type 2 diabetes and cardiovascular diseases. In this study, our clinical observation of natural variation in fat cell lipolysis in individuals reveals that a high lipolytic rate is associated with low insulin sensitivity. Furthermore, partial genetic and pharmacologic inhibition of hormone-sensitive lipase, one of the enzymes involved in the breakdown of white adipose tissue lipids, results in improvement of insulin sensitivity in mice without gain in body weight and fat mass. We undertake a series of mechanistic studies in mice and in human fat cells to show that blunted lipolytic capacity increases the synthesis of new fatty acids from glucose in fat cells, a pathway that has recently been shown by others to be a major determinant of whole body insulin sensitivity. In conclusion, partial inhibition of adipose tissue lipolysis is a plausible strategy in the treatment of obesity-related insulin resistance.

(ATGL) and leads to the formation of diacylglycerols (DGs) that are in turn hydrolyzed by hormone-sensitive lipase (HSL) [2,3]. HSL also shows TG hydrolase activity. The final step of this catabolic process is the hydrolysis of monoacylglycerols by monoglyceride lipase, leading to the release of one molecule of glycerol and three molecules of FA.

Obese individuals are at increased risk of type 2 diabetes and cardiovascular disease. Insulin resistance is viewed as a cornerstone of the underlying pathogenic processes, and there is a wide disparity in insulin resistance among obese individuals [4]. FAs have been postulated to play a critical role in the development of insulin resistance [5]. Plasma NEFA levels and fluxes are not directly determined by the amount of body fat and are partly controlled by WAT lipolysis [6]. Furthermore, the relationship between circulating NEFA concentrations and insulin sensitivity in vivo is not straight forward. In that context, the influence of variation in fat cell lipolysis and lipase expression on insulin sensitivity and glucose metabolism remains elusive. Different consequences of diminished WAT lipolysis that are not mutually exclusive can be hypothesized. It could favour the development of obesity through retention of TG within adipocytes. It can also be viewed as a mechanism limiting an excess of FA release and alleviating the development of insulin resistance and metabolic abnormalities. This effect may be direct through the deleterious action of FA on insulin-sensitive tissues [7]. An indirect action may be considered via the modulation of WAT inflammation-induced insulin resistance as FAs produced by adipocytes stimulate cytokine production by macrophages [8]. Moreover, there is no clear picture of the relation between WAT lipolysis and glucose metabolism in WAT, skeletal muscle, and liver. Mice with full knockout of HSL and ATGL show complex phenotypes including marked alterations of fat mass that preclude conclusions on the effect of WAT lipolysis inhibition on insulin sensitivity [9]. Therefore, a major question of clinical relevance that remains unanswered is the role of FA release from WAT on insulin sensitivity and glucose metabolism and whether this control operates with an effect on fat mass.

By a combination of clinical, animal, and cellular studies, we investigated the role of WAT lipolysis, including the specific contribution of HSL, in the control of insulin sensitivity and glucose metabolism. HSL level is a determinant of lipolytic capacity in human WAT [10]. Reduction of HSL activity and blunted stimulated lipolysis has been observed in obesity [11,12]. To gain mechanistic insights in this relationship, we investigated HSL haploinsufficient ($HSL^{+/-}$) mice that showed impaired HSL expression and enzymatic activity and diminished WAT lipolysis. When fed a high-fat diet (HFD), $HSL^{+/-}$ mice did not become more obese than wild type (WT) littermates and their WAT was not more inflamed. Lipid metabolism studied dynamically in vivo revealed a global reduction of FA fluxes in $HSL^{+/-}$ mice. The slowdown of FA turnover was accompanied by an amelioration of glucose metabolism, including glucose uptake and de novo lipogenesis in insulin-sensitive tissues. Insulin tolerance was improved both in mice with HSL haploinsufficiency and in mice treated with a HSL inhibitor. Improved adipocyte insulin-stimulated glucose uptake, observed both in vivo in mice and in vitro in human adipocytes, led to cell autonomous induction of de novo lipogenesis, which may contribute to improved insulin sensitivity when WAT lipolysis is decreased. The relevance of these observations was established in humans. Investigation of several cohorts of individuals with a wide range of BMI showed a positive association between fat cell lipolytic rate and indexes of insulin resistance and a negative association between lipolysis and expression of genes involved in fatty acid synthesis including the lipogenic transcription factor ChREBP (carbohydrate responsive element-binding protein). Moreover, chronic treatment of obese individuals with an antilipolytic drug resulted in up-regulation of WAT de novo lipogenesis gene expression.

Results

Association between WAT Lipolysis and Insulin Sensitivity in Humans

To investigate the relationship between WAT lipolysis and insulin sensitivity in humans, we first studied a large cohort of subjects presenting a wide range of BMI. A positive association was found in 367 individuals between spontaneous glycerol release measured ex vivo on WAT explants obtained after an overnight fast and the homeostasis model of indirect assessment of insulin resistance (HOMA-IR) (Figure 1A). Variation in lipolysis explained 28% of the variance in HOMA-IR. When adjusted for age, gender, and BMI, 8% of the variance in HOMA-IR remained explained by lipolysis ($p<0.0001$). Dividing the cohort according to WHO criteria for normal weight, overweight, and obesity (i.e., $18.5<BMI<25$, $25<BMI<30$, $30<BMI<35$, $35<BMI<40$, $BMI>40$ kg/m^2), a correlation coefficient of 0.3 was found for each range of BMI ($p<0.01$), indicating that the relationship between high lipolysis and insulin resistance exists across the spectrum of fat mass. We then assessed insulin tolerance in 126 subjects, after an intravenous bolus injection of insulin. A negative association was found between insulin tolerance and lipolysis (Figure 1B). To gain further insight, this relationship was investigated in 25 morbidly obese individuals who underwent bariatric surgery (Figure 1C). WAT lipolysis and HOMA-IR were measured before and 2 years after bariatric surgery. A correlation was found between the change in lipolysis and the change in HOMA-IR (Figure 1D). The higher the decrease in lipolysis, the stronger the improvement of insulin resistance. Altogether, these data suggest, in both cross-sectional and longitudinal studies, that, in humans, WAT lipolytic capacity may contribute to the control of insulin sensitivity.

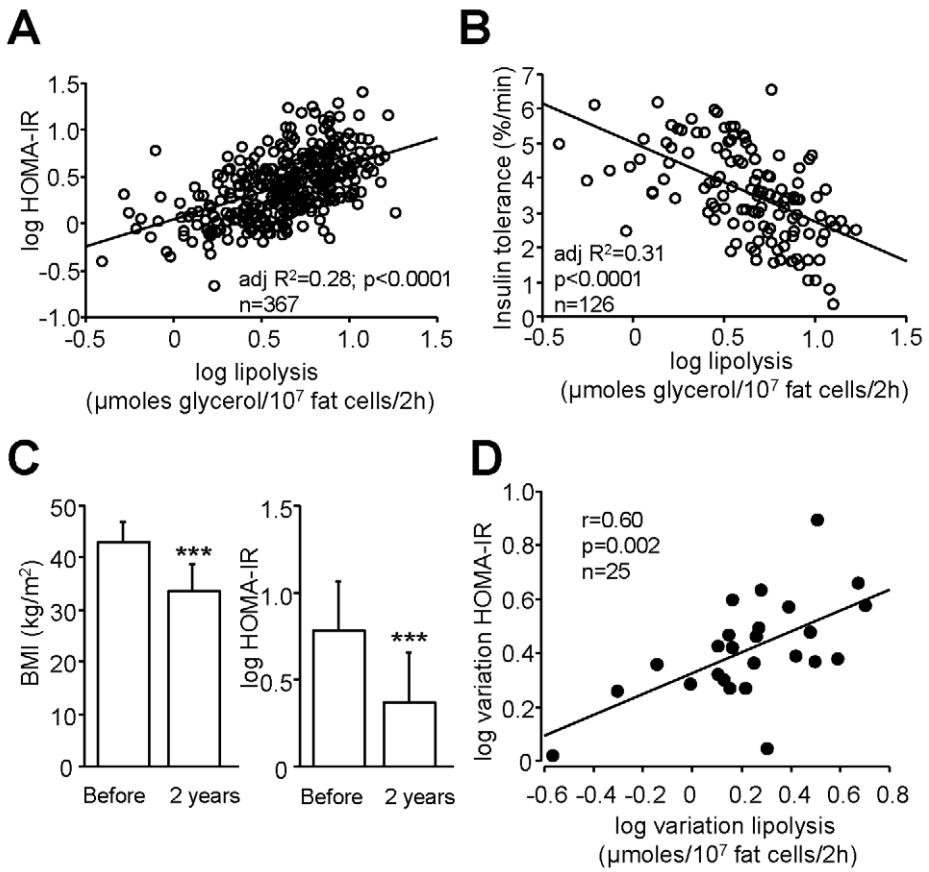

Figure 1. Relationship between WAT lipolytic capacities and insulin sensitivity in human subjects. (A) Simple linear regression between lipolysis and HOMA-IR ($n = 367$). (B) Simple linear regression between lipolysis and insulin tolerance ($n = 126$). (C) BMI and HOMA-IR before and 2 y after bariatric surgery ($n = 25$). (D) Correlation between variations in lipolysis and changes in HOMA-IR following bariatric surgery ($n = 25$).
doi:10.1371/journal.pbio.1001485.g001

HSL Haploinsufficient Mice Show Reduced Lipolytic Capacities without Alteration of Fat Mass and Adipose Tissue Inflammation

In search for an animal model with diminished WAT lipolysis and no marked alterations of WAT development, $HSL^{+/-}$ mice were generated by mating WT and $HSL^{-/-}$ mice. HSL (lipe) mRNA expression was 50% lower in epididymal WAT of $HSL^{+/-}$ mice compared to WT mice fed chow and HFD (Figure S1A and Figure 2A, respectively). A similar difference between genotypes was obtained in subcutaneous WAT (unpublished data). mRNA expression of ATGL (pnpla2), its co-activator CGI-58 (abhd5), and perilipin 1 (plin1) was similar in WT and $HSL^{+/-}$ mice, suggesting that no compensatory mechanism occurred as a result of the reduction in HSL expression (Figure 2A and Figure S1A). HSL protein expression was also reduced by 50% in $HSL^{+/-}$ compared to WT mice and undetectable in $HSL^{-/-}$ mice (Figure 2B), whereas ATGL protein expression was not significantly altered in $HSL^{+/-}$ mice (Figure 2C). In vitro total hydrolase activities against cholesterol ester (Figure 2D and Figure S1B) and TG (Figure 2E and Figure S1C) were reduced in WAT of $HSL^{+/-}$ mice, indicating that reduced expression of HSL had the expected impact on cognate enzymatic activities. HSL-specific TG hydrolase activity (expressed as total activity minus activity in the presence of the HSL inhibitor) was significantly decreased in $HSL^{+/-}$ compared to WT mouse WAT (1.45 ± 0.11 versus 2.61 ± 0.52 nmol/min.mg prot, $p < 0.05$, respectively). ATGL activity determined in the presence of the HSL inhibitor was not affected (Figure 2E). In HFD-fed mice, consistent with reduced expression and activity of HSL in WAT, adipocytes had reduced in vitro lipolytic response to isoproterenol stimulation (Figure 2F). In addition, in vivo β-adrenergic-stimulated lipolysis was also significantly reduced in $HSL^{+/-}$ mice (Figure 2G). Therefore, decreased expression of HSL alters lipolytic function at a cellular as well as at a organism level.

On chow diet, the evolution of body weight (Figure S1D) and fat mass (Figure S1E) were similar in WT and $HSL^{+/-}$ mice. The consequences of diminished HSL function were then investigated in mice fed HFD. As previously reported, $HSL^{-/-}$ mice were paradoxically resistant to diet-induced obesity [13]. WT and $HSL^{+/-}$ mice gained weight at a comparable rate and both became obese (Figure 3A). After 12 weeks of HFD, WT and $HSL^{+/-}$ presented similar fat mass, while fat mass of $HSL^{-/-}$ mice was markedly lower (Figure 3B). Fat pad weights were similar between WT and $HSL^{+/-}$ mice (Figure 3C). Accordingly, plasma levels of leptin were identical in the two genotypes (Table 1). No difference in fat cell morphology was observed by histochemistry (Figure 3D). Mean adipocyte diameter was not modified in $HSL^{+/-}$ mice compared to WT mice (Figure 3E). Differentiation of WAT-derived progenitor cells into adipocytes was similar in WT and $HSL^{+/-}$ mice but markedly reduced in $HSL^{-/-}$ mice (Figure 3F). Profound alterations in WAT gene expression involving PPARγ targets, FA synthesis and esterification, and

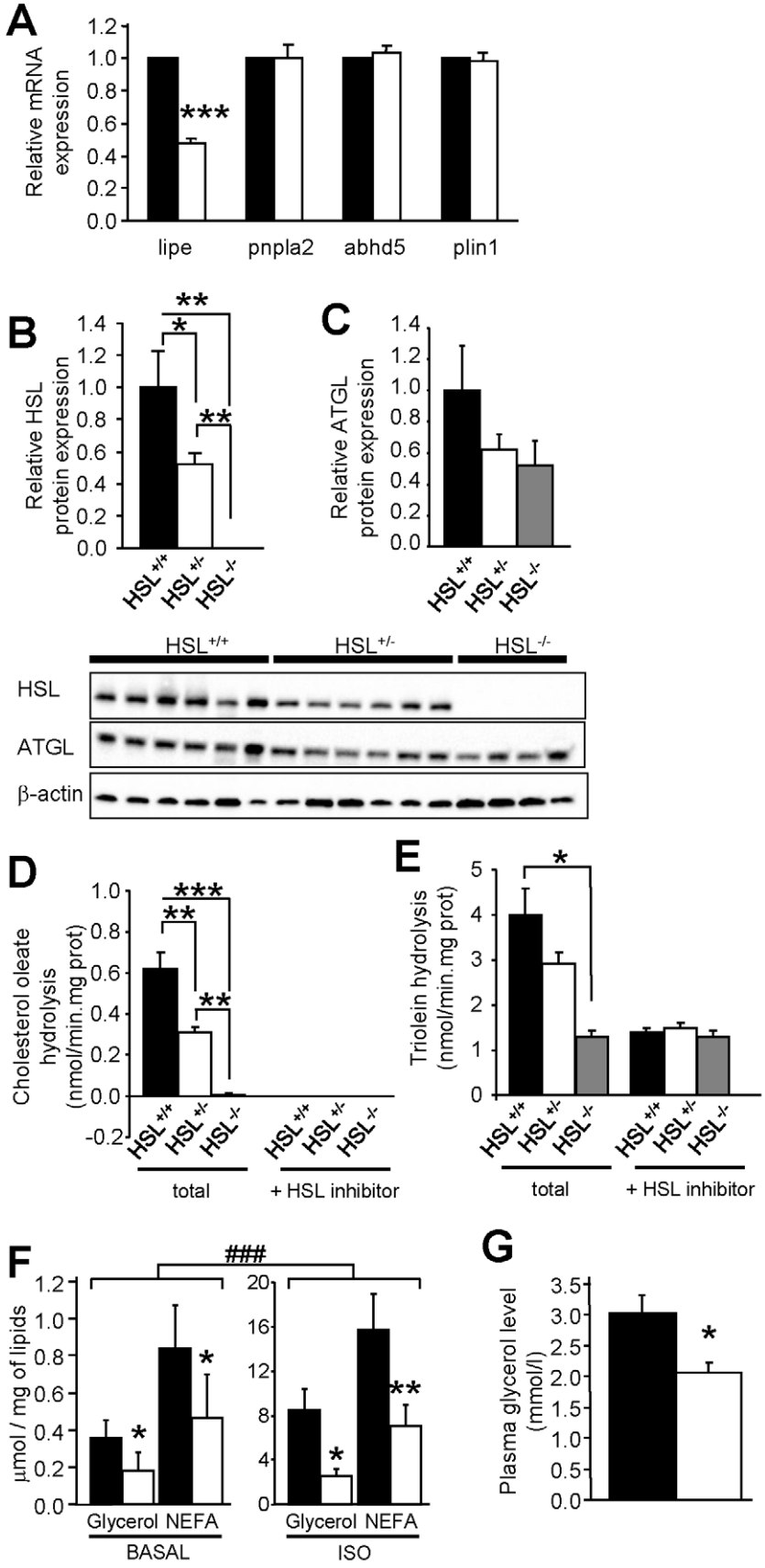
A
Relative mRNA expression
1.2
1.0
0.8
0.6
0.4
0.2
0.0
***
lipe
pnpla2
abhd5
plin1
B
Relative HSL protein expression
1.4
1.2
1.0
0.8
0.6
0.4
0.2
0.0
**
*
**
HSL+/+
HSL+/-
HSL-/-
C
Relative ATGL protein expression
1.4
1.2
1.0
0.8
0.6
0.4
0.2
0.0
HSL+/+
HSL+/-
HSL-/-
HSL+/+
HSL+/-
HSL-/-
HSL
ATGL
β-actin
D
Cholesterol oleate hydrolysis (nmol/min.mg prot)
1.0
0.8
0.6
0.4
0.2
0.0
-0.2
***
**
**
HSL+/+
HSL+/-
HSL-/-
HSL+/+
HSL+/-
HSL-/-
total
+ HSL inhibitor
E
Triolein hydrolysis (nmol/min.mg prot)
5
4
3
2
1
0
*
HSL+/+
HSL+/-
HSL-/-
HSL+/+
HSL+/-
HSL-/-
total
+ HSL inhibitor
F
###
µmol / mg of lipids
1.2
1.0
0.8
0.6
0.4
0.2
0.0
*
*
20
16
12
8
4
0
*
**
Glycerol NEFA
BASAL
Glycerol NEFA
ISO
G
Plasma glycerol level (mmol/l)
3.5
3.0
2.5
2.0
1.5
1.0
0.5
0.0
*

Figure 2. WAT lipases and lipolysis in HFD-fed WT, HSL$^{+/-}$, and HSL$^{-/-}$ mice. (A) mRNA expression of HSL (lipe), ATGL (pnpla2), CGI-58 (abhd5), and plin1 in epididymal WAT. (B–C) Western blot analysis of HSL (B) and ATGL (C) protein expression. (D–E) In vitro hydrolase activities against cholesterol ester (D) and TG (E) analogs in the absence and presence of HSL specific inhibitor. (F) In vitro basal and isoproterenol-stimulated (ISO) lipolysis in isolated adipocytes. (G) In vivo lipolysis expressed as fold increase over saline. Plasma glycerol levels were measured 15 min after saline or isoproterenol injection. Values are means ± SEM. WT mice (black bars) ($n = 6$–8); HSL$^{+/-}$ mice (white bars) ($n = 6$–9); HSL$^{-/-}$ mice (gray bars) ($n = 4$). * $p<0.05$, ** $p<0.01$, *** $p<0.001$ versus WT mice; ### $p<0.001$ versus basal condition.
doi:10.1371/journal.pbio.1001485.g002

retinoid and oxidative metabolisms have been reported in HSL null mice [13–16]. No alteration was observed in HSL$^{+/-}$ mice (Figure S2). There was no difference in WAT TG, DG, cholesterol ester, or free cholesterol contents between HSL$^{+/-}$ and WT mice (Figure 3G). The assessment of energy balance showed similar food intake and energy expenditure in HSL$^{+/-}$ and WT mice (Figure 3H and Figure 3I). Therefore, the data show that decreased expression of HSL, unlike complete lack of the enzyme, neither influences adipocyte differentiation and fat mass nor alters energy imbalance during diet-induced obesity.

Since FA released from adipocytes may modulate WAT inflammation [8,17], we investigated WAT macrophages and inflammatory molecules. The number of macrophages in the stroma-vascular fraction of WAT did not differ between HSL$^{+/-}$ and WT mice fed a HFD (Figure 4A). Accordingly, mRNA levels of macrophage markers were not different (Figure 4B). Gene expression of inflammatory markers was similar in WAT from HSL$^{+/-}$ and WT mice (Figure 4C). Therefore, the decreased lipolytic capacity of HSL$^{+/-}$ mice does not induce a decrease in WAT inflammation.

Modification of Fatty Acid Fluxes in HSL Haploinsufficient Mice

The decreased expression of HSL did not affect fasting plasma parameters (Table 1). NEFA, glycerol, TG, and total cholesterol levels were similar in both genotypes. As no noticeable alteration of metabolic parameters was observed in steady-state measurements, we determined FA fluxes in HFD-fed mice by stable perfusion of radiolabelled palmitate. Global tracer clearance that represents exit of the radioactive tracer from the blood compartment (FA disappearance) is an index of the combined ability of the tissues to take up FAs [18]. Clearance was markedly decreased in HSL$^{+/-}$ mice, indicating that partial HSL depletion has reduced peripheral FA uptake (Figure 5A, left panel). The data suggest that the decreased rate of appearance of FAs in the blood due to decreased WAT lipolysis is, in a steady-state situation with constant plasma NEFA levels, matched by a similar rate of disappearance of FAs (i.e., decreased FA clearance). Global FA oxidation represented by radioactive water measured in plasma was reduced (Figure 5A, right panel). Total radioactive FA storage, deduced from these measurements, was markedly decreased in HSL$^{+/-}$ mice (Figure 5A, right panel). Global FA turnover estimated through the evolution of plasma radioactive palmitate isotopic dilution (which is influenced by the clearance and dilution by cold and radioactive FA released from WAT in the fasted state) was in turn reduced in HSL$^{+/-}$ mice compared to WT mice (Figure 5A, right panel). Therefore, since the mice have been studied in steady-state condition, this suggests that the production rate (WAT lipolysis in accordance with direct measurements shown on Figure 2F, Figure 2G, and liver TG production) was lower as well. Tissue-specific radioactive FA incorporation into the TG pool was evaluated and showed reduction in WAT, heart, and *soleus* muscle of HSL$^{+/-}$ mice (Figure 5B), further supporting the presumed decrease in peripheral FA uptake. Total TG content was not affected in WAT of HSL$^{+/-}$ mice, whereas it was decreased in *soleus* muscle, heart, and liver (Figure 5C). Hence, the decreased lipolytic capacity in WAT induced by partial HSL deficiency provokes a diminution in FA uptake and storage in peripheral tissues. These changes take place without influencing total WAT mass.

Genetic and Pharmacological Inhibition of HSL Improves Insulin Tolerance and Glucose Metabolism

As a negative association was observed in humans between WAT lipolysis and insulin sensitivity (Figure 1), we next investigated peripheral insulin tolerance in HSL$^{+/-}$ mice. Insulin and glucose tolerance tests performed repeatedly on HFD-fed mice revealed that partial HSL depletion improved insulin and glucose tolerance in vivo with no difference in body weight between genotypes (Figure 6A and Figure 6B). However, a gain in peripheral insulin sensitivity could not be observed during hyperinsulinemic euglycemic clamp at 6 mU kg^{-1} min^{-1} of insulin (unpublished data). During clamp studies, insulin is infused at a constant rate to reach a steady state in which WAT lipolysis, which is highly sensitive to the antilipolytic action of the hormone, is strongly suppressed. Indeed, plasma NEFA levels measured during the clamp represented less than one third of fasting levels and were identical in HSL$^{+/-}$ and WT mice (unpublished data). This chronic suppression may explain the lack of differences between genotypes during the clamp studies. Time course insulin tolerance tests first performed on animals fed a chow diet and then challenged after 6 wk of HFD confirmed the protective effect of HSL haploinsufficiency (Figure 6C) and indicated that the relationship between high lipolysis and insulin resistance exists across the spectrum of fat mass in agreement with human data when various ranges of body mass index are considered as reported above. To confirm that HSL haploinsufficiency protects against the development of insulin resistance, WT and HSL$^{+/-}$ mice were fed a high fructose diet known to appreciably alter insulin sensitivity (Figure S3). Insulin tolerance tests performed after 45 wk of diet showed that HSL$^{+/-}$ mice remained more insulin tolerant than WT mice (Figure 6D), supporting the data obtained previously with the fat-enriched diet.

In a therapeutic perspective, we tested the effect of pharmacological inhibition of HSL on insulin tolerance. Twelve-week HFD-fed mice were treated *per os* with a specific HSL inhibitor or vehicle for 7 d [11,19]. HSL inhibitor-treated animals showed an improvement of insulin sensitivity as shown by QUICKI (Table 1) and of insulin tolerance (Figure 6E) compared to vehicle-treated mice without an effect on body weight and fat mass (Figure 6F). Similar data were obtained on another genetic background (Figure 6G). Treatment with the HSL inhibitor was also performed for 2 wk in 6-wk-old Lepr^{db}/Lepr^{db} mice that carry homozygous mutation of the leptin receptor and are genetically prone to obesity and diabetes. The treatment induced no change in body weight. Glycemia was comparable between HSL inhibitor- and vehicle-treated animals at different time points during glucose tolerance test (Figure 6H). However, plasma insulin level at 15 min was lower in mice treated with the HSL inhibitor, indicating a better control of glycemia by insulin when HSL is inhibited (Figure 6I). Similarly to partial genetic HSL depletion, pharmacological HSL inhibition protects mice from insulin and glucose intolerance.

Molecular Mechanisms Underlying Improvement of Insulin Sensitivity in Mice with Partial Inhibition of HSL

The improvement of insulin sensitivity in HFD-fed HSL$^{+/-}$ and HSL inhibitor-treated mice could result from changes in levels of adipokines with action on insulin signalling. Adiponectin plasma levels were not different from control animals in mice with partial

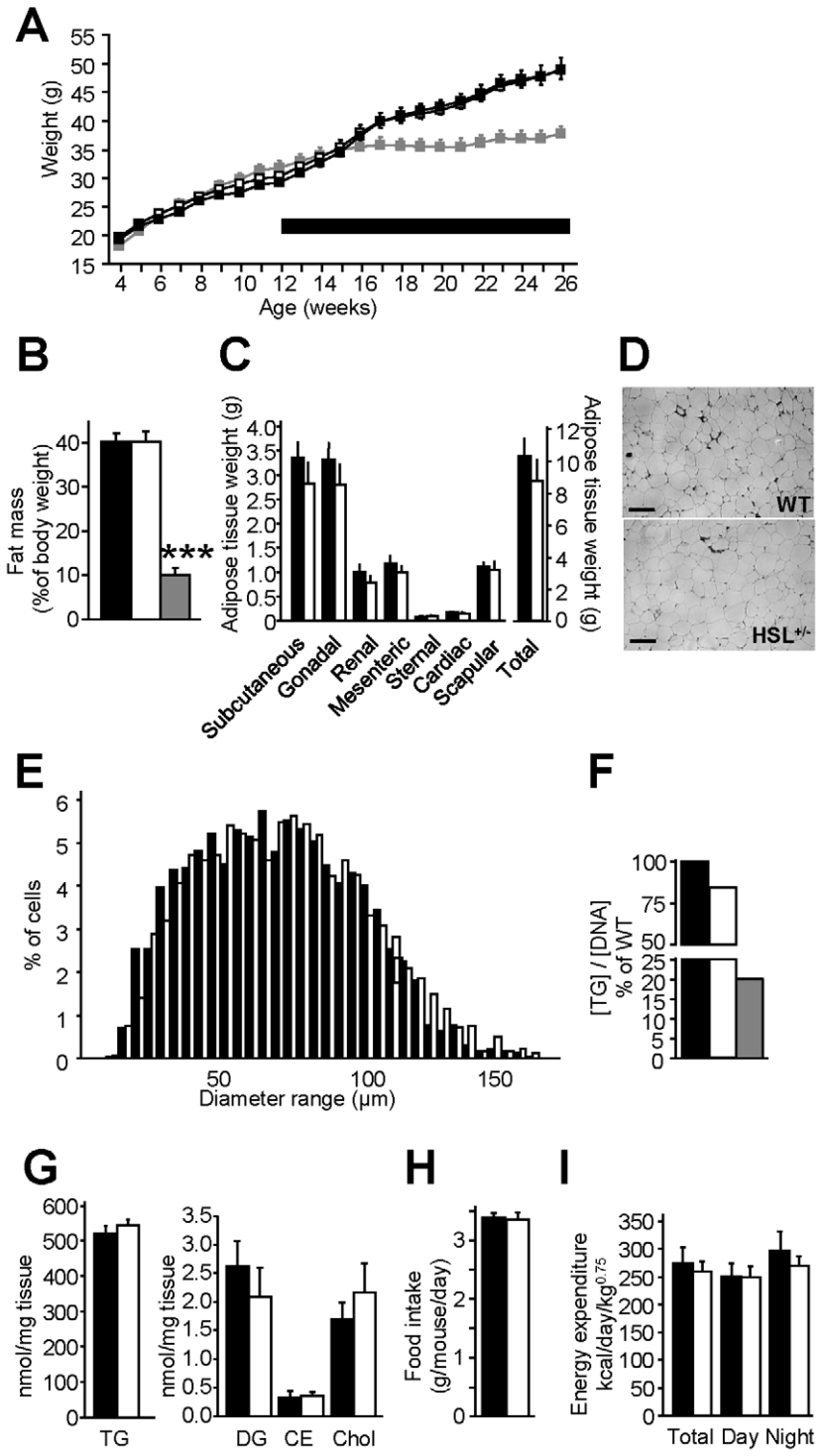

Figure 3. Energy balance of HFD-fed HSL$^{+/-}$ and WT mice. Mice were first provided *ad libitum* access to a standard diet for 8 wk after weaning. Then they received a HFD shown as a thick line for 12 to 16 wk. (A) Body weight curves. (B) Fat mass. (C) Fat pad weight. (D) WAT morphology. Scale bar, 100 µm. (E) Frequency of adipocyte diameter observed on histological preparation of WAT. (F) In vitro adipogenesis of progenitor cells from the subcutaneous WAT stromavascular fraction. Values show results of WAT pools from 2–3 mice. (G) WAT neutral lipids. CE, cholesterol ester; chol, free cholesterol; DG, diacylglycerol; TG, triacylglycerol. (H) Food intake. (I) Energy expenditure assessed by indirect calorimetry. Values are means ± SEM. WT mice (black bars) ($n = 5$–10), HSL$^{+/-}$ mice (white bars) ($n = 5$–10), and HSL$^{-/-}$ mice (gray bars) ($n = 4$). *** $p<0.001$ versus WT mice.
doi:10.1371/journal.pbio.1001485.g003

genetic or pharmacologic inhibition of HSL (Table 1). Similarly, plasma concentrations of retinol binding protein 4 (RBP4), an adipokine involved in the development of insulin resistance [20], were not modified in HSL$^{+/-}$ and HSL inhibitor-treated mice compared to control mice. To shed light on the origin of the global improvement in insulin tolerance in HSL$^{+/-}$ mice, in vivo insulin-

Table 1. Fasting plasma parameters in 12-wk wild type (WT) and $HSL^{+/-}$ HFD-fed mice and in 12-wk wild type HFD-fed mice treated with vehicle or HSL specific inhibitor (HSLi) for 7 consecutive days.

	WT	$HSL^{+/-}$	*p*	Vehicle	HSLi	*p*
Glucose (g/l)	1.54±0.11	1.46±0.07	*ns*	1.22±0.05	1.05±0.07	*ns*
Insulin (µg/l)	1.43±0.17	1.18±0.22	*ns*	1.46±0.39	0.88±0.43	*ns*
QUICKI	0.270±0.007	0.280±0.007	*ns*	0.286±0.011	0.376±0.039	0.05
NEFA (mmol/l)	1.02±0.02	0.98±0.10	*ns*	0.88±0.04	0.81±0.05	*ns*
Glycerol (mmol/l)	0.87±0.09	0.88±0.08	ns	0.55±0.06	0.34±0.07	*ns*
Triacylglycerol (mmol/l)	1.43±0.09	1.26±0.10	*ns*	1.63±0.11	1.54±0.10	*ns*
Total cholesterol (mmol/l)	3.07±0.25	3.02±0.24	*ns*	3.33±0.09	3.51±0.09	*ns*
Adiponectin (µg/ml)	5.62±0.20	5.75±0.20	*ns*	6.86±0.53	6.06±0.47	*ns*
Leptin (ng/ml)	28.0±0.9	28.3±0.9	*ns*	17.9±2.5	14.7±2.1	*ns*
RBP4 (µg/ml)	18.0±0.7	18.1±0.6	*ns*	15.2±0.7	15.4±1.0	*ns*

Values ($n = 6$–17) are means ± SEM. NEFA, nonesterified fatty acid; QUICKI, quantitative insulin sensitivity check index; RBP4, retinol binding protein 4.
doi:10.1371/journal.pbio.1001485.t001

stimulated glucose uptake was determined in various tissues. Glucose uptake was increased in *soleus* (oxidative) muscle and showed a tendency to increase in *biceps femoris* (glycolytic) muscle (Figure 7A). An increase in glucose uptake was also observed in WAT. Furthermore, glucose oxidation measured ex vivo in *soleus* muscle was increased (Figure 7B). There were no differences in DG and glycogen contents between $HSL^{+/-}$ and WT skeletal muscle (unpublished data). Interestingly, respiratory quotient was increased in $HSL^{+/-}$ mice showing a shift from FA to glucose as energy substrate (Figure 7C). To determine whether liver was involved in the improvement of glucose and insulin tolerance in $HSL^{+/-}$ mice, we administered a bolus of insulin and measured

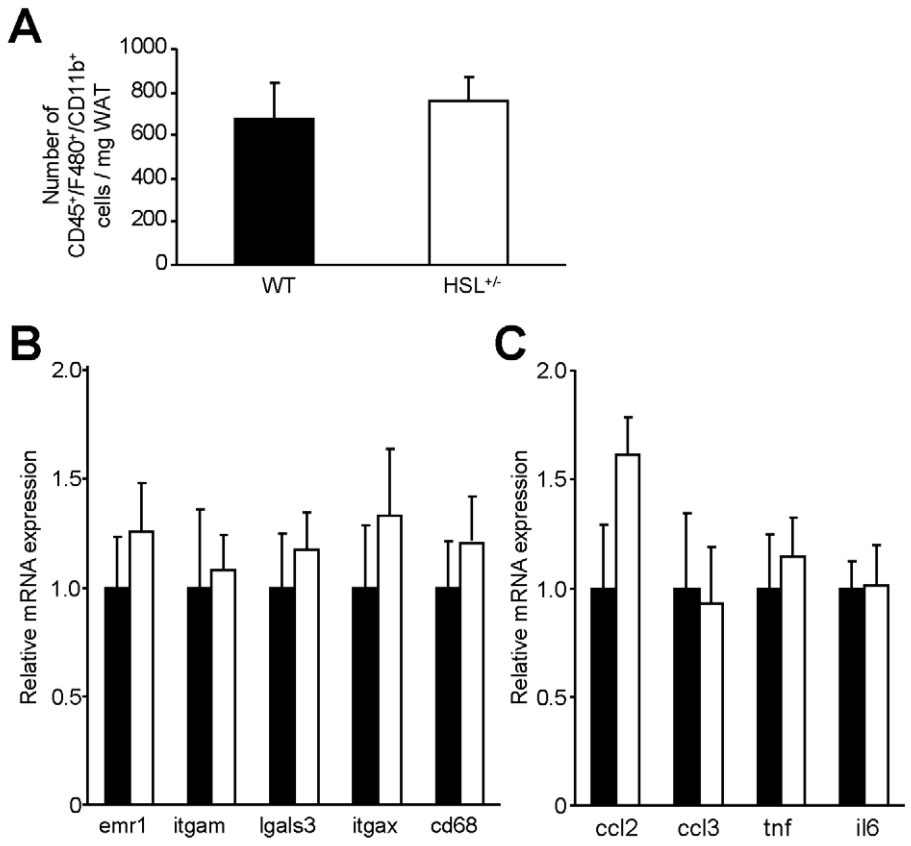

Figure 4. WAT inflammation in 12-wk HFD-fed $HSL^{+/-}$ and WT mice. (A) Macrophage (CD45/F480/CD11b triple positive cells) number per milligram of WAT assessed by flow cytometry. (B) mRNA expression of WAT macrophage surface markers. (C) mRNA expression of WAT inflammatory markers. Values are means ± SEM. WT mice (■) ($n = 7$) and $HSL^{+/-}$ mice (□) ($n = 8$).
doi:10.1371/journal.pbio.1001485.g004

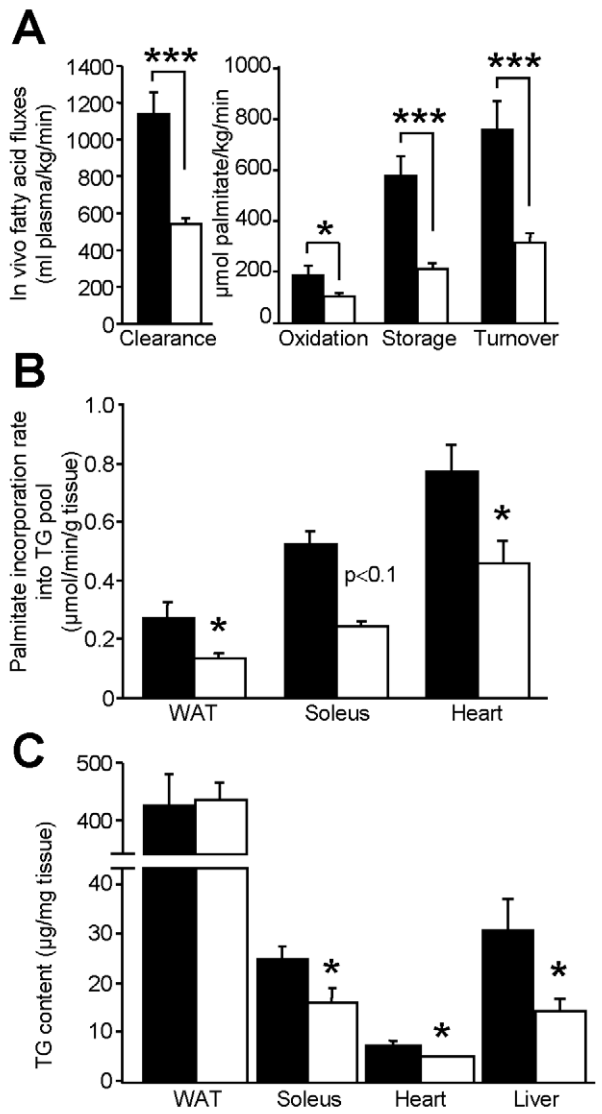

Figure 5. In vivo fatty acid fluxes in HFD-fed HSL$^{+/-}$ and WT mice. (A) Plasma parameters of fatty acid fluxes. (B) Rate of radiolabelled fatty acid incorporation in the TG pool of tissues. (C) Total TG content in tissues. Values are means ± SEM. WT mice (■) ($n=5$) and HSL$^{+/-}$ mice (□) ($n=6$). * $p<0.05$, *** $p<0.001$ versus WT mice.
doi:10.1371/journal.pbio.1001485.g005

the effects on the hepatic insulin signalling pathway. In agreement with an improved insulin tolerance, the decrease of glycemia was greater in HSL$^{+/-}$ mice than in WT mice (Figure 7D). In response to exogenous insulin administration, levels of phosphorylated insulin receptor substrate 1 and Akt were increased in the liver of HSL$^{+/-}$ mice supporting an improvement of insulin signalling (Figure 7E). HSL$^{+/-}$ mice infused with radiolabelled glucose showed a rise in glucose carbon incorporation into hepatic lipids—that is, de novo lipogenesis—compared to WT mice (Figure 7F). Pyruvate tolerance test revealed that gluconeogenesis was reduced in HSL$^{+/-}$ mice (Figure 7G). The reduced hepatic glucose production was associated with decreased glucose storage as demonstrated by reduced glycogen content in HSL$^{+/-}$ mice (Figure 7H). Liver DG content was unchanged in HSL$^{+/-}$ mice (unpublished data). As changes in the capacity of the pancreas to produce insulin could modify glucose tolerance, we then investigated pancreatic function in vivo and in vitro. Neither arginine tolerance test performed on 12-wk HFD-fed animals (Figure S4A) nor in vitro glucose-stimulated insulin secretion of isolated pancreatic islets (Figure S4B) revealed changes in insulin secretion in HSL$^{+/-}$ compared to WT mice, arguing against a direct effect of HSL haploinsufficiency on the capacity of pancreatic β cells to secrete insulin. Altogether, adaptations in WAT, skeletal muscle, and liver explain the global improvement in glucose and insulin tolerance observed in mice with HSL haploinsufficiency.

HSL Gene Silencing in Vitro and Partial Inhibition of Lipolysis In Vivo Affects Nutrient Partitioning and Promotes De Novo Lipogenesis in Human Adipocytes

In order to determine whether modifications of fat cell metabolism observed in vivo in HSL$^{+/-}$ mice were cell autonomous, expression of HSL was knocked down in human hMADS adipocytes. Adipocytes transfected by HSL siRNA showed a 70% reduction in LIPE mRNA expression compared to GFP siRNA transfected cells (Figure 8A, upper panel). HSL protein expression was also reduced in HSL-silenced adipocytes (Figure 8A, lower panel). As observed at the whole body level in HSL$^{+/-}$ mice (Figure 5A), HSL gene silencing resulted in a decrease of FA oxidation in human adipocytes (Figure 8B). HSL gene silencing also led to an increase in insulin-stimulated glucose uptake (Figure 8C) as shown in vivo in HSL$^{+/-}$ mouse WAT (Figure 7A), accompanied by a rise in insulin-stimulated glucose oxidation (Figure 8D). The enhanced influx of glucose was associated with an increase in glyceroneogenesis and de novo lipogenesis in adipocytes knocked down for HSL (Figure 8E and Figure 8F). Expression of the glucose transporter GLUT4 and of glycolytic and fatty acid synthesis genes showed coordinated up-regulation in HSL-silenced adipocytes (Figure 9A and Figure 9B). RBP4 mRNA (1.4-±0.2-fold siHSL/siGFP, $n=9$, $p<0.05$) and secreted protein levels (1.2-±1.0-fold siHSL/siGFP, $n=11$, $p<0.001$) were slightly but significantly increased in hMADS adipocytes transfected with HSL siRNA (Figure S5). This piece of data does not support a role of this adipokine in the improvement of insulin action and glucose metabolism when HSL expression is lowered. As glucose uptake and fatty acid synthesis were upregulated in vitro in human adipocytes with low HSL level, we investigated correlations between lipolysis and expression of key genes of these pathways in vivo in human WAT. Simple regression analysis showed negative associations between GLUT4, fatty acid synthase or the lipogenic transcription factor ChREBP mRNA levels, and WAT lipolytic rates (Figure 9C). The negative associations persisted in multiple linear regression analyses with BMI as the covariate (partial $R=0.3$, $p<0.05$). No association was found between mRNA level of SREBP1c, another transcription factor controlling expression of FA synthesis genes, and lipolysis ($p=0.96$). As further proof supporting the link between human fat cell lipolysis and fat cell de novo lipogenesis, 8-wk treatment of obese male individuals with nicotinic acid, which inhibits lipolysis through activation of a fat cell Gi protein-coupled receptor [1], resulted in up-regulation of adipocyte de novo lipogenesis gene expression (Figure 9D).

Discussion

Insulin resistance is a critical pathogenic process linking obesity to type 2 diabetes and cardiovascular diseases. To date, there is convincing evidence in humans that FAs cause deleterious effects on insulin signalling in peripheral organs [21]. The working

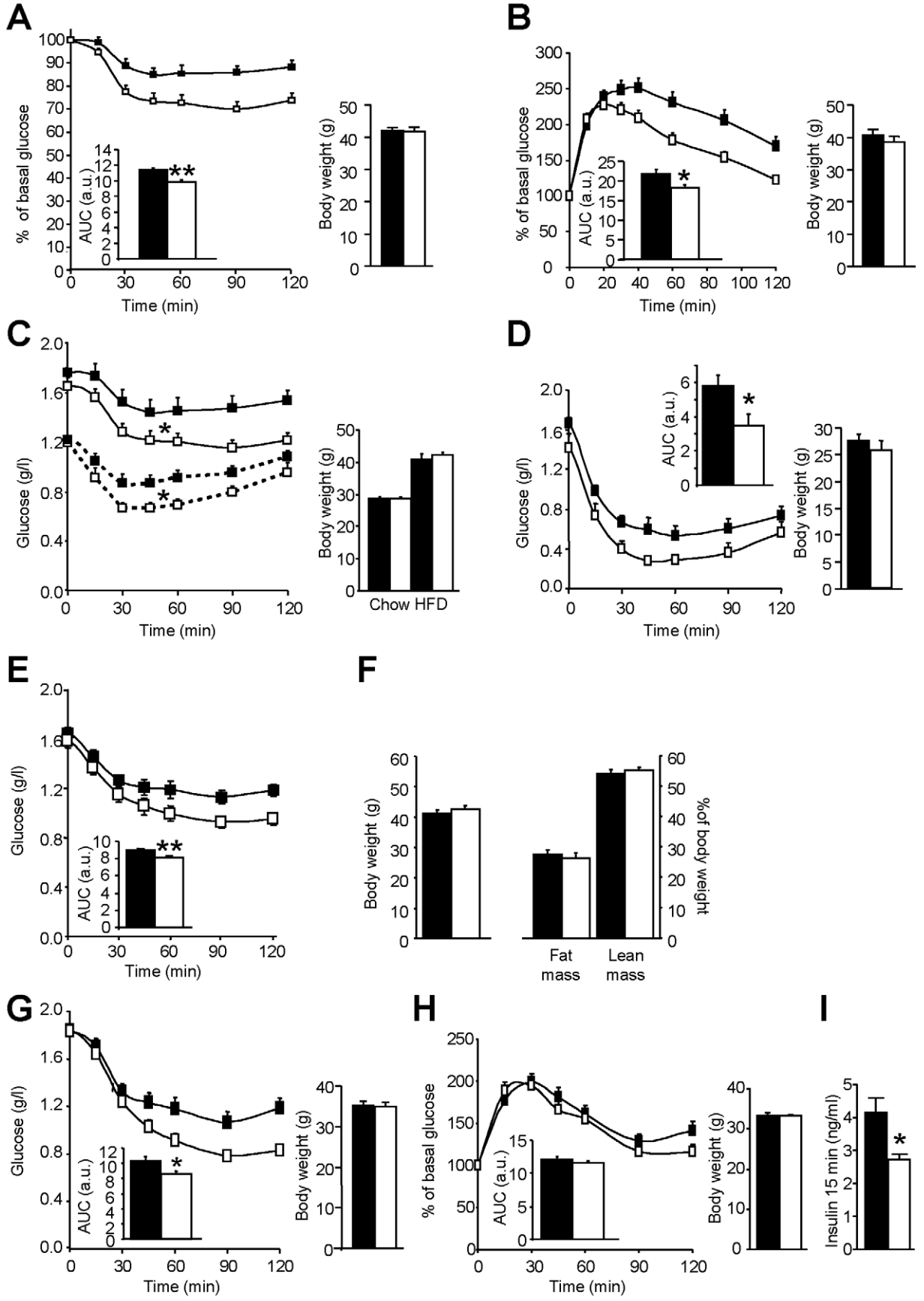
A
% of basal glucose
Time (min)
AUC (a.u.)
**
Body weight (g)
B
% of basal glucose
Time (min)
AUC (a.u.)
*
Body weight (g)
C
Glucose (g/l)
Time (min)
*
*
Body weight (g)
Chow HFD
D
Glucose (g/l)
Time (min)
AUC (a.u.)
*
Body weight (g)
E
Glucose (g/l)
Time (min)
AUC (a.u.)
**
F
Body weight (g)
%of body weight
Fat mass
Lean mass
G
Glucose (g/l)
Time (min)
AUC (a.u.)
*
Body weight (g)
H
% of basal glucose
Time (min)
AUC (a.u.)
Body weight (g)
I
Insulin 15 min (ng/ml)
*

Figure 6. Insulin and glucose tolerance in mice with diminished HSL activity. (A) Insulin tolerance test performed on wild type and $HSL^{+/-}$ mice fed a HFD for 12 wk. (B) Glucose tolerance test performed on wild type and $HSL^{+/-}$ mice fed a HFD for 12 wk. (C) Insulin tolerance test performed on the same animals fed first a chow diet for 6 wk (dotted curve) and then a HFD for 6 wk (solid curve). (D) Insulin tolerance test performed on wild type and $HSL^{+/-}$ mice fed a diet enriched in fructose for 45 wk after weaning. (E–F) Insulin tolerance test (E) and body weight and body composition (F) in 12-wk HFD-fed B6D2 mice treated with a specific HSL inhibitor for 7 d. (G) Insulin tolerance test in 7-wk HFD-C3H/HeJ mice treated with a specific HSL inhibitor for 7 d. (H–I) Glucose tolerance test (H) and plasma insulin at 15 min (I) in $LepR^{db}/LepR^{db}$ mice treated with a specific HSL inhibitor for 13 d. AUC, area-under-curve expressed as arbitrary units (a.u.). Body weights at the time of the tolerance tests are shown. Values are means ± SEM. WT mice (■) ($n = 6$–10) and $HSL^{+/-}$ mice (□) ($n = 8$–10). B6D2 (■) and HSL inhibitor-treated B6D2 (□) mice ($n = 10$). C3H/HeJ (■) and HSL inhibitor-treated C3H/HeJ (□) mice ($n = 8$–10). Vehicle- (■) and HSL inhibitor-treated $LepR^{db}/LepR^{db}$ (□) mice ($n = 12$). * $p<0.05$, ** $p<0.01$ versus control mice.
doi:10.1371/journal.pbio.1001485.g006

models are based on overload of lipids from exogenous sources—that is, dietary FA for HFD or FA produced by lipoprotein lipase-mediated hydrolysis of TG during lipid and heparin infusion [7,22]. However, little is known on the effect of FAs released by WAT lipolysis on the modulation of fat mass and insulin sensitivity. The physiological significance of lipolysis may be seen in two, not necessarily mutually exclusive, ways. Impaired lipolytic capacity could contribute to the development of obesity through impairment in the mobilization of fat stores. Alternatively, the defect may protect against excessive FA release and ensuing deleterious action of FAs on insulin sensitivity. To address this clinically relevant question, we used a translational approach combining human and animal studies together with cellular investigations. As we previously showed that the level of HSL expression controls lipolytic rate in human fat cells and is altered in obesity [10–12], the association between WAT lipolysis, fat mass, and insulin sensitivity was investigated in mice with HSL haploinsufficiency. To address this relationship, lipase total knockout mouse models may not prove suitable. HSL null mice show impaired development of WAT when fed a HFD and marked WAT inflammation in the absence of obesity [13,23]. Metabolic defects are observed in multiple organs of ATGL global knockout mice, causing a complex modulation of insulin sensitivity [9,24–26]. WAT-specific ablation of ATGL shows markedly altered thermogenesis [27]. Therapeutic relevance was provided by studies on mice treated with a specific HSL inhibitor. Cell-autonomous effects of HSL deficiency were investigated in hMADS adipocytes, a validated model for the study of human fat cell metabolism [2,28]. The relationship between WAT lipolysis and glucose metabolism was further explored in four independent cohorts of individuals with a wide range of BMI. The results are summarized on Figure 10.

Phenotyping obese mice with reduced HSL activity in WAT first revealed that a partial defect in lipolysis did not modify adiposity and, hence, that chronic inhibition of FA release from WAT did not contribute to the development of obesity. Strikingly, complete HSL deficiency leads to resistance to HFD-induced obesity [13] and impaired adipogenesis (present work). However, the increase in body fat mass, weights of fat depots, and adipocyte size was not compromised in $HSL^{+/-}$ mice fed HFD. It may be hypothesized that the presence of an active allele is sufficient to compensate for the defect in adipogenesis, which has been linked to an impaired production of signalling lipolytic by-products [16,29]. The identical fat mass in $HSL^{+/-}$ and WT mice was supported by similar food intake, energy expenditure, and leptin levels in the two genotypes. The normal development of WAT in a condition of diminished adipose lipolysis raised questions on the dynamics of lipid fluxes. Using a fluxomics approach [18], we show that $HSL^{+/-}$ mice presented altered global FA turnover, decreased WAT lipolysis being balanced by reduced FA esterification in WAT. Accordingly, we have previously reported a coupling between FA release and re-esterification in vitro in human adipocytes [2]. The decreased FA oxidation observed in human adipocytes with altered lipolytic capacity may result from decreased FA availability. In heart and brown adipose tissue, it has been postulated that FA need to be esterified into TG and then mobilized for being properly oxidized in mitochondria [30,31]. Moreover, enhanced de novo lipogenesis in adipocytes knocked down for HSL results in an increase of the levels of malonyl-CoA, which inhibits the rate-limiting step in FA oxidation, carnitine palmitoyl transferase 1b [32]. Therefore, partial inhibition of WAT lipolysis results in a modification of FA fluxes in vivo and in fat cells without alteration of fat mass.

Our data in humans show, on a large number of individuals, a strong association between WAT lipolysis and indexes of insulin resistance independently of fat mass. This relation was confirmed in a longitudinal study. Two years after bariatric surgery in morbidly obese individuals, the diminution of lipolytic rate was positively correlated with the improvement of insulin sensitivity. In obese HSL haploinsufficient mice, we observed an improvement of glucose metabolism and insulin tolerance. It happens with a global slowdown of FA turnover and unchanged plasma FA levels in the overnight fasted state, a condition observed in many obese individuals [6]. Results from insulin and glucose tolerance tests were supported by organ-specific adaptations. In the liver, insulin action was improved as revealed by an increase in tyrosine phosphorylation of insulin receptor substrate 1 and serine phosphorylation of Akt. An improvement in hepatic insulin sensitivity has been reported in one model of total HSL deficiency [33]. Hepatic glucose fluxes were modified in HSL haploinsufficient mice. The decrease in glucose production, which could partially result from the reduced glycerol availability, is balanced by a decrease of glucose storage as glycogen. The shift in respiratory quotient could sign an increase in carbohydrate usage and decreased lipid utilisation but could also result from the conversion of carbohydrate to lipid and its subsequent oxidation as this process has the same respiratory quotient as direct oxidation of carbohydrates. Accordingly, *soleus* muscle glucose oxidation and hepatic de novo lipogenesis were increased in $HSL^{+/-}$ mice. In vivo insulin-stimulated glucose uptake was increased in WAT and skeletal muscles of HFD-fed $HSL^{+/-}$ mice, suggesting an improvement in peripheral insulin sensitivity. It is now well established that lipid-induced insulin resistance in skeletal muscle stems from defects in insulin-stimulated glucose transport [7]. Moreover, a better glucose uptake in fat cells may participate in the amelioration of insulin sensitivity at the whole body level. Indeed, adipocyte-specific invalidation of GLUT4 abolishes insulin-stimulated glucose uptake in WAT and impairs insulin action in liver and skeletal muscle [34]. RBP4 was described as a potential mediator of insulin resistance in these mice [20]. However, in vivo data in mice as well as in vitro data in human adipocytes show that it is unlikely that RBP4 contributes to the improvement of insulin tolerance and glucose metabolism promoted by diminished WAT lipolysis. The rise in insulin-stimulated glucose uptake was also observed in a cell-autonomous manner in human adipocytes with diminished HSL expression. It

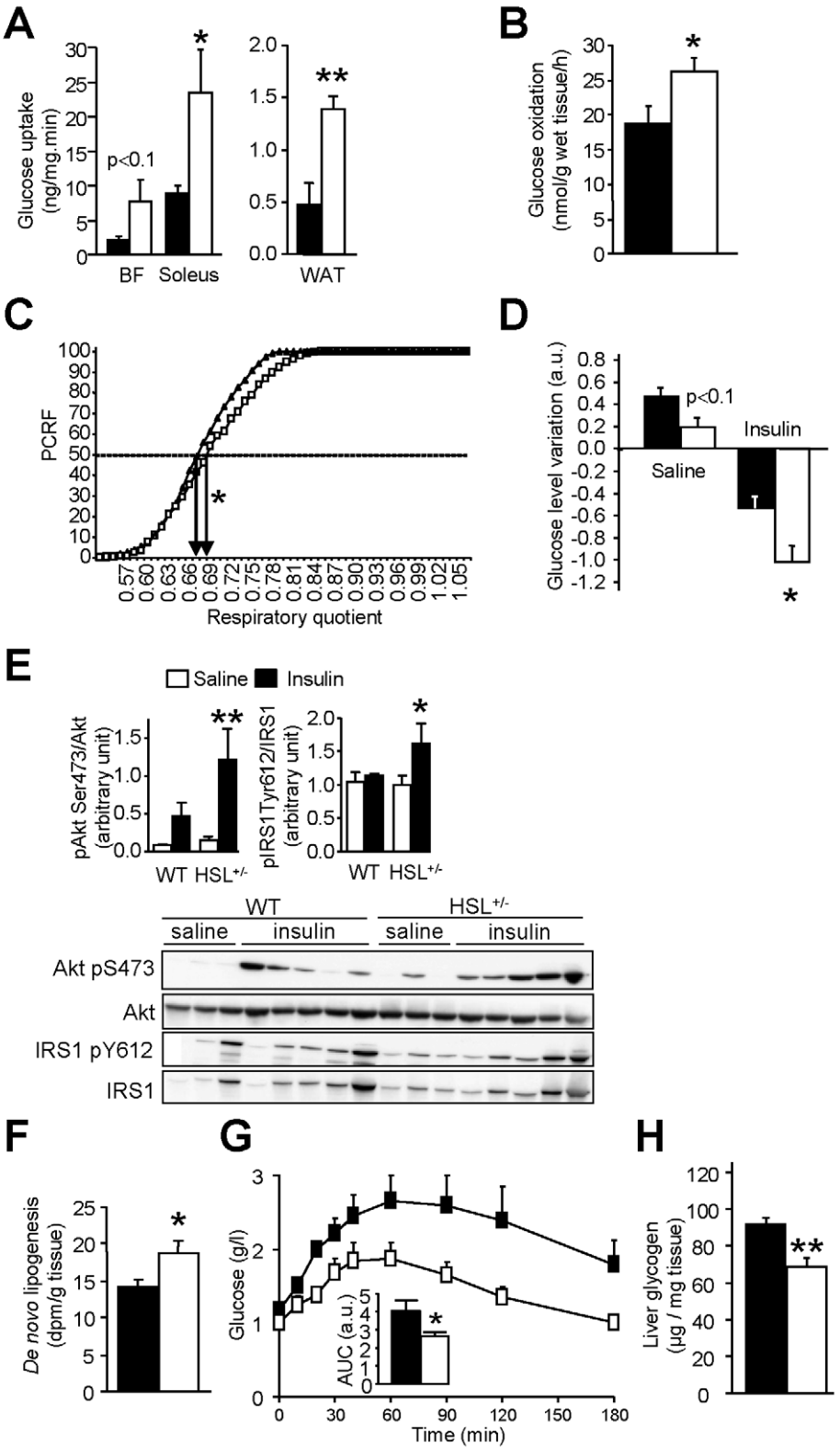

Figure 7. Glucose metabolism and insulin sensitivity in mice with reduced HSL activity. (A) In vivo 2-deoxy-D-[^{3}H] glucose uptake under stimulation by insulin in skeletal muscle (*biceps femoris*—BF—and *soleus*) and WAT. (B) Ex vivo glucose oxidation in *soleus* muscle. (C) Respiratory quotient assessed by indirect calorimetry and expressed as percentage of cumulative relative frequencies (PCRF). EC_{50} are represented by arrows. (D) In vivo insulin bolus. Variation in plasma glucose 15 min after injection of saline or insulin (a.u., arbitrary unit). (E) Effect of insulin bolus in vivo on hepatic insulin signalling. IRS1, insulin receptor substrate 1; Akt, protein kinase B. (F) Hepatic de novo lipogenesis. Measurement of radiolabelled glucose incorporation in lipid fraction of liver after insulin stimulation. (G) Pyruvate tolerance test. (H) Liver glycogen content assessed in mice starved for 24 h and then refed for 18 h. Values are means ± SEM. WT mice (■ or ▲) and $HSL^{+/-}$ mice (□) mice ($n = 4$–10 in each group). * $p<0.05$, ** $p<0.01$ versus WT mice.

doi:10.1371/journal.pbio.1001485.g007

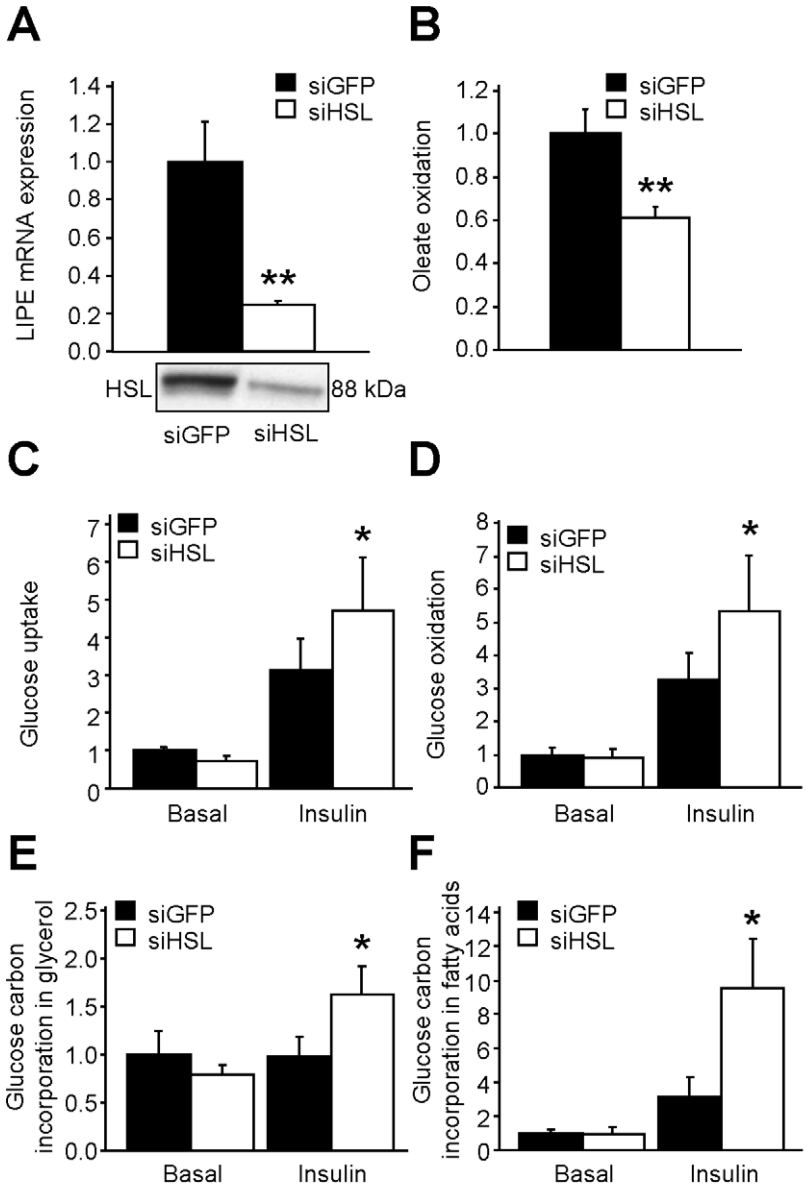

Figure 8. Fate of glucose and fatty acid in hMADS adipocytes. (A) HSL (LIPE) expression as mRNA (upper panel) and protein (lower panel). (B) Fatty acid oxidation. (C) Basal and insulin-stimulated glucose uptake. (D) Basal and insulin-stimulated glucose oxidation. (E–F) Basal and insulin-stimulated glucose carbon incorporation into glycerol (E) or fatty acid (F) of neutral lipids. hMADS adipocytes were transfected either with a siRNA against GFP (control; siGFP) or HSL (siHSL). Data are fold induction of siGFP values (means ± SEM). siGFP adipocytes (■) and siHSL adipocytes (□) ($n = 5$–10). * $p<0.05$, ** $p<0.01$ versus siGFP.
doi:10.1371/journal.pbio.1001485.g008

was accompanied by increased glucose oxidation and glucose carbon incorporation into FA and glycerol—that is, increased de novo lipogenesis and glyceroneogenesis. Glucose uptake controls adipocyte de novo lipogenesis, which has recently appeared as a major determinant of whole body insulin sensitivity [35,36]. The negative correlations between GLUT4, ChREBP, or fatty acid synthase mRNA levels and WAT lipolytic rate in vivo in humans strongly support that notion. As further proof of concept, chronic inhibition of WAT lipolysis with nicotinic acid resulted in an increase of fat cell de novo lipogenesis gene expression in obese individuals. In HFD-fed obese $HSL^{+/-}$ mice, the concomitant up-regulation of de novo lipogenesis in WAT and liver may play an important part in the favourable metabolic profile [35,37,38]. Altogether, the modifications in FA metabolism resulting in enhanced fat cell glucose uptake and de novo lipogenesis are therefore likely to contribute to the improvement of insulin sensitivity.

Increase in WAT macrophage number and expression of immune cell-derived cytokines and chemokines may contribute to obesity-induced insulin resistance [39]. As FAs released from 3T3-L1 adipocytes have been shown to stimulate pro-inflammatory cytokine production by RAW264 macrophages, it could be hypothesized that inflammation would be diminished in WAT from obese $HSL^{+/-}$ mice [8]. However, neither macrophage number nor gene expression of macrophage markers and inflammatory factors were modified, indicating that chronic

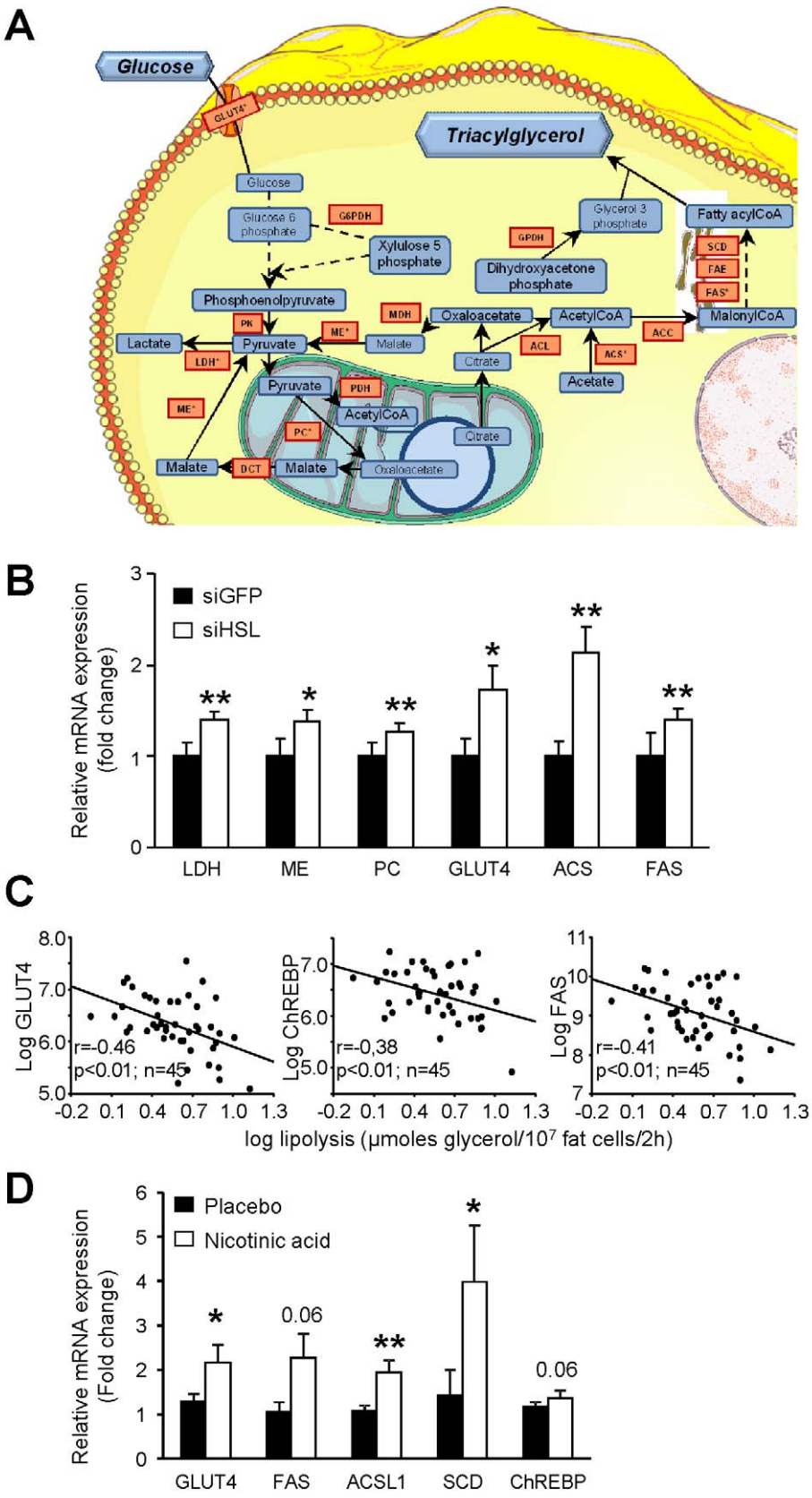
A
Glucose
GLUT4*
Triacylglycerol
Glucose
Glucose 6 phosphate
G6PDH
Xylulose 5 phosphate
Glycerol 3 phosphate
GPDH
Dihydroxyacetone phosphate
Fatty acylCoA
SCD
FAE
FAS*
Phosphoenolpyruvate
PK
MDH
Oxaloacetate
AcetylCoA
MalonylCoA
ACC
Lactate
Pyruvate
ME*
Malate
ACL
Citrate
ACS*
Acetate
LDH*
Pyruvate
PDH
ME*
AcetylCoA
PC*
Citrate
Malate
DCT
Malate
Oxaloacetate
B
siGFP
siHSL
Relative mRNA expression (fold change)
LDH
ME
PC
GLUT4
ACS
FAS
C
Log GLUT4
r=-0.46
p<0.01; n=45
Log ChREBP
r=-0,38
p<0.01; n=45
Log FAS
r=-0.41
p<0.01; n=45
log lipolysis (µmoles glycerol/10^7 fat cells/2h)
D
Placebo
Nicotinic acid
Relative mRNA expression (Fold change)
0.06
0.06
GLUT4
FAS
ACSL1
SCD
ChREBP

Figure 9. Relationship between WAT lipolysis and de novo lipogenesis. (A) Up-regulation of glucose transporter 4 and de novo lipogenesis-related pathways. Induction of gene expression (red boxes) in hMADS adipocytes with HSL gene silencing were determined by DNA microarray analysis and validated by reverse transcription-quantitative PCR (indicated by *). (B) Up-regulation of glucose transporter 4 and de novo lipogenesis-related pathway gene expression in hMADS adipocytes. mRNA levels were determined by reverse transcription-quantitative PCR ($n = 9–12$). ** $p<0.01$ versus siGFP. (C) Correlations between glucose transporter 4, carbohydrate responsive element-binding protein, and fatty acid synthase mRNA levels and, lipolysis in human WAT ($n = 45$). (D) Up-regulation of glucose transporter 4 and de novo lipogenesis-related pathway gene expression in adipocytes from obese individuals treated with placebo or nicotinic acid ($n = 12$ per group). * $p<0.05$, ** $p<0.01$ versus before treatment. ACC, acetylCoA carboxylase; ACL, ATP citrate lyase; ACS, acetyl-CoA synthase; ChREBP, carbohydrate responsive element-binding protein; DCT, dicarboxylate transporter; FAE, fatty acid elongase; FAS, fatty acid synthase; GPDH, glycerol-3-phosphate dehydrogenase; GLUT4, glucose transporter 4; G6PDH, glucose-6-phosphate dehydrogenase; LDH, lactate dehydrogenase; MDH, malate dehydrogenase; ME, malic enzyme; PC, pyruvate carboxylase; PDH, pyruvate dehydrogenase; PK, pyruvate kinase; SCD, stearoylCoA desaturase.
doi:10.1371/journal.pbio.1001485.g009

inhibition of lipolysis, unlike acute stimulation, does not modify the content of macrophages in WAT [17]. In $HSL^{+/-}$ mice, the lack of alteration in WAT inflammation is, however, in line with the lack of change in fat mass.

This work has relevance on therapeutic strategies aimed at preventing the development of obesity-associated insulin resistance. The interest in antilipolytic drugs has been shown with nicotinic acid, which has been used for decades as a lipid-lowering drug. This compound acts through a G-protein-coupled receptor with antilipolytic action in fat cells [1]. However, the receptor is expressed in other cell types than adipocytes, and nicotinic acid shows receptor-independent effects in the liver. The use of the drug has been restricted due to upper-body skin flushing. Moreover, data on insulin sensitivity are conflicting [40]. A search for alternative drugs with an antilipolytic effect has led to synthesis of several series of HSL inhibitors [41]. The compounds are highly selective in part because of the low homology between HSL and known mammalian lipases [42]. We show here that chronic pharmacological inhibition of lipolysis using a selective HSL inhibitor improved insulin action in HFD-fed mice and genetically obese $LepR^{db}/LepR^{db}$ mice. From the clinical data presented here, it appears that insulin-resistant individuals with a high lipolytic rate will benefit the most from treatment with antilipolytic molecules such as HSL inhibitors. An additional clinical advantage with HSL inhibition is the lack of effect, at least in mice, on fat mass. As discussed earlier, plasma levels of FA poorly correlate with insulin sensitivity [6]. Our data do not dispute this notion but suggest that it is FA fluxes rather than FA levels that determine insulin sensitivity.

In summary, a decrease in WAT lipolysis results in a slowdown of FA turnover associated with improved insulin tolerance and glucose metabolism and no change in fat mass (Figure 10). Long-term moderate inhibition of WAT lipolysis can therefore be beneficial in the treatment of obesity-related insulin resistance.

Materials and Methods

Ethics Statement

Clinical studies were approved by the ethics committee of Karolinska Institute University Hospital and Toulouse University Hospitals. Informed consent was obtained from each participant.

All experimental procedures on mice were performed according to INSERM and Genotoul Anexplo animal core facility guidelines for the care and use of laboratory animals.

Generation of Transgenic Mice, Treatments, and Phenotypic Analyses

Targeted disruption of the HSL gene and generation of $HSL^{-/-}$ mice have been described elsewhere [43]. Four- to 5-wk-old B6D2 mice were fed chow diet (10% kCal fat, D12450B, Research Diets Inc.) for 6 or 28 wk, HFD (45% kCal fat, D12451, Research Diets Inc.) for 12 to 16 wk, or fructose-enriched diet (D11743, Research Diets Inc.) for 45 wk. C3H/HeJ mice were purchased from Jackson Laboratories. They were fed a HFD for 7 wk. For fasting-refeeding experiments, 12-wk HFD-fed WT and $HSL^{+/-}$ male mice were overnight fasted and refed for 18 h before sacrifice. For chronic HSL inhibition, the specific HSL inhibitor synthesized by IDEALP PHARMA was given orally at 70 mg/kg/d [19]. B6D2 and $LepR^{db}/LepR^{db}$ mice were, respectively, treated once daily during 7 or 13 consecutive d. Body weight was measured weekly. Food intake was measured

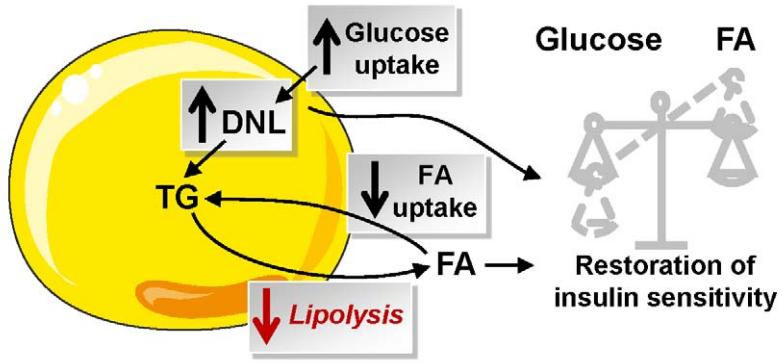

Figure 10. Consequence of partial inhibition of WAT lipolysis on fatty acid and glucose metabolism and insulin sensitivity. Partial inhibition of lipolysis modifies FA flux with a decrease in WAT FA uptake concurring to maintenance of fat mass and an increase in glucose uptake that favours de novo lipogenesis, which may be a key player in the restoration of insulin sensitivity. DNL, de novo lipogenesis; FA, fatty acid; NEFA, nonesterified fatty acid; TG, triacylglycerol.
doi:10.1371/journal.pbio.1001485.g010

daily during 4 d in animal housed individually. Body mass composition was evaluated by quantitative nuclear magnetic resonance system (EchoMRI 3-in-1, Echo Medical Systems). In vivo lipolytic challenge by intraperitoneal (ip) injection of the β-adrenergic agonist isoproterenol (10 mg/kg) on mice fasted for 7 h was performed as previously reported [44].

For ip insulin tolerance tests, an injection of 0.6 U/kg insulin was given to 6-h–fasted mice. For oral glucose tolerance tests, an oral administration of 1.5 g/kg D-Glucose was given to 16-h–fasted mice with, in $LepR^{db}/LepR^{db}$ mice, supplemental blood sampling performed at 15 min for insulin measurement. For pyruvate tolerance test, an ip injection of 2 g/kg pyruvate was performed on 16-h–fasted mice. Blood glucose levels were monitored from the tip of the tail vein with a glucometer (Accucheck, Roche). Arginine tolerance test was performed on WT and $HSL^{+/-}$ mice fed a HFD for 12 wk. The 16-h–fasted mice anesthetized with isoflurane were ip injected with 3 g/kg of L-arginine (Sigma). Blood sampling for insulin measurement was performed at the retro-orbital sinus.

For the measurement of in vivo glucose utilization in individual tissues, an intravenous bolus of 50 μCi 2-deoxy-D-[^{3}H] glucose (Perkin Elmer) was given during euglycemic hyperinsulinemic clamp (6 mU kg^{-1} min^{-1} of insulin). Disappearance of plasma 2-deoxy-D-[^{3}H] glucose and glucose concentrations were determined in 5 μl blood samples from the tail vein. Different tissues were dissected and dissolved in 1 M NaOH during 1 h. 2-deoxy-D-[^{3}H] glucose 6-phosphate and 2-deoxy-D-[^{3}H] glucose were differentially precipitated by the use of zinc sulfate (0.3 M), barium hydroxide (0.3 M), and perchloric acid solutions (6%).

For the measurement of in vivo hepatic de novo lipogenesis, livers were harvested after an euglycemic hyperinsulinemic clamp (1.5 mU kg^{-1} min^{-1} of insulin) with D-[3-^{3}H]glucose (Perkin Elmer) infusion at 15.9 kBq/min. After homogenization in a lysis buffer, lipids were extracted by a Folch method and the organic phase was counted for radioactivity.

For in vivo measurements of phospho-insulin receptor substrate 1 and phospho-Akt, animals fed a HFD for 12 wk were fasted for 6 h before ip injection of 10 U/kg insulin. Liver was harvested 15 min after injection. Liver proteins were solubilised in RIPA buffer containing protease and phosphatase inhibitors. Protein samples were resolved by SDS-PAGE, blotted, and incubated with anti-phospho insulin receptor substrate 1 (Tyr^{612}), phospho Akt (Ser^{473}), total insulin receptor substrate 1, or total Akt antibodies (Cell Signaling). Equal loading was confirmed using anti-GAPDH protein.

To investigate FA fluxes, a catheter was inserted into the femoral vein in $HSL^{+/-}$ and WT animals under isoflurane anaesthesia. Mice were allowed to recover for 4–5 d before assessing FA fluxes in awake free-moving mice. Mice were then infused in fasting conditions (during 6 h from 08:00) with a tracer solution freshly prepared each day. Infusate was prepared with 50 μM palmitate and [9,10-^{3}H] palmitic acid. Infusions were performed at a constant rate of 0.2 μCi/4 μl/min for 2 h. Blood samples (30 μl) were collected from the tip of the tail at −30, 0, 60, 75, 90, and 120 min. Tracer infusion was stopped at 120 min, and additional blood samples were collected at 125, 130, and 140 min. Blood samples were rapidly centrifuged to prepare plasma, which was kept at −80°C until biochemical measurements. Total plasma NEFA and TG were measured with a colorimetric enzymatic method (respectively, NEFA C, Wako, and TG PAP150, Biomerieux). Lipid extraction and separation procedure were performed to determine plasma ^3H_2O, ^{3}H-NEFA and ^{3}H-TG as described by Oakes et al. [18]. During a first step, ^3H_2O was separated from lipid phase using an isopropanol-hexane-H_2SO_4 0.5 M mixture. In a second step, TGs were separated from neutral lipids using an alkaline methanol solution. Finally, NEFAs were extracted from neutral lipid phase using an acid hexane solution. Radioactivity was counted in each fraction. Whole body rates of FA clearance, appearance, oxidation, and storage were determined as described by Oakes et al. [18]. At 140 min, the last blood sample was collected from retro-orbital sinus. Mice were euthanized with an intravenous bolus of pentobarbital. Different tissues were collected and weighed before freezing in liquid nitrogen and storage at −80°C for total TG content assessment. A sample of WAT, *soleus* muscle, and heart was homogenized in water. Non-^3H_2O products were extracted using an isopropanol-hexane-H_2SO_4 0.5 M mixture, and radioactivity was counted. NEFA incorporation rates into tissue-specific storage products were calculated between 120 and 140 min.

Oxygen (VO_2) and carbon dioxide (VCO_2) production was measured using a four-chamber oxylet system (Bioseb). Temperature was maintained at 21±1°C, and the light was on from 07:00 to 19:00. System setting included a flow rate of 0.3 l/min, a sample purge of 5 min, and a measurement period of 5 min every 25 min. Twenty-four h prior to data collection, mice were placed in separate calorimetry chambers (each with a volume of 2.5 l), with free access to food and water. The respiratory quotient was calculated as the ratio of VCO_2/VO_2; results were expressed as percent of relative cumulative frequency along the measurement period [45].

For measurements of plasma parameter concentrations, insulin, NEFA, and glycerol were determined by ELISA (Mercodia), an enzymatic colorimetric reaction (NEFA C, Wako), and with the hydrazine buffer method or with a commercial kit (Sigma), respectively. TG and cholesterol were determined with a COBAS-MIRA + analyzer (ABX Diagnostics). Adiponectin, leptin, and RBP4 were measured with commercial ELISA kits (R&D Systems).

In Vitro Measurements on Mouse Tissues

Overnight fasted mice were euthanized at various weeks of age depending on experiments, blood was collected in EDTA tubes, and various tissues were removed, immediately weighed, frozen in liquid nitrogen, and stored at −80°C.

Epididymal fat samples were fixed in 1% formalin (Sigma), embedded in paraffin, and processed to hematoxylin and eosin staining. Digital images were captured using light microscope coupled to a camera and analyzed using a morphometric programme (Lucia IMAGE, version 4.81; Laboratory Imaging). Adipocyte size was determined on a histological preparation measuring area of at least 200 adipocytes.

In adipogenesis test, the stromavascular fraction (SVF) was isolated from subcutaneous WAT of 12-wk HFD-fed WT, $HSL^{+/-}$, and $HSL^{-/-}$ mice. WAT from 2–3 mice were pooled together. SVF cells were plated at a density of 70,000 cells per well, in a 48-well plate, in 10% FBS-endothelial cell basal medium. Media were replaced at Day 1 and Day 4. At Day 5, the medium was replaced with 2% FBS—endothelial cell basal medium supplemented with 20 nM insulin, 0.2 nM T3, 100 nM cortisol, 0.01 mg/ml transferrin, and then changed every 2 d. At Day 14, lipid accumulation was estimated through Oil Red O staining normalized by total DNA amount measured using PicoGreen (InVitrogen).

For flow cytometry analysis of WAT, SVF cells were obtained by collagenase digestion as previously described [46]. After digestion, the suspension was filtered through 150 μm sieves and centrifuged (100 g, 10 s) to collect the infranatant containing the SVF. The lower phase was centrifuged (400 g, 10 min), and the

pellet containing the SVF was incubated for 10 min in erythrocyte-lysis buffer (155 mM NH_4Cl, 5.7 mM KH_2PO_4, and 0.1 mM EDTA), filtered through 40 µm sieves, and centrifuged again (400 g, 10 min). The pellet was then resuspended in PBS containing 2 mM EDTA and 0.5% bovine serum albumin. The total number of cells was counted using Trypan blue (Gibco, Courbevoie, France) and a Neubauer hematocytometer (Poly Labo, Paul Block & Cie, Strasbourg, France). The cell count was confirmed by DNA determination using fluorometric assay (Picogreen, Invitrogen, Cergy Pontoise, France). We incubated 100,000 cells of the SVF with FITC-conjugated antibodies (F4/80), PerCP-conjugated antibody (CD45), PE-Cy7-conjugated antibody (CD11b), and respective isoptype control. Analyses were performed using a FACSCanto flow cytometer and the BD FACS Diva software (BD Bioscience). The total number of each cell population present in the fat depot was calculated as a product of the percentage of each cell type determined by the flow cytometry analyses and the total number of SVF cells. Results were presented per milligram of WAT.

In vitro triolein and cholesterol oleate hydrolase activities were performed as previously described [2]. Briefly, total protein from gonadal WAT were extracted and mixed with ^{14}C-labelled triglyceride or cholesterol ester analogue, and subsequent radiolabelled fatty acids were extracted and counted. In order to estimate the enzymatic activity resulting from other lipases than HSL in these assays, the HSL-specific inhibitor was used at 1 µM [11].

For gene expression analysis, WAT was homogenized in Qiazol buffer (Qiagen) using Precellys tissue homogenizer. Total RNA from WAT was extracted using RNeasy kit (Qiagen). RNA concentration and purity were assessed spectrophotometrically using NanoDrop (DigitalBio). After treatment with DNase I (Invitrogen) and reverse transcription of 1 µg of total RNA with Superscript II (Invitrogen) or Multiscribe Reverse Transcriptase (Applied Biosystems), real-time quantitative PCR was performed with Applied Biosystems Step One Plus real-time PCR system. A standard curve was obtained using serial dilutions of WAT cDNA prior to mRNA quantitation. 18s rRNA and HPRT mRNA were used as controls to normalize gene expression.

For neutral lipid measurement, small pieces of tissues were homogenized in 1 ml 5 mM EGTA water:Methanol (1:2) using Precellys tissue homogenizer. Lipids were extracted with a mixture Methanol/Chloroform/Water (2.5/2.5/1.7 volume) purified with SPE column, dried, and dissolved in ethyl acetate. The fraction was measured by gas chromatography.

For glycogen measurement, liver and hind limb muscles were dissected from mice either fasted for 24 h or fasted and refed for 18 h and snap frozen in liquid nitrogen. Tissues were then dissolved in 200 µl of 1 N NaOH 1 h at 55°C. Digestion is neutralized by 200 µl of 1 N HCl and centrifuged to remove cell debris. Amyloglucosidase (50 U/ml) is then added and incubated for 1 h at 55°C. Glucose content is then measured by the RTU kit method (Biomerieux, France). Results are normalized by mg of tissue.

To determine ex vivo glucose oxidation, *soleus* skeletal muscles were homogenized with a polytron homogenizer in a buffer containing 0.25 M Sucrose, 1 mM EDTA, 1 µM Tris-HCl, and 2 mM ATP at pH 7.4. We incubated 80 µl of homogenized sample at 37°C for 2 h with 0.2 mM cold D-glucose, 1 µCi/ml [U-^{14}C]glucose, 0.5% BSA, 125 mM Sucrose, 25 mM Potassium phosphate monobasic, 200 mM Potassium chloride, 2.5 mM Magnesium chloride, 2.5 mM L-Carnitine, 0.25 mM Malic acid, 20 mM Tris-HCl, 2.5 mM DTT, 0.25 mM NAD+, 4 mM ATP, and 0.125 mM Coenzyme A. Following incubation, 40 µl of 70% perchloric acid was added to trap CO_2 production for 1 additional hour at room temperature. We counted 200 µl of NaOH, containing trapped CO_2, using a scintillation counter (Tri-Carb2100TR; Pakard). An acidified portion was collected, placed at 4°C overnight, centrifuged at 15,000 g for 15 min at 4°C, and the supernatant was counted. A sample of the incubation medium was used to quantify specific activity.

To measure ex vivo glucose-stimulated insulin secretion by pancreatic islets, WT and $HSL^{+/-}$ mice fed a HFD for 12 wk were anesthetized by ip injection of 50 mg/kg of pentobarbital. The common bile duct was catheterized and pancreas infused with a pre-oxygenated fixative solution [2 mg/ml of liberase (Roche) in Hanks–Hepes buffer]. Mice were sacrificed, and the pancreas was removed and digested for 8 min at 37°C. Digestion was stopped by addition of Hanks buffer supplemented with 2% BSA. After rinsing, the pellet was dissolved in 20 ml of Histopaque (Sigma) and 20 ml of Hanks/BSA buffer before being centrifuged 20 min at 1,000 g at room temperature. Pancreatic islets were collected by aspiration at the interphase. After purification, pancreatic islets were selected according to morphology and size and incubated three per well in a ACROPREP 96-well filter plate (VWR, France) in 200 µl of a medium containing 2.8 or 16.7 mM of glucose for 90 min at 37°C in an incubator. Insulin was assessed in the medium after centrifugation of the filter plate.

Culture, siRNA Transfection, Metabolic Measurements, and Gene Expression Analysis in hMADS Adipocytes

hMADS cells were maintained in proliferation medium (Dulbecco's modified Eagle's medium low glucose, 10% fetal bovine serum, 2 mM L-glutamine, 10 mM Hepes buffer, 50 units/ml of penicillin, 50 µg/ml of streptomycin, supplemented with 2.5 ng/ml of human fibroblast growth factor 2). The cells were inoculated in 100 mm dishes at a density of 525,000 cells and kept at 37°C in 5% CO2. Six days postseeding, fibroblast growth factor 2 was removed from proliferation medium. On the next day (day 0), the cells were incubated in differentiation medium (DM: serum-free proliferation medium/Ham's F-12 medium containing 10 µg/ml of transferrin, 5 µg/ml of insulin, 0.2 nM triiodothyronine, 100 µM 3-isobutyl-1-methylxanthine, 1 µM dexamethasone, and 100 nM rosiglitazone). At day 3, dexamethasone and 3-isobutyl-1-methylxanthine were omitted from DM, and at day 10, rosiglitazone was also omitted. For glucose metabolism experiments, insulin concentration was 10 nM from day 7. The experiments were carried out between days 12 and 15.

RNA interference was achieved by small interfering RNA. Briefly, on day 7 of differentiation, hMADS cells were detached from culture dishes with trypsin/EDTA (Invitrogen) and counted. Control siGFP or gene-specific small interfering RNAs for HSL (Applied Biosystems) were delivered into adipocytes with a microporator (Invitrogen) with the following parameters: 1,100 V, 20 ms, 1 pulse. The targeted sequences, flanked with dTdT overhangs, are: GFP, 5′-GCAGCACGACUUCUU-CAAG-3′; HSL, 5-AGGACAACAUAGCCUUCUU-3′.

Human fibroblast growth factor 2, insulin, triiodothyronine, transferrin, 3-isobutyl-1-methylxanthine, and dexamethasone were from Sigma; L-glutamine, penicillin, and streptomycin from Invitrogen; Hepes, Dulbecco's modified Eagle medium low glucose, and Ham's F-12 medium from Lonza; and rosiglitazone from Alexis Biochemicals.

To determine FA oxidation, cells were incubated during 3 h in 1 ml Krebs Ringer Buffer containing 3% BSA, 1 mM L-Carnitine, 80 µM oleic acid, and 20 µM [1-^{14}C] oleic acid (PerkinElmer). For medium-trapped $^{14}CO_2$ extraction, medium was transferred and acidified with 1 M sulfuric acid in closed vials

containing a central well filled with benzethonium hydroxide. After 2 h incubation, trapped $^{14}CO_2$ was measured by liquid scintillation counting. Cells were washed twice with PBS and then scraped in cold buffer (0.25 M sucrose; 10 mM Tris HCl; 1 mM EDTA; 1 mM dithiothreitol, pH 7.4). Neutral lipids and aqueous soluble metabolites were separated by adding 5 volumes chloroform/methanol (2:1) and 0.4 volume 1 M KCl/HCl. Acid soluble products, ^{14}C-labeled oxidative intermediates, were measured in aqueous phase by liquid scintillation counting. Specific activity was measured and used to calculate total oxidation as equivalent of oxidized oleic acid.

Glucose uptake was measured using 2-deoxy-D-glucose. The day before the assay, insulin was removed from culture medium. After two washes with PBS, cells were incubated 50 min at 37°C with or without 100 nM insulin. Then, 125 µM 2-deoxy-D-glucose and 0.4 µCi 2-deoxy-D-[^{3}H] glucose per well were added for 10 min incubation. Culture plates were put on ice and rinsed with 10 mM glucose in ice-cold PBS and then with ice-cold PBS. Cells were scraped in 0.05 N NaOH, and 2-deoxy-D-glucose uptake was measured by liquid scintillation counting of cell lysate.

To determine glucose oxidation, insulin was removed from culture medium the day before the assay. Cells were incubated for 3 h in Krebs Ringer buffer supplemented with 2% BSA, 10 mM HEPES, 2 mM glucose, and 1 µCi D-[^{14}C(U)]glucose (PerkinElmer) with or without 100 nM insulin. A 2×2 cm Whatman 3M paper was placed on top of each well and wet with 100 µl 1 N NaOH. After incubation, filter-trapped $^{14}CO_2$ was measured by liquid scintillation counting. Medium-trapped $^{14}CO_2$ was measured as described previously for oleate oxidation. Specific activity was counted and used to determine the quantity of oxidized glucose equivalent.

To determine glucose carbon incorporation into fatty acid and glycerol, neutral lipids were extracted after glucose oxidation as described above. They were dried and hydrolyzed in 1 ml 0.25 N NaOH in chloroform/methanol (1:1) for 1 h at 37°C. The solution was neutralized with 500 µl 0.5 N HCl in methanol. FA and glycerol were separated by adding 1.7 ml chloroform, 860 µl water, and 1 ml chloroform/methanol (2:1). Incorporation of ^{14}C into glycerol and FA was measured by liquid scintillation counting of upper and lower phases, respectively. Specific activity was counted and used to determine the quantity of incorporated glucose equivalent.

Results from metabolic measurements were normalized to total protein content of cell extracts and expressed relative to siGFP condition without insulin.

DNA microarray and reverse transcription-quantitative PCR analysis were performed as previously described [47].

Clinical Studies

The first clinical study cohort was comprised of 295 women and 72 men aged 18–65 years (mean 38 years), with a BMI range of 19–63 kg/m^2 (mean 35 kg/m^2). Thirty-eight were treated for type 2 diabetes, hypertension, and/or dyslipidemia. The remaining subjects were healthy according to self-report. They came to the laboratory in the morning after an overnight fast. A venous blood sample was obtained for the determination of fasting plasma glucose and insulin [48], which were used to calculate HOMA-IR. Thereafter, a subcutaneous fat biopsy was obtained from the abdominal area using a needle biopsy technique [49]. In 97 women and 29 men, an intravenous insulin tolerance test was performed immediately after the biopsy in order to directly estimate insulin sensitivity [48]. In the second clinical study, 25 obese individuals were investigated before and 2 years after bariatric surgery with gastric banding. At the time of the first investigation, none had undergone a slimming attempt for at least 1 year and body weight had been stable for at least 3 mo according to self-report. The third cohort, described in detail in [50], comprised 56 healthy women (age 23–72 years; mean 43 years) with a large interindividual variation in BMI (20–53 kg/m^2; mean 33 kg/m^2). They were investigated in the morning after an overnight fast as for the first cohort above. DNA microarray and reverse transcription-quantitative PCR analyses were performed in 45 individuals as previously described [50]. In the fourth clinical study, 24 obese men (mean BMI 32.7, [29.3; 36.5]) were randomly assigned to two groups and received placebo or nicotinic acid for 8 wk. Nicotinic acid was administered as Niaspan LP in progressive doses, reaching 2,000 mg from the fifth week to the end of the period. The study was registered in Clinical Trials NCT01083329 and EudraCT 2009-012124-85. A needle biopsy of subcutaneous WAT was performed before and after the treatment. Adipocytes were isolated by collagenase digestion for total RNA preparation. Fat cell de novo lipogenesis gene expression was determined using reverse transcription-quantitative PCR with microfluidic qPCR device (Biomark Dynamic Array, Fluidigm) [51].

In Vivo and In Vitro Measurement of WAT Lipolysis

In mouse studies, in vitro lipolysis on isolated adipocytes was performed as previously reported [44]. In human studies, WAT was brought to the laboratory and was immediately subjected to investigation. One portion of the tissue was used for incubation in vitro exactly as described [48]. At the end of the incubation, an aliquot was removed for analysis of glycerol levels as lipolysis index. After incubation, lipids were extracted from the lWAT. In a parallel sample, isolated fat cells were prepared and mean fat cell weight determined [48]. Glycerol release was related to number of fat cells incubated by dividing total lipid weight of the sample with the mean lipid weight of a fat cell.

Statistical Analyses

Results were expressed as mean ± SEM. Student's *t* tests, nonparametric Mann Whitney and Wilcoxon tests, and repeated measures ANOVA were used for comparisons between WT and HSL$^{+/-}$ mice. When experiments also involved HSL$^{-/-}$ mice, one-way ANOVA with Welch correction test was applied. Simple and multiple linear regression analyses and ANCOVA were used to analyze clinical data. Differences were considered significant for $p<0.05$ (*), $p<0.01$ (**), and $p<0.001$ (***).

Supporting Information

Figure S1 Lipolysis in chow diet-fed HSL$^{+/-}$ and WT mice. Mice were provided *ad libitum* access to a standard diet for 12 wk after weaning. (A) mRNA expression of HSL (lipe), ATGL (pnpla2), and plin1 in epididymal WAT. (B–C) In vitro hydrolase activities against a cholesterol ester (B) and a TG (C) were determined in WAT homogenates in the presence and absence of a HSL-specific inhibitor to calculate the activities due to HSL. (D) Body weight curve. (E) Fat mass expressed as percentage of body weight. Values are means ± SEM. Wild type mice (■) ($n = 6–10$) and HSL$^{+/-}$ mice (□) ($n = 6–10$). * $p<0.05$ versus WT mice.
(PDF)

Figure S2 Gene expression in WAT of 12-wk HFD-fed HSL$^{+/-}$ and WT mice. mRNA gene expression assessed by qRT PCR. Values are means ± SEM. WT mice (■) ($n = 8$) and HSL$^{+/-}$ mice (□) ($n = 8$).
(PDF)

Figure S3 Insulin tolerance test in chow and high fructose diet-fed WT mice. Mice were provided *ad libitum* access to standard or fructose-enriched diet for 45 wk. AUC, area under the curve in arbitrary unit. Body weight at the time of insulin tolerance test is presented below the curve. High fructose diet-fed mice (■) ($n = 7$) and chow diet-fed mice (□) ($n = 5$). * $p<0.05$ versus chow diet-fed mice.
(PDF)

Figure S4 Pancreatic function in 12-wk HFD-fed $HSL^{+/-}$ and WT mice. (A) Blood insulin during an arginine tolerance test. Values are means ± SEM. WT mice (■) ($n = 8$) and $HSL^{+/-}$ mice (□) ($n = 9$). (B) In vitro glucose-stimulated insulin secretion in pancreatic islets. Values are means ± SEM. The islets of three mice from each genotype have been pooled. Incubations and measurements were performed in quadruplicates. WT mice (■) ($n = 4$) and $HSL^{+/-}$ mice (□) ($n = 4$).
(PDF)

Figure S5 Retinol binding protein 4 measurement in media from adipocytes with HSL knockdown. RBP4 was measured in media of hMADS cells transfected with GFP or HSL siRNA. siGFP adipocytes (■) and siHSL adipocytes (▲) ($n = 11$). ** $p<0.01$ versus siGFP.
(PDF)

Acknowledgments

We gratefully acknowledge the GenoToul Animal Care, Anexplo, Quantitative Transcriptomics, and Lipidomic facilities. We especially thank Anne Bouloumié, Alexia Zakaroff-Girard, and Coralie Sengenès for flow cytometry experiments and Valentin Barquissau for critical reading of the manuscript.

Author Contributions

The author(s) have made the following declarations about their contributions: Conceived and designed the experiments: AG GT CT NV TS RB PA DL. Performed the experiments: AG GT CV CM NM ALD MH ABP MC LMir LMonbrun VB BPM AW IV KL MAM AM MLR JG. Analyzed the data: AG GT CV CM NM BR BPM SCB TS CH EM RB PA DL. Contributed reagents/materials/analysis tools: CH. Wrote the paper: AG DL.

References

1. Lafontan M, Langin D (2009) Lipolysis and lipid mobilization in human adipose tissue. Prog Lipid Res 48: 275–297.
2. Bezaire V, Mairal A, Ribet C, Lefort C, Girousse A, et al. (2009) Contribution of adipose triglyceride lipase and hormone-sensitive lipase to lipolysis in hMADS adipocytes. J Biol Chem 284: 18282–18291.
3. Zimmermann R, Strauss JG, Haemmerle G, Schoiswohl G, Birner-Gruenberger R, et al. (2004) Fat mobilization in adipose tissue is promoted by adipose triglyceride lipase. Science 306: 1383–1386.
4. McLaughlin T, Abbasi F, Lamendola C, Reaven G (2007) Heterogeneity in the prevalence of risk factors for cardiovascular disease and type 2 diabetes mellitus in obese individuals: effect of differences in insulin sensitivity. Arch Int Med 167: 642–648.
5. McGarry JD (1992) What if Minkowski had been ageusic? An alternative angle on diabetes. Science 258: 766–770.
6. Karpe F, Dickmann JR, Frayn KN (2011) Fatty acids, obesity, and insulin resistance: time for a reevaluation. Diabetes 60: 2441–2449.
7. Samuel VT, Petersen KF, Shulman GI (2010) Lipid-induced insulin resistance: unravelling the mechanism. Lancet 375: 2267–2277.
8. Suganami T, Nishida J, Ogawa Y (2005) A paracrine loop between adipocytes and macrophages aggravates inflammatory changes: role of free fatty acids and tumor necrosis factor alpha. Arterioscler Thromb Vasc Biol 25: 2062–2068.
9. Girousse A, Langin D (2012) Adipocyte lipases and lipid droplet-associated proteins: insight from transgenic mouse models. Int J Obes 36: 581–594.
10. Large V, Arner P, Reynisdottir S, Grober J, Van Harmelen V, et al. (1998) Hormone-sensitive lipase expression and activity in relation to lipolysis in human fat cells. J Lipid Res 39: 1688–1695.
11. Langin D, Dicker A, Tavernier G, Hoffstedt J, Mairal A, et al. (2005) Adipocyte lipases and defect of lipolysis in human obesity. Diabetes 54: 3190–3197.
12. Large V, Reynisdottir S, Langin D, Fredby K, Klannemark M, et al. (1999) Decreased expression and function of adipocyte hormone-sensitive lipase in subcutaneous fat cells of obese subjects. J Lipid Res 40: 2059–2066.
13. Harada K, Shen WJ, Patel S, Natu V, Wang J, et al. (2003) Resistance to high-fat diet-induced obesity and altered expression of adipose-specific genes in HSL-deficient mice. Am J Physiol Endocrinol Metab 285: E1182–E1195.
14. Strom K, Gundersen TE, Hansson O, Lucas S, Fernandez C, et al. (2009) Hormone-sensitive lipase (HSL) is also a retinyl ester hydrolase: evidence from mice lacking HSL. FASEB J 23: 2307–2316.
15. Strom K, Hansson O, Lucas S, Nevsten P, Fernandez C, et al. (2008) Attainment of brown adipocyte features in white adipocytes of hormone-sensitive lipase null mice. PLoS ONE 3: e1793. doi:10.1371/journal.-pone.0001793
16. Zimmermann R, Haemmerle G, Wagner EM, Strauss JG, Kratky D, et al. (2003) Decreased fatty acid esterification compensates for the reduced lipolytic activity in hormone-sensitive lipase-deficient white adipose tissue. J Lipid Res 44: 2089–2099.
17. Kosteli A, Sugaru E, Haemmerle G, Martin JF, Lei J, et al. (2010) Weight loss and lipolysis promote a dynamic immune response in murine adipose tissue. J Clin Invest 120: 3466–3479.
18. Oakes ND, Thalen PG, Jacinto SM, Ljung B (2001) Thiazolidinediones increase plasma-adipose tissue FFA exchange capacity and enhance insulin-mediated control of systemic FFA availability. Diabetes 50: 1158–1165.
19. Claus TH, Lowe DB, Liang Y, Salhanick AI, Lubeski CK, et al. (2005) Specific inhibition of hormone-sensitive lipase improves lipid profile while reducing plasma glucose. J Pharmacol Exp Ther 315: 1396–1402.
20. Yang Q, Graham TE, Mody N, Preitner F, Peroni OD, et al. (2005) Serum retinol binding protein 4 contributes to insulin resistance in obesity and type 2 diabetes. Nature 436: 356–362.
21. Boden G (2011) Obesity, insulin resistance and free fatty acids. Curr Op Endocrinol Diabetes Obesity 18: 139–143.
22. Schenk S, Saberi M, Olefsky JM (2008) Insulin sensitivity: modulation by nutrients and inflammation. J Clin Invest 118: 2992–3002.
23. Cinti S, Mitchell G, Barbatelli G, Murano I, Ceresi E, et al. (2005) Adipocyte death defines macrophage localization and function in adipose tissue of obese mice and humans. J Lipid Res 46: 2347–2355.
24. Haemmerle G, Lass A, Zimmermann R, Gorkiewicz G, Meyer C, et al. (2006) Defective lipolysis and altered energy metabolism in mice lacking adipose triglyceride lipase. Science 312: 734–737.
25. Hoy AJ, Bruce CR, Turpin SM, Morris AJ, Febbraio MA, et al. (2011) Adipose triglyceride lipase-null mice are resistant to high-fat diet-induced insulin resistance despite reduced energy expenditure and ectopic lipid accumulation. Endocrinology 152: 48–58.
26. Kienesberger PC, Lee D, Pulinilkunnil T, Brenner DS, Cai L, et al. (2009) Adipose triglyceride lipase deficiency causes tissue-specific changes in insulin signaling. J Biol Chem 284: 30218–30229.
27. Ahmadian M, Abbott MJ, Tang T, Hudak CS, Kim Y, et al. (2011) Desnutrin/ATGL is regulated by AMPK and is required for a brown adipose phenotype. Cell Metab 13: 739–748.
28. Rodriguez AM, Elabd C, Delteil F, Astier J, Vernochet C, et al. (2004) Adipocyte differentiation of multipotent cells established from human adipose tissue. Biochem Biophys Res Commun 315: 255–263.
29. Shen WJ, Yu Z, Patel S, Jue D, Liu LF, et al. (2011) Hormone-sensitive lipase modulates adipose metabolism through PPARgamma. Biochim Biophys Acta 1811: 9–16.
30. Haemmerle G, Moustafa T, Woelkart G, Buttner S, Schmidt A, et al. (2011) ATGL-mediated fat catabolism regulates cardiac mitochondrial function via PPAR-alpha and PGC-1. Nat Med 17: 1076–1085.
31. Mottillo EP, Bloch AE, Leff T, Granneman JG (2012) Lipolytic products activate peroxisome proliferator-activated receptor (PPAR) alpha and delta in brown adipocytes to match fatty acid oxidation with supply. J Biol Chem 287: 25038–25048.
32. McGarry JD, Mannaerts GP, Foster DW (1977) A possible role for malonyl-CoA in the regulation of hepatic fatty acid oxidation and ketogenesis. J Clin Invest 60: 265–270.
33. Voshol PJ, Haemmerle G, Ouwens DM, Zimmermann R, Zechner R, et al. (2003) Increased hepatic insulin sensitivity together with decreased hepatic triglyceride stores in hormone-sensitive lipase-deficient mice. Endocrinology 144: 3456–3462.
34. Abel ED, Peroni O, Kim JK, Kim Y-B, Boss O, et al. (2001) Adipose-selective targeting of the Glut4 gene impairs insulin action in muscle and liver. Nature 409: 729–733.
35. Herman MA, Peroni OD, Villoria J, Schon MR, Abumrad NA, et al. (2012) A novel ChREBP isoform in adipose tissue regulates systemic glucose metabolism. Nature 484: 333–338.
36. Roberts R, Hodson L, Dennis AL, Neville MJ, Humphreys SM, et al. (2009) Markers of de novo lipogenesis in adipose tissue: associations with small adipocytes and insulin sensitivity in humans. Diabetologia 52: 882–890.
37. Benhamed F, Denechaud PD, Lemoine M, Robichon C, Moldes M, et al. (2012) The lipogenic transcription factor ChREBP dissociates hepatic steatosis from insulin resistance in mice and humans. J Clin Invest 122: 2176–2194.

38. Lodhi IJ, Wei X, Semenkovich CF (2011) Lipoexpediency: de novo lipogenesis as a metabolic signal transmitter. Trends Endocrinol Metab 22: 1–8.
39. Bourlier V, Bouloumie A (2009) Role of macrophage tissue infiltration in obesity and insulin resistance. Diabetes Metab 35: 251–260.
40. Karpe F, Frayn KN (2004) The nicotinic acid receptor—a new mechanism for an old drug. Lancet 363: 1892–1894.
41. Wang M, Fotsch C (2006) Small-molecule compounds that modulate lipolysis in adipose tissue: targeting strategies and molecular classes. Chem Biol 13: 1019–1027.
42. Langin D, Laurell H, Holst LS, Belfrage P, Holm C (1993) Gene organization and primary structure of human hormone-sensitive lipase: possible significance of a sequence homology with a lipase of Moraxella TA144, an antarctic bacterium. Proc Natl Acad Sci USA 90: 4897–4901.
43. Mulder H, Sorhede-Winzell M, Contreras JA, Fex M, Strom K, et al. (2003) Hormone-sensitive lipase null mice exhibit signs of impaired insulin sensitivity whereas insulin secretion is intact. J Biol Chem 278: 36380–36388.
44. Lucas S, Tavernier G, Tiraby C, Mairal A, Langin D (2003) Expression of human hormone-sensitive lipase in white adipose tissue of transgenic mice increases lipase activity but does not enhance in vitro lipolysis. J Lipid Res 44: 154–163.
45. Riachi M, Himms-Hagen J, Harper ME (2004) Percent relative cumulative frequency analysis in indirect calorimetry: application to studies of transgenic mice. Can J Physiol Pharmacol 82: 1075–1083.
46. Duffaut C, Galitzky J, Lafontan M, Bouloumie A (2009) Unexpected trafficking of immune cells within the adipose tissue during the onset of obesity. Biochem Biophys Res Commun 384: 482–485.
47. Klimcakova E, Roussel B, Marquez-Quinones A, Kovacova Z, Kovacikova M, et al. (2011) Worsening of obesity and metabolic status yields similar molecular adaptations in human subcutaneous and visceral adipose tissue: decreased metabolism and increased immune response. J Clin Endocrinol Metab 96: E73–E82.
48. Bolinder J, Ostman J, Arner P (1982) Postreceptor defects causing insulin resistance in normoinsulinemic non-insulin-dependent diabetes mellitus. Diabetes 31: 911–916.
49. Kolaczynski JW, Morales LM, Moore JH, Jr., Considine RV, Pietrzkowski Z, et al. (1994) A new technique for biopsy of human abdominal fat under local anaesthesia with Lidocaine. Int J Obesity 18: 161–166.
50. Arner E, Mejhert N, Kulyté A, Balwierz PJ, Pachkov M, et al. (2012) Adipose tissue microRNAs as regulators of CCL2 production in human obesity. Diabetes 61: 1986–1993.
51. Viguerie N, Montastier E, Maoret JJ, Roussel B, Combes M, et al. (2012) Determinants of human adipose tissue gene expression: impact of diet, sex, metabolic status, and cis genetic regulation. PLoS Genet 8: e1002959. doi:10.1371/journal.pgen.1002959

De novo lipogenesis-derived fatty acids released during human adipocyte lipolysis promote lipid storage but not macrophage activation

C.I. Kolditz[1,2], S. Caspar-Bauguil[1,2,3], C. Lefort[1,2], I. K. Vila[1,2], M. Houssier[1,2], L. Mir[1,2], S. Nicolas[1,2], A.C. de Gouville[4], N. Viguerie[1,2], E. Montastier[1,2,3], C. Thalamas[1,2,5], D. Langin[1,2,3]

[1]INSERM, UMR1048, Obesity Research Laboratory, Institute of Metabolic and Cardiovascular Diseases, Toulouse, France;

[2]University of Toulouse, UMR1048, Paul Sabatier University, France;

[3]Toulouse University Hospitals, Departments of Clinical Biochemistry and Nutrition, Toulouse, France;

[4]GlaxoSmithKline, Les Ulis, France;

[5]Toulouse University Hospitals, Clinical Investigation Center, Inserm, CIC-9302, Department of clinical pharmacology, Toulouse, France

C.I. Kolditz and S. Caspar-Bauguil contributed equally to this study.

Corresponding author : Dominique Langin; Institut des Maladies Métaboliques et Cardiovasculaires, I2MC, Inserm UPS U1048, Laboratoire de Recherches sur les Obésités, Equipe 4, CHU Rangueil, 1 avenue Jean Poulhès, BP 84225, 31432 Toulouse Cedex 4, France. Tel : +33561325628; FAX : + 33561325623; E-mail : dominique.langin@inserm.fr

Word Count Abstract : 248

Word Count Main Text : 3942

Abstract

Aims/Hypothesis Toll-like receptor 4 (TLR4)-mediated activation of macrophages by saturated fatty acids is a potential mechanism linking obesity to adipose tissue inflammation. Here, we investigated whether fatty acids produced during adipocyte lipolysis induce activation of macrophages.

Methods Human THP-1 macrophages were treated with conditioned media from human hMADS adipocytes stimulated with lipolytic and antilipolytic drugs. Macrophages were also treated with a mixture of fatty acids mimicking the lipolytic conditioned medium and with a TLR4 signaling inhibitor. mRNA levels and secretion of inflammation-related molecules were measured in macrophages. Triglyceride accumulation and fatty acid composition were determined in adipocytes and macrophages. The effect of chronic inhibition of fat cell lipolysis on adipose tissue immune response was also investigated in high fat diet-fed mice carrying or not a mutation in the *Tlr4* gene and in obese individuals.

Results Human adipocyte conditioned media was composed of de novo lipogenesis-derived fatty acids. There was no change in interleukin, chemiokine and cytokine gene expression and production by macrophages and no involvement of TLR4 signaling. Similarly, the fatty acid mixture had no effect. Adipocyte lipolysis fatty acids were stored as triglyceride droplets in macrophages. In vivo, treatment with antilipolytic drugs did not modify adipose tissue macrophage marker gene expression in obese mice with intact or defective Tlr4 and, in obese individuals.

Conclusions/interpretation Our data suggest a role for adipose tissue macrophages in buffering fatty acids released by fat cell lipolysis that could take place as an initial defense preventing lipotoxicity, notably when fatty acids derive from de novo lipogenesis.

Keywords : Lipolysis . De Novo Lipogenesis . Adipose Tissue . Adipocyte . Macrophage . TLR4 . Insulin Resistance

Abbreviations : AT, adipose tissue ; ATM, adipose tissue macrophages ; FA, fatty acid; HSLi, hormone-sensitive lipase inhibitor ; lipopolysaccharide ; MCP-1, monocyte chemoattractant protein 1; PMA, phorbol myristate acetate ; TG, triglycerides ; TLR4, Toll-like receptor 4

Introduction

Chronic low grade inflammation is associated with insulin resistance and obesity-related metabolic disorders such as type 2 diabetes mellitus [1, 2] . This inflammatory state appears to initiate in adipose tissue (AT), as immune cell infiltration in this tissue has been shown, in rodent models, to take place gradually during the time-course of obesity prior to the development of insulin resistance [3, 4] Notably, infiltrated adipose tissue macrophages (ATM) represent a major source of proinflammatory cytokines and chemiokines, such as TNFα, IL1β, IL6 and MCP-1, which may impair insulin sensitivity [1, 2, 5, 6] and interfere with adipocyte functions [7, 8], thereby aggravating the metabolic dysfunction of AT. On the other hand, excessive release of fatty acids (FAs) from expanded AT has been hypothesized to cause insulin resistance [9, 10]. Thus, there is growing evidence that both adipocytes and ATM contribute to the development of insulin resistance. Cross-talk between the two cell types may play a key role in this process. The metabolic factors regulating ATM immune response remain poorly defined. Saturated FAs have been reported, in several murine models, to have pro-inflammatory effects via the endotoxin receptor, Toll-like receptor 4 (TLR4), expressed in ATM [11-15] .We therefore hypothesized that FAs released by stimulation of human adipocyte lipolysis could promote activation of inflammatory pathways in ATM through TLR4 signalling. To test this hypothesis, conditioned media were prepared from human mesenchymal stem cell-derived (hMADS) adipocytes stimulated with lipolytic and antilipolytic drugs and used to treat human THP-1 macrophages [16, 17]. Human macrophages were also treated with a mixture of FAs similar to that in the lipolytic medium. The involvement of TLR4 was assessed using a blocker of TLR4 signalling, TAK-242 [18]. The effect of chronic inhibition of lipolysis on AT inflammation was investigated in vivo in two strains of mice expressing or not functional TLR4 and in obese individuals.

Methods

hMADS cell culture hMADS cells were cultured and differentiated as previously described in 6-well plates at a density of 44,000 cells/ml and kept at 37 °C in 5% CO_2 [16]. hMADS cells were maintained in proliferation medium supplemented with 2 ng/ml fibroblast growth factor 2. Six days post-seeding, fibroblast growth factor 2 was removed from proliferation medium. On the next day (day 0), the cells were incubated in differentiation medium (serum-free DMEM low glucose/ Ham's F-12 medium containing 10µg/ml of transferrin, 5µg/ml of insulin, 0.2 nM triiodothyronine, 100µM 3-isobutyl-1-methylxanthine, 1 µM dexamethasone, and 100 nM rosiglitazone). At day 3, dexamethasone and 3-isobutyl-1-methylxanthine were omitted from the medium, and rosiglitazone was omitted at day 9. At day 13, cells were fully differentiated into adipocytes.

Fat cell lipolysis Lipolytic challenges were performed by treating adipocytes for 3h with 10^{-5}M of forskolin (Sigma-Aldrich, Saint-Louis, MO, USA), isoproterenol (Sigma-Aldrich), OPC3911 (Otsuka Pharmaceutical, Tokyo, Japan) [19, 20] and/or BAY 59-9435 (NoValix, Illkirch, France) [21] in RPMI 1640 medium (Gibco, GrandIsland, NY, USA) supplemented with 1 mmol/L sodium pyruvate, 1.5 g/L sodium bicarbonate, 2.9 g/L glutamine, 100 U/mL penicillin, 100 mg/L streptomycin and 2% BSA (A7030, Sigma-Aldrich). Control cells were treated with vehicle (0.2% DMSO). The same treatments were carried out in parallel in cell-free wells used as controls of hMADS conditioned medium for THP-1 cell treatment. Culture supernatants were collected, centrifuged for 10 minutes at 13000 rpm, 4°C and then maintained at -80°C until use. Aliquots of conditioned media were thawed only once prior to analysis or use on THP-1 culture cells after supplementation with 10% vol/vol FBS and 4.5 g/L glucose. To evaluate lipolysis, glycerol and NEFA released in the medium were measured using commercially available kits (free glycerol reagent from Sigma-Aldrich and NEFA-HR2

from Wako Chemicals, Neuss, Germany). Protein concentration was determined in cellular fraction to normalize data. Cells were washed twice with PBS and scraped with extraction buffer (10 mM Tris-HCl, pH 7.4, 0.25 M sucrose, 1 mM EDTA, 1 mM dithiothreitol). Protein concentrations were determined with Bio-Rad protein assay using BSA as standard.

THP-1 macrophage culture THP-1 cells were routinely cultured at 5% CO_2 in 75-cm^2 tissue culture flasks at 37°C in RPMI 1640 medium (Gibco) supplemented with 10% vol/vol fetal bovine serum, 4.5 g/L glucose, 10 mmol/L Hepes, 1 mmol/L sodium pyruvate, 1.5 g/L sodium bicarbonate, 0.05 mmol/L 2-β-mercaptoethanol, 2.9 g/L glutamine, 100 U/mL penicillin and 100 mg/L streptomycin. For the induction of monocyte–macrophage differentiation, cells were seeded in 12-well tissue culture plates (5.5×10^5 cells/well) in complete RPMI medium without 2-β-mercaptoethanol and treated for 24 h with 100 nM of phorbol myristate acetate (PMA) (Sigma-Aldrich). Differentiated, plastic-adherent cells were washed twice with sterile Dulbecco's PBS (Sigma-Aldrich). Treatments with conditioned media were carried out immediately after PMA removal.

Fatty acid mixture The mixture of FAs used to mimic the composition of lipolysis conditioned media was 20% palmitic acid, 20% palmitoleic acid, 50% oleic acid and 10% vaccenic acid (molar %), and was used at 100 μM final concentration. FAs were mixed according to the indicated proportions to a final concentration of 40 mM in a solvent of 0.1 N NaOH / 70% ethanol, and heated to 70◦C until dissolved. The final FA:albumin ratio used in experiments was approximately 3:1.

THP-1 cell treatments PMA-differentiated THP-1 cells were treated with hMADS conditioned media or exogenous FAs in RPMI 1640 complete medium without 2-β-mercaptoethanol for 72 h, in the presence or absence of 10^{-6}M of TAK-242, a specific inhibitor of TLR4 signaling pathway [18]. PMA-differentiated THP-1 cells treated with complete RPMI medium supplemented with 2% BSA were used as non-vehicle controls.

Incubation media containing FAs were prepared by diluting the FA stock solutions (40 mmol/L FA in 70% ethanol, 0.1N NaOH). Vehicle controls were obtained by diluting a FA-free stock solution 0.1% ethanol 0.1N NaOH to the same proportion. PMA-differentiated THP-1 cells were also treated for 72 h with 10^{-5}M of forskolin, isoproterenol or OPC3911 in pilot experiments. Effects of conditioned media and FAs on measured parameters were determined using one or several of the corresponding controls. At the end of the 72h-treatment, culture supernatants were collected, centrifuged for 10 minutes at 13000 rpm, 4°C and then maintained at -80°C until use for cytokine measurements. PMA-differentiated THP-1 cells cultured in complete RPMI medium were also treated with TLR4-specific lipopolysaccharide (LPS) (InVivogen, San diego, LA, USA) for 72h in the presence or absence of 10^{-6}M of TAK-242. Total RNA was extracted using the RNeasy total RNA mini kit (Qiagen, Hilden, Germany) and maintained at -80°C until use for gene expression measurements. All the experiments were carried out in triplicates.

Differentiation of THP-1 macrophages into M1 and M2 phenotypes Cells were incubated for 72h in complete RPMI medium supplemented either with 2ng/ml LPS (Sigma-Aldrich) and 10ng/ml interferon γ (Sigma-Aldrich), or with 20 ng/ml IL4 (Sigma-Aldrich) for a differentiation toward the M1 or M2 phenotype, respectively. The non-activated state, M0, was obtained after PMA removal without further treatment.

Gas chromatography analysis of triglyceride (TG) FAs FA composition was determined by capillary gas chromatography as previously described [22].

Bodipy staining of neutral lipids Cells were washed with PBS, fixed with 4% of paraformaldehyde solution for 20minutes at room temperature and washed 3 times again with fresh PBS. Cells were then incubated with PBS supplemented with 1% BSA to block non-specific interactions. Lipid droplets and nuclei were stained with 2 µg/ml green-fluorescent Bodipy neutral lipid probe 493/503 (Invitrogen, Paisley, UK) and 10µg/ml blue-fluorescent

Hoechst33342 (Invitrogen) in PBS for 30 minutes. Cells were then washed twice with PBS and visualized under reverse fluorescent microscopy.

Cytokine quantification Aliquots of culture media were thawed only once prior to analysis. IL6, IL10 and MCP1 proteins were measured in cell culture supernatants using ELISA kits (IL6, Invitrogen; MCP1, Ray Biotech, Norcross, GA, USA; IL10, Enzo life sciences, Farmingdale, NY, USA) following manufacturer's instructions.

Isolation of human adipose tissue fat cells and macrophages Adipocytes and stromavascular fraction cells were isolated from subcutaneous abdominal AT by collagenase digestion. ATM was purified from stroma vascular fraction by immunoselection and DNA microarray analyses were performed as previously described [23].

Animal study Animal studies followed the INSERM and Louis Bugnard Institute Animal Core Facility guidelines. Five week C3H/HeJ male mice which have defective TLR4 signaling due to a missense mutation in the TLR4 gene and wild-type C3H/HeOuJ male mice were purchased from the Jackson Laboratory (Bar Harbor, Maine, USA). After weaning, C3H/HeJ and C3H/HeOuJ mice were fed high-fat diet (45% energy as fat, Research Diets D12451, New Brunswick, NJ, USA) for 8 weeks. Treatments with BAY 59-9435 at 70 mg/kg or vehicle were given orally once a day in the last two weeks of diet. At sacrifice, epididymal fat pads were collected and snap frozen in liquid nitrogen then stored at -80°C.

Flow cytometry analysis One epididymal fat pad was digested by collagenase (Serlabo Technologies, Entraigues, France). Digested tissues were filtered through a 225µm pore filter. The stromavascular fraction was separated from remaining fibrous material and floating adipocytes by centrifugation at 300g. Stromavascular fraction cells were then filtered through a 70 µm pore filter followed by an incubation step in an erythrocyte lysing buffer. 10^6 cells were incubated 10 minutes at room temperature with Fcblock (BD Biosciences, Le Pont de Claix, France) in FACS buffer (PBS, 0.2% BSA, 2mM EDTA). Pools of specific fluorescent-

labeled antibodies (PerCP-CD45, FITC-F4/80 from BD Biosciences) were prepared and added to the stromavascular cell solution. After an incubation of 30 min on ice in the dark, cells were washed with 2 mL of PBS and centrifuged at 300×g, 10 min at 4°C. Supernatant was discarded and the cell pellet was resuspended in 0.5ml of PBS. Analyses were performed using a FACSCalibur flow cytometer and the CellQuest Pro software (BD Biosciences).

Clinical study The clinical study was conducted at Toulouse Clinical Investigation Center. Eleven obese men (mean BMI 32.7, [29.3; 36.5]) received nicotinic acid for 8 weeks. Nicotinic acid was administered as Niaspan® LP in progressive doses, reaching 2 g from the fifth week to the end of the period. A biopsy of subcutaneous AT was performed before and at the end of the treatment. Total RNA was prepared to assess gene expression. Plasma parameters were determined using standard clinical biochemistry techniques. The protocol was approved by the ethics committee of Toulouse University Hospitals. All subjects gave written informed consent. The study is registered in Clinical Trials NCT01083329 and EudraCT 2009-012124-85.

Measurements of mRNA levels Total RNA extraction and mRNA quantitation was performed as previously described [24, 25]. Values were normalized to the levels of 18S rRNA (Applied Biosystems, Foster city, CA, USA) or proteasome 26S subunit ATPase 4 (Applied Biosystems) for THP1 and low density lipoprotein receptor-related protein 10 for hMADS.

Statistics All data are presented as mean ± SEM. Data were analyzed by Student's t test, Mann-Whitney test or Wilcoxon non parametric test and paired t-test using GraphPad Prism Software (GraphPad Software, Inc., San Diego, CA) whenever appropriate. Statistical significance was set at $p<0.05$.

Results

The profile of FAs released by hMADS adipocytes reflects the composition of intracellular TG

At day 13 of differentiation, hMADS cells were fully differentiated into adipocytes and had readily accumulated TG droplets (Fig. 1a). NEFAs and cholesterol esters were not detected in the cellular fraction (data not shown). Differentiation is accompanied by robust induction of de novo lipogenesis gene expression (Fig. 1b). The major FAs found in the TG fraction were oleic (C18:1n-9), palmitic (C16:0) and palmitoleic (C16:1 n-7) acid (Fig. 1c). Smaller amounts of vaccenic (C18:1 n-7) and stearic (C18:0) acid were also found. The essential FAs C18:2 n-6 (linoleic acid) and C18:3 n-3 (α-linolenic acid) and C20 to C22 FAs represented less than 0.3 % (not shown). The FA profile of the TG fraction reflects that expected in a situation of strict de novo lipogenesis, the differentiation process being carried out in serum-free condition without exogenous lipids. Therefore, FAs chiefly derive from the glucose provided in the differentiation medium.

To investigate the effect of fat cell lipolysis on macrophage activation, we first screened for a drug with lipolytic potency on hMADS adipocytes yet minimal direct effects on THP-1 cells. Three commonly used lipolytic agents were tested: forskolin (an adenylylcyclase activator), isoproterenol (an agonist of β-adrenergic receptors), and OPC3911 (a cyclic nucleotide phosphodiesterase 3B inhibitor). Forskolin induced the strongest lipolytic response on hMADS adipocytes (ESM Fig. 1). However, it also potently induced *IL6* and *IL10* gene expression in THP-1 cells. Isoproterenol showed a weak lipolytic action on hMADS adipocytes. It had modest direct effect on THP-1 cell IL6 mRNA level but induced *IL10* gene expression as strongly as forskolin. OPC3911 readily stimulated adipocyte lipolysis with minimal direct activation of THP-1 cell inflammatory marker gene expression and was therefore selected as lipolytic agent (ESM Fig. 1, Fig. 1c). Inhibition of lipolytic induction was obtained by adding the specific hormone-sensitive lipase isoxazolone inhibitor BAY 59-9435 (HSLi). HSLi had no effect on FA and glycerol release when used alone but decreased

the lipolytic effect of OPC3911 by >90% (Fig. 1c). We then analysed the nature of FAs that were released in the medium in response to lipolytic stimulation (Fig. 1d). The major FAs found in the culture media were oleic, palmitic and palmitoleic acids. Vaccenic and stearic acids were also detected at lower concentrations. Thus, the profile of FAs released by hMADS adipocytes upon lipolytic stimulation largely reflected that of their TG fraction before the treatment.

FAs released by hMADS during lipolytic challenges do not induce inflammatory response in THP-1 macrophages To explore the role of lipolytic products released by adipocytes in the activation of macrophages, we studied the effects of hMADS cell conditioned media on the inflammatory response in THP-1 macrophages. To validate our culture protocol and for comparison with the effects of conditioned media, THP-1 macrophages were differentiated into M1 and M2 phenotypes. Gene expression of the pro-inflammatory markers *IL1B*, *IL6* and *TNF* were robustly increased in M1 macrophages whereas mRNA level of the anti-inflammatory marker *IL10* was markedly induced in M2 macrophages (ESM Fig. 2). Conditioned media of hMADS adipocytes with lipolytic stimulation or inhibition did not modify *IL1B*, *IL6* and *TNF* gene expression suggesting that adipocyte-derived lipolytic products do not induce the activation of inflammatory pathways in THP-1 cells (Fig. 2a). Indeed, when a modest increase in gene expression was observed following conditioned media treatment, a similar increase was observed in THP-1 cells treated with hMADS cell-free control media supplemented with OPC, suggesting a direct modest effect of the drug used to stimulate hMADS cell lipolysis on THP-1 cell gene expression. The lack of response to conditioned media was also observed for the M2 marker *IL10* and the chemiokine *CCL2* (MCP1). Concordant data were obtained when measuring IL6 and MCP1 production in culture media (Fig. 2b). The modest increase in IL10 content in the media was

incommensurate with the levels typically observed in macrophages with the anti-inflammatory M2 phenotype (ESM Fig. 2).

The possible implication of TLR4 in the effect of FAs released from adipocyte lipolysis on macrophages was assessed by treating THP-1 macrophages with TAK-242, a specific inhibitor of the TLR4 signalling pathway. First, we tested whether TLR4 was functional and TAK-242 was efficient in THP-1 cells (ESM Fig. 3). PMA-differentiated THP-1 macrophages were treated with ultra-pure LPS, the prototypical TLR4 ligand. LPS markedly stimulated *IL1B*, *TNF* and *IL10* mRNA levels in THP-1 macrophages. This induction was completely blocked in the presence of TAK-242. However, TAK-242 had no significant effect on inflammation-related marker gene expression in THP-1 cells treated with conditioned media from OPC3911-stimulated hMADS adipocytes (Fig. 2c).

To confirm the lack of stimulation of inflammatory pathways by adipocyte lipolysis-derived FAs, we exposed THP-1 macrophages to a FA mixture with a composition that reflects that of hMADS fat cells stimulated with a lipolytic agent. Compared to the FA-free control, treatment of THP-1 macrophages with the FA mixture induced no change in *IL1B*, *IL6*, *TNF*, *IL10* and *CCL2* gene expression (Fig. 2d). However, treatment with palmitate alone increased mRNA levels of *IL1B*, *IL6*, *TNF* and *IL10* (ESM Fig. 4).

THP-1 macrophages readily store TG in the presence of adipocyte lipolysis-derived FA Upon treatment with lipolysis-induced conditioned media, THP-1 macrophages accumulated intra-cytoplasmic droplets that gave them the appearance of foam cells. Cells were stained with Bodipy which binds neutral lipids revealing that the droplets were lipid-filled. Untreated THP-1 macrophages and macrophages treated with unstimulated conditioned media contained very few intracellular stained structures, whereas abundant staining was observed in THP-1 macrophages treated with OPC-treated conditioned media (Fig. 3a). To determine the nature of the neutral lipids stored in the droplets, we analysed the lipid composition of the cellular

fractions of THP-1 cells. The TG sub-fraction was the most affected by the treatments with the different conditioned media (Fig. 3b). Very few NEFAs and no cholesterol esters were detected (data not shown). At the same time, NEFA concentration in the culture medium from THP-1 cells exposed to hMADS OPC3911-stimulated conditioned media drastically felt after 72h of culture (Fig. 3c). Overall, the FA profile of the THP-1 TG sub-fraction (Fig. 3d) reflected that of the lipolysis conditioned media (Fig. 1e) and that of the hMADS adipocyte TG (Fig. 1c). When cultured in medium supplemented with 100μM of FA mixture, THP-1 macrophages exhibited plentiful intracellular Bodipy-stained structures that were not observed in THP-1 cells maintained in FA-free condition (Fig. 3e). TG content gradually increased with time in THP-1 cells whereas NEFA level in the media decreased in a concomitant manner (Fig. 3e). In THP-1 macrophages treated with FA-free control media, there was a progressive modest increase in intracellular TG content and media NEFA level. This indicates that THP-1 cells have a capacity for de novo lipogenesis and subsequent esterification of FAs into TG and lipolysis. The magnitude of TG synthesis and storage is however much lower than when FAs are provided as an external source.

In vivo inhibition of lipolysis does not modulate immune cell gene expression in mouse and human AT The relationship between lipolysis and inflammation in AT was further explored in vivo. High fat diet-fed C3H/HeJ mice with defective TLR4 signaling ($TLR4^{mut}$) and wild-type (WT) C3H/HeOuJ mice were treated for 15 days with HSLi or vehicle. Gene expression of ATM markers such as CD68 (*Cd68*), F4/80 (*Emr1*) and CD11c (*Cd11c*) was significantly lower in $TLR4^{mut}$ mice than in WT mice (Fig. 4a). Deficiency in TLR4 signaling showed also lower mRNA levels of pro- (*Tnf*) and anti- (*Il10*) inflammatory markers and of the chemiokine MCP1 (*Ccl2*). Compared to vehicle, treatment with HSLi decreased plasma glycerol levels in $TLR4^{mut}$ (455±69 μM vs. 732±50 μM, $p<0.005$, n=12 per group) and WT (635±57 μM vs. 1029±55 μM, $p<0.0001$, n=12 per group) obese mice. However, chronic

inhibition of lipolysis has no effect on ATM- and inflammation-related marker gene expression (Fig. 4a). Accordingly, treatment with HSLi did not modify ATM content determined by flow cytometry analysis (Fig. 4b). The lack of changes in inflammation-related gene expression and ATM number was observed in mice with intact or defective TLR4 signalling demonstrating in vivo a lack of interactions between AT lipolysis, TLR4 and AT inflammation.

To establish that the contention was true in humans, obese men were treated with the antilipolytic drug, nicotinic acid. At the end of the 8-week treatment, the decrease in fasting plasma TG (1.3 ± 0.2 vs 1.8 ± 0.3 mmol/L, $p<0.05$) and VLDL-C (0.6 ± 0.1 vs 0.8 ± 0.1 mmol/L, $p<0.05$) and increase in HDL-C (1.3 ± 0.1 vs 1.1 ± 0.1, $p<0.05$) were in accordance with expected actions of the drug on blood lipid profile. No significant change was observed for *IL1B*, *IL6*, *TNF*, *IL10* and *CCL2* mRNA levels in AT after treatments with placebo or nicotinic acid (Fig. 4c). Of note, these markers are expressed at much higher levels in human ATM than in adipocytes (ESM Fig. 5). As in mice, chronic inhibition of lipolysis had no effect in vivo on human AT inflammation.

Discussion

In the present study, we investigated the effects of a modulation of adipocyte lipolysis on human ATM activation. During lipolysis, FAs and other molecules are released from fat cells. Using in vitro and in vivo approaches, we show that stimulation or inhibition of adipocyte lipolysis does not modulate inflammation-related response of macrophages. TLR4, a receptor of innate immunity activated by saturated FA, is not involved. The lack of response is most likely related to the composition of lipolysis-derived FAs, notably the presence of monounsaturated FAs produced by de novo lipogenesis. ATM, however, play a role in scavenging FAs released by fat cell lipolysis.

Mouse studies suggest that saturated FAs induce a proinflammatory response by ATM [12-14, 26]. These effects are mostly dependent on TLR4. However, some studies argue against a direct activation of TLR4 signalling by saturated FAs [27, 28]. Recently, evidence for resolution of this paradox was provided. Fetuin-A, a liver-derived glycoprotein, acts as an adaptor between saturated FAs and TLR4 allowing activation of intracellular signal transduction pathways [29]. In our in vitro experiments, the concentration of fetuin A (>1.5 mg/mL) provided by FBS is sufficient to ensure maximal effect of the adaptor protein. Indeed, addition of the saturated FA, palmitate, elicites an inflammatory response on macrophages. Therefore, the lack of immune response to lipolytic media and to a FA mixture similar in composition to lipolytic media cannot be ascribed to the absence of an adaptor protein. Instead, the nature of the FAs released during lipolysis may explain the lack of effect. Monounsaturated FAs do not stimulate TLR4-mediated activation of NF-κB [29, 30]. Unsaturated FAs have been shown to inhibit LPS-induced NF-κB signaling pathway in macrophages [26, 31]. Moreover, monounsaturated FAs such as oleate have protective effects on various lipotoxic effects of palmitate [32-35]. It is therefore likely that the ratio of monounsaturated to saturated FAs produced during adipocyte lipolysis explains the absence

of inflammatory response in macrophages. In our serum-free in vitro condition, the FA composition of fat cell TG is entirely derived from de novo lipogenesis [36]. Here, we show that FAs produced through lipolysis reflect that composition and do not induce ATM activation. This piece of data may constitute a novel facet in the beneficial effect of AT de novo lipogenesis on whole body insulin sensitivity [37-41]. The lack of induction of inflammatory pathways by de novo lipogenesis-derived FAs is indeed in accordance with the positive effect on insulin action. In vivo, our data, in humans and mice, show that chronic inhibition of AT lipolysis does not modulate AT immune response. Coherent with in vitro data, TLR4 is not involved in this adaptation.

De novo lipogenesis-derived FAs were readily stored into macrophage TG as multi-locular lipid droplets. The rapid fall in NEFA concentrations from the medium demonstrates the propensity of macrophages to efficiently absorb local excess of lipid from their environment. Accordingly, mouse ATM accumulate lipid in response to lipolysis during fasting [42]. The data indicate a role for ATM in buffering local increase in FA concentrations within AT to prevent lipotoxicity. This adaptation may be transient as long term lipid accumulation promotes M1 polarization and AT inflammation [43]. However, monounsaturated FAs have been shown to protect against macrophage proinflammatory response and may allow a prolonged delay in the development of AT inflammation-associated insulin resistance [31]. Altogether, these results dissociate fat cell lipolysis-derived FA uptake and subsequent storage as TG in ATM from the induction of inflammatory pathways.

In summary, FAs released during AT lipolysis especially the FA mixture derived from fat cell de novo lipogenesis do not induce TLR4-mediated production of cytokines, chemiokines and interleukins by ATM. Instead, macrophages scavenge FAs in excess and convert them into TG stored within multilocular lipid-droplets. This may reflect an adaptive function of ATM to

preserve AT homeostasis in times of moderate or short term increase in lipid flux within AT, a mechanism that might be overridden with excess food supply in saturated fat.

Ackowledgments We thank Marion Combes and Marie-Adeline Marques for expert technical assistance.

Funding This work was supported by grants from Fondation pour la Recherche Médicale (to D.L.), Agence Nationale de la Recherche (LIPOB and OBELIP projects; to D.L.), Région Midi-Pyrénées (to D.L.), GlaxoSmithKline (to D.L.), Inserm/DHOS (to C.T. and D.L.), CHU de Toulouse (AOL 08 163 02 to C.T. and D.L.), and the Commission of the European Communities (Projects ADAPT and DIABAT to D.L.).

Duality of interest The authors declare that there is no duality of interest associated with this manuscript.

Contribution statement CIK, SCB, ACdG, NV, CT, DL designed the research. CIK, SCB, CL, IV, MH, LM, SN, NV, EM, CT researched and analysed data. CIK, SCB and DL wrote the manuscript. All authors approved the final version of the manuscript.

References

[1] Lumeng CN, Saltiel AR (2011) Inflammatory links between obesity and metabolic disease. J Clin Invest 121: 2111-2117

[2] Olefsky JM, Glass CK (2010) Macrophages, inflammation, and insulin resistance. Annu Rev Physiol 72: 219-246

[3] Weisberg SP, McCann D, Desai M, Rosenbaum M, Leibel RL, Ferrante AW, Jr. (2003) Obesity is associated with macrophage accumulation in adipose tissue. J Clin Invest 112: 1796-1808

[4] Xu H, Barnes GT, Yang Q, et al. (2003) Chronic inflammation in fat plays a crucial role in the development of obesity-related insulin resistance. J Clin Invest 112: 1821-1830

[5] Hotamisligil GS, Peraldi P, Budavari A, Ellis R, White MF, Spiegelman BM (1996) IRS-1-mediated inhibition of insulin receptor tyrosine kinase activity in TNF-alpha- and obesity-induced insulin resistance. Science 271: 665-668

[6] Kanda H, Tateya S, Tamori Y, et al. (2006) MCP-1 contributes to macrophage infiltration into adipose tissue, insulin resistance, and hepatic steatosis in obesity. J Clin Invest 116: 1494-1505

[7] Duncan RE, Ahmadian M, Jaworski K, Sarkadi-Nagy E, Sul HS (2007) Regulation of lipolysis in adipocytes. Annu Rev Nutr 27: 79-101

[8] Langin D, Arner P (2006) Importance of TNFalpha and neutral lipases in human adipose tissue lipolysis. Trends Endocrinol Metab 17: 314-320

[9] Samuel VT, Petersen KF, Shulman GI (2010) Lipid-induced insulin resistance: unravelling the mechanism. Lancet 375: 2267-2277

[10] Suganami T, Nishida J, Ogawa Y (2005) A paracrine loop between adipocytes and macrophages aggravates inflammatory changes: role of free fatty acids and tumor necrosis factor alpha. Arterioscler Thromb Vasc Biol 25: 2062-2068

[11] Lee JY, Sohn KH, Rhee SH, Hwang D (2001) Saturated fatty acids, but not unsaturated fatty acids, induce the expression of cyclooxygenase-2 mediated through Toll-like receptor 4. J Biol Chem 276: 16683-16689

[12] Nguyen MT, Favelyukis S, Nguyen AK, et al. (2007) A subpopulation of macrophages infiltrates hypertrophic adipose tissue and is activated by free fatty acids via Toll-like receptors 2 and 4 and JNK-dependent pathways. J Biol Chem 282: 35279-35292

[13] Shi H, Kokoeva MV, Inouye K, Tzameli I, Yin H, Flier JS (2006) TLR4 links innate immunity and fatty acid-induced insulin resistance. J Clin Invest 116: 3015-3025

[14] Suganami T, Tanimoto-Koyama K, Nishida J, et al. (2007) Role of the Toll-like receptor 4/NF-kappaB pathway in saturated fatty acid-induced inflammatory changes in the interaction between adipocytes and macrophages. Arterioscler Thromb Vasc Biol 27: 84-91

[15] Tsukumo DM, Carvalho-Filho MA, Carvalheira JB, et al. (2007) Loss-of-function mutation in Toll-like receptor 4 prevents diet-induced obesity and insulin resistance. Diabetes 56: 1986-1998

[16] Bezaire V, Mairal A, Ribet C, et al. (2009) Contribution of adipose triglyceride lipase and hormone-sensitive lipase to lipolysis in hMADS adipocytes. J Biol Chem 284: 18282-18291

[17] Rodriguez AM, Elabd C, Delteil F, et al. (2004) Adipocyte differentiation of multipotent cells established from human adipose tissue. Biochem Biophys Res Commun 315: 255-263

[18] Ii M, Matsunaga N, Hazeki K, et al. (2006) A novel cyclohexene derivative, ethyl (6R)-6-[N-(2-Chloro-4-fluorophenyl)sulfamoyl]cyclohex-1-ene-1-carboxylate (TAK-242), selectively inhibits toll-like receptor 4-mediated cytokine production through suppression of intracellular signaling. Mol Pharmacol 69: 1288-1295

[19] Eriksson H, Ridderstrale M, Degerman E, et al. (1995) Evidence for the key role of the adipocyte cGMP-inhibited cAMP phosphodiesterase in the antilipolytic action of insulin. Biochim Biophys Acta 1266: 101-107

[20] Tavernier G, Galitzky J, Valet P, et al. (1995) Molecular mechanisms underlying regional variations of catecholamine-induced lipolysis in rat adipocytes. Am J Physiol 268: E1135-1142

[21] Langin D, Dicker A, Tavernier G, et al. (2005) Adipocyte lipases and defect of lipolysis in human obesity. Diabetes 54: 3190-3197

[22] Caspar-Bauguil S, Fioroni A, Galinier A, et al. (2012) Pro-inflammatory phospholipid arachidonic acid/eicosapentaenoic acid ratio of dysmetabolic severely obese women. Obes Surg 22: 935-944

[23] Klimcakova E, Roussel B, Kovacova Z, et al. (2011) Macrophage gene expression is related to obesity and the metabolic syndrome in human subcutaneous fat as well as in visceral fat. Diabetologia 54: 876-887

[24] Girousse A, Tavernier G, Valle C, et al. (2013) Partial inhibition of adipose tissue lipolysis improves glucose metabolism and insulin sensitivity without alteration of fat mass. PLoS Biol 11: e1001485

[25] Viguerie N, Montastier E, Maoret JJ, et al. (2012) Determinants of human adipose tissue gene expression: impact of diet, sex, metabolic status, and cis genetic regulation. PLoS Genet 8: e1002959

[26] Lee JY, Plakidas A, Lee WH, et al. (2003) Differential modulation of Toll-like receptors by fatty acids: preferential inhibition by n-3 polyunsaturated fatty acids. J Lipid Res 44: 479-486

[27] Erridge C, Samani NJ (2009) Saturated fatty acids do not directly stimulate Toll-like receptor signaling. Arterioscler Thromb Vasc Biol 29: 1944-1949

[28] Schaeffler A, Gross P, Buettner R, et al. (2009) Fatty acid-induced induction of Toll-like receptor-4/nuclear factor-kappaB pathway in adipocytes links nutritional signalling with innate immunity. Immunology 126: 233-245

[29] Pal D, Dasgupta S, Kundu R, et al. (2012) Fetuin-A acts as an endogenous ligand of TLR4 to promote lipid-induced insulin resistance. Nat Med

[30] Dasu MR, Jialal I (2011) Free fatty acids in the presence of high glucose amplify monocyte inflammation via Toll-like receptors. Am J Physiol Endocrinol Metab 300: E145-154

[31] Chang CF, Chau YP, Kung HN, Lu KS (2012) The lipopolysaccharide-induced pro-inflammatory response in RAW264.7 cells is attenuated by an unsaturated fatty acid-bovine serum albumin complex and enhanced by a saturated fatty acid-bovine serum albumin complex. Inflamm Res 61: 151-160

[32] Collins JM, Neville MJ, Hoppa MB, Frayn KN (2010) De novo lipogenesis and stearoyl-CoA desaturase are coordinately regulated in the human adipocyte and protect against palmitate-induced cell injury. J Biol Chem 285: 6044-6052

[33] Ishiyama J, Taguchi R, Akasaka Y, et al. (2011) Unsaturated FAs prevent palmitate-induced LOX-1 induction via inhibition of ER stress in macrophages. J Lipid Res 52: 299-307

[34] Kadotani A, Tsuchiya Y, Hatakeyama H, Katagiri H, Kanzaki M (2009) Different impacts of saturated and unsaturated free fatty acids on COX-2 expression in C(2)C(12) myotubes. Am J Physiol Endocrinol Metab 297: E1291-1303

[35] Staiger K, Staiger H, Weigert C, Haas C, Haring HU, Kellerer M (2006) Saturated, but not unsaturated, fatty acids induce apoptosis of human coronary artery endothelial cells via nuclear factor-kappaB activation. Diabetes 55: 3121-3126

[36] Collins JM, Neville MJ, Pinnick KE, et al. (2011) De novo lipogenesis in the differentiating human adipocyte can provide all fatty acids necessary for maturation. J Lipid Res 52: 1683-1692

[37] Abel ED, Peroni O, Kim JK, et al. (2001) Adipose-selective targeting of the GLUT4 gene impairs insulin action in muscle and liver. Nature 409: 729-733

[38] Eissing L, Scherer T, Todter K, et al. (2013) De novo lipogenesis in human fat and liver is linked to ChREBP-beta and metabolic health. Nat Commun 4: 1528

[39] Herman MA, Peroni OD, Villoria J, et al. (2012) A novel ChREBP isoform in adipose tissue regulates systemic glucose metabolism. Nature 484: 333-338

[40] Roberts R, Hodson L, Dennis AL, et al. (2009) Markers of de novo lipogenesis in adipose tissue: associations with small adipocytes and insulin sensitivity in humans. Diabetologia 52: 882-890

[41] Cao H, Gerhold K, Mayers JR, Wiest MM, Watkins SM, Hotamisligil GS (2008) Identification of a lipokine, a lipid hormone linking adipose tissue to systemic metabolism. Cell 134: 933-944

[42] Kosteli A, Sugaru E, Haemmerle G, et al. (2010) Weight loss and lipolysis promote a dynamic immune response in murine adipose tissue. J Clin Invest 120: 3466-3479

[43] Prieur X, Mok CY, Velagapudi VR, et al. (2011) Differential lipid partitioning between adipocytes and tissue macrophages modulates macrophage lipotoxicity and M2/M1 polarization in obese mice. Diabetes 60: 797-809

Figure Legends

Fig. 1 Lipid metabolism in hMADS adipocytes. (**a**) Photomicrograph of adipocytes at Day 0 (left panel) and Day 13 (right panel) of differentiation; (**b**) mRNA levels of de novo lipogenesis enzymes at Day 0 (D0) and Day 13 (D13) of differentiation (n=4, *** $p<0.001$). (**c**) Fatty acid (FA) composition of fat cell triglycerides (TG) in differentiated adipocytes (n=4). (**d**) Glycerol (open bars) and NEFA (black bars) concentrations in lipolysis medium from adipocytes exposed or not to 10^{-5}M OPC3911 (OPC) and 10^{-5}M hormone-sensitive lipase inhibitor (HSLi) (n=4). *** $p<0.001$ relative to basal condition, $^{\$\$\$}$ $p<0.001$ relative to the OPC condition. (**e**) FA composition of lipolysis medium NEFAs (n=4).

Fig. 2 Effects of hMADS adipocyte lipolysis conditioned media and exogenous fatty acid (FA) mixture on THP-1 macrophage inflammation markers. (**a**) mRNA levels in macrophages treated with control and conditioned media. OPC3911 (OPC) and hormone-sensitive lipase inhibitor (HSLi) were, respectively, used as lipolytic and antilipolytic drugs (n=6). (**b**) Levels of interleukins and chemiokine released by macrophages exposed to conditioned media from hMADS adipocytes treated with OPC or vehicle (V) (n=6); (**c**) mRNA levels in macrophages exposed to conditioned media from OPC-stimulated hMADS adipocytes in the presence or absence of TAK-242 (TAK) (n=6). (**d**) mRNA levels in macrophages treated with vehicle (V) or FA mixture (Mix) (n=6). * $p < 0.05$, ** $p<0.01$ relative to the control condition (open bars).

Fig. 3 Effects of hMADS adipocyte lipolysis conditioned media and exogenous fatty acid (FA) mixture on lipid storage in THP-1 macrophages. (**a**) Fluorescent microscopy of neutral lipid accumulation in macrophages exposed to conditioned media from non-stimulated (Basal) or OPC3911-stimulated (OPC) adipocytes. Neutral lipid droplets and nuclei show green and blue fluorescence, respectively. (**b**) Triglyceride (TG) content in macrophages exposed to

conditioned media from non-stimulated (C) or OPC-stimulated adipocytes. (n=8), *** $p<0.001$ relative to control condition; (**c**) NEFA concentration in the macrophage culture medium before and after 72h-treatment with conditioned media from non-stimulated (-) or OPC-stimulated (+) adipocytes (n=6). *** $p<0.001$ relative to NEFA concentration at time 0 before THP-1 macrophage exposure with conditioned media from non-stimulated adipocytes, $^{\$\$\$}$ $p<0.001$ relative to NEFA concentration at time 0 before macrophage exposure with conditioned media from OPC3911-stimulated adipocytes. (**d**) FA composition of the macrophage TG fraction after 72h of treatment with conditioned media from OPC-stimulated adipocytes. (**e**) Fluorescent microscopy of neutral lipid accumulation in macrophages exposed to FA mixture or vehicle. Neutral lipid droplets and nuclei show green and blue fluorescence, respectively. (**f**) Time-course of NEFA concentrations in the macrophage culture media and TG content of macrophages exposed to FA mixture (black squares) or vehicle (open diamonds) (n=6).

Fig. 4 In vivo effect of chronic inhibition of lipolysis on adipose tissue gene expression of macrophage and inflammation markers. (**a**) mRNA levels in epididymal adipose tissue of C3H/HeJ carrying a mutation of *TLR4* ($TLR4^{mut}$) and C3H/HeOuJ (WT) obese male mice treated with vehicle (open bars) or hormone-sensitive lipase inhibitor (HSLi) (black bars) (n=12 per group). (**b**) Quantitation of adipose tissue macrophages by flow cytometry in $TLR4^{mut}$ and WT mice treated vehicle (open bars) or HSLi (black bars) (n=12 per group). (**c**) mRNA levels in subcutaneous adipose tissue of obese men before (open bars) and after (black bars) 8 weeks of treatment with nicotinic acid (n=11).

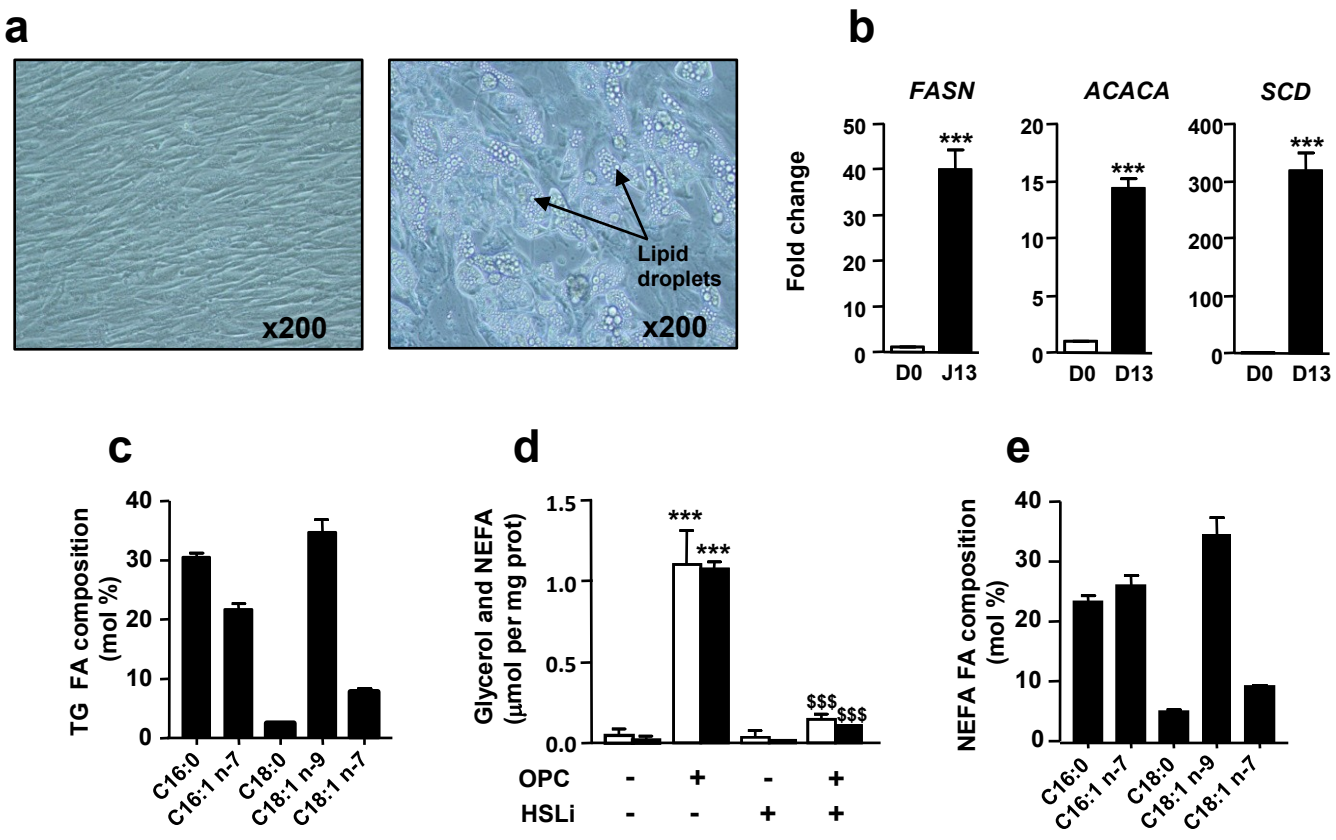
a
x200
Lipid droplets
x200
b
FASN
ACACA
SCD
Fold change
***
D0 J13
D0 D13
D0 D13
c
TG FA composition (mol %)
C16:0
C16:1 n-7
C18:0
C18:1 n-9
C18:1 n-7
d
Glycerol and NEFA (µmol per mg prot)
OPC
HSLi
$$$
e
NEFA FA composition (mol %)

Figure 1

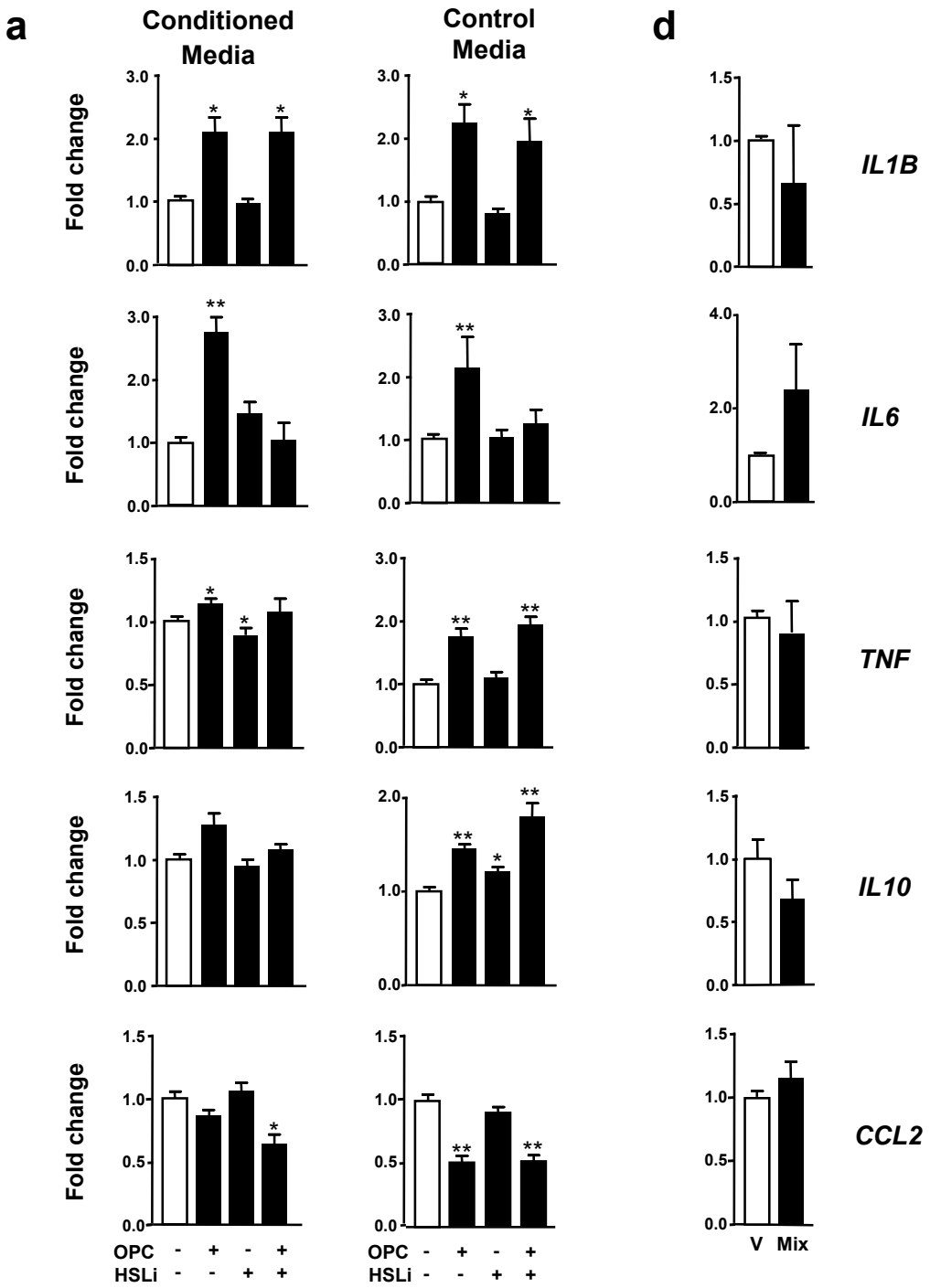
a
Conditioned Media
Control Media
Fold change
OPC - + - +
HSLi - - + +
d
IL1B
IL6
TNF
IL10
CCL2
V Mix
b
IL6
IL10
MCP1
pg/µg protein
V OPC
c
IL1β
IL6
TNFα
IL10
CCL2
Fold change
TAK - +

Figure 2

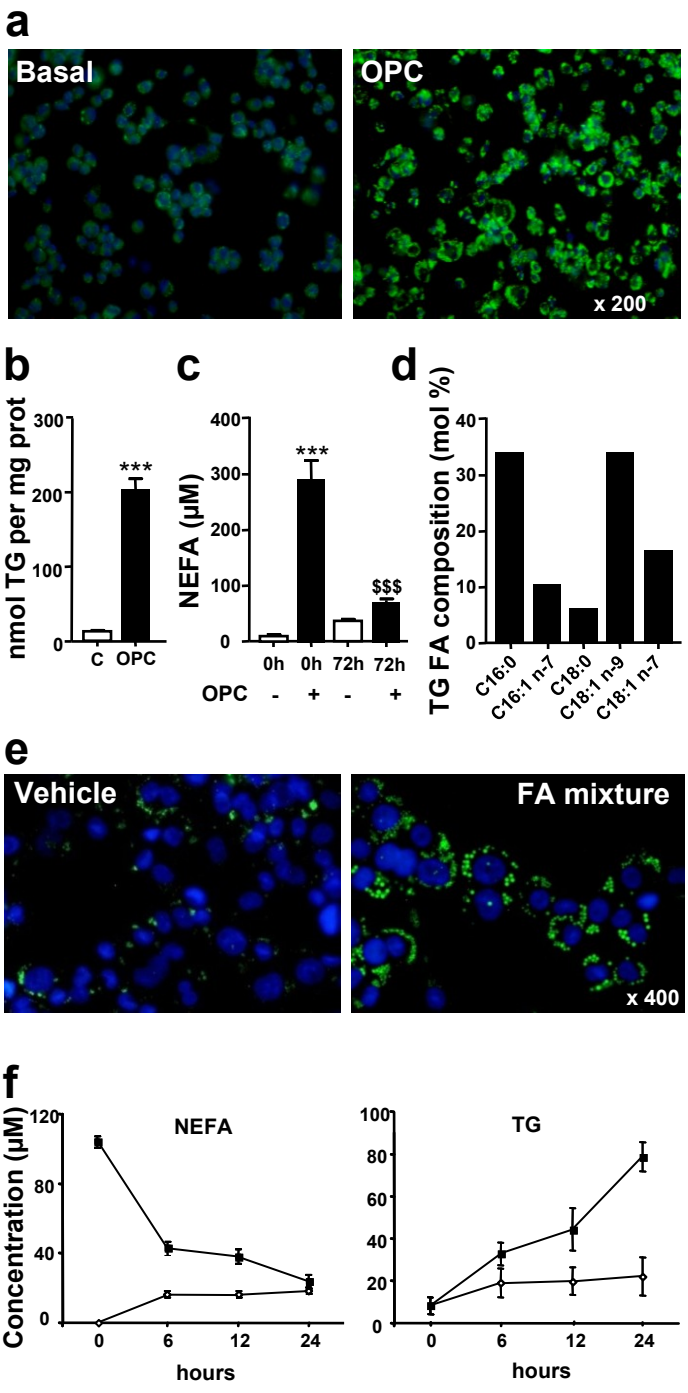
a
Basal
OPC
x 200
b
nmol TG per mg prot
300
200
100
0
***
C
OPC
c
NEFA (µM)
400
300
200
100
0
***
$$$
0h
0h
72h
72h
OPC
-
+
-
+
d
TG FA composition (mol %)
40
30
20
10
0
C16:0
C16:1 n-7
C18:0
C18:1 n-9
C18:1 n-7
e
Vehicle
FA mixture
x 400
f
Concentration (µM)
NEFA
120
80
40
0
0
6
12
24
hours
TG
100
80
60
40
20
0
0
6
12
24
hours

Figure 3

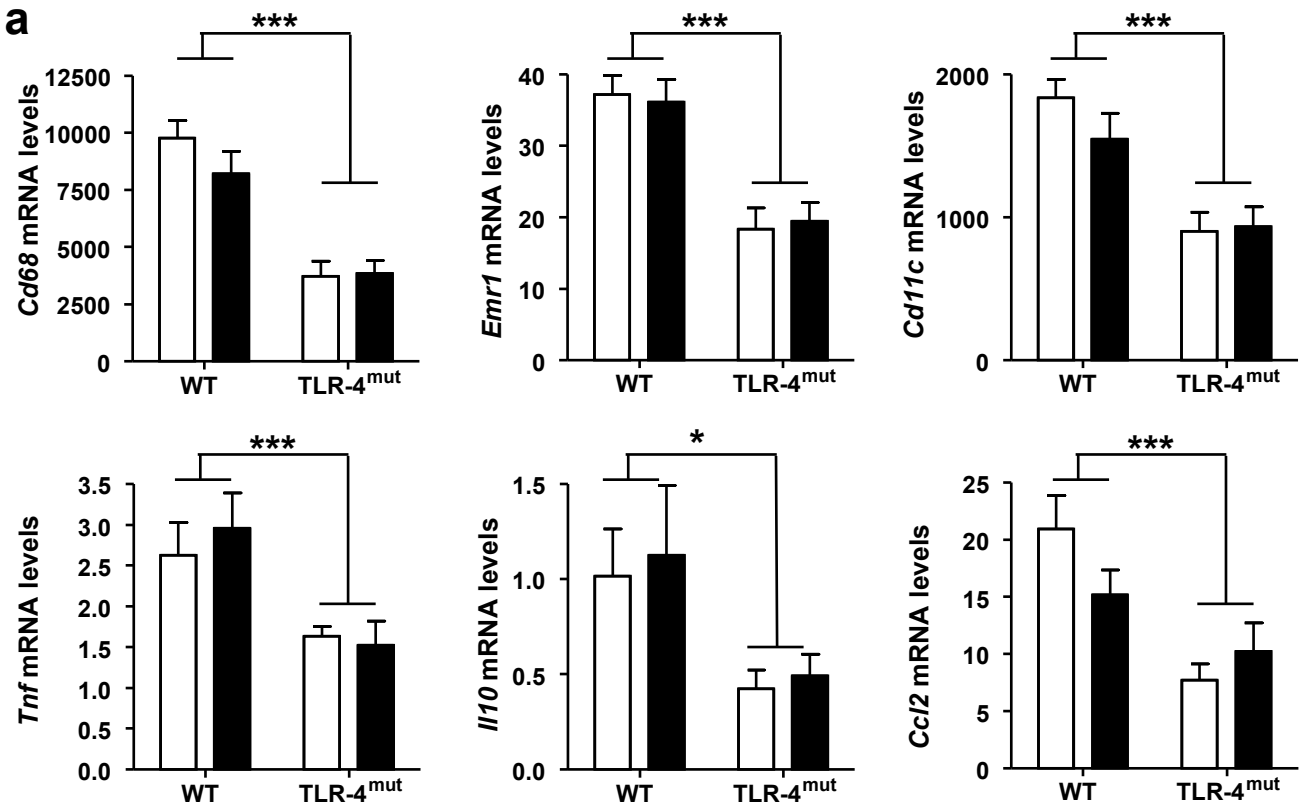
a
***
Cd68 mRNA levels
12500
10000
7500
5000
2500
0
WT
TLR-4mut
***
Emr1 mRNA levels
40
30
20
10
0
WT
TLR-4mut
***
Cd11c mRNA levels
2000
1000
0
WT
TLR-4mut
***
Tnf mRNA levels
3.5
3.0
2.5
2.0
1.5
1.0
0.5
0.0
WT
TLR-4mut
*
Il10 mRNA levels
1.5
1.0
0.5
0.0
WT
TLR-4mut
***
Ccl2 mRNA levels
25
20
15
10
5
0
WT
TLR-4mut

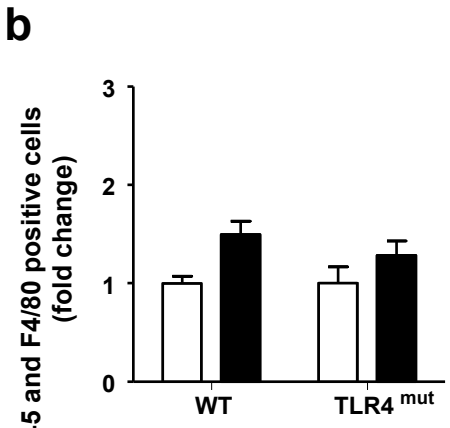
b
CD45 and F4/80 positive cells
(fold change)
3
2
1
0
WT
TLR4 mut

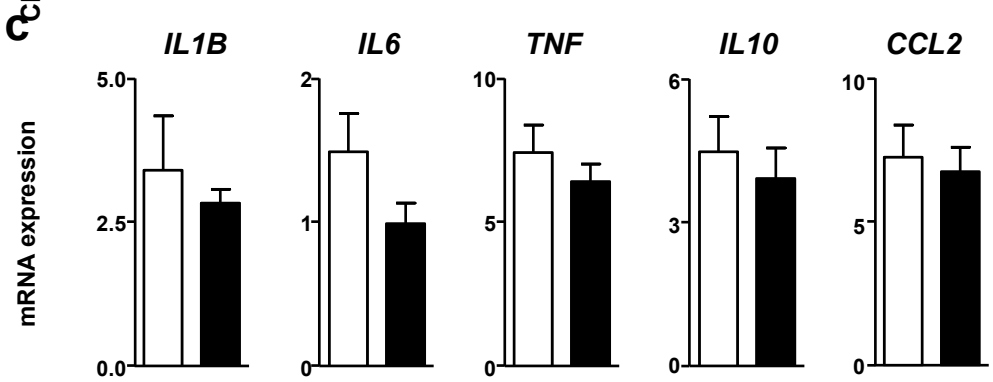
c
IL1B
IL6
TNF
IL10
CCL2
mRNA expression
5.0
2.5
0.0
2
1
0
10
5
0
6
3
0
10
5
0

Figure 4

Electronic Supplementary Material

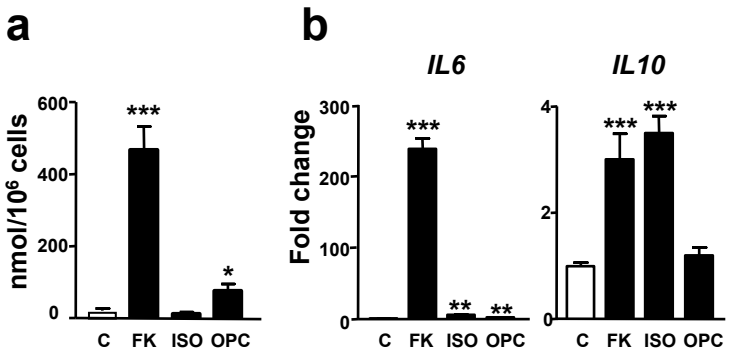

ESM Fig. 1 Selection of lipolytic agents. (**a**) NEFA levels in media from differentiated hMADS adipocytes treated without (C) or with forskolin (FK), isoproterenol (ISO) or OPC3911 (OPC) for 3h (n=6). (**b**) Effect of 72h treatment with lipolytic drugs on THP-1 macrophage interleukin gene expression (n=6). * $p < 0.05$, ** $p<0.01$, *** $p<0.001$ relative to the control condition (open bars).

Electronic Supplementary Material

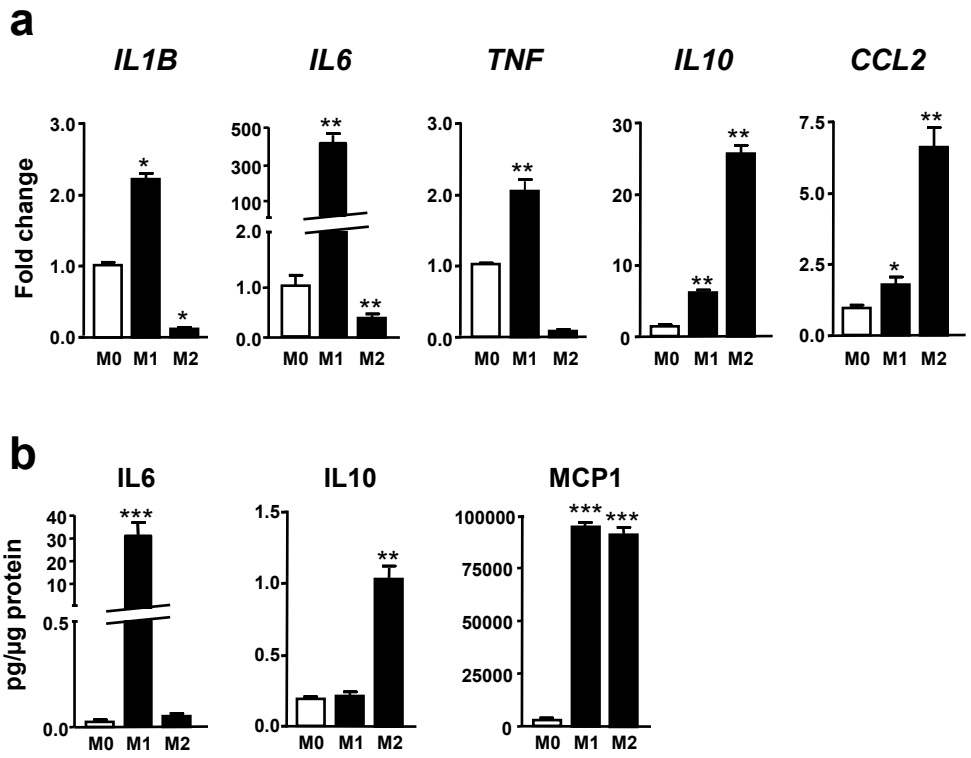

ESM Fig. 2 Induction of inflammation markers in THP-1 macrophage differentiated into M0 (untreated), M1 (treated in the presence of lipopolyssacharide and interferon and interferon γ) and M2 (treated with interleukin 4) phenotypes. (**a**) mRNA levels (n=6); (**b**) Levels of interleukins and chemiokine released in culture media (n=6). * $p < 0.05$, ** $p<0.01$, *** $p<0.001$ relative to the M0 condition (open bar).

Electronic Supplementary Material

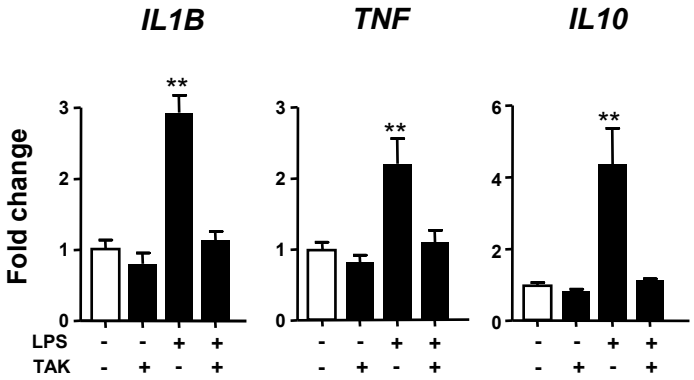

ESM Fig. 3 Validation of TAK-242 as an inhibitor of the TLR-4 signalling pathway. THP-1 macrophages were stimulated or not with lipopolysaccharide (LPS) for 72h in the presence or absence of TAK-242 (TAK) (n=6). **p<0.01 relative to the control condition (open bars).

Electronic Supplementary Material

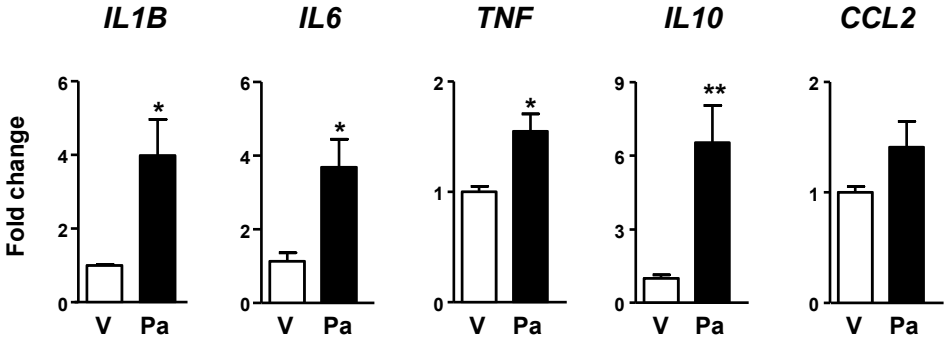

ESM Fig. 4 Effect of exogenous palmitate on THP-1 macrophage inflammation marker gene expression. Macrophages were treated with vehicle (V) or 100 µM palmitate (Pa) (n=4-6) . * p < 0.05, ** p<0.01 relative to the control condition (open bars).

Electronic Supplementary Material

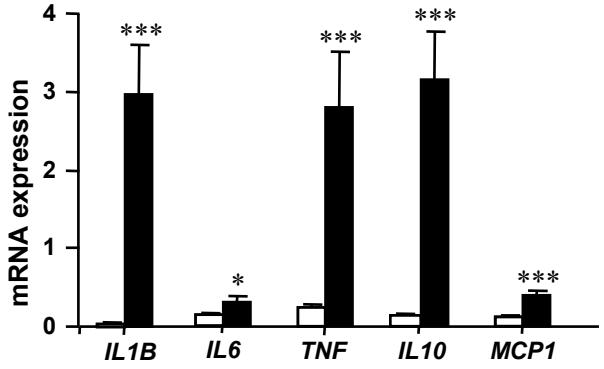

ESM Fig. 5 Human adipose tissue macrophage and adipocyte inflammation-related gene expression. Gene expression assessed using microarray analyses in adipocytes (open bars) and macrophages (black bars) isolated from subcutaneous adipose tissue (n=6) * $p<0.05$, *** $p<0.001$.

Author: Isabelle VILA

Title: Immune Cell Toll-like Receptor 4 (TLR4) Mediates the Development of Obesity-associated Adipose Tissue Fibrosis.

Supervisor : Pr Dominique Langin

Place and date of thesis defense : Toulouse 8th July 2013

Abstract:

In a first part, the study focuses on the implication of the immune Toll-like Receptor 4 (TLR4) in adipose tissue fibrosis. The natural ligand of this innate immunity receptor is lipopolysaccharide (LPS). In many studies, TLR4 was involved in fibrogenesis in various tissues such as liver and kidney. To highlight the mechanisms of fibrogenesis in adipose tissue, we worked with C3H/HeJ mice which carry a missense mutation in the TLR4 gene and C3H/HeOuJ as controls. The use of a high fat diet, inducing inflammation and fibrosis in this model, as well as an irradiation/bone marrow reconstitution experiment, which allowed us to identified the key role of the immune TLR4 in the genesis of adipose tissue fibrosis. We also showed the appearance of a lipolytic adipose tissue dysfunction accompanied by adipocyte death with the appearance of adipose tissue fibrosis.

In the second part of this thesis, we looked at the regulation of skeletal muscle lipases during a high fat diet in mice. A previous publication of the laboratory, done in an *in vitro* model, showed the negative impact on insulin signaling of the dysregulation of the expression of two major lipases, though diacylglycerol (DAG) accumulation. In this context we wanted to verify these results *in vivo*. We used C3H/HeOuJ mice on standard diet or high fat diet for 4 weeks. The study of different actors in insulin signaling and muscle lipases has allowed us to confirm *in vivo* results previously obtained.

Key words : TLR4, fibrosis, adipose tissue, inflammation, lipolysis, skeletal muscle.

Auteur: Isabelle VILA

Titre: Rôle du Toll-like receptor 4 (TLR4) immun dans le développement de la fibrose du tissu adipeux.

Directeur de thèse : Pr Dominique Langin

Lieu et date de soutenance : Toulouse le 8 Juillet 2013

Résumé :

Ce manuscrit est principalement axé sur le rôle du Toll-like Receptor 4 (TLR4) immun dans le développement de la fibrose du tissu adipeux. Récepteur de l'immunité innée dont le ligand naturel est le lipopolysaccharide (LPS), le TLR4 a été impliqué dans la fibrogenèse de différents tissus tels que le foie et le rein. Afin de mettre en évidence les mécanismes de genèse de la fibrose dans le tissu adipeux, nous avons travaillé avec des souris C3H/HeJ, modèle de mutation ponctuelle/perte de fonction du TLR4 et leurs contrôles C3H/HeOuJ. L'utilisation d'un régime hyperlipidique, inducteur d'inflammation et de fibrose dans ce modèle, ainsi que l'utilisation d'une expérience d'irradiation/reconstitution de moelle osseuse, nous a permis d'identifier le rôle clé du TLR4 immun dans la mise en place de la fibrose adipeuse. Nous avons également montré l'apparition d'une dysfonction lipolytique du tissu adipeux accompagnée d'une importante mort adipocytaire avec l'apparition de cette fibrose

En deuxième partie de ce manuscrit, nous avons regardé la régulation des lipases du muscle squelettique au cours d'un régime gras *in vivo*. Une précédente publication du laboratoire, dans un modèle *in vitro,* a montré le rôle néfaste pour le signal insulinique d'une dérégulation de l'expression des deux principales lipases de la lipolyse, via l'accumulation de diacylglycérols (DAG). Dans ce contexte nous avons voulu vérifier ces résultats *in vivo*. Pour cela nous avons mis des souris C3H/HeOuJ en régime standard ou en régime riche en lipides durant 4 semaines. L'étude de différents acteurs de la voie de l'insuline ainsi que des lipases musculaires nous a permis de confirmer les résultats *in vitro* précédemment obtenus dans un modèle *in vivo.*

Mots clés : TLR4, fibrose, tissu adipeux, inflammation, lipolyse, muscle squelettique.

Discipline : Pharmacologie

Intitulé et adresse du laboratoire : Equipe 4, Laboratoire de recherche sur les obésités, INSERM U1048, Institut Moléculaire de Rangueil, Bât L4, 1 avenue du Prof.Poulhès, BP84225, 31432 Toulouse Cedex 4